Preliminary Reports, Memoranda and Technical Notes of the ARPA Materials Summer Conference

Woods Hole, Massachusetts

VOLUME II

Environmental Degradation of Stressed Materials

July 1971

Sponsored by
Advanced Research Projects Agency
ARPA Order No. 0236

Department of Materials and Metallurgical Engineering

EC

SEE AD744204

318

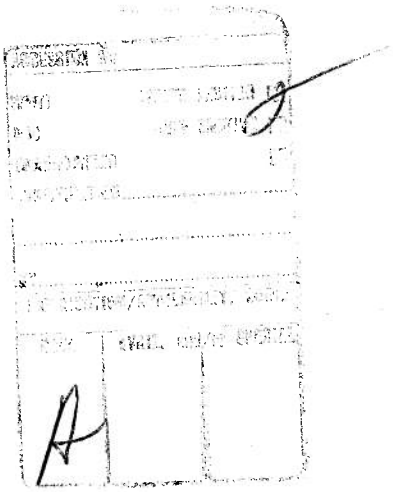

ARPA MATERIALS RESEARCH COUNCIL

Conference on

ENVIRONMENTAL DEGRADATION OF STRESSED MATERIALS

at

Woods Hole, Massachusetts

July 1971

ARPA Order Number: 0236
Program Code Number: 1D10
Contractor: The Regents of the University of Michigan
Effective Date of Contract: 1 May 1971
Contract Expiration Date: 30 April 1972
Amount of Contract: $254,000
Contract Number: DAHC15-71-C-0253
Principal Investigator: Professor Edward E. Hucke
Department of Materials & Metallurgical Engineering
The University of Michigan
Ann Arbor, Michigan 48104
(313) 764-3302

The views and conclusions contained in this document are those of the authors and should not be interpreted as necessarily representing the official policies, either expressed or implied, of the Advanced Research Projects Agency or the U.S. Government.

VOLUME II TABLE OF CONTENTS

VOLUME I TABLE OF CONTENTS

ENVIRONMENTAL DEGRADATION OF MATERIALS

J.P. Hirth and F.A. McClintock

Abstract

The Conference was organized so that fundamental aspects of stress-corrosion cracking were discussed on the first day from a number of different viewpoints. Next, three groups met to consider the possible application of these ideas to the diverse problems of cracking of stainless steel, particularly in nuclear reactors; of the corrosion of high-strength alloys, particularly aluminum and titanium; and of degradation of silicon nitride. The results of these deliberations were presented and discussed with the entire group on the final day, on which a general discussion of the field also ensued.

The initial paper in the following report is both a summary of the results of the Conference and an overview of the field generated by the authors subsequent to the meeting. The remainder represents the Proceedings of the Conference.

ENVIRONMENTAL DEGRADATION OF STRESSED MATERIALS

I. SUMMARY REPORT

by

H.H. Johnson, A.J. Sedriks and M. Cohen

1. Introduction

This Conference was organized by Professors J.P. Hirth and F.A. McClintock under the auspices of the ARPA Materials Research Council, and took place at Woods Hole, Massachusetts, during 21-23 July 1971. Although there was some attempt to deal generally with the problem of environmental degradation of materials under stress, most of the emphasis was directed to stress-corrosion cracking (SCC) phenomena.

Thirteen of the presented papers are assembled here as the Proceedings of the Conference. In addition, there were three separate sessions on related engineering problems involving (a) stainless steels, (b) high-strength aluminum and titanium alloys, and (c) silicon nitride. Here, the objective was to assess both the interplay and the gaps between recent basic research on the subject and actual service experience. Digests of these three sessions are given in Sections 7.1, 7.2 and 7.3.

This Summary Report also aims to provide a critical overview of the Conference, cutting across many of the informal discussions as well as the papers themselves. In such an undertaking, it should be recognized that the summarizers (HHJ, AJS and MC)

could not possibly do justice to all the arguments and opinions expressed; moreover, some of their own viewpoints may well have entered the picture that emerges here.

2. Participants

J. P. Hirth, Ohio State University
M. Cohen, Massachusetts Institute of Technology
F. A. McClintock, Massachusetts Institute of Technology
D. C. Drucker, University of Illinois
E. E. Hucke, University of Michigan
J. J. Gilman, Allied Chemical Corporation
R. Gomer, University of Chicago
J. R. Rice, Brown University
R. M. Thomson, Institute of Applied Technology
S. H. Bush, Battelle-Northwest
B. Cohen, AF Materials Laboratory
H. L. Gegel, AF Materials Laboratory
H. H. Johnson, Cornell University
R. P. Kambour, General Electric Company
R. Latanision, Research Institute for Advanced Studies
J. R. Low, Jr., Carnegie-Mellon University
R. A. Oriani, United States Steel Corporation
P. C. Paris, Del Research Corporation
H. W. Paxton, Carnegie-Mellon University
R. Pelloux, Massachusetts Institute of Technology
E. N. Pugh, University of Illinois
A. J. Sedriks, Research Institute for Advanced Studies
M. O. Speidel, Boeing Scientific Laboratory
R. W. Staehle, Ohio State University
A. R. Troiano, Case Western Reserve University
H. H. Uhlig, Massachusetts Institute of Technology
H. G. F. Wilsdorf, University of Virginia
J. Westbrook, General Electric Research & Development Center
A. R. C. Westwood, RIAS

3. Delineation of Mechanisms

After a detailed examination of the various SCC mechanisms discussed, we present herewith a classification scheme which seems reasonable, at least to the summarizers. It should not be inferred, however, that general agreement was obtained on the matter among the conferees.

Starting with B. F. Brown's working definition, "Stress-corrosion cracking (SCC) denotes a cracking process caused by the conjoint action of stress and a corrodent," it is evident that both mechanical and chemical factors can operate, in varying degree, relative to each other. Accordingly, in Table I, the proposed categories are arranged to indicate the interdependent roles of these factors in the SCC mechanisms.

In the dissolution mechanisms, the crack is thought to propagate mainly through the removal of atoms by dissolution from the crack tip. In this category, the film-rupture and stress-accelerated subsets differ in certain ways. In the former (A.1), the role of plastic deformation is to prevent re-passivation at the crack tip [1,2] whereas in the stress-accelerated case (A.2), plastic deformation is presumed to accelerate the ongoing dissolution process by increasing the number of sites favorable for dissolution[3]. A major distinction between these two types lies in the following: in A.1 there is a tendency for the crack tip to re-passivate by film formation, while in A.2 the crack tip is considered to be film-free (i.e. dissolution will occur along an "active path," such as a grain boundary, even in the absence of stress).

In the mechanical mechanisms, the SCC process takes place by mechanical separation of the opposing crack surfaces. Here, it is convenient to distinguish between two environmental subsets: (B.1) hydrogen embrittlement at the crack tip and (B.2) adsorption of a surface-active specie at the crack tip. Of course, these two cases may not be mutually exclusive.

TABLE I

Suggested Classification of Stress-Corrosion Cracking Mechanisms

A. Dissolution Mechanisms

A.1 Film-rupture
Crack propagates by local dissolution of metal at crack tip due to prevention of passivation there by plastic deformation.

A.2 Stress-accelerated dissolution
Crack propagates by localized anodic dissolution. Principal role of plastic deformation is to accelerate the dissolution process.

B. Mechanical Mechanisms

B.1 Hydrogen embrittlement
Hydrogen accumulates within metal in the crack-tip region, leading to localized weakening either by void formation or lowering of cohesive strength. Crack propagates by mechanical fracture of weakened region.

B.2 Adsorption
Surface-active species adsorb and interact with strained bonds at the crack tip, causing reduction in bond strength and leading to crack propagation.

C. Mixed Mechanisms

C.1 Brittle film
Crack propagates by repeated formation and rupture of a brittle film which grows into metal at crack tip.

C.2 Tunnel model
Crack propagates by formation of deep pits or tunnels via dissolution followed by linking of these pits or tunnels by ductile rupture.

The cause of hydrogen brittleness remains obscure. It appears that the interaction between hydrogen and the host material leads to a reduction in cohesive strength, either at an external surface or an internal interface or in a small volume. An alternate possibility is that void formation and growth are catalyzed by hydrogen. However, the embrittlement observed in low-pressure hydrogen gas is strong evidence against a crack-growth mechanism that depends on high-pressure hydrogen precipitating in internal voids. Whatever the mechanism, the brittleness occurs in a localized region and cannot be described as a bulk effect; the brittle crack propagates by mechanical fracture of the weakened region. In some stress-corrosion systems at least, the hydrogen must be generated by reaction between the metal and its environment, and the quantity of hydrogen available may then be controlled by dissolution processes. Consequently, dissolution may play a direct role even in mechanical SCC mechanisms.

The adsorption concept suggests that surface-active species are adsorbed and interact with strained atomic bonds at the tip of a stressed crack, resulting in reduction of the atomic-bond strength across the crack tip. This again is a localized process, and the brittle crack is visualized to propagate through the weakened atomic bonds. If hydrogen acts as a surface-active specie in this sense, then hydrogen brittleness (B.1) can be included in the adsorption subset (B.2). However, it is not yet clear whether hydrogen exerts its influence exter-

nally or internally, and it seems advisable to distinguish between the B.1 and B.2 cases for the time being.

In the category of mixed mechanisms, two unit processes are thought to be necessary, the first involving the formation of a brittle or weakened corrosion product at the crack tip, and the second involving the mechanical fracture of this product. Such phases may consist of oxides (e.g., Cu_2O in the brass/ammonia system[4]) or regions of corrosion sponge formed by the loss of one of the alloying elements (e.g., the gold-rich sponge formed in nickel-gold alloys exposed to ferric chloride[5]). Both the formation of the Cu_2O and the gold-rich sponge are thought to involve dissolution, whereas the crack actually advances by the mechanical rupture of these corrosion products. It is difficult to separate the processes in terms of importance, inasmuch as both appear to be necessary in the total stress-corrosion phenomenon.

We now apply these SCC concepts to various types of engineering materials: high-strength steels, aluminum alloys, titanium alloys, stainless steels, glass and ceramics.

High-strength steels are very sensitive to environment-induced cracking under certain circumstances. The yield strength threshold for general susceptibility is around 180,000 to 200,000 psi, and water is the most common component in the aggressive environments. With lower yield strengths, there is relatively little incidence of SCC in simple aqueous environments, but at higher strength levels the problem can become epidemic unless

appropriate measures are taken. Fracture-mechanics techniques are most useful in characterizing this SCC system, since crack propagation, rather than initiation, seems to be the dominant feature in practical situations. Analysis of service failures show that the water-accelerated fracture crack tends to emanate from a prior flaw, such as a pre-existent crack or a localized brittle structure resulting from unsatisfactory welding.

Only two SCC mechanisms are presently considered as serious explanations of the water-induced cracking process: localized anodic dissolution and hydrogen brittleness. It has been known for many years, although perhaps not widely appreciated in stress-corrosion circles, that a steel membrane with water at one surface can emit hydrogen at the other surface. This presumably results from an interaction between the steel and the water, with hydrogen as a reaction product. A portion of the hydrogen bubbles off as gas; the remainder is free to adsorb and enter the steel where, because of its very high diffusivity, the hydrogen will shortly appear at the output surface.

Relatively few experimental techniques are available to differentiate between the dissolution and embrittlement mechanisms. Fractography has been helpful in that analysis of fracture surfaces has revealed no distinction between those fractures known to be produced by hydrogen brittleness and those which result from SCC in aqueous environments. However, such evidence can scarcely be considered definitive.

A second and potentially more discriminating approach has been to determine the influence of applied macroscopic potentials upon the SCC kinetics as expressed by, say, the time to failure. It is frequently found that increasing the cathodic potential will shorten the time to failure, indicating an acceleration of the fracturing process. It seems reasonable to attribute this SCC to a hydrogen-brittleness mechanism, since these are the conditions under which hydrogen brittleness is often deliberately caused. Special significance has been attached to results obtained under increasing anodic potentials, because these experiments also indicate a decreasing fracture time and, hence, an acceleration of the cracking process. In the past, this was often considered evidence of an anodic dissolution process, for it was not at all clear that hydrogen would be present at the tip of the crack under these conditions.

However, recent investigations suggest that hydrogen is, in fact, available at the crack tip even under bulk anodic potentials. Barth, Steigerwald, and Troiano[6] have used a permeation technique to ascertain the conditions under which hydrogen is discharged into a steel from an aqueous environment. Even under anodic potentials, they find that hydrogen does permeate through the steel if pitting is produced on the input surface. Hydrogen permeation is not observed in the absence of pitting. This suggests a close connection between the pitting (or dissolution) phenomenon and the availability of hydrogen to the steel in an aqueous environment.

This correlation has been clarified by the extensive studies of B. F. Brown, et al.[7-9] into the electrochemistry of aqueous solutions in cracks. From measurements of local pH and potential in the vicinity of a propagating crack, it was demonstrated conclusively that the electrochemistry of the aqueous solution at the tip of a crack is usually quite different from the bulk chemistry of the environment. The aqueous-solution chemistry in the vicinity of a crack tip always becomes sufficiently acidic to favor the breakdown of water and the reduction of H+ ions. This is so even when the bulk solutions are highly alkaline, or when the bulk specimen is at a substantial anodic potential. This acidification process of the solution in cracks is postulated to result from hydrolysis of dissolving metal ions.

The stress-corrosion cracks in high-strength steels in simple aqueous environments always seem to propagate under conditions where the solution chemistry at the crack tip is thermodynamically favorable for the discharge of hydrogen upon the surface of the crack tip. This is strong presumptive evidence that the mechanism of the cracking process is one of hydrogen brittleness, and there is at present no equally compelling experimental reason to envision any other mechanism. Here again, however, dissolution appears to play an important part in furnishing the necessary electrochemical conditions for generating the hydrogen.

From a practical standpoint, the problem of environmental cracking of high-strength steels remains troublesome. A typical threshold stress intensity for crack growth in aqueous environments corresponds to stresses of approximately 10-15% of the unaxial yield strength of the material. Failure times are short, ranging from a few minutes to a few hours. There have been substantial efforts to improve the environmental-cracking performance of high-strength steels by various thermal treatments, but with comparatively little success. It has been possible to devise procedures for increasing the failure time, but not in sufficient magnitude to be of practical benefit. No real progress has been achieved in raising the threshold stress intensity for crack growth, other than by lowering the yield strength of the steel. These conclusions stem from investigations such as those of Paxton, et al.[10,11] who explored the environmental-cracking behavior of maraging steels in aqueous environments after many types of thermal treatment, and of 4340 steel with ultrafine austenitic grain sizes. It was found possible to manipulate the failure time to some extent, but the threshold stress intensity for SCC remained discouragingly low.

Service problems in the stress-corrosion cracking of high-strength steels almost invariably involve crack growth from a pre-existing flaw, and so the current route to improvement in this system is one of eliminating flaws. In the absence of flaws, the susceptibility of high-strength steels to environmental cracking in aqueous environments can be much reduced.

With regard to the SCC of aluminum alloys, Pryor and Bothwell[12] concluded in 1969 that no strong evidence existed to favor either the hydrogen-embrittlement or brittle-film mechanisms. They noted, however, that the classical electrochemical mechanism of Dix, which in terms of Table I would be a dissolution mechanism, appeared to attract a large number of proponents. This still seems to be the general opinion today.

More recent studies on aluminum alloys have led to further insights into the SCC mechanisms, particularly in the case of the high-strength 7000 series. Speidel and co-workers[13] have demonstrated from an analysis of their crack velocity (V) vs. stress intensity (K) curves that different activation energies govern the propagation of cracks in the K-dependent and K-independent regimes of the V-K curves. Brown, et al.[14] have shown that the aqueous solution at the tip of a stress-corrosion crack exhibits a pH = $\sim$ 3.5, while Sedriks, et al.[15] found that this pH can be predicted from the solubility product of freshly precipitated aluminum hydroxide. These observations are consistent with a crack-propagation mechanism involving dissolution. Moreover, in the K-dependent regime, the reported activation energy of 20-30 kcal/mole is also consistent with a dissolution mechanism.

However, in the K-independent regime, the activation energy is only about 4 kcal/mole, which is considered much too

low for a dissolution process and which may be related to the mass transport of chemical species in the aqueous solution[13]. Thus, the low activation energy in the K-independent regime poses questions for further studies on the SCC mechanism under such conditions. This also happens to be where crack-branching is observed.

Titanium alloys exhibit both intergranular and transgranular modes of fracture, and there is now evidence to suggest that the intergranular type, which takes place primarily in halogen-containing organic liquids, can be categorized as stress-accelerated dissolution[16] (A.2 in Table I). On the other hand, the mechanism of the transgranular type of failure, which occurs in high-strength titanium alloys in many environments, is subject to continuing controversy. Powell and Scully[17] have proposed that transgranular failure results from an ingress of hydrogen into the metal at the crack tip. Beck[18], in contrast, considers that certain ions or species selectively attack the stressed metal atoms at the crack tip, leading to a cleavage process. Although Beck does not identify this mechanism as adsorption-induced embrittlement (i.e., B.2 in Table I), this seems to be a likely possibility. Dissolution would appear to be ruled out by the high velocities at which such cracks propagate. For example, Pugh, et al.[19] have noted that the observed propagation rates of transgranular cracks in a Ti-8-1-1 alloy exposed to aqueous halide solutions would require current densities at the crack tip of the order of 600 amperes/cm^2, if the cracking were to proceed by anodic dissolution.

Strong evidence against a hydrogen-embrittlement mechanism being operative in titanium alloys is that (a) failure does not occur in acidic fluoride solutions which are known to introduce hydrogen into titanium alloys[20], and (b) SCC does occur in purified carbon tetrachloride containing traces of water[14].

Concerning the mechanism of failure of titanium alloys in nitrogen tetroxide, two mechanisms have been proposed. Sedriks, et al.[21] have suggested, primarily on the basis of metallographic studies, that the brittle-film model is operative (i.e., C.1 in Table I), whereas more recently Moreland and Boyd[22] have proposed an electrochemical-dissolution mechanism (i.e., A.1 in Table I) involving the formation of a $TiO(NO_3)_2$ complex. However, definitive studies on the titanium/nitrogen tetroxide system are rendered difficult by the hazardous nature of this environment.

Understanding of the SCC mechanisms in austenitic stainless steels remains in an ambiguous state. There is perhaps no other alloy system where the observations are so complex and difficult to interpret. As a result, this aspect of the SCC problem is especially controversial. It is not feasible to summarize all the possible mechanisms and associated observations in this Summary Report. Comprehensive reviews from different viewpoints have appeared recently[23-25]; and so the emphasis here will be on matters of broad interest and argument.

Instances of SCC in nuclear-power systems[25] continue to emphasize the deleterious influence of chloride ions in aqueous

media. Although SCC in practical systems may occasionally occur in the absence of chloride ions, the latter is a causative agent in the overwhelming majority of failures. It is, therefore, disappointing that the role of chloride ions in the cracking process is poorly understood. It is often presumed that they somehow degrade a protective film. This degradation process is further considered to be heterogeneous and localized in the areas where cracks will appear. Clearly, a deeper understanding of the action of chloride ions in the SCC of stainless steels warrants further attention, and may even suggest a route to improved service performance.

The literature on SCC of austenitic steels leads to the inescapable conclusion that films are an essential consideration. Immunity to SCC can conceivably result from a tight and continuous film, while susceptibility to SCC can result from localized breakdown of the film (A.1 in Table I). Accordingly, the circumstances surrounding film formation, its general and localized destruction, and film reformation on austenitic stainless steels should be explored in detail.

In this connection, Staehle[26] has advanced the intriguing concept that SCC susceptibility may perhaps be deduced from the potential vs. current-density curve for a particular alloy/environment system. The suggestion is that SCC is associated neither with full passivation nor with relatively rapid general dissolution, but rather with the transition regimes between these two conditions. Under such circumstances, the protective film is presumably meta-

stable, and passivation may be destroyed locally by deleterious factors such as chloride ions, emerging dislocations, etc. It would be highly desirable to establish whether or not this concept is generally applicable.

The localized destruction of passivating films due to emerging slip steps is an essential feature of the slip/dissolution mechanism (A.1 in Table I) for SCC in austenitic stainless steels[24]. The film-free area produced at the slip step is thought to be the site of intense dissolution of the underlying metal. Obviously, the repassivation kinetics are an important feature of this mechanism. The walls of the advancing fissure are assumed to be repassivated by film formation, with the sequences of slip-step formation and metal dissolution being repeated over and over at the fissure tip.

A major difficulty with this model for the SCC of stainless steels is that fractographic analyses of the crack surfaces often show no evidence of dissolution or chemical activity. Instead, the visual appearance of the surface seems to be quite compatible with crack propagation by mechanical processes. It may be that the dissolution event occurs on too fine a scale to be detected by current techniques; in any event, this observation is perhaps the primary obstacle to the proposed slip/dissolution model.

Substantial controversy also centers upon the question of whether or not hydrogen is a key agent in SCC of austenitic stainless steels in aqueous media. It has been generally held that

austenitic stainless steels are immune to hydrogen brittleness, and that there is no evident way in which aqueous media could generate hydrogen at the crack tip. However, recent experiments have refuted these objections. It has been shown that:

(a) copious hydrogen gas can be evolved near the tips of propagating stress-corrosion cracks[23];

(b) the aqueous solution becomes highly acid, with a pH of approximately unity, in the crack-tip vicinity, independent of the bulk solution chemistry[23,24];

(c) hydrogen brittleness occurs in 310 stainless steel after cathodic charging[27]; although the hydrogen concentrations required are much higher than for ferritic steels; and

(d) hydrogen permeation through 310 steel takes place under anodic polarization[28].

The first two observations demonstrate unambiguously that hydrogen is present at the tips of propagating stress-corrosion cracks in austenitic stainless steels, although the concentration is certainly controlled by the metal-dissolution reaction. Much more work is required to fill out the picture suggested by the last two observations, but they do suggest the conceptual feasibility of hydrogen brittleness as a cracking mechanism.

In summary, three major and somewhat interrelated topics have been identified as important for future research on the SCC of austenitic stainless steels:

(a) role of chloride ions;

(b) all aspects of film formation, destruction, and reformation; and

(c) role of hydrogen.

Resolution of these three controversial areas would establish scientific understanding and perhaps point new ways to improved service performance.

In comparison with metals and alloys, the environment-sensitive mechanical behavior of glass and ceramic materials has received relatively little attention. The state of knowledge in this area has been recently reviewed by Westwood and Latanision[29]. Three categories of fracture behavior are defined for glass: (a) those dependent on adsorption-induced reduction in the surface-free energy[30], (b) those in which the presence of water is critical, leading to stress-enhanced corrosion[31]; and (c) those which depend on adsorption-induced variations in the flow properties of the near-surface regions.

In discussing these mechanisms, Westwood and Latanision[29] have argued that, since certain organic environments are more active than water in influencing fracture behavior, one should question explanations of environment-sensitive fracture behavior

which depend on the corrosive influence of water. At the same time, mechanisms based on adsorption-induced reduction in surface-free energy and variations in flow properties require further experimental verification. For example, very little is known about the actual mechanism of flow in glasses, and hence any mechanism proposed for the environment-sensitive flow or fracture of glasses can only be speculative in nature at this stage.

The effects of environment on the fracture of crystalline ceramics also demand critical study. Inasmuch as the hardness of ceramic solids can be significantly affected by the presence of surface-active species[29], their fracture processes would be expected to be environment-sensitive. The effect of environment on hardness, known as the "Rebinder effect," has been recognized for several decades, and has been ascribed to an adsorption-induced reduction in the surface free energy[32]. However, extensive studies by Westwood and co-workers[29] indicate that the environmental effect may be manifestation of adsorption-induced changes in flow processes in the near-surface regions. Specifically, Westwood suggests that adsorption of surface-active species will change the ease with which dislocations (a) can move and interact so as to initiate cracks, or (b) can be generated and move in the vicinity of crack tips, thereby influencing crack propagation.

4. Some New Elements of Understanding in SCC

4.1 Fracture Mechanics, Initiation Vs. Propagation

The greatly expanded use of high-performance systems has led to increased difficulties in the utilization of high-strength materials. Premature and low-stress failures have been encountered in high-strength structures even in relatively mild environments. As a result of an epidemic of failures in high-strength steels during the late 1950's, serious attention has been concentrated on the problem of predicting fracture performance of high-strength materials in aggressive environments.

In many instances, failures occurred with material/environment systems which were considered safe on the basis of testing procedures current at the time. These were mainly fracture-initiation tests. Examination of service failures in high-strength steels, however, showed that cracks almost invariably initiated from flaws present in the material. These were mechanical and/or metallurgical flaws or cracks arising from improper processing and fabrication. It was, therefore, essential to develop test procedures which focused on crack propagation.

It has now been amply demonstrated that test specimens designed on the basis of fracture mechanics offer an adequate method for measuring and interpreting environmental-cracking phenomena when crack propagation is the controlling feature. The validity of this approach is at present limited to high-strength and intermediate-strength materials, where the service

conditions are such that the plastic zone around the crack tip is a small fraction of the smallest dimension of the section; that is, the material is loaded in plane strain. The fracture-mechanics approach may be characterized as a "worst possible case." In static loading, it may be used to estimate the maximum load-carrying capacity of a high-strength material in a specified environment as a function of the stress-intensity parameter.

The stress-intensity parameter is an appropriate normalizing factor in the sense that it "normalizes out" the effects of specimen and load geometry. This means that the maximum stress intensity observed to be safe in laboratory testing may also be interpreted as the maximum stress intensity that a service component can carry under static load in the given environment. This threshold stress intensity, designated K_{Iscc}, is an important measure of the resistance to environmental cracking. Unfortunately, the various mechanisms which proport to explain environmental cracking have not yet been developed in sufficiently quantitative fashion to enable prediction or even understanding of the observed K_{Iscc} values. This knowledge-gap should be a major item on the agenda of future work.

In addition to providing a parameter which may be correlated with service applications, fracture mechanics also allows quantitative measurement of the crack-growth rate as a function of environmental and material variables. Crack-growth rates are of considerable assistance in attempting to determine the mecha-

nisms responsible for environmental cracking. With the use of conventional smooth-section specimens, the study of crack-growth kinetics would be a difficult and uncertain business because of crack-initiation and multiple-crack problems.

It should be emphasized that the fracture-mechanics approach is one of measuring crack propagation from a prior flaw. If crack propagation is not operative for most of the service life, then estimates of time-to-failure in SCC based on fracture-mechanics testing may not be realistic. This situation will arise in smooth-section applications where the failure crack often originates at a pit in the surface of the material. In that case, the majority of the service life may be consumed by the formation and growth of the pit, rather than by the kinetics of crack propagation. The transition from a pit to a crack is not well understood.

Film formation and reformation may be key factors in the relative importance of crack initiation vs. propagation in SCC. This is evident from experience with titanium alloys in both laboratory and service tests. SCC susceptibility is not observed in the testing of smooth sections of titanium alloys in aqueous media. With a pre-cracked specimen, however, if the stress is applied when the flaw is in the presence of an aqueous environment, then considerable susceptibility to environmental cracking may be observed. On the other hand, if the environmental exposure comes after the stress is applied, then there may be sufficient time for a protective film to reform on the surface of the crack

before the aggressive exposure. Under these circumstances, a much reduced susceptibility to environmental cracking is observed. The latter case seems to correspond to service experience in which film reformation often occurs at the tips of flaws or crevices, thus limiting the susceptibility to environmental cracking. As a result, titanium alloys have a better record in service than they do in the laboratory testing of SCC with fracture-mechanics specimens.

4.2 Stress-Corrosion Cracking Regimes

An interesting correlation between crack-growth rate (V) and stress intensity (K) is evident from environmental-cracking experiments:

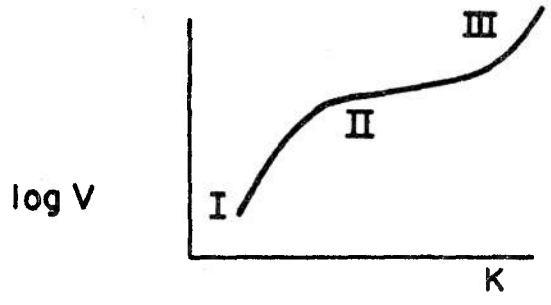

V-K curves of this characteristic shape have been observed for a wide variety of material/environment systems, including steels, titanium and aluminum alloys, and glass. However, not all material/environment systems necessarily exhibit all three regimes.

The essential point is that three regimes of crack propagation may be identified, with the attendant possibility that a different mechanism is operative in each regime. Environmental parameters, e.g., temperature and solution chemistry, are often observed to have different effects in the three regimes. In some instances, regime II is associated with crack branching, and this may represent a quasi-steady-state situation in which reaction with the environment occurs just fast enough to keep up with the propagating crack.

In some instances, notably with steels and titanium alloys, regime I becomes vertical at sufficiently low stress intensities, suggesting the existence of a true threshold for environmental crack extension (K_{Iscc}). Further, in the case of steels, crack-growth rates cannot be manipulated over orders of magnitude by variations in composition, heat treatment or environmental parameters.

For aluminum alloys, the existing data do not indicate a true threshold stress intensity; rather, the curve in regime I simply becomes steeper at low stress intensities but does not appear to approach a true vertical asymptote. Thus, growth rates may be controlled over many orders of magnitude by appropriate variations in composition, processing and heat treatment schedules for the aluminum-base materials. Safe performance may be attained by this approach, even though a threshold stress intensity is not observed.

4.3 Crack-Tip Chemistry; Pourbaix Diagrams

It is now realized that the local chemistry within a crevice, corrosion pit, or growing crack will often be quite different from that of the bulk environment. There is reduced circulation in such restricted regions, and corrosion products tend to seal off the occluded area from the bulk environment.

From the work of B.F. Brown and his collaborators[8,14], one can conclude that, for a wide range of alloy compositions and microstructures, the electrochemical conditions in an occluded corrosion cell shift toward a steady state in which there is a driving force for the reduction of hydrogen ions. As previously mentioned, this has been determined from measurements of local pH and potential in aqueous solutions near the tip of a growing crack. For example, with high-strength steels, even in highly alkaline bulk environments, the solution at the crack tip invariably becomes acidic at a pH value of about 3, and the local potential becomes favorable for the reduction of hydrogen ions. Similar situations prevail for aluminum alloys, magnesium alloys, and titanium alloys, and most likely result from the hydrolysis of metal ions.

In the light of the above findings, interest has been further increased in hydrogen as a potential embrittling agent in many alloy systems, even under bulk environmental conditions which would otherwise appear unfavorable for the production of hydrogen. Under an overall anodic potential, a hydrogen-induced

failure crack in a smooth section must presumably originate at a pit, inasmuch as restricted geometry is required for the acidification process and allows the local electrochemistry to become favorable for the generation of hydrogen.

There are still many unanswered questions regarding the electrochemistry of an occluded corrosion cell. For example, will the same experimental results be obtained for cracks growing in cyclic loading as for cracks growing in static loading? One also wonders whether the crack-tip chemistry is a significant factor in the SCC of stainless steels. Furthermore, a wider range of chemical parameters in the bulk enviroment (including dissolved oxygen) should be explored in relation to the electrochemical conditions arising in the occluded corrosion cell.

The Pourbaix diagram[14] is most helpful in interpreting corrosion and SCC phenomena in aqueous media. This type of diagram is the electrochemical analog to a phase diagram, and as such, it summarizes the thermodynamic characteristics of the environment/material system in graphical and compact form.

The information is presented as a plot of potential vs. pH, where the lines on the diagram indicate the various chemical equilibria involved. When suitable criteria have been adopted, it becomes possible to delineate those regions in the Pourbaix diagram which correspond to environmental-cracking susceptibility, and those which are regions of immunity.

Although Pourbaix diagrams are now available for a number of metals in relatively pure aqueous media at room temperature, it is hoped that they will eventually be developed for aqueous media containing specific ions, such as chloride and sulphide ions. Theoretical and experimental work on the effect of temperature would also be of interest. The continued accumulation of thermodynamic information in this compact form will provide an invaluable compendium of data for the corrosion analyst of the future. Of course, it goes without saying that such diagrams are based on equilibria rather than on kinetics.

Sedriks, et al.[15] have recently suggested that in certain cases, particularly with aluminum and magnesium alloy systems in salt solutions, the composition of the solution at the crack tip may be deduced from the solubility product of the least soluble corrosion product. This may be a promising approach to prediction of crack-tip chemistry from equilibrium electrochemistry.

4.4 Borderline Passivity Vs. SCC Susceptibility

It has been suggested[1,2,26] that in certain alloy/environment systems, the conditions required to produce susceptibility to SCC correspond to the borderline between active and passive behavior. It is assumed that a passive film forms and is then ruptured at the crack tip by plastic deformation, enabling localized anodic dissolution to occur (A.1 in Table I); the (nondeforming) crack walls are thought to remain passive and as cathodes.

On the basis of this mechanism, some association is to be expected between the onset of passivity at the crack tip and susceptibility to SCC.

An example of the correlation between borderline passivity and the initiation of SCC in Fe-Cr-Ni alloys is reported by Staehle[24], who found that SCC occurs in the potential-current regimes represented by either the onset of passivity or the onset of transpassive behavior. Another example of the correlation between borderline passivity and the propagation of stress-corrosion is provided by the Al-Zn-Mg alloy/aqueous chloride system[15]. Here, the composition of the solution at the crack tips in these alloys appears to be determined by the onset of aluminum hydroxide precipitation; this implies that, close to the crack tip, equilibrium is approached between dissolving aluminum ions and aluminum hydroxide, and is one in which borderline conditions exist. Thus, a viewpoint is emerging that it may become possible to define the environmental regimes of susceptibility in terms of the conditions which correspond to borderline passivity.

4.5 Co-Planar Slip Vs. Easy Cross-Slip; Slip Bands Vs. Distributed-Slip

Interest in correlations between the deformation characteristics of metals and alloys and their stress-corrosion susceptibility arose from attempts to explain the relative immunity from stress-corrosion of certain "pure" metals. In addition, the

transitions from intergranular to transgranular cracking in susceptible alloys have also been related to the mechanical behavior. Much of these considerations have been in terms of the film-rupture mechanism of failure (A.1 in Table I) particularly since surface films are more likely to be ruptured by coarse than by fine slip. The height of slip steps in pure metals and dilute alloys is small, and therefore film rupture is less probable. Correspondingly, alloys of low stacking-fault energy or in which ordering exists exhibit coarse slip, and so film rupture should be more prevalent in these materials.

On the basis of the above argument, a correlation should be manifest between susceptibility to transgranular SCC and the occurrence of coarse slip (i.e., the formation of planar dislocation arrays). This seems to be the case for brasses in non-tarnishing aqueous ammonia solutions[19] and for titanium alloys in aqueous-chloride[33] and methanol[16] solutions. For example, in titanium-aluminum alloys, increasing the aluminum content to >5 w/o restricts cross-slip[33], enhances co-planar slip, and introduces susceptibility to transgranular cracking[16].

While the generality of these correlations between deformation behavior (co-planar slip or discrete slip bands vs. well-distributed slip) and SCC characteristics has not been established, such relationships may ultimately prove to be a valuable interpretive aid, especially in cases where film-rupture mechanisms are operative.

4.6 Relation of Metallurgical Structure to SCC

There are very few well-delineated relationships between metallurgical structure and SCC. Even the conditions which control transgranular vs. intergranular crack propagation are not yet clearly defined. As indicated above (Section 4.5), co-planar slip tends to favor transgranular SCC. In fact, coarse slip seems to be more detrimental than distributed slip in promoting both transgranular and intergranular SCC.

Although impurity precipitates at grain boundaries are considered to be undesirable, their behavior with respect to SCC is not clear-cut. Perhaps it depends on their electrochemical action and on the way they impede slip transfer across grain boundaries.

There is evidence, at least in precipitation-hardened aluminum-base alloys, that an overaged state is less susceptible to SCC than that corresponding to peak hardness.

In high-strength steels, the refinement of grain size may retard environmentally-induced crack propagation to some extent, but it does not raise K_{Iscc}. Thusfar, even ultrafine-grain refinement holds little promise as a practical solution.

The most general rule, however qualitative and unattractive, is that improved resistance to SCC can often be gained by sacrificing the strength level of the alloy being tested.

5. Some Important Issues

5.1 Role of Hydrogen

The idea that hydrogen is a causative agent in stress-corrosion cracking in aqueous media is currently under much debate. Interest in this concept has intensified following the demonstration that the aqueous-solution chemistry at a crack tip may differ substantially from that of the bulk solution, and in a direction so as to favor the discharge of hydrogen. This has been shown for steels and for alloys of titanium, aluminum, and magnesium. Furthermore, copious hydrogen gas evolution from the tip region of propagating stress-corrosion cracks has been observed. Clearly, then, the crack-tip material is exposed to hydrogen during crack propagation.

This does not prove that hydrogen is the agent responsible for SCC, but it does suggest a possibility which cannot be dismissed. The amount of hydrogen produced is controlled by the metal-dissolution reaction, and hence it may be exceedingly difficult to distinguish mechanisms based upon metal dissolution and hydrogen embrittlement. Measurement of the temperature-dependence of crack-propagation parameters might be discriminating. Fractographic evidence in most systems at present indicates a mechanical mode of crack propagation, which is compatible with a hydrogen-brittleness mechanism.

Unfortunately, there is no atomistic mechanism of hydrogen brittleness that commands general agreement. The mechanism

is probably not better understood than it was many years ago. Several observations suggest that hydrogen brittleness is localized, but controversy still exists over whether the local site is at the surface, or at an internal interface, or within the bulk metal. It appears that the brittleness induced by hydrogen may be of external or internal origin.

Crack propagation in low-pressure hydrogen gas is not compatible with a pressure (void formation) mechanism, and this has focussed attention on the hypothesis that hydrogen may decrease the cohesive strength relative to the shear strength by weakening atomic bonds, either at an interface or in the bulk. Gilman presented some novel ideas along these lines at this Conference (see Paper XII). An experimental technique independent of cracking observation and capable of assessing the influence of hydrogen upon the cohesion of a strained solid would be most welcome, indeed.

It is also interesting to note a phenomological analogy to hydrogen brittleness in the area of field-ion microscopy. Here, the addition of hydrogen to the environment lowers the electric field at which evaporation of atoms from the filament tip will occur. The presence of very minute quantities of hydrogen in the system probably decreases the cohesion of the surface layer of atoms with the bulk material underneath, conceivably by the formation of hydride-like compounds. It is not known, however, whether this analogy between hydrogen-promoted evaporation

under a strong electric field and the brittleness induced by hydrogen in a high mechanical-stress field is physically real.

5.2 Role of Stress in Pit Formation; Pit/Crack Transition

The pitting process in halide solutions can be divided into an initiation stage and a propagation stage. We shall consider the latter first. The propagation stage may be described as follows: The dissolution of metal within the pit produces an excess of positive ions. As a result, the negatively charged chloride ions concentrate within the pit. There is also a local increase in the concentration of hydrogen ions due to the hydrolysis of metal ions. Both the increased acidity and concentration of chloride ions further stimulate the dissolution of the metal ions. The pit propagation process is, therefore, self-sustaining, and does not require the presence of stress.

If the pit is growing in a stress field, plastic deformation can occur at the base of the pit, and some acceleration of dissolution may be expected due to an increase in the number of active sites at the tip. The stress-assisted pitting process is the basis of the stress-accelerated corrosion mechanism (A.2) of SCC shown in Table I. Intuitively, one might assume that the pit/crack transition would occur at the stage at which yielding commences (or reaches some critical stage) at the base of the pit. However, it is known that metal/environment systems in which pitting occurs do not necessarily exhibit SCC. The problem of pit/SCC transitions warrants much more study.

The initiation process for pitting remains a matter of dispute. While some consider that pits originate randomly on the surface, others favor the view that they form at surface defects. Plastic deformation leading to slip-step emergence at the surface along with the rupture of a protecting film would be expected to increase the number of pitting sites.

Qualitatively, then, localized plastic deformation is believed to increase both the initiation-probability and growth-rate of pitting, but the critical details remain obscure, as is also the case for pit/SCC transitions.

5.3 Local Stress-Strain Conditions at a Crack Tip

We have seen that fracture-mechanics concepts are useful in characterizing environmental-cracking systems when crack propagation is dominant. The central parameter in this approach is the stress-intensity factor, a quantitative measure of the locally-elevated elastic stress field in the vicinity of a crack tip. However, this parameter provides no direct information on the local stress-strain behavior in the plastic zone at the crack tip, and it is the plastically-deforming material which interacts with the environment.

To describe the environmental interactions at a crack tip more accurately, it is necessary to develop some understanding of the stress-strain state within the plastic zone and at the interface between the material and the environment. New ideas are needed as to how this should be done. Possibly, a

continuum approximation involving plasticity theory will prove to be sufficiently discriminating for practical approximations. Another point of view is that the critical events are occurring on such a small scale that it will be necessary to develop a discrete lattice approach to this particular problem (see Paper IV by Thomson and Hirth at this Conference). Such calculations will surely be difficult to develop on a realistic basis, in view of the heterogeneous microstructure of many SCC-susceptible alloys. In any event, the lack of quantitative description of the plastic zone stands as a major barrier to the scientific understanding of the environmental cracking.

5.4 Control of Fracture Paths; Transgranular Vs. Intergranular Cracks; Single Vs. Branching Cracks

As indicated in Section 4.5, there appears to be some correlation between changes in fracture path from intergranular to transgranular when the deformation behavior changes from generally-distributed slip to co-planar slip for certain alloy/environment systems. Nevertheless, there are instances in which the intergranular/transgranular transition can be accomplished simply by altering the environment. For example, Bush has reported that with sensitized stainless steels, varying the pH will change the crack path (see Paper IX of this Conference). At pH = 5, cracking is transgranular; at pH = 4.5, it is mixed; and at pH = 3.0 - 3.5, it is often intergranular. Bush also notes that the stress level can shift these values.

There is little agreement on what governs such environmentally-induced transitions in a crack path in stainless steels. Available explanations remain unsubstantiated, and we shall not enumerate them here. An important gap in knowledge is the aqueous-solution chemistry at the tips of stress-corrosion cracks in stainless steels, such as has already been obtained for high-strength steels, aluminum, titanium and magnesium alloys[14]. It is desirable to know whether there are any differences in solution chemistry at the crack tips between transgranular and intergranular cracks.

There is equally little fundamental understanding regarding the metallurgical and environmental factors governing crack branching. In their studies of high-strength aluminum alloys, Hyatt and Speidel[13] have found certain conditions under which branching occurs. They have established that cracks will branch in alloys which exhibit equiaxed grain structures, but only during propagation in the K-independent part of the crack-velocity (V) vs. stress-intensity (K) regime. Hence, a correlation for the onset of branching exists only relative to the V-K curve, and not in terms of environmental or metallurgical variables. Staehle[26] has pointed out that the tendency toward crack branching is greater in the more ductile materials, such as copper alloys and stainless steels.

5.5 Question of Environmental Specificity; Trends Relative to Strength Level

Much emphasis has been placed on the specificity of environments in causing SCC. However, with the development of higher-strength alloys, the environments capable of inducing SCC have multiplied. A striking example is given by Sandoz[34] who tested a high-strength Ti-8Al-8Mo-1V alloy in salt water and most alcohols and alkanes. He found that all of the environments examined caused crack propagation at stress intensities below that required to produce fracture in dry air.

The specificity idea may still be valid for low-strength materials. However, even in the case of alpha brass, which at one stage was thought to crack only in ammoniacal environments, the number of SCC-inducing environments has now increased to include citrate and tartrate solutions[35].

In considering the SCC of high-strength steels, Phelps[36] has attempted to correlate the susceptibility with yield strength. He was able to distinguish between chloride-induced and H_2S-induced types of failure: the "threshold" for chloride-cracking came at a yield strength of 180,000 psi, and for hydrogen-sulphide-cracking at a yield strength of only 115,000 psi. Accordingly, in this comparison, the chloride environment was less aggressive relative to SCC than the H_2S environment, and so tolerated a higher strength level in the steel.

5.6 Mechanisms of Liquid-Metal Embrittlement

The important issues concerning liquid-metal embrittlement are well defined in the accompanying paper by Westwood and Latanision. They argue that, since the influence of any charged adsorbate is likely to be screened out (in metals) within a distance of a few atomic diameters from the surface, one would not expect the macroscopic tensile or flow properties to be affected by adsorbed liquid metal. Consequently, they favor a failure mechanism based on the weakening of strained atomic bonds at the crack tip.

While such short-range adsorption effects can provide some rationalization of liquid-metal embrittlement, the details of the failure mechanism remain in doubt. A deeper understanding of the nature of electronic interactions at the solid-metal/liquid-metal interface should prove helpful in this connection.

5.7 Nature of Available Models; Quantification; Questions of Predictability

Although many of the models or mechanisms of environmentally-induced failure are subject to continuing argument, nevertheless a valuable body of knowledge has accumulated, both from fundamental and parametric studies. However, the quantitative aspects of available theories are, at best, limited to hindsight explanations or to very narrow conditions. The problem is further confused by the competitive SCC failure mechanisms at play, ranging from hydrogen embrittlement to stress-assisted dissolution.

In general, the operative mechanisms cannot be predicted, let alone their kinetics.

At the present stage, one must conclude that reliable guidelines for materials selection against environmental failures have to be derived from experiment and experience rather than from basic understanding. Furthermore, the gap is still very large.

5.8 Static vs. Cyclic Loading

A major limitation of the critical threshold stress intensity (K_{Iscc}) for crack growth in an aggressive environment is that it is essentially a static-loading parameter. Although the evidence is limited, it appears that the static K_{Iscc} value is of little relevance in situations involving dynamic or cyclic loading. In fact, environment-accelerated crack growth has been observed in cyclic loading at stress intensities well below the threshold for static crack growth. In addition, environmental crack growth under cyclic loading is strongly sensitive to the loading frequency, as would be anticipated for any process involving interaction with the environment.

In some structures, particularly in aerospace and military applications, environment-accelerated fatigue cracking may well be the life-limiting phenomenon. In spite of this rather serious circumstance, there is a sobering scarcity of experimental data which can be used to analyze the situation. This should be a key

area for future experimental attention.

5.9 Direct-Measurement Techniques

A discouraging aspect of many SCC models is that they are essentially after-the-fact rationalizations of stress-corrosion cracking observations. Although the concepts may sound elegant, in many instances they do little more than redescribe experimental results, and do not contain either predictive capacity or failure-prevention assurance. There is pressing need for independent measurement or analytical techniques which can characterize SCC systems without producing cracking. This is particularly important for those models which envision adsorption upon the surface as weakening atomic bonds, or which postulate deleterious effects of hydrogen on the cohesion of some materials. These ideas would be much more convincing if the adsorption or the alleged weakening could be demonstrated by independent methods which are not cracking experiments in themselves. It would also help eliminate the redundant nature of certain current models, and thereby allow independent evaluation of the physical concepts in the operative mechanisms.

5.10 Long-Range and Parametric Research in SCC

To date, basic research on SCC has opened up the possibility of several operative mechanisms, but for the most part, this thrust has not led to reliable guidelines for material de-

velopment or for anticipating failures. As a case in point, if the uncertainty about the way in which hydrogen exerts harmful effects in the SCC of high-strength steel were to be settled, this would still not tell us what to do about it for a practical solution.

Much of the fundamental work on SCC is in this vein. Perhaps such is the very nature of the problem, but it is beginning to look as though parametric research with systematic control over the experimental variables will be required well into the foreseeable future. It is likely that the latter approach may well have to point the way for basic research because of the many-sided nature of the SCC phenomenon. The longer-range studies will continue to make their contributions through clarification and understanding and stimulation, and can be justified on those grounds.

6. Education in the Field of SCC

There are presently two primary educational needs in the field of SCC:

(a) The current understanding and technological importance of SCC should be brought into the corrosion-teaching core in engineering curricula. To that end, an appropriate textbook on the subject would be highly desirable. We understand that B. F. Brown has this project well in hand.

(b) It is also urgent that design and operating engineers be made fully aware of the seriousness of SCC

and the available ways of coping with it. A handbook would seem like the most effective and realistic approach to meet that purpose, and we recommend that steps be taken in that direction.

7. Application of Fundamental Ideas to Engineering Problems in SCC

7.1 Stainless Steels

The object of the session on SCC of stainless steels was to define the extent of the current practical problems and to examine their solution. In particular, consideration was given (a) to what extent failures could be prevented by "designing around them," (b) to the more effective utilization of current knowledge, and (c) to the necessity of undertaking further research with a view to developing more stress-corrosion resistant materials. An approach utilizing current knowledge more effectively involves educational aspects, and these are dealt with in Section 6. Accordingly, this section will call attention to:

(a) Documented service failures in nuclear reactors.

(b) Future trends in materials selection for nuclear reactors.

(c) Current understanding of the mechanisms of SCC failures in stainless steels.

(d) General discussion.

(a) Documented Service Failures in Nuclear Reactors

A description of some eleven fully-documented

failures in nuclear reactors, together with corrective actions taken and lessons learned, was presented by S. H. Bush (see Paper IX of this Conference). The corrective actions included variations in material, heat treatment, stress level, and chemistry of the environment, as well as re-design of components to change flow patterns, reduce vibration, and prevent crevice conditions.

Bush also commented on the lessons learned from such failures and noted the effect on SCC of parameters such as sensitization, halogens, alkalinity, concentration effects, stress, neutron irradiation, cyclic loading, acidity, and pickling. The multiplicity of factors influencing stress-corrosion resistance was recognized, as were the difficulties associated with keeping a close check on these diverse variables in materials selection, reactor construction, and operation.

(b) Future Trends in Materials Selection for Nuclear Reactors

Bush also discussed possible alternates to the current nuclear technology which employs stainless steel:

(i) Utilization of stabilized grades of stainless steel.

(ii) Change toward alloys containing higher nickel and chromium contents.

(iii) Utilization of low-alloy steels in conjunction with close control of environmental chemistry.

The main foreseeable problem associated with (i) is the relatively poor welding characteristics of the stabilized grades of stainless steel. Hence, research and development leading to improved weldability of these materials would seem desirable.

Regarding (ii), there are two obvious disadvantages: (1) the higher cost associated with materials containing more nickel and chromium, and (2) the present lack of knowledge concerning their environment-sensitive mechanical behavior. The higher nickel-chromium alloys may find application in the Liquid Metal Fast Breeder Reactors, where the operation temperatures are high enough to sensitize the conventional grades of stainless steel. Further research into the environment-sensitive behavior

of the high nickel-chromium alloys was recommended.

Bush suggested that the use of lower-alloy steels, i.e. alternate (iii) above, is an approach that should be seriously considered for certain types of reactors. The idea here would be to use corrodable materials whose environmental reactions are controlled by closely adjusting the purity of the water. The primary advantage of this approach lies in the significantly lower cost of the low-alloy steels.

(c) Current Understanding of the Mechanisms of SCC Failures in Stainless Steels

As indicated in Section 3, the mechanisms of stress-corrosion failure in stainless steels are not well defined. Among mechanisms discussed during this session on stainless steel were (i) dissolution, (ii) hydrogen embrittlement, and (iii) martensite formation. In the dissolution mechanism, the crack advances by the dissolution of metal at slip steps, whereas in the hydrogen-embrittlement mechanism, the crack advances as a result of hydrogen adsorption or entry at the crack tip (Table I). The martensite hypothesis involves some entry of

hydrogen into the metal, thus causing an increase in M_d temperature*, and then a mechanical fracture of the martensitic region.

Staehle presented the case for the dissolution mechanism, Troiano for hydrogen embrittlement, and Paxton commented on the martensite mechanism. Staehle's and Troiano's arguments are covered in Papers III and XIII of this Conference. With reference to the martensitic mechanism, Paxton noted that the M_s temperature of 25Cr - 20Ni stainless steel is below the liquid-nitrogen temperature, and that the postulated M_d temperature* would have to be as high as ~150° C, which seems doubtful. He also pointed out that these low-carbon martensites are not necessarily brittle.

(d) General Discussion

In attempting to apply fundamental ideas to practical problems, Staehle proposed an explanation of the incidence of failures in BWR and PWR reactors in terms of potential-anodic current diagrams. He described the BWR reactor

*M_d is the temperature above which martensite cannot be formed by plastic deformation of the austenite.

environment as having an oxygen content of ~1 ppm and a pH = 6 to 7, and the PWR environment an oxygen content of ~0.001 ppm and a pH = 10. He suggested that these environments placed stainless steels in regimes exhibiting borderline passivity, with the PWR environment being near the passive-to-transpassive regime and the BWR near the active-to-passive regime.

The implication was that a generalized concept, based on correlating borderline passivity with the occurrence of SCC, might be developed in terms of potential-current diagrams. No serious objections were raised to this idea, although Bush questioned its applicability to failures encountered prior to start-up (i.e., during the construction of a reactor).

Paxton reported that, in the case of maraging steels containing a pre-crack, the lowest stress level at which SCC occurred (K_{Iscc}) was insensitive to structural changes. He also noted that variations in pH and potential affected the time taken for the cracking to commence but <u>not</u> the K_{Iscc} value. This indicated that the borderline-passivity concept was probably not applicable to maraging steels, even though it might

be valid for stainless steels.

Troiano stated that, in his view, hydrogen embrittlement could not be ruled out as the failure mechanism in stainless steels. In this connection, he mentioned that the ductility of K-monel and 25Cr - 20Ni steels can be reduced by charging these materials with hydrogen.

Some doubts were raised as to whether sufficient knowledge on failure mechanisms exist at the present time to contribute significantly to the solution of practical problems. It was generally felt that further study of factors affecting failures, including such variables as environment, temperature, residual stress, and cyclic loads, would be beneficial.

7.2 Aluminum and Titanium Alloys

The discussion in this session ranged over a very broad spectrum of topics, with emphasis upon the practical aspects of SCC failures in aluminum and titanium-alloy systems. Speidel first presented a summary of the characteristics of some 3,000 aerospace service failures due to SCC. The materials covered were high-strength steels, and alloys based on titanium, aluminum, and magnesium. A striking feature was the low incidence of stress-

corrosion failures with titanium alloys in non-exotic environments. The alloys in current use are apparently immune in aqueous environments. This contrasts with results obtained in the laboratory testing of pre-cracked specimens which show a substantial susceptibility in aqueous environments, at least for some alloys. The contradiction presumably reflects both the role of crack initiation versus crack propagation and the filming characteristics of titanium alloys. Fracture-mechanics tests are essentially propagation tests, but the service design and operating environments are evidently such that there is little opportunity for cracks to initiate, and therefore the propagation characteristics are not controlling. Presumably the filming properties of titanium alloys tend to protect any flaws present prior to the stress application.

This does not mean that SCC research on titanium alloys is unnecessary. Laboratory tests have shown a potential susceptibility to environment-enhanced propagation, which must be guarded against in material selection and component design. Nor is current understanding of SCC sufficiently secure to predict that new alloys under development and to be used in the future will display similar immunity to service failures.

The applications picture is more disturbing for high-strength aluminum alloys. There has been substantial incidence of SCC, mainly in the short-transverse direction of forgings and with an intergranular crack path. This difficulty does not seem

to exist with thin sheet. It appears that residual stresses arising from the fabrication processes are an important aspect of the aluminum-alloy problem. Another feature of aluminum alloys is that a threshold stress intensity for stress-corrosion crack propagation is not a definable parameter in the sense that SCC is observed at longer and longer times for lower and lower stress intensities; a true threshold in stress intensity has not been reached in laboratory testing.

In the discussion of these two alloy systems, it was interesting to find that rather little attention was directed to the current mechanisms of stress-corrosion cracking, perhaps because the discussers were not strong adversaries on the subject. It seemed to be generally agreed that current alloy development programs are largely semi-empirical in nature, and are not built upon any acceptance or rejection of the available SCC mechanisms.

There has been considerable success in developing new aluminum alloys with improved SCC resistance and only a minor loss in strength. These alloys have been evolved by semi-empirical procedures, in which systematic variations in purity and thermal treatment followed by laboratory stress-corrosion testing have been the guiding factors. This approach has resulted in lengthening the SCC failure times by a factor of approximately 10^7, thus guaranteeing satisfactory performance for many applications, even though the threshold stress intensity for crack growth remains low.

A similar viewpoint has been adopted in current programs to improve the SCC resistance of titanium alloys. It has been shown that crack growth tends to propagate on a crystallographic plane inclined at about 11° to the basal plane of the titanium unit cell. Efforts are currently underway to develop processing techniques which will so orient this plan as to resist SCC relative to the applied stress in sheet applications.

The semi-empirical approach is necessitated largely because current models of SCC are not expressed in quantitative form and hence lack predictive capability. This, in turn, reflects the fact that SCC phenomena are extremely complex and involve an intricate combination of metallurgical, chemical,and mechanical parameters. For this reason, improvements in SCC resistance are largely evolutionary, with alloy composition and processing methods advancing by incremental steps based on feedback from laboratory testing and service experience.

7.3 Silicon Nitride

In this part of the Conference, it was decided to examine a relatively new engineering material from the standpoint of potential difficulties with environmental degradation. The material thus selected was silicon nitride, which shows considerable promise for high-temperature applications in gas turbine engines for automobiles* and power plants*. As it happens, significant prog-

* We are indebted to representatives of the Ford Motor Company and Westinghouse Electric Company for background information concerning these developmental programs.

ress has been made along these lines with rather limited knowledge of the composition/processing/structure/property/performance relationships involved. In other words, the material and processing developments are coupled directly to the design and performance developments.

The silicon nitride parts to be discussed are ceramic bodies, prepared by hot pressing or reaction-bonding, which are quite brittle but which display noteworthy resistance to severe thermal shock in air or combustion atmospheres. Reaction-bonded specimens have survived thousands of cycles of flame-heating to 1400° C and air-blast quenching to room temperature with no appreciable deterioration in tensile strength, as determined by modulus-of-rupture bend tests. The thermal coefficient of expansion is only about 2.5×10^{-6} per °C. Some mechanical-property determinations have been made with respect to test temperature, and the strength seems to be essentially maintained up to the expected operating range of ~1400° C, without any evidence of macroplasticity. A few fracture-toughness (notched-specimen) measurements have been conducted at room temperature, and appear to show that control of the effective flaw size is still a critical problem in the processing. Studies of microstructure, phase relationships, processing variables, and physical properties are in a comparatively elementary state, as might be expected at this point. Moreover, the simultaneous role of stress and environment, which is so critical in numerous metallurgical applications, ap-

pears not to have been investigated with respect to silicon nitride. It is obvious, then, that silicon nitride is an ideal material for the purposes of the present exercise.

Discussion leaders at this session were Eldon Hermann of Ford Motor Company, Robert Katz of the Army Materials and Mechanics Research Center, and Michael Lindley of the British Admiralty Research Laboratory. It is intended that silicon nitride will be developed for gas-turbine stator vanes, combustion chambers, rotor blades, and even rotor shafts. Silicon nitride is much cheaper than the superalloys to be replaced in these applications, and the expected operating temperature of 1400°C far exceeds the ~900°C maximum level for superalloys.

Silicon nitride exists in two phases: α - $Si_{11.5}O_{0.5}N_{15}$ and β - Si_6N_8. The α modification is evidently a three-component phase based on $Si_{12}N_{16}$ with part of the silicon replaced by oxygen and part of the nitrogen by vacancies. Both types of silicon nitride have hexagonal unit cells, the α showing an ABCD stacking and the β an ABAB stacking. Little is known about the difference in properties between these two modifications of silicon nitride. There is some thought that a true polymorphic change is not involved, but that the β is converted to α merely because of oxygen contamination.

Hot-pressed silicon nitride (HPSN) is prepared from silicon nitride powder that is obtained by reacting $SiCl_4$ with ammonia gas or nitrogen. About 1% MgO may be added to the powder for lubrication and bonding purposes, and the subsequent hot pressing

is carried out isostatically or in graphite dies. A pressure/temperature/time sequence has been worked out to maximize the density (~3.2 gm/cm^3), minimize the porosity (<2%), minimize the grain size (0.3 - 0.4 μm), and minimize the pore size (2 - 5 μm). The final step in the hot pressing sequence is a hold at 1700° C for about 1/2 hour under a pressure of 4000 psi. The room-temperature modulus of rupture is then approximately 115 ksi.

Reaction-bonded silicon nitride (RBSN) starts with cold-pressed silicon powder having a particle size of 10 μm (mean) and 25 - 50 μm (maximum). An organic binder is mixed with the silicon powder to aid the cold pressing. After sintering for 24 hours in nitrogen at 1250° - 1350° C, the resulting compact is chalky and can be machined. The subsequent sintering is carried out at 1450 - 1480° C for 24 hours, this being above the melting point of silicon (1420° C). During the first firing, interlocking whiskers of α-silicon nitride form within the pores among the silicon particles, producing a skeleton or matte that helps bind the compact together. This stage is accompanied by a 5 - 10% gain in weight, but the external dimensions remain essentially unchanged. During the second firing, the metallic silicon melts, and further reaction with the nitrogen atmosphere produces both α- and β-silicon nitride, but the reaction does not go to completion. Moreover, the density achieved is only about 75% of theoretical and the modulus of rupture is only some 20 ksi. The pore size is about 20 μm, but judging from the mechanical properties, the effective flaw size seems to be at least 10 times larger.

It is not clear what determines this large effective flaw size, but clumps of grains may be involved. Embrittling films of SiO_2, or of other impurities, could be playing a part here.

The following paragraphs summarize many of the questions raised about silicon nitride as an engineering material and the suggestions offered to narrow the knowledge gap.

(a) Mechanical Behavior. There is need for systematic determinations of K_{Ic} as a function of temperature, time of holding, and micro-structural and processing variables. In this connection, the effects of environmental conditions should be brought into the picture. Thusfar, it appears that oxidizing and combustion atmosphere are not unduly harmful, but reducing atmospheres could be deleterious. The influence of cyclic stressing also demands attention. In these tests, the fractured surfaces should be examined carefully in an effort to determine what controls the effective flaw size and also the role played by the silicon nitride whiskers previously mentioned.

(b) Processing Studies. Clearly, there are many processing variables operative in both the hot-pressed and reaction-bonded silicon nitrides. Impurity effects (such as oxygen, iron, etc.) can be investigated by controlled additions to delineate their

correlation with the resulting nitriding and densification kinetics as well as with the generated microstructures and mechanical properties. The temperature/time cycles in the firing operations might be optimized to permit freer access of the nitrogen gas through the interconnecting channels between the particles. Inasmuch as SiO_2-glassy phases may coat the particles due to oxygen contamination, $N_2 + H_2$ mixtures might be considered for reacting with the silicon particles. Long-time sintering treatments may enhance the strength by rounding-off the pores.

(c) Surface Treatments. It was suggested that surface treatments might be applied to both HPSN and RBSN bodies as a final step in the processing. Diffusion barriers against environmental attack in service could be formed in this way. In fact, the inadvertent development of SiO_2 protective layers may contribute materially to the excellent oxidation resistance of silicon nitride. This further indicates the need to investigate the potentially harmful effects of reducing atmospheres. It is also conceivable that the formation of diffusion barriers could induce a favorable state of compressive stress in the surface layers.

(d) Phase Relationships. The equilibria existing between the α- and β-silicon nitrides as a function of the nitrogen and oxygen activities require elucidation. The resulting phase relationships would provide a fundamental baseline for understanding the conditions under which these phases occur.

(e) Nitriding of Bulk Silicon. Quantitative knowledge is lacking concerning the kinetics of surface reactions, diffusion and compound formation during the nitriding of silicon. Such phenomena can be studied on bulk specimens, and perhaps even on monocrystals and bicrystals. This would also provide an opportunity to see how the kinetics are affected by additions to the nitrogen atmosphere and by doping of the silicon nitride.

(f) Experimental Techniques. Many experimental methods, now quite common for metals, will require further development for application to silicon nitride bodies. This is particularly the case because of the complex and uncertain microstructures. Suitable etching reagents, electron microscopy, accoustical-emission testing, etc. should receive attention.

(g) Strength Calculations. It should be possible to model the pore structure of RBSN bodies to calculate the internal-notch and grain-size effects, and to estimate the potential benefits from altering the

structures. This would seem like a good system for applying the principles of elastic mechanics.

In attempting to assess the extent to which available knowledge on SCC phenomena can be of help in anticipating the premature failure of new engineering materials where service experience is still lacking, one can only call attention to the potential dangers of environmental degradation. This awareness can then lead to the formulation of intelligent test and research programs to investigate the controlling factors which may point the way to improve performance. However, predications based on what we know do not look realistic at the present time.

8. Prospects and Concluding Remarks

As yet, the principles of SCC do not provide a suitable basis for assessing the reliability of real material/environment systems. Actually, this is too much to expect, if one recalls how much remains unknown even about mechanical behavior in benign environments and about chemical behavior in the absence of stress. The interactive possibilities of the two sets of phenomena, each vast in itself, are truly prodigious. In the light of this complex situation, optimum progress will require a balanced program of fundamental (long-term) and parametric (more-oriented) research. This phase of the SCC problem might well receive due attention at the next meeting of the ARPA Materials Research Council.

Many areas for further research on SCC have come to light at this Conference. It might be a valuable exercise for the Council to attempt some placing of priorities among the various approaches to be taken. In any event, the idea of a handbook on SCC has received rather general endorsement among the participants and the way is now open for the Council to plan the content of such a handbook.

REFERENCES

1. F. A. Champion, "Symposium on Internal Stresses in Metals and Alloys," Institute of Metals, London (1948) 468.

2. H. L. Logan, J. Res. Nat. Bur. Stds. 48 (1952) 99.

3. T. P. Hoar, Fundamental Aspects of Stress-Corrosion Cracking (R. W. Staehle, A. J. Forty and D. van Rooyen, eds.) N.A.C.E., Houston (1969) 98.

4. E. N. Pugh, "The Mechanisms of Stress-Corrosion Cracking of Alpha-Brass in Aqueous Ammonia," paper presented at the NATO Conference on The Theory of Stress-Corrosion Cracking in Alloys, Ericeira, Portugal (March 1971).

5. P. R. Swann and W. R. Duff, Met. Trans 1 (1970) 69.

6. C. F. Barth, E. A. Steigerwald, and A. R. Troiano, "Hydrogen Permeability and Delayed Failure of Polarized Martensitic Steels," Corrosion 25 (1969) 353-358.

7. B. F. Brown, C. T. Fujii, and E. P. Dahlberg, "Methods of Studying the Solution Chemistry Within Stress Corrosion Cracks," J. Electrochem. Soc. 116 (1969) 218-219.

8. B. F. Brown, Final Technical Report, ARPA Coupling Program on Stress Corrosion Cracking, September 21, 1970.

9. J. A. Smith, M. H. Peterson, and B. F. Brown, "Electrochemical Conditions at the Tip of an Advancing Stress Corrosion Crack in AISI 4340 Steel," Corrosion 26 (1970) 539-542.

10. R. P. M. Proctor and H. W. Paxton, "The Effect of Prior Austenite Grain Size on the Stress Corrosion Susceptibility of AISI 4340 Steel," ASM Trans. Quart. 62 (1969) 989.

11. A. J. Stavros and H. W. Paxton, "Stress Corrosion Cracking Behavior of an 18% Ni Maraging Steel," Met. Trans. 1 (1970) 3049.

12. M. J. Pryor and M. R. Bothwell, "Fundamental Aspects of Stress-Corrosion Cracking (R. W. Staehle, A. J. Forty and D. van Rooyen, eds.) N.A.C.E., Houston, (1969) 465.

13. M. V. Hyatt and M. O. Speidel, ARPA Technical Report on the State-of-the-Art of Stress-Corrosion Cracking of High Strength Aluminum Alloys, to be published.

14. B. F. Brown, Final Technical Report on ARPA Coupling Program on Stress-Corrosion Cracking, NRL Report 7168, U.S. Naval Research Laboratory, Washington, D.C., 1970.

15. A. J. Sedriks, J. A. S. Green and D. L. Novak, Corrosion-NACE 27 (1971) 198.

16. A. J. Sedriks and J. A. S. Green, Jnl. of Metals, 23, No. 4 (1971) 48.

17. D. T. Powell and J. C. Scully, Corrosion-NACE, 24 (1968) 151.

18. T. R. Beck, Fundamental Aspects of Stress-Corrosion Cracking (R. W. Staehle, A. J. Forty and D. van Rooyen, eds.) NACE, Houston (1969) 607.

19. E. N. Pugh, J. A. S. Green and A. J. Sedriks, in Interfaces (R. C. Gifkins, ed.) Butterworths, London (1969) 237.

20. T. R. Beck, M. J. Blackburn and M. O. Speidel, Boeing Scientific Research Laboratories Quarterly Progress Report No. 11, NAS7-489, March 1969.

21. A. J. Sedriks, P. W. Slattery and E. N. Pugh, Fundamental Aspects of Stress-Corrosion Cracking (R. W. Staehle, A. J. Forty and D. van Rooyen, eds.) NACE, Houston (1969) 673.

22. P. J. Moreland and W. K. Boyd, Corrosion-NACE 26 (1970) 153.

23. N. A. Nielsen, 1970 Gillett Memorial Lecture, ASTM.

24. (a) R. Staehle, paper presented at Conference on Mechanistic Concepts of Stress Corrosion Cracking, sponsored by NATO, held in Portugal, March 1971.

    (b) R. M. Latanison and R. W. Staehle, Proceedings of Conference on Fundamental Aspects of Stress Corrosion Cracking, Ohio State University, 1967.

25. S. A. Bush, Stress Corrosion in Nuclear Systems, this Conference.

26. R. W. Staehle, document prepared for this Conference.

27. M. B. Whiteman and A. R. Troiano, Corrosion 21 (1965) 53.

28. J. H. Shively, R. F. Hehemann, and A. R. Troiano, Corrosion 23 (1967) 215.

29. A. R. C. Westwood and R. M. Latanision, Environment-Sensitive Machining Behavior of Non-metals, 2nd Technical Report to ONR, RIAS TR 70-10c, October 1970.

30. E. Orowan, Nature 154 (1944) 341.

31. R. J. Charles and W. B. Hillig, Symposium on Mechanical Strength of Glass and Ways of Improving It, Union Scientifique du Verre, Charleroi, Belgium (1962) 511.

32. P. A. Rebinder, Proc. Sixth Physics Conf., State Press, Moscow, USSR (1928) 29.

33. M. J. Blackburn and J. C. Williams, "Fundamental Aspects of Stress-Corrosion Cracking," (R. W. Staehle, A. J. Forty and D. van Rooyen, eds.), NACE, Houston (1969) 620.

34. G. Sandoz, "Fundamental Aspects of Corrosion Cracking," (R. W. Staehle, A. J. Forty and D. van Rooyen, eds.) NACE, Houston (1969) 684.

35. J. A. S. Green and E. N. Pugh, Met. Trans. 2 (1971) 1379.

36. E. H. Phelps, Proc. of Seventh World Petroleum Congress, Spottiswoode, Ballantyne and Co., London (1969) 201.

II. COMMENTS ON ADSORPTION-SENSITIVE CRACKING

by

A.R.C. Westwood and R.M. Latanision

1. Introduction

Some of the most fascinating examples of environment-sensitive fracture behavior are associated with the adsorption of surface-active species. Such phenomena include liquid-metal embrittlement (L-ME), complex-ion embrittlement, and various examples of Rebinder-type effects. At this time, the mechanisms of such phenomena are not understood in detail, although useful working hypotheses are being developed. One purpose of this paper is to draw attention to the apparently significant role of charge double-layers in adsorption-sensitive mechanical behavior. We will attempt to show that many examples of such behavior can be understood, at least conceptually, on the basis of considerations of the type, concentration, mobility, and adsorption-induced redistribution of the charge carriers in the solid. Some of the current controversies in this field of research will be indicated, and the fact that more sophisticated and definitive studies are needed will become evident.

2. Metals

2.1 Liquid-Metal Embrittlement

Metals contain a high concentration of highly mobile electrons. Consequently, the influence of any charged adsorbate is likely to be screened out within a distance of a few atomic diameters of the surface[1]. Knowing this, one might anticipate that the influence of adsorbed species on the mechanical behavior of metals is likely to be confined to phenomena related to true surface effects (as opposed to "near-surface" effects), e.g., phenomena strongly dependent on the surface free energy of the solid or the strength of bonds between surface atoms. Intuitively, therefore, one would not expect macroscopic tensile or flow properties to be affected, because these involve the movement of dislocations through the bulk of the solid.

On the other hand, it is possible that the motion of dislocations which intersect the surface can be influenced by adsorbates. For example, an edge dislocation in a metal may be considered to possess an electrical field, as pointed out earlier by Cottrell, et al.[2] in their considerations of interactions between dislocations and solutes. It is conceivable, therefore, that the mobility of near-surface edge dislocations could be influenced by adsorption-induced changes in the surface double layer, Figure 1(a). This could lead either to

enhanced mobility, or to reduced mobility ("adsorption-locking")[3]. Because of the highly restricted range of influence of adsorbates on metal surfaces, however, one would not expect that their presence would affect the ease of generating dislocations from sources situated, say, a micron or so from the surface, Figure 1(b), unless loops produced by that source produced surface steps.

This realization is useful in providing an interpretation of the tensile behavior of solid metals in liquid-metal environments[4,5] as follows: Consider the crack shown in Figure 2 and the possible influence of an adsorbed, surface-active liquid metal atom (B) at the crack tip $A\text{-}A_0$. For an embrittling species, it is assumed that the magnitude of the tensile fracture stress of the bond constituting the crack tip, σ, will be reduced[6,7]. However, because of conduction electron screening, it is considered unlikely that atom (B) can influence the strength of bonds across the slip-plane, S-P, for any sufficient distance from S to significantly affect the ease of operation of any nearby dislocation source, D. If so, then the shear stress, τ, to initiate slip on this plane should not be significantly affected by the precence of (B).

If the adsorption process leads to a reduction in σ, while τ is unaffected, then the ratio (σ/τ) will decrease. The effect of this, on the basis of arguments presented by a number of workers, including Kelly, et al.[8], will be an in-

creased tendency for the crack tip to propagate by cleavage rather than by ductile shear. In other words, liquid-metal embrittlement will result, and the severity of embrittlement will be related to the magnitude of the reduction in σ. It has been observed that an extremely active liquid metal can reduce the ratio of (σ/τ) of even a normally ductile, pure f.c.c. metal sufficiently to cause it to fail by cleavage. For example, Figure 3 shows the cleavage failure of a notched, 1 cm. diam., super-pure aluminum monocrystal exposed to liquid gallium. The cleavage surface was found to be predominantly $\{100\}$[4].

An alternative way of increasing the severity of liquid-metal embrittlement is to increase τ. This can be done by alloying the solid. Figure 4(a) shows the dramatic effect of alloying on the susceptibility of polycrystalline zinc to embrittlement by mercury[9]. Note that the fracture stress of zinc is reduced from 1.4 kg/mm^2 to 0.4 kg/mm^2. The association of this increase in susceptibility to embrittlement with increased yield stress, Figure 4(b) is quite apparent.

Alloying can also be used to counteract susceptibility, however. For example, silver is embrittled by gallium, whereas gold is not, and alloying silver with gold substantially inhibits its embrittlement by gallium, Figure 5[10].

One factor in L-ME which requires further attention is the variation in susceptibility to embrittlement with chemical composition of the liquid metal. A new approach to this prob-

lem, in which a potentially active metal is dissolved in an "inert-carrier" liquid metal of lowering melting point, has made it possible to evaluate the embrittlement behavior of a number of new systems, and to compare the influence of several elements effectively in the liquid state at the same temperature[5,11,12]. The need for such a technique arises because direct investigation of many potentially interesting solid metal-pure liquid metal couples is not feasible because, at the melting temperature of the pure liquid metal, the solid metal either is too ductile to maintain the stress concentrations necessary to initiate and propagate a brittle crack, or is excessively soluble in the liquid metal, resulting in crack blunting. Recent studies with liquid metal solutions indicate that L-ME is not as specific as had been previously thought. For example, polycrystalline pure aluminum is only slightly embrittled by mercury at room temperature, but additions of as little as 1-3 a/o of a number of elements to the mercury produce marked effects on the severity of embrittlement[5], Figure 6.

The severity of embrittlement by liquid metal solutions can also be extremely temperature sensitive[5,13,14]. Figure 7 illustrates, for example, the occurrence of brittle-to-ductile transitions in polycrystalline pure aluminum, the critical temperatures, T_c, for which are determined by the composition of the mercury-gallium solution environment. Similar effects have been observed for silver and brass[14].

It appears that previous analyses of apparently similar transitions occurring in bcc or hcp metals tested in inert environments are inappropriate for such environment-sensitive transitions because the assumptions on which they are based are not valid for the latter case. The assumptions are (i) that the temperature dependence of the yield stress is the controlling factor, and (ii) that T_c is the temperature at which the yield stress equals the fracture stress. For fcc metals such as aluminum, however, the yield stress decreases only slightly with temperature over the temperature range involved, and a significant amount of plastic deformation occurs before embrittlement results, even below T_c. Thus, the yield stress does not equal the fracture stress at any temperature of relevance to this work. An alternate possibility[14] is that such transitions are associated with the temperature-sensitive behavior of the ratio (σ/τ). T_c is considered to be the temperature at which (σ/τ) increases above some critical value. While τ is a relatively temperature-insensitive parameter, σ is temperature sensitive because adsorption (desorption) is a dynamic and thermally activated process.

While appreciation of the short range nature of the influence of adsorbed species on metals, and of the influence of adsorption on the ratio (σ/τ) can provide a useful rationalization of L-ME phenomena, the fundamental question of mechanism still remains unanswered. It is insufficient to say that the surface free energy of the solid is reduced--we need to know

how this is accomplished. Detailed work on the nature of electronic interactions at solid metal-liquid metal interfaces is required of the specificity if L-ME is to be explained. The possible role of non-equilibrium, strain-activated processes might also be worth investigating, since embrittlement can occur in systems which are otherwise so incompatible that the two elements are immiscible in the liquid state (e.g., Cd_S-Ga_L,Fe_S-Cd_L.) Other topics worthy of study are listed at the end of Reference 5.

2.2 Electrocapillary Effects

Although the generation of dislocations from "near-surface" sources is not likely to be affected by adsorption, the motion of a dislocation line which meets the surface, and whose Burgers vector contains a component normal to the surface, may experience an environment-dependent resistance to motion[15]. This effect may have been demonstrated recently in studies of the influence of electrolytes and applied potential on the hardness of metal monocrystal electrodes (the electrocapillary effect). The surface tension, γ, of an electrode is a function of the potential difference across its electrical double-layer. A net surface charge density, q, of either sign is considered to reduce γ, and the relation between γ, q, and the applied potential, E, for an ideal polarized electrode in the absence of specifically adsorbed ions is (at constant

temperature, pressure, and chemical potential) given by the Lippmann equation:

$$(\partial\gamma/\partial E)_{T,P,\mu_i} = -q.$$

Thus, when γ is plotted versus E, γ is maximum at $q = 0$; i.e., at the potential of zero charge or electrocapillary maximum.

Recently, we have begun a study of the environment-sensitive indentation hardness of the basal and first-order prism planes of zinc monocrystals[16]. Observable slip about hardness indentations on the basal plane occurs on second-order pyramical planes, {1122}, and in {1123} directions, so that {1122} steps are generated on the {0001} surface about such indentations. When indentations are made on a {1010} prism plane, dislocations on the pyramidal system that intersect the prism surface have their Burgers vectors in the plane of the surface, and thus produce no surface steps. Surface steps are created, however, by basal slip about indentations on the prism surface. We have found, Figure 8, that the microhardness of the basal plane passes through a maximum (nearly a two-fold increase) at -1200mV (SCE) in a $1N \cdot Na_2SO_4$ solution. Similar measurements over the range -1000 to -1500 mV on prism planes, however, indicate that the hardness of this surface is insensitive to potential variations. Dislocation etch pit distributions about the indentations are consistent with these observations.

Now, if the motion of pyramidal dislocations produced about the indentation on the basal plane is resisted in part by the energy of the {1122} steps left in their trail, one might expect that, at the potential of zero charge (where γ is a maximum), the extent of glide of such dislocations about the impression would be minimized -- i.e., the hardness would be a maximum. The motion of pyramidal dislocations intersecting the prism surfaces should be less sensitive to changes in potential, however, since in this case, slip step creation is not involved.

The observation that the hardness of the prism surface is indeed potential independent implies further than changes in the surface energy of the basal plane ($\sim$100 ergs/cm^2) may have less influence on the mobility of dislocations moving in this plane and intersecting the free surface than changes in γ for less densely packed slip planes (for which γ is likely to be considerably greater, say $\sim$1000 ergs/cm^2).

These observations suggest that changes in the charge density of the double-layer present at the electrode/solution interface can indeed affect localized mechanical behavior. Recognizing then that the potential of zero charge depends not only on the adsorption of species from solution but also on the work function of the metal surface, and that the latter is anisotropic, one would expect that the detailed nature of the double-layer will differ for each of the many crystal faces

exposed on a polycrystalline specimen. Unfortunately, there is a dearth of information regarding double layers at solid surfaces, and hardly any data exist on their variation with crystal orientation. Yet, such information could well facilitate our understanding of stress-corrosion cracking and corrosion fatigue, etc. For example, consider the possibility that the influence of applied potentials on susceptibility to SCC reflects, in part and in turn, the influence of this variable on (i) adsorption, (ii) adsorption-dependent near-surface dislocation behavior, and (iii) flow-dependent fracture behavior. The possible existence of such a "chemo-mechanical effect" might be worth investigating. (Note, however, that such an effect should be distinguished from the "mechano-chemical effect," in which deformation processes at the crack tip are considered to influence dissolution. Incidentally, this possibility is now considered unlikely.[17])

3. Semiconductors

It is well known that the yield and flow behavior of solids can be significantly influenced by doping with appropriate elements at concentrations of $>\sim 10^{17}/cm^3$. For example, the addition to silicon of electron donating species such as antimony facilitates dislocation motion, leading to a reduction in yield stress, while electron acceptor species; e.g., gallium, produce the opposite effect.[18] This phenomenon has

been interpreted in terms of the influence of electron concentration on either the formation (at charged dislocation acceptor sites) or mobility of dislocation kinks.

The environment-sensitive microhardness of semiconductors (e.g., Figure 9)[19], can be interpreted in essentially the same way. Such effects are considered to result from adsorption-induced changes in the electronic core structure of near-surface dislocations (for review, See Reference 20). Few studies have been made of the adsorption-dependent fracture behavior of semiconductors, however, although it has been shown[21] that liquid-metal environments can produce significant embrittlement. Figure 10, for example, illustrates the effects of liquid-gallium coatings on the bend strength of germanium monocrystals over the temperature range of 0-600°C. For temperatures between 100-350°C, the fracture stress in bending was reduced from about 120 kg/mm^2 in air to about 10 kg/mm^2 in gallium. This remarkable effect is not a genuine example of adsorption-induced liquid-metal embrittlement, however, being caused by a combination of selective dissolution and the intrinsic notch brittleness of germanium. Cracks were observed to have initiated at crystallographic notches (left inset of Figure 10) etched into the surface by the liquid metal. This observation, incidentally, has obvious implications for the ultrahigh-strength materials of the future. Such materials, while intrinsically notch brittle, are likely to be too hard to be notched mechani-

cally under ordinary working conditions, but may be notched by chemical means with potentially disastrous results.

At temperatures above about 400°C, on the other hand, germanium crystals exhibited "true" liquid-metal embrittlement, sometimes fracturing below the upper yield stress following measurable plastic strain (Figure 10, right inset). The variation in susceptibility to embrittlement with group of the liquid metal, and the variation with the solubility of germanium in the liquid metal were investigated. It was found that the severity of embrittlement was not related to the solubility of germanium in the environment, nor did extensive solubility prevent embrittlement. Group IV liquid metals were least embrittling, but groups II, III and V liquid metals all induced approximately the same degree of embrittlement, and there was no correlation between degree of embrittlement and electron affinity of the liquid metal. Several other possible correlations were examined, but none was found to be significant.

Further work on this topic, and especially on the relative influences of electron donor versus electron acceptor liquid metals on microhardness (above the ductile/brittle temperature) would appear to be worthwhile.

4. Non Metallic Solids

4.1 Silver Halides

If the charges carriers in the solid are not electrons,

but point defects, and these are mobile at room temperature, then the adsorption of charged species at the surface of the crystal can lead to concentration of these charge carriers in the near-surface regions of the solid. Such an effect is considered to be responsible for the embrittlement of silver chloride in aqueous complex-forming environments; that is, complex-ion embrittlement[22,23]. In this phenomenon, the adsorption of ions such as $AgCl^{3-}$ or Ag_4Br^{3+} cause normally ductile polycrystalline AgCl to fracture in an extremely brittle manner at stresses as low as one-seventh of its macroscopic flow stress. The failure mechanism proposed for this phenomenon[23] is illustrated in Figure 11. It appears that failure results from the repeated formation and rupture of Frenkel defect-hardened, charge double-layers at the surface of the solid. The mechanism is very similar to the film-rupture mechanism for stress-corrosion cracking in certain systems.

Although complex-ion embrittlement is not likely to be too important technologically, its introduction does provide an opportunity to make an important point regarding environmental embrittlement. This is that when the critical species causing embrittlement are known, the possibility of preventing failure is considerably enhanced. For AgCl, for example, it is known that the critical species are highly charged complex-ions, and it is the charge on the complex, or perhaps the charge density, which is the key factor. Thus, to prevent embrittlement, we simply add to the environment some "counter-ion" of opposite

charge, chosen so that it forms either a mixed complex of lower charge or charge density, or a different, more stable, but non-embrittling complex. Figure 12, for example, shows the influence of adding to a 6N NaCl, $AgCl_4^{3-}$ containing environment (very embrittling) small quantities of cesium or potassium ions. Note that the time to failure for a given stress is increased from 10 sec to more than 100,000 sec when 10^{-1}N of cesium ions are added[22].

4.2 Crystalline Ceramics

For most non-metals, however, the charge carriers at room temperature are not Frenkel defects, but electrons or holes, and these are present in concentrations several orders of magnitude less than those of the carriers in a metal. Consequently, the influence of adsorbed, surface-active species can extend distances of order microns into semi-conductor or insulator materials. An important consequence of this is the existence of the Rebinder Effect.

Recent work at RIAS[24,25] has shown that this phenomenon is extremely complex in nature. Adsorbed species can lead both to reductions in microhardness, which is the normal manifestation of the Rebinder Effect, or to significant increases. An example of this complexity is seen in Figure 13[24]. The material is freshly cleaved MgO. ΔL is the extent of edge dislocation motion occurring around a diamond indenter in the time period from 2 sec to 1000 sec after application of 10g load.

It is related to the "softness" of the crystal. The greater ΔL (fixed time) the softer the crystal. We see that ΔL is a very complicated function of the composition of the environment.

In the past, Rebinder Effects have been interpreted in terms of adsorption-induced reductions in surface-free energy. For various reasons, this view is no longer considered correct[20,24]. An alternative explanation is as follows[24,25]. The mobility of dislocations in a non-metallic solid such as a ceramic or an oxide film is determined by the interactions of dislocations with point defects, vacancies, impurities, etc. The chemisorption process on such non-metallic solids involves--at least in part--the transfer of electrons or holes between the various impurities or point defects in the near-surface region of a solid and the adsorbate[26]. It is considered, therefore, that adsorption-induced changes in the electronic state of near-surface point defects and dislocations--whether caused by direct interactions with the adsorbate or as a result of band bending effects--introduce variations in their mutual interactions. Such variations are then manifested as environmentally-induced changes in dislocation mobility, and hence in microhardness.

Now the influence of adsorbed species on near-surface dislocation mobility can influence directly the fracture behavior of notch-sensitive ceramics. For such materials, crack initiation controls failure and, of course, crack initia-

tion itself is a consequence of dislocation generation and interaction. An interesting relationship between environment-sensitive flow and fracture behavior may be seen in data on the influence of liquid environments on the drilling behavior of MgO or CaF_2 monocrystals, Figures 14 and 15[27]. Note the direct correlation between environment-sensitive dislocation mobility (as indicated by ΔL (1000)) and depth of penetration of a carbide spade drill in 600 sec (D (600)). A possible explanation for this correlation is as follows: For a notch brittle solid, the fracture stress is determined by, and closely approximates, the flow stress. Thus, any environment which facilitates dislocation motion in the near-surface regions of a notch brittle solid (lowers its flow stress) will facilitate crack initiation, and so facilitates material removal.

Although surface-active environments, such as DMSO or DMF, do not affect the propagation of fast moving cracks[28]--probably because they do not significantly influence lattice cohesion--it seems not unreasonable to expect that they will influence the propagatability of slow moving cracks by affecting dislocation mobility in the vicinity of the crack tip. Such an effect could either facilitate sub-critical crack growth by the dislocation emission processes discussed by Clarke, et al.[29] and others, leading to static fatigue failure, or result in crack blunting and reduced propagatability.

This would be an interesting and possibly important topic for study, being directly relevant to the anticipated future use of ultrahard, notch-brittle solids as structural materials. A more detailed investigation of the proposed explanation for Rebinder Effects in ceramics also will be required before predictability of occurrence and magnitude can be expected. Research seeking to apply this phenomenon to machining, comminution, rock drilling, compaction, control of wear, etc. also should be undertaken.

4.3 Amorphous Solids - SiO_2 Base Glasses

Explanations for the environment-sensitive fracture behavior of oxide-type glasses (e.g., static fatigue) usually fall into one of two categories: (i) those dependent upon adsorption-induced reductions in surface free energy[30] and (ii) those which assume the presence of water to be critical, and of which the stress-enhanced corrosion mechanism of Charles and Hillig[31] is perhaps most widely accepted. For explanations in category (ii), the role of testing media other than water is usually considered to be simply that of screening the highly reactive water molecules from the glass surface.

However, there is evidence that, under conditions where fracture is induced by abrasion or grinding, certain organic environments are considerably more active than water[32]. For such examples of environment-sensitive fracture behavior it would certainly appear that explanations dependent upon the

dominant presence and corrosive influence of water could not be valid. Likewise, recent work by Westwood and Latanision[33,34] has revealed that the n-alcohols and n-alkanes can exert a profound influence on the hardness and machinability of silica-base glasses. The data of Figure 17(a) show, for example, that under otherwise identical testing conditions, a soda-lime glass may be drilled with a diamond bit some twenty times faster in heptyl alcohol than in water (N_C is the number of carbon atoms in the molecule). And other experiments have shown that binary solutions of the n-alcohols (or n-alkanes) of different molecular chain lengths can produce hardnesses or drilling efficiencies equivalent to those produced by n-alcohols (or n-alkanes) of intermediate chain length.

Consideration of these results, of data from measurements of the fracture energy of soda-lime glass as a function of environment (determined by means of the double cantilever technique), and of the water contents and other physical parameters of test environments has led to the realization that such variations in machinability are not related either to adsorption-induced reductions in surface free energy, or to stress-accelerated corrosion effects. It seems more likely that--as with similar phenomena in crystalline solids--they are associated with adsorption-induced variations in the flow behavior (e.g., microhardness, Figure 17(b)) and flow-dependent fracture properties of the near-surface regions of the glass. The problem now is to determine the mechanism involved.

One possibility is that a stress-plus-chemisorption-induced redistribution of charge-carrying ionic species (Na^+, OH^-) in the near-surface regions is involved--leading to changes in hardness. This possibility is supported by the observation[35] that the hardness of glass in liquid environments is related to its zeta-potential in these environments. For example, the variation in the ξ-potential of glass in aqueous solutions of KCl or $Th(NO_3)_4$ has been determined by Rutgers and de Smet[36] and is shown in Figure 17(a). The variation in pendulum hardness of a soda-lime glass in the same environments is shown in Figure 17(b). It may be deduced that this glass is hardest when $\xi \simeq 0$, and is softened by environments in which the ξ-potential of the glass is either positive or negative. This finding has been confirmed in studies using non-aqueous environments, Figure 19[37].

Following the general principles established by Grimley[38] and others (e.g., Reference 39), a possible interpretation of this relationship between ξ-potential and hardness is as follows: When the environmental composition is such that $\xi \simeq 0$, the long-range electrostatic forces acting on the near-surface region of the glass are minimized, and so the concentration and distribution of charge carriers there will correspond essentially to those in the bulk. When ξ is negative, however, the response of the solid must be to bring into the near-surface region a charge counterbalancing concentration of positive charge carriers, i.e., Na^+ ions. This locally in-

creased sodium ion concentration reduces the hardness of this region. When ξ is positive, on the other hand, it may be presumed that an above-average concentration of negative charge carriers in the near-surface regions is required to perform the charge-balancing function. Apparently, charge balancing is not achieved by the migration of Na^+ ions away from the surface; otherwise the hardness of the glass would increase, not decrease, as ξ became positive. A controversial alternative suggestion is that mobile OH^- ions are involved, and that their migration to the near-surface layers is responsible for the observed softening. On this hypothesis, glass should be hardest at its zero point of charge, as is observed.

The remarkable influence of the n-alcohols on drilling efficiency, Figure 17(a), could then be interpreted in the same way, because it is known that the sign of the ξ-potential of non-metallic solids can be reversed by the adsorption of monovalent organic molecules, and that the ability to cause charge reversal increases with N_C. It is also known that the ξ-potential of soda lime glass in the lower n-alcohols is negative. Presumably, therefore, ξ for soda lime glass becomes ~0 when $N_C \simeq 7$, and is positive when $N_C > 7$.

By mixing two alcohols which, independently, produce different ξ-potentials, it should be possible to produce a range of intermediate ξ-potentials, and, hence, the range of hardnesses appropriate to these values of ξ. This would seem to be a likely explanation for effects of binary solutions mentioned above.

An important practical conclusion from this work is that the effectiveness of heptyl alcohol (N_C=7) as a drilling aid for soda lime glass is not specific to this compound, but is specific to the surface charge (approximately zero) it produces at the glass surface.

Another interesting recent development is the observation of what appears to be adsorption-controlled, flow-facilitated, slow crack growth in soda lime glass, stressed in non-corrosive environments, Figure 20[35]. Of course, both Marsh[40] and Linger and Holloway[41] have suggested previously that localized plastic flow can occur in the vicinity of crack tips in soda lime glass. However, in their considerations, flow was not thought of as a means of facilitating crack growth.

The data shown in Figure 20 was obtained using the center-loaded crack technique developed by Panasyuk and Kovchik[42], Figure 21. The specific advantage of this technique is that, within the dimensional restrictions shown in Figure 21, the load required to propagate the crack increases with crack length (the converse of the "Griffith-crack" situation). The crack thus extends in a stable manner at a velocity dependent upon its length and the rate of loading. The energy ϕ_B, required to propagate center-loaded cracks in a stable mode is calculated from the relationship[42].

$$\phi_B = P^2(1 - \nu^2) / 2c \pi Eh^2$$

in which P is the instantaneous load to continue slow propagation of a crack of length 2c, ν is Poisson's ratio (0.22), E is Young's modulus (7.34×10^{11} dyn/cm^2), and h is the thickness of the glass sheet.

Comparison of the data in Figure 20 with those in Figure 17 reveals that ϕ_B for this soda lime glass varies in essentially the same manner with environmental composition as does ease of drilling with a diamond bit, and pendulum hardness. The characteristic maximum in heptyl alcohol is especially noticeable. Other experiments have also demonstrated that the maximum in ϕ_B which occurs in heptyl alcohol ($N_C = 7$) can be reproduced by solutions of octyl alcohol in pentyl alcohol, Figure 22(a). Likewise, the maximum (at $N_C \simeq 10$) and minimum at ($N_C \simeq 14$) in the ϕ_B versus N_C (alkanes) plot can be reproduced by, respectively, solutions of tetradecane in pentane and pentadecane in undecane, Figures 22(b) and 22(c).

Clearly, the behavior illustrated in Figures 20 and 22 is unlikely to be related to any corrosion phenomenon--since most of the environments used were, as far as can be ascertained, non-corrosive, and the effects of binary solutions are inconsistent with such a possibility--or to lattice "compaction" effects. Nor can such behavior be rationalized in terms of adsorption-induced reductions in the brittle fracture energy of glass for, if this were so, then ϕ_B should have been a minimum in heptyl alcohol because this environment maximizes the hardness of soda lime glass, and so would have been expected

to facilitate its failure by brittle processes. It follows that ϕ_B should not be regarded as a measure of the true surface energy of glass, but rather as a relative measure of the energy required to propagate a sub-critical crack in a semi-brittle manner at a rate dictated, in part, by the rate of loading. The data in Figures 20 and 22 can then be interpreted as follows: Non-corrosive environments which, by adsorption, soften soda-lime glass (e.g., ethyl alcohol or tetradecane), facilitate slow crack growth by localized flow processes. Therefore, the external load (P) required to maintain crack propagation at a particular rate is reduce, and ϕ_B, which is proportional to P^2, then is relatively low. Environments which maximize the hardness of glass, on the other hand (e.g., heptyl alcohol), restrict flow-assisted crack growth, and in such cases ϕ_B is relatively high.

It is of particular interest to note that tetradecane is as effective as water in reducing the hardness and value of ϕ_B of the soda lime glass used in this work (Figures 17(b) and 20). Since tetradecane may certainly be considered non-corrosive, one wonders then if the corrosive action of water is as critical in facilitating slow crack growth in glass as previously thought. Moreover, on the basis of this work, it seems possible that adsorption-sensitive, flow-enhanced, sub-critical crack growth may well play a role in determining both the static and dynamic fatigue behavior of soda-lime glass in moisture-containing environments.

At present, the mechanism proposed to explain these effects must be regarded as speculative. It is conceivable that mobile Na^+ or OH^- ions have little to do with the observed phenomena. An alternative, and certainly controversial, possibility is that flow in glass involves the movement of line defects--possibly dislocations of variable Burgers vector[43]--the mobility of which can be influenced by adsorption-induced changes in their electronic environment. Clearly, this field of research represents an area in which almost everything worthwhile remains to be done.

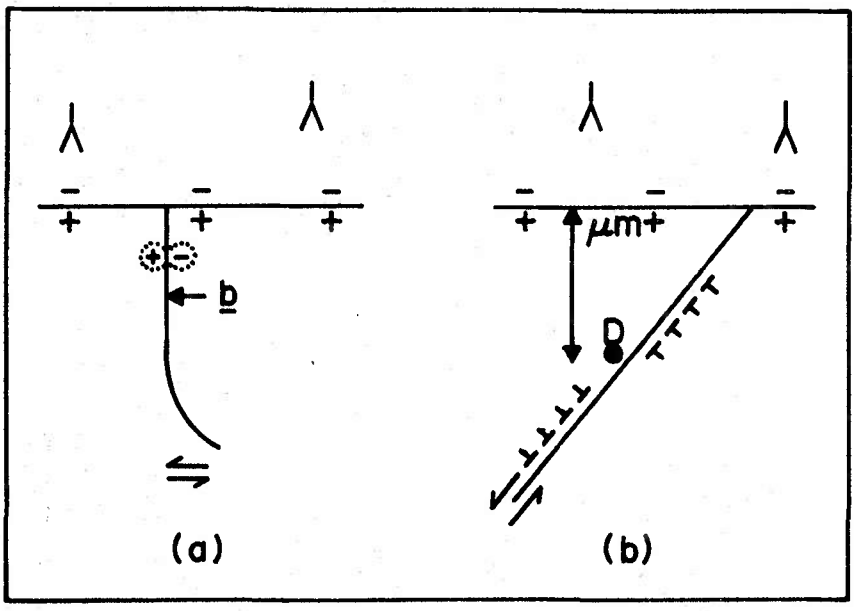

Figure 1: The charge double layer and (a) a dislocation line intersecting the surface, and (b) dislocations parallel to the surface generated from a source, D, a micron or so away from the surface.

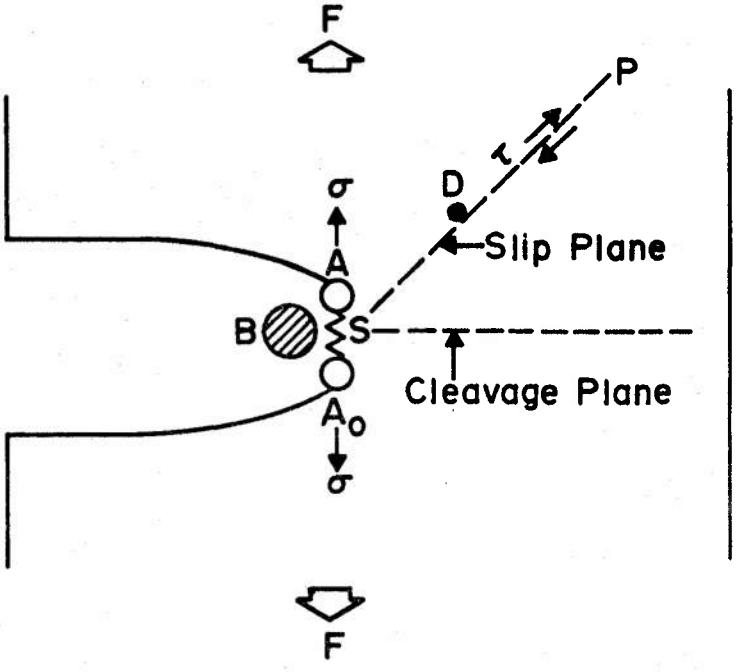

Figure 2: Schematic of a crack in a solid, subjected to an increasing force F. The bond A-A_o constitutes the crack tip, and B is a surface-active liquid metal atom. D is a dislocation source (5).

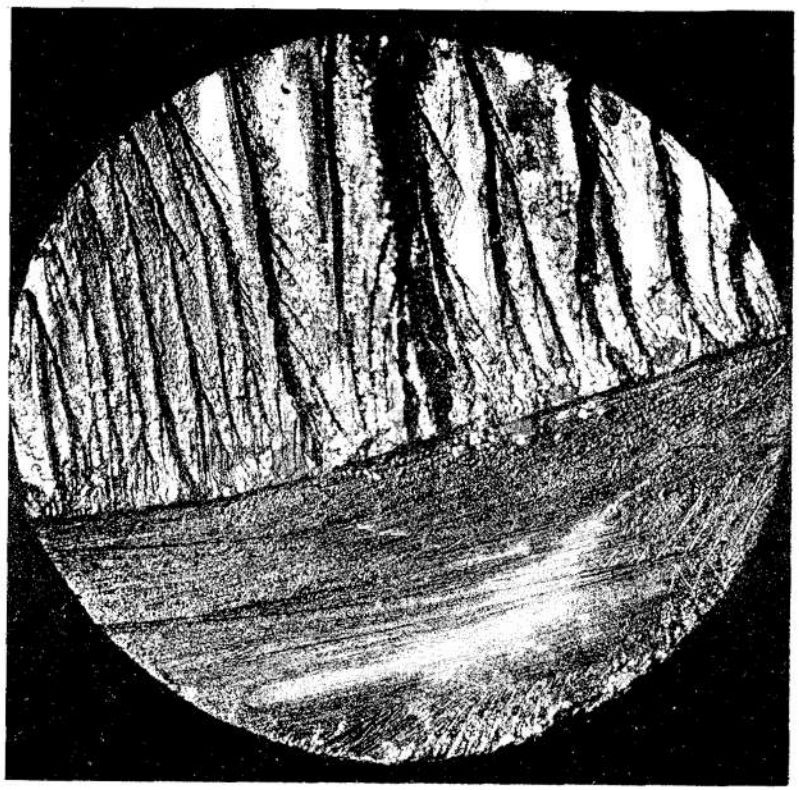

Figure 3: Cleavage failure of a notched, 12 mm diameter aluminum monocrystal stressed in liquid gallium. Fracture surface is predominantly {100}[4].

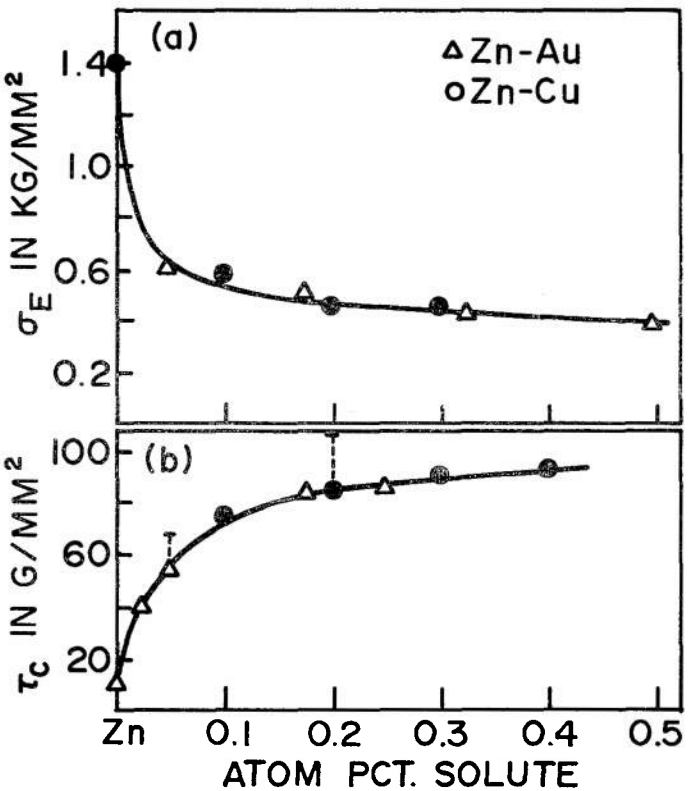

Figure 4: (a) Effect of solute content on fracture stress, σ_F, of polycrystalline zinc in liquid mercury. (b) Variation of critical resolved shear stress, τ_C, with solute content for zinc monocrystals.[9]

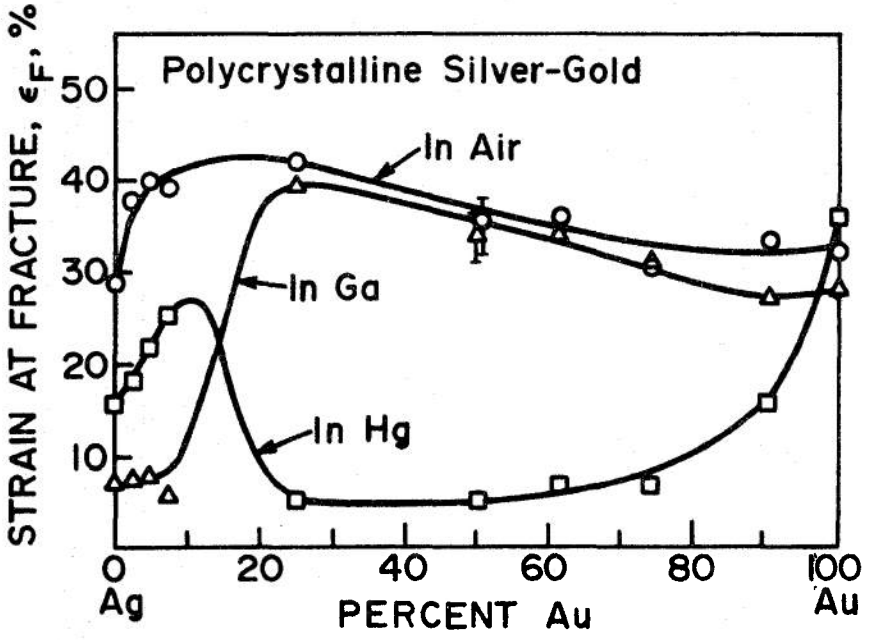

Figure 5: Influence of mercury and gallium environments on the strain at fracture of silver-gold alloys.[10]

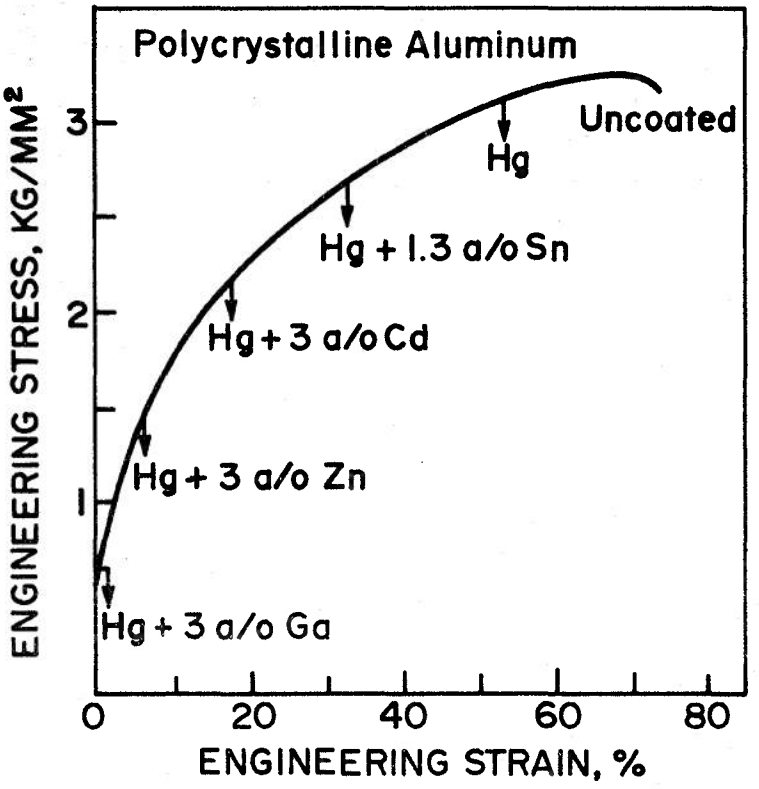

Figure 6: Embrittlement of polycrystalline pure aluminum by various mercury solutions.[4]

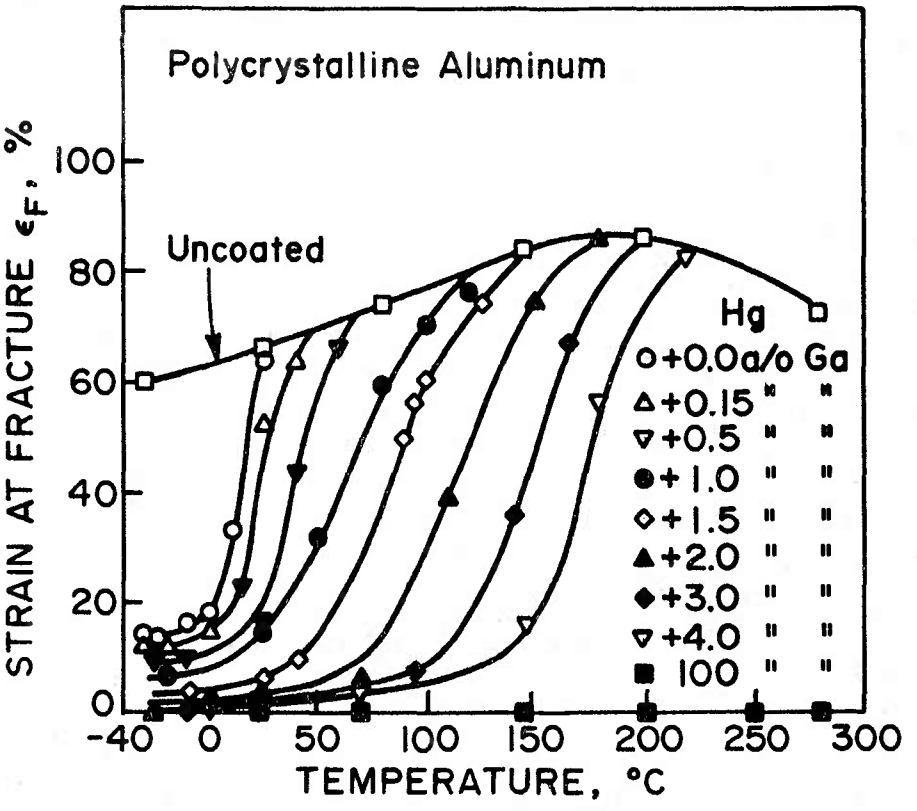

Figure 7: Temperature dependence of strain at fracture for polycrystalline aluminum specimens in mercury, gallium and mercury-gallium solutions.[14]

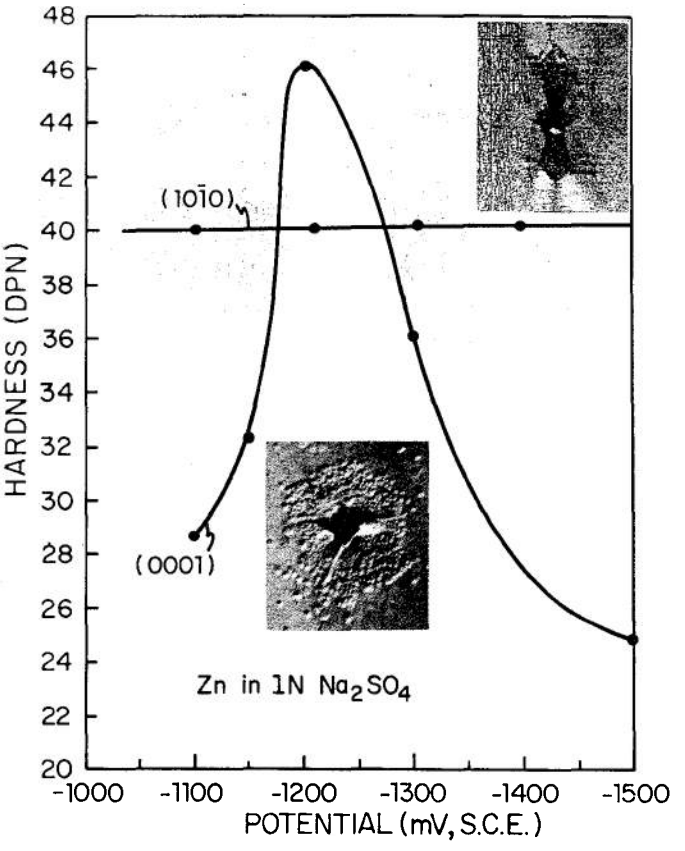

Figure 8: The variation in diamond-pyramid hardness with potential for zinc monocrystal surfaces in 1N Na_2SO_4.[16]

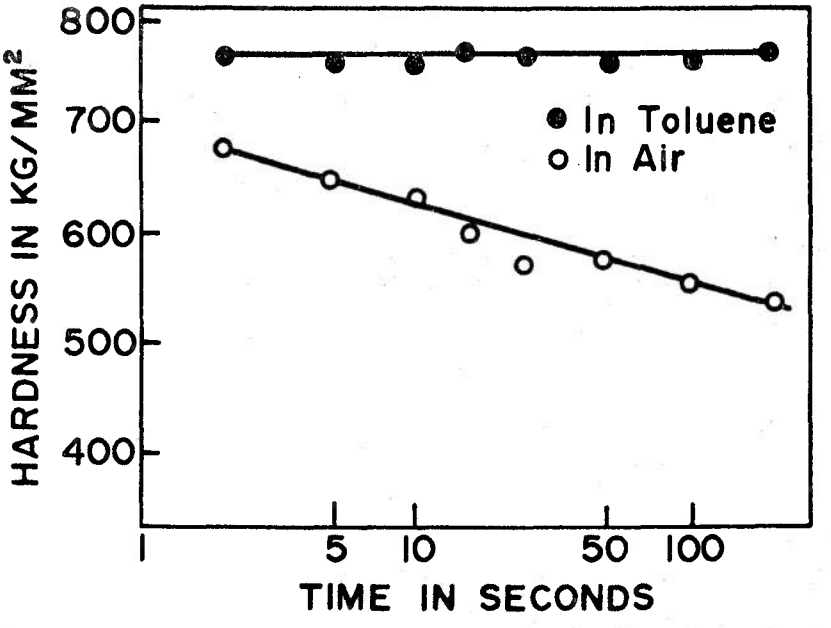

Figure 9: Time dependence of hardness (anomalous creep-indentation effect) of germanium in (moist) air.[19]

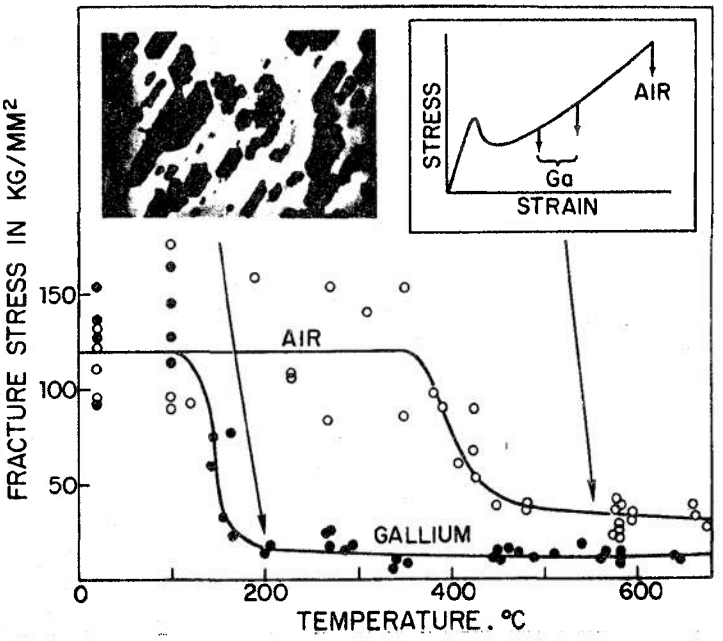

Figure 10: Embrittlement of germanium by liquid gallium. Below about 350° C, embrittlement is associated with the notch-etching effect illustrated in left inset. Above about 450° C, true liquid-metal embrittlement effects predominate, right inset.[21]

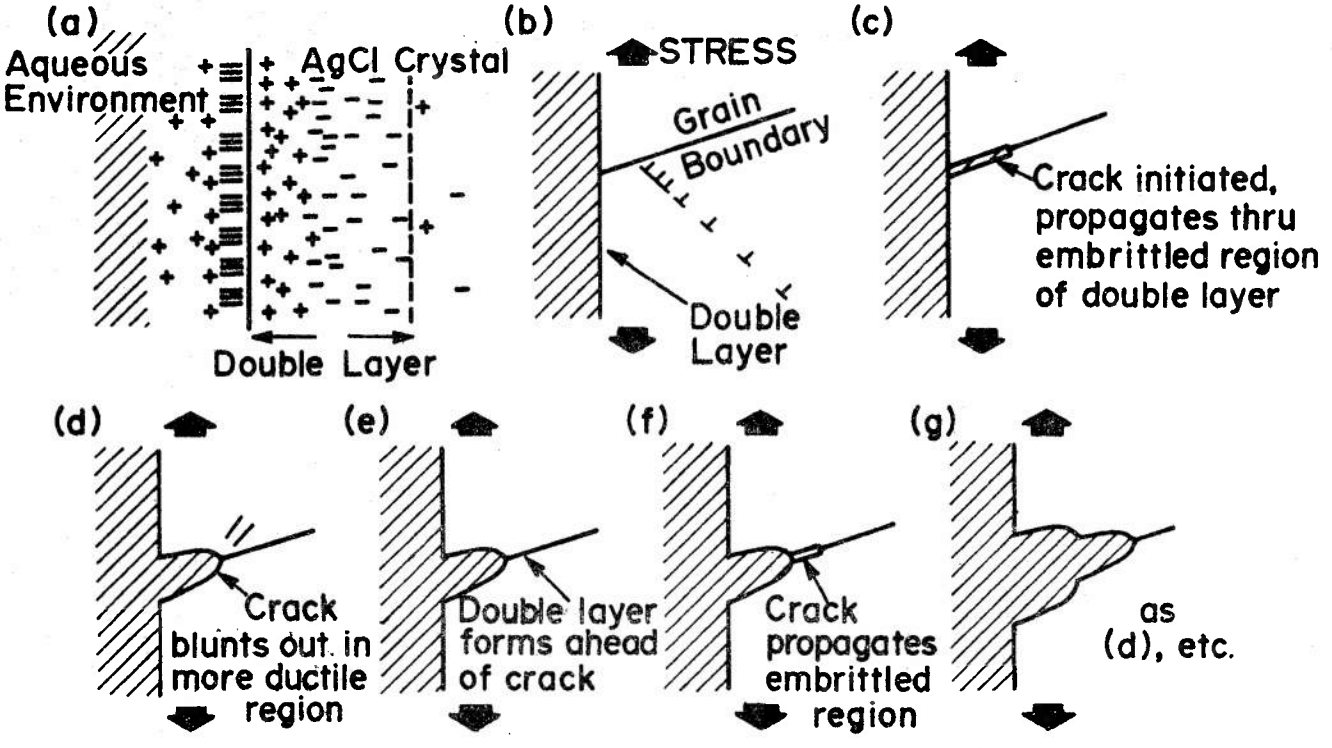

Figure 11: Schematic of the double layer mechanism for the complex-ion embrittlement of AgCl. The charge carriers in the solid are Frenkel defects.[23]

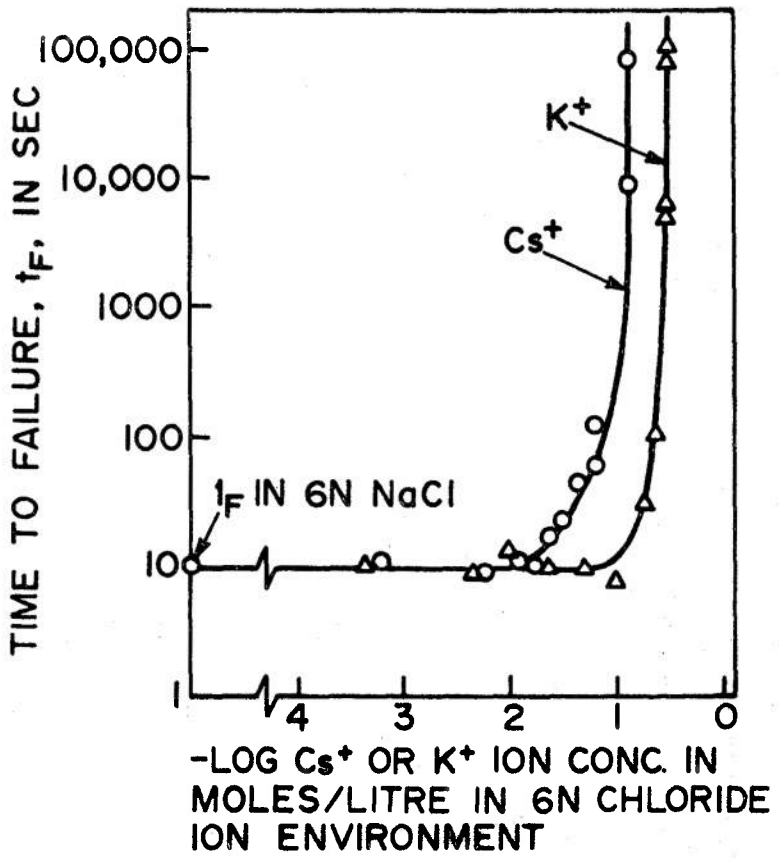

Figure 12: Inhibition of embrittlement of AgCl in a 6N chloride environment resulting from the replacement of Na+ ions by K+ or Cs+ ions. The applied stress was $600 g/mm^2$.[22]

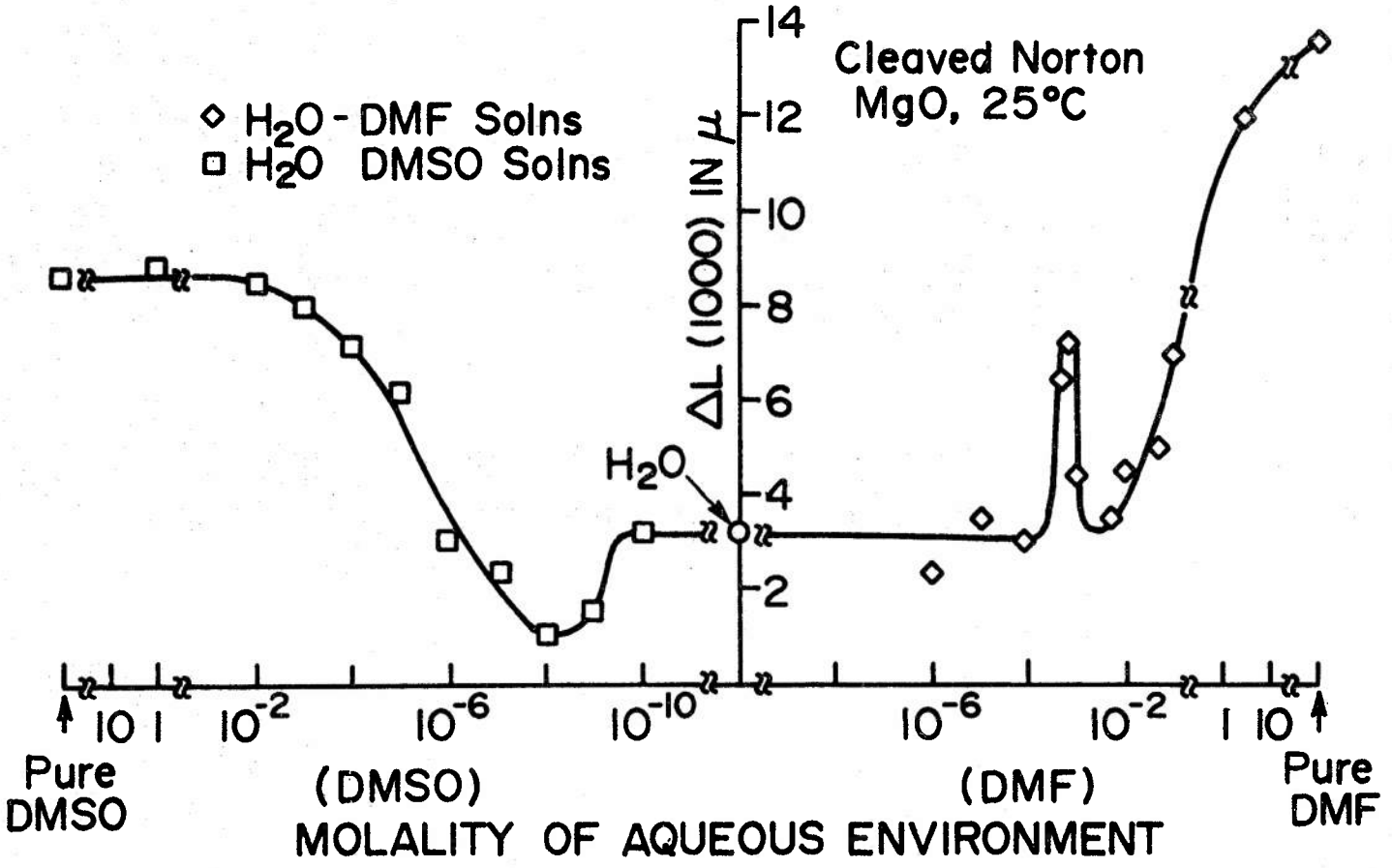

Figure 13: Variation of ΔL with molality of aqueous solutions of dimethyl formamide (DMF) or dimethyl sulphoxide (DMSO) for freshly cleaved MgO.[24]

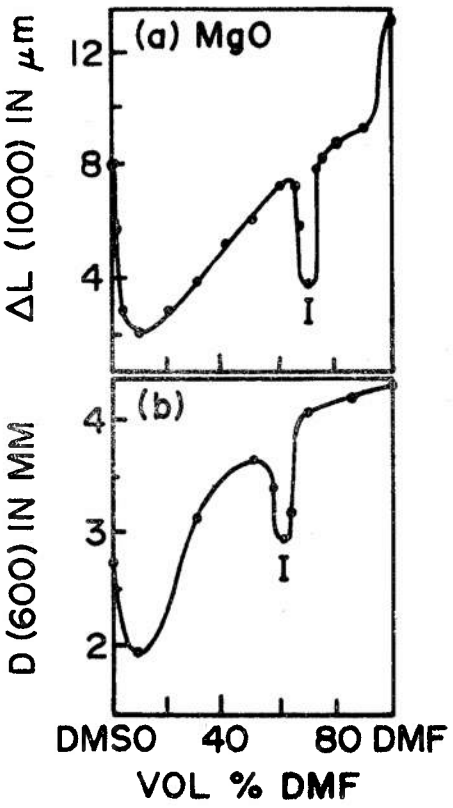

Figure 14: Influence of DMF-DMSO environments on (a) extent of edge dislocation motion produced during indentation period between 2 and 1000 s around indentation in freshly cleaved {100} MgO surface, and (b) depth of penetration of a carbide spade drill in 600 s, D(600), in [100] direction into similar crystal. Note similarity in variation of ΔL(1000) and D(600) with environmental composition.[27]

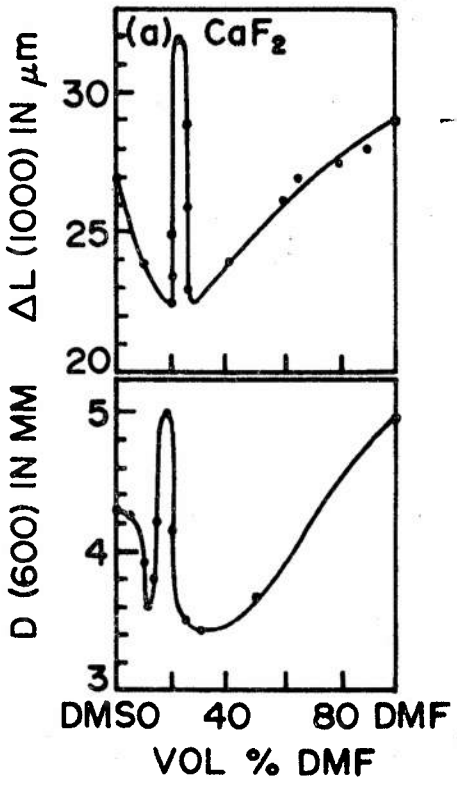

Figure 15: Data similar to that in Figure 14 for CaF_2 crystals. This material cleaves on {111} planes and was drilled in a direction perpendicular to this plane.[27]

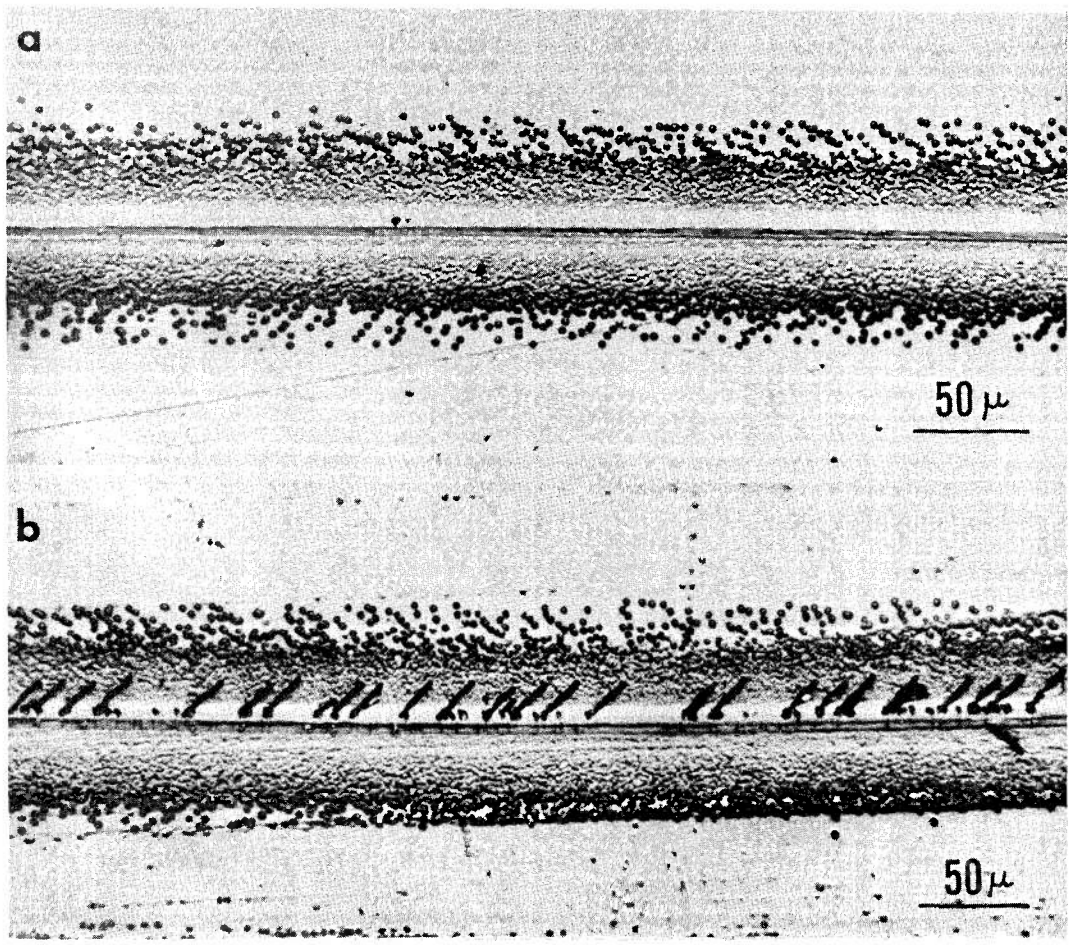

Figure 16: Indenter tracks in freshly cleaved MgO surface produced (a) in air (i.e. with adsorbed water present) and (b) under n-hexadecane. Cracks produced in latter environment are present in {110} planes at the surface (b) and on {100} planes below the surface. Load on indenter was 20 g; it was moved from left to right.[27]

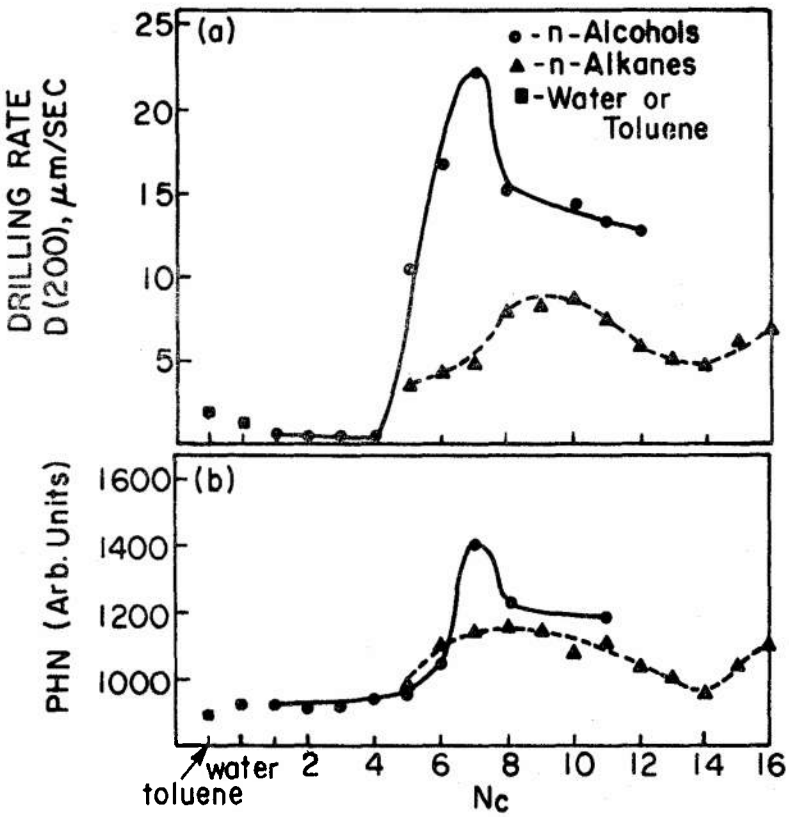

Figure 17: Effects of environment on (a) drilling rate after 200 sec. with a diamond bit, D(200), and (b) pendulum hardness (PHN), of a soda-lime glass. N_C is the number of carbon atoms in the molecule.[33]

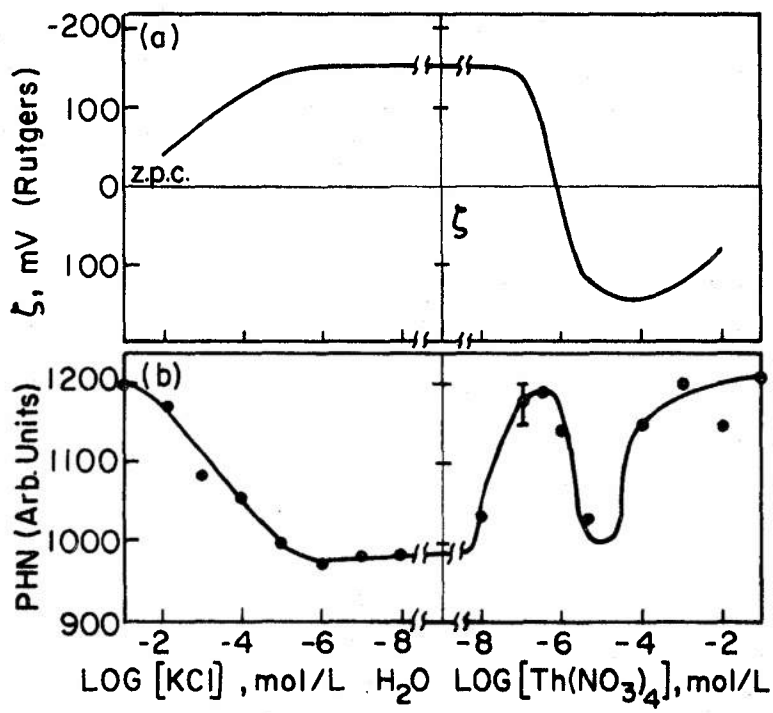

Figure 18: Effect of composition of aqueous environments on (a) ξ - potential and (b) pendulum hardness of a soda-lime glass. Note that the glass is hardest when $\xi \simeq 0$.[35]

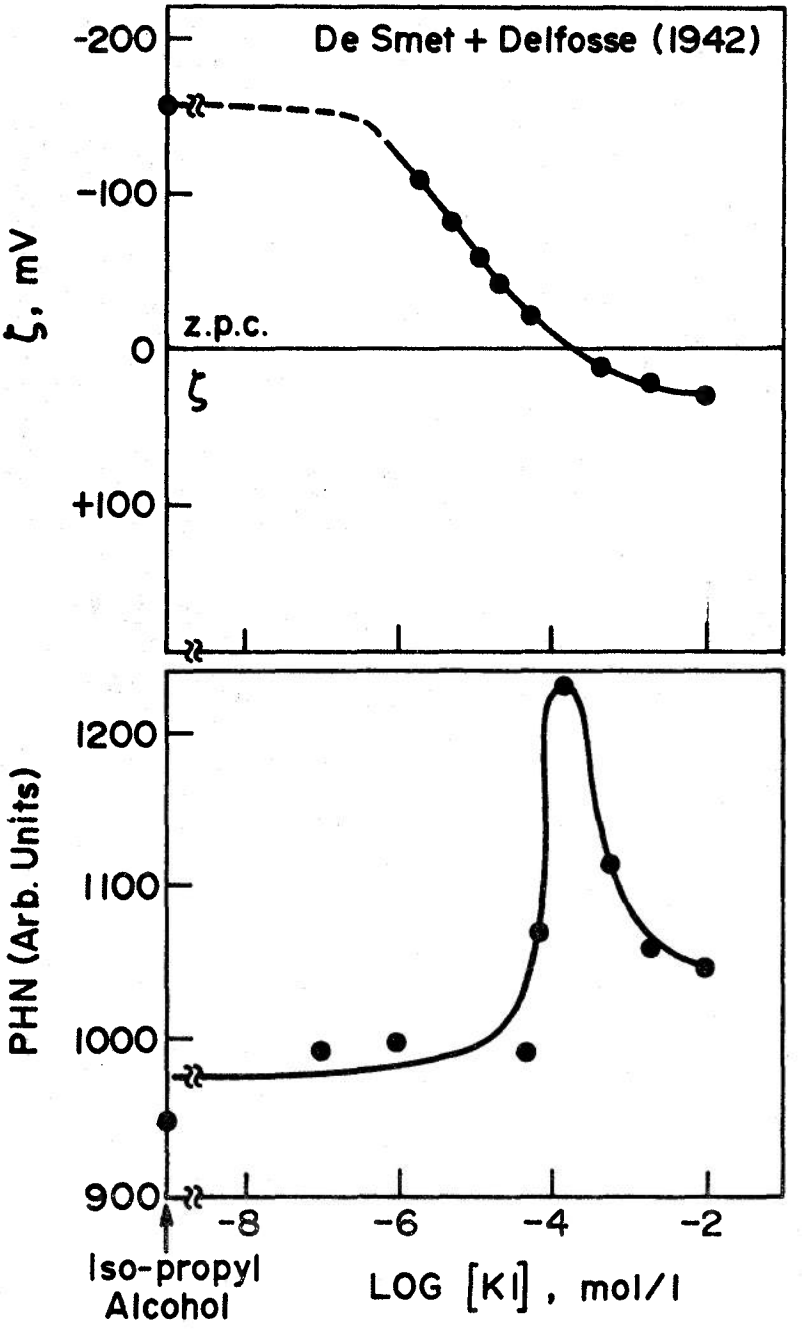

Figure 19: Effect of KI additions to iso-propyl alcohol on (a) ξ-potential and (b) pendulum hardness of a soda-lime glass.[37]

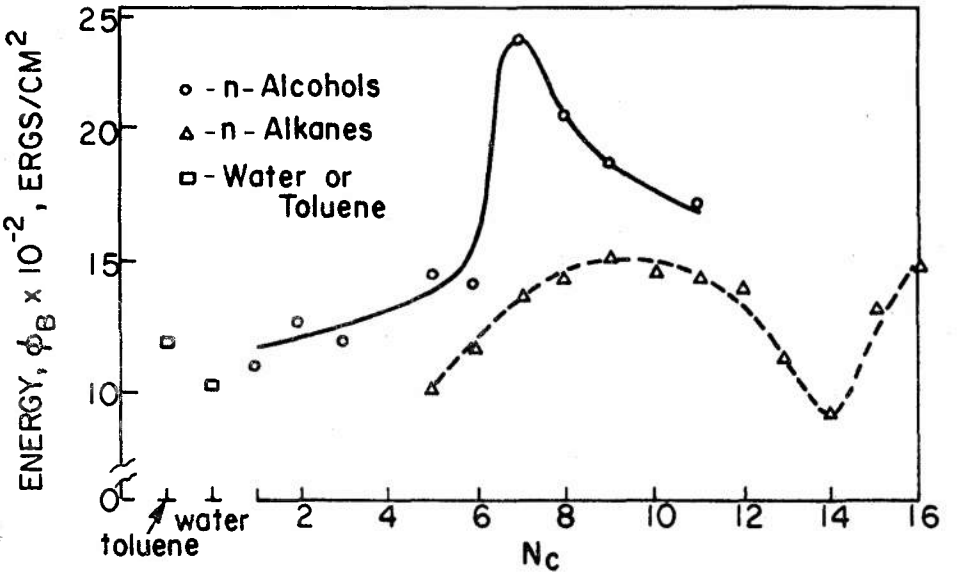

Figure 20: Influence of environment on the energy (ϕ_B) required to propagate a stable crack in a semi-brittle manner in soda-lime glass.[35]

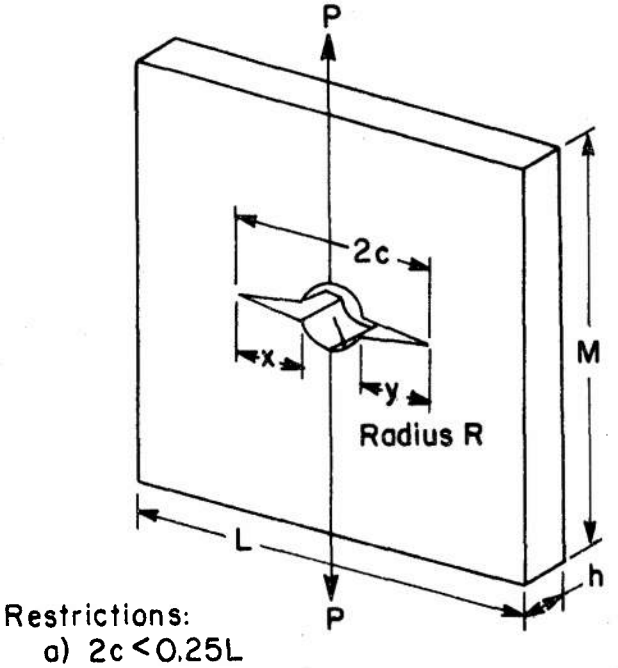

Restrictions:
a) $2c < 0.25L$
b) $x = y > R$
c) $M \cong L$

Figure 21: Schematic of specimens used in studies of environment-sensitive slow crack growth in soda-lime glass.[35]

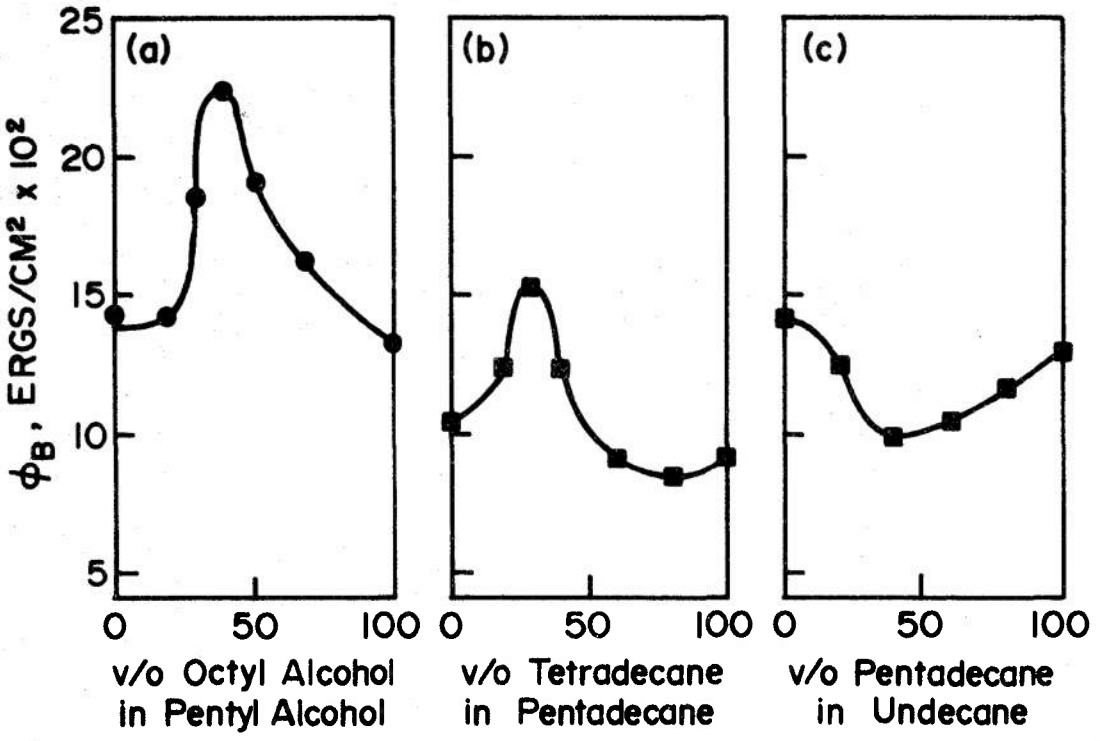

Figure 22: Effects of various binary n-alcohols or n-alkane solutions on ϕ_B, illustrating ability to reproduce values of ϕ_B characteristic of intermediate alcohols or alkanes.[35]

REFERENCES

1. W.H. Brattain, "The Surface Chemistry of Metals and Semiconductors," John Wiley, New York, 9 (1959).

2. A.H. Cottrell, S.C. Hunter and F.R.N. Nabarro, Phil. Mag., 44, 1064 (1953).

3. A.R.C. Westwood, Phil. Mag., 7, 633 (1962).

4. A.R.C. Westwood, C.M. Preece and M.H. Kamdar, Trans. ASM, 60, 723 (1967).

5. A.R.C. Westwood, C.M. Preece and M.H. Kamdar, Treatise on Fracture, Ed. H. Liebowitz, Academic Press, New York, III, 590.

6. A.R.C. Westwood and M.H. Kamdar, Phil. Mag., 8, 787 (1963).

7. N.S. Stoloff and T.L. Johnston, Acta Met., 11, 251 (1963).

8. A. Kelly, W.R. Tyson and A.H. Cottrell, Phil. Mag., 15, 567 (1967).

9. C.M. Preece and A.R.C. Westwood, Acta Met., 16, 1335 (1968).

10. C.M. Preece and A.R.C. Westwood, "Corrosion by Liquid Metals," Plenum Press, New York, 441 (1970).

11. M.H. Kamdar and A.R.C. Westwood, Phil. Mag., 15, 641 (1967).

12. C.M. Preece and A.R.C. Westwood, Fracture 1969, Chapman and Hall, London, 439 (1969).

13. A.R.C. Westwood, C.M. Preece and D.L. Goldheim, Molecular Processes on Solid Surfaces, McGraw-Hill, New York, 591 (1969).

14. C.M. Preece and A.R.C. Westwood, Trans. ASM, 62, 418 (1969)

15. J.J. Gilman, Phil, Mag., 6, 159 (1961).

16. R.M. Latanision, H. Opperhauser and A.R.C. Westwood, unpublished work, RIAS, 1970-1.

17. T.P. Hoar, Proc. NATO Conf. on Mechanisms of Stress-Corrosion Cracking, Ericeira, Portugal, 1971. To be published.

18. J.R. Patel and P.E. Freeland, Phys. Rev. Letters, 18, 833 (1967).

19. J.H. Westbrook, Environment-Sensitive Mechanical Behavior, Gordon and Breach, New York, 247 (1966).

20. A.R.C. Westwood, Microphasticity, Interscience, New York, III, 365 (1968).

21. E.N. Pugh, A.R.C. Westwood and T.T. Hitch, Phys. Stat. Solidi, 15, 291 (1966).

22. A.R.C. Westwood, D.L. Goldheim and E.N. Pugh, Mat. Sci. Research, 3, 533 (1966).

23. A.R.C. Westwood, D.L. Goldheim, E.N. Pugh, Phil. Mag., 15, 105 (1967).

24. A.R.C. Westwood, D.L. Goldheim and R.G. Lye, Phil. Mag., 16, 505 (1967); ibid, 17, 951 (1968).

25. A.R.C. Westwood and D.L. Goldheim, J.Appl. Phys., 39, 3401 (1968).

26. F.F. Volkenstein, "The Electronic Theory of Catalysis on Semi-Conductors," Pergamon, 1963. Also Sov. Phys. Uspekhi, 9, 743 (1967).

27. A.R.C. Westwood and D.L. Goldheim, J. Am. Ceram. Soc., 53, 142 (1970).

28. D.A. Shockey and G.W. Groves, J. Am. Ceram. Soc., 52, 82 (1969).

29. F.J.P. Clarke, R.A.J. Sambell and H.G. Tattersall, Phil. Mag., 7, 393 (1962).

30. E. Orowan, Nature, 154, 341 (1944).

31. R.J. Clarke and W.B. Hillig, Sump. on Mechanical Strength of Glass and Ways of Improving It, Union Scientifique du Verre, Charleroi, Belgium, 511 (1962).

32. W.V. Engelhardt, Naturwiss, 33, 195 (1946).

33. A.R.C. Westwood, G.H. Parr and R.M. Latanision, Proc. 3rd Intl. Conf. on Non-Crystalline Solids, Wiley, London. In press (1971).

34. A.R.C. Westwood and R.M. Latanision, Proc. Symp. on Science of Ceramic Machining and Surface Finishing, NBS Monograph. In press (1971). (RIAS TR 71-10c).

35. A.R.C. Westwood and R.D. Huntington, Proc. Intl. Conf. on Mechanical Behavior of Solids, Kyoto, Japan, August 1971. To be published. (RIAS TR 71-12c).

36. A.J. Rutgers and M. deSmet, Trans. Faraday Soc., 41, 758 (1945).

37. A.R.C. Westwood and R.D. Huntington. Unpublished work, RIAS (1971).

38. T.B. Grimley, Proc. Roy. Soc., A201, 40 (1950).

39. E.P. Honig, Trans. Faraday Soc., 65, 2248 (1969).

40. D.M. Marsh, Proc. Roy. Soc., A279, 420 (1964).

41. K.R. Linger and D.G. Holloway, Phil. Mag., 18, 1269 (1968).

42. V.V. Panasyuk and S.E. Kovchik, Sov. Phys. - Doklady, 7, 835 (1963).

43. J.J. Gilman, Dislocation Dynamics, McGraw-Hill, New York, 3 (1968).

2. Background References

2.1 Stress Corrosion Symposia, Monographs and Reviews

1. Physical Metallurgy of Stress Corrosion Fracture, Interscience, New York, 1959, AIME.

2. W. D. Robertson, ed. Stress Corrosion Cracking and Embrittlement, Wiley, New York, 1956.

3. Stress Corrosion Cracking of Metals, ASTM-AIME, 1945.

4. H. L. Logan, The stress Corrosion of Metals, Wiley, Electrochemical Society, 1966, New York.

5. I. A. Levin, Intercrystalline Corrosion and Corrosion of Metals Under Stress, 1962, Consultants Bureau.

6. Stress Corrosion Cracking of Titanium, STP 397, ASTM, 1966.

7. Ake Bresle, ed. Recent Advances in Stress Corrosion, Almquist and Wiksell, Stockholm, 1961.

8. V. V. Romanov, Stress Corrosion Cracking of Metals, Jerusalem: Israel Program for Scientific Translations, 1961.

9. R. W. Staehle, A. J. Forty, D. van Rooyen, eds., Fundamental Aspects of Stress Corrosion Cracking, National Association of Corrosion Engineers, 1969, Houston, Texas.

10. R. Hochman, J. C. Scully, Stress Corrosion Cracking of Titanium, Conference held January, 1971 at Georgia Tech, Proceedings to be published by NACE.

11. J. C. Scully, Conference on Mechanistic Aspects of SCC Sponsored by NATO, held in Portugal, March 1971. Proceedings published by NATO.

12. B. F. Brown, Report on ARPA Sponsored Stress Corrosion Program. Published 1971.

13. B. F. Brown, Engineering Text on Stress Corrosion Cracking in preparation.

14. M. O. Speidel and M. D. Hyatt, "Stress Corrosion Cracking of High Strength Aluminum Alloys", Advances in Corrosion Science and Technology, Volume II, Plenum Press. To be published by the end of 1971.

15. M. J. Blackburn, J. S. Feeney, and T. R. Beck, "Stress Corrosion Cracking of Titanium Alloys", Advances in Corrosion Science and Technology, Volume III, Plenum Press. To be published early 1972.

2.2 Corrosion Fatigue

16. M. Achter, "Effect of Environment on Fatigue Cracks," ASTM-STP-415, 1967.

17. O. Devereux, A. J. McEvily, and R. W. Staehle, Conference on Chemistry, Mechanics and Microstructure of Corrosion Fatigue, held at University of Connecticut, June 1971. Proceedings to be published by NACE.

2.3 Surface--Mechanical Effects

18. V. I. Likhtman, P. A. Rehbinder, and G. V. Karpenko, Effect of Surface-Active Media on Deformation of Metals, Chemical Publishing Company.

19. R. M. Latanision and A. R. C. Westwood, Volume I, Advances in Corrosion Science and Technology. Plenum Press

20. A. R. C. Westwood and N. S. Stoloff, eds. Environment Sensitive Mechanical Behavior, Gordon and Breach (1966) New York, AIME.

2.4 Liquid Metal Embrittlement

21. W. Rostoker, J. M. McCaughey, H. Markus, Embrittlement by Liquid Metals, Reinhold, 1960.

22. A. R. C. Westwood, C. M. Preece and M. H. Kamdar, Treatise on Brittle Fracture, Academic Press, New York.

23. See Westwood and Latanision. This conference.

2.5 Temper Embrittlement

24. ASTM-STP-407, Temper Embrittlement, 1967.

25. C. J. McMahon, Progress in Metal Physics, Edited Chalmers, and Hume Rovhey.

2.6 SCC of Glass

26. See Wiederhorn and Doremus in Reference #17.

2.7 SCC of Polymers

27. See Kambour, Marshall, and Lake in Reference #17.

2.8 Hydrogen Embrittlement

28. M. Smialowski, Hydrogen in Steel, Pergamon Press, 1962, New York.

29. A. R. Elsea, E. E. Fletcher, "Hydrogen-Induced, Delayed, Brittle, Failures of High-Strength Steels", DMIC Report 196, January 20, 1964.

30. A. R. Troiano, "The Role of Hydrogen and Other Interstitials in the Mechanical Behavior of Metals", Trans. ASM, Volume 52, 1960, p. 54-80.

31. E. E. Fletcher, A. R. Elsea, "The Effects of High-Pressure, High-Temperature Hydrogen on Steel", DMIC Report 202, March 1964.

32. E. E. Fletcher, W. E. Berry, A. R. Elsea, "Stress Corrosion Cracking and Hydrogen-Stress Cracking of High Strength Steel", DMIC Report 232, July 1966.

33. P. Cotterill, "The Hydrogen Embrittlement of Metals", Progress in Metal Physics, Volume 9, p. 205-301.

34. See articles by Oriani, McBreen and Genshaw, Tetelman, H. H. Johnson in reference #9.

3. The Politics of the Problem

3.1 The Extent

The stress corrosion problem has cost the country enormous quantities of money.

The amount of money spent on understanding the problem and developing preventative measures is ridiculous relative to the losses incurred in this country as well as others.

The traditional alarm caused by such failures have nucleated transiently enthusiastic research efforts which have usually produced more technical papers than useful engineering solutions.

Important examples of these failures are listed as follows:

1. The Silver Bridge on the Ohio River failed due to an SCC failure apparently related to sulfide contamination.

2. The turbine at Hinkley Point in England exploded due to SCC of the blade ring.

3. The liquid metal cooled Seawolf reactor failed by caustic SCC causing deactivation of that submarine until the power plant was replaced by a pressurized water unit.

4. The catastrophic pipeline failures appear to be nucleated by SCC.

5. The Nine Mile Point nuclear reactor failed at a six inch pipe and was down seven months (losing $40,000 per day of revenues).

6. The Oyster Creek nuclear reactor required complete replacement of about 130 stub tubes at the reactor bottom at a rumored cost of $50,000,000 excluding the cost of down time.

7. Approximately 1/4 of all component failures in the duPont Company are listed as being due to SCC.

8. Caustic induced failures in the paper industry have been responsible for major explosives.

9. Wing boxes (D6AC) in the F-111 incurred cracks before the aircraft left the manufacturer.

10. H_2S failures in the oil industry continue to be a major problem.

The listing of such failures could go on extensively--to an unbelievable extent and total cost. A summary of such failures and costs relative to what has been spent in understanding would be a study in ridiculous economics.

3.2 SCC is Not a Product

A major difficulty in funding research on corrosion and SCC in particular is that this research does not produce a product.

There is a peculiar mentality involved which encourages

the funding of work on new products which have doubtful profitability and spends nothing on saving money in cases where the possibility of premature failure is previously demonstrated.

3.3 The Pre-Existing Crack

The new approach to SCC utilizing fracture mechanics suggests that designers assume the existence of prior flaws. Utilizing the K_{Iscc} concept, it is possible for designers to relate their needs to metallurgically definable parameters. However, there are some problems which deserve continued and further attention:

1. The flaw size which can initiate SCC is too small to be routinely detectable by NDT techniques for high strength steels.

2. Despite the high sensitivity of the very high strength steels to SCC and the relative ease with which defects can be produced, there is a relatively small incidence of SCC. On the other hand, the necessity to work with such fragile materials when better high strength ones or low strength versions of the same ones are available seems a curious lack of communication (as well as of intelligence?). Also, many of the coatings; i.e., cadmium offer little protection from the onset of SCC.

3. The SCC of lower strength materials (stainlesses, carbon steels, copper alloys, nickel base alloys) appear to depend less on the question of prior defects than on the initiation aspect. The concept of prior defects in this class of alloys seems not to be significant criterion. This lack of dependence prevents using a fracture mechanics design criteria. For these alloys, a better relationship between SCC properties and design is needed.

3.4 The Total Environment

Many SCC failures occur under conditions for which plans were never made and tests never conducted. Thus, exhaustive testing to determine the possibility of SCC at normal and operating conditions for a component usually neglects the possibility that the component will fail due to the chloride impurities in machining lubricants. The current development of the LMFBR has selected constructional materials (austenitic stainless steels) for compatibility only with liquid sodium while totally neglecting possible premature debilitation by outside-in cracking due to chloride or caustic and neglecting materials of adequate compatibility with sodium (Inconel), but excellent resistance to outside-in problems. This oversight may be one of the costlier yet.

Examples of these non-anticipated and "spurious" causes are environments due to:

1. Hydrostatic Testing
2. Drops From Leaking Valves
3. Insulation
4. Lubricants
5. Gaskets
6. Cleaning Agents
7. NDT Agents

3.5 Solving the Problem of Education

We must consider the objective of our deliberations with respect to SCC. Is it to prevent SCC or to conduct research? What is the balance between educational efforts, engineering tests, and scientific studies?

It would seem that the natural answer is that a major effort is appropriate in the educational area in proportion to the fact that most failures of significant proportions have occurred by processes for which fixes were already known. However, this conclusion should reflect upon the following:

1. Despite the fact that type 304 stainless steel is among the most susceptible of all alloys to a variety of SCC processes, engineers continue to specify its use. This continued use is specified despite the fact that manufacturers know well the risks in using this material. Part of the problem relates to alternative alloys. Manufacturers and users feel that they would rather take the risks

with a "known" material than incur more risks in other areas (welding, fabrication, etc.) with less well known materials.

Since all the information relative to SCC of this alloy has been available to engineers for years, one wonders why it is never used.

2. Despite the fact that the D6AC, 4340, and 300M alloys are well known to be highly susceptible to SCC with their attendant small critical initial flaw size, they continue to be used. It seems incredible in view of the vast resources of the agencies and organizations involved.

Despite the intransigence, let us consider what forms "education" might take and along what paths it might follow. Education appears needed along the following lines:

1. There appears to be a large group of people, technicians and designers, who do not understand the importance of identifying the broad sources of deleterious environmental impurities. Further, the same group does not understand that failures can occur or be nucleated at any point during construction, fabrication, testing, and operation.

2. Another group, maybe metallurgists, does not understand the importance of prior engineering tests for complex situations. Typical of this group, it is

believed that SCC occurs only in liquids or only in the presence of chlorides; typical also is the neglect of variations of alloy structure and alloy chemistry normally occurring in engineering materials with respect to designing tests. The amount of prior testing should be in proportion to the seriousness of possible failure and the cost of the project.

3. There seems to be a total lack of understanding in design manuals. Where it is tacitly assumed that all metals operate in antiseptic conditions.

To address the ignorance of the above groups as well as other considerations, the following educational routes might be considered.

1. Making movies aimed at certain objectives may give the most effective way of transmitting the appropriate information. These can be packaged for presentation to technicians, management, designers, etc. These groups, after all, do not have the time nor the background to either read or digest the references. We, as a group, have a responsibility to pre-digest and to transmit effectively to our technical bretheren. To assume that our responsibility ends with the clever experiment and that the designers must dig the information out themselves is an inappropriate use by us of public research monies.
2. A systematic approach to materials pathology needs

developing and ennunciation. The stress corrosion problem is a part of a whole series of pathogenic phenomena.

3. Serious attempts need to be made to interface effectively with designers.
4. A series of highly focused technical meetings need organizing. A great deal of unfocused information is available. Examples of areas which need focusing and can be focused are:
   a. Crack tip phenomena in aqueous environments
   b. Hydrogen entry in iron
   c. Properties of passive films on iron

   The thought (often mentioned to me) that intelligent scientists cannot get together to bore into narrowly defined problems is a figment of limited imaginations.

There has been a recent attempt by NASA to prepare a design manual for interpreting SCC to the designer. This effort was a truly pathetic activity. It is misleading, lacking in quantitative contribution, and would lead people into errors as bad as the ones it is trying to prevent.

3.6 Composite Materials

Many of the SCC problems are thought of in terms of alloys having the same composition throughout the thickness in a material. The possibility of using composite materials should be considered more widely. Thus, the inside surface may be

resistant to one environment, with the outside being resistant to another. This approach seems somehow to have not been received due to the wide attention it deserves.

3.7 Coordination Among Funding Agencies

There is no coordinated national policy in the area of corrosion. Rather than bringing the country's resources together for coordinated attacks on special problems of national interest, the pervading idea seems to be to "spread it around."

The country has no explicit technical objectives in the area of corrosion. There is no sense of dedication or urgency. There is no explicit consciousness of the enormous economic losses. A useful activity would involve formulating such policies and then arranging appropriate implementation.

3.8 The Specific Ion Concept is Dead

For years, it has been thought that SCC was always a matter of being associated with a specific ion. This is not true. Stainless steels SCC in pure water. Aluminum cracks in water vapor, and so does high strength steel.

As is illustrated in the section on film concepts, the SCC problem is a part of a continuum. SCC is just one of a series of corrosion modes which depend for their existence on various conditions of pH, potential, and anion.

This matter is probably an item belonging under the discussion of Section 3.5. But it is worth identifying explicitly because it is the source of many errors in judgment both in the

analysis of failures and in the design of equipment.

3.9 The Absolute Necessity for Coordinated Interdisciplinary Programs

The major advances in SCC have not been made by small and scattered efforts. The most significant advances have been made by intensive coordinated efforts. Examples of these have been the ARPA program, the coordinated attack maintained at RIAS, the AEC sponsored effort at Ohio State, and the coordinated program at BSRL.

4. The Generality of the SCC Problem

SCC occurs in all materials: metals, glasses, ionic solids, polymers. For appropriate materials, all environments cause SCC. These include fused salts, liquid metals, gases, organic liquids, etc. Illustrations of this ambiguity are below:

1. Gases
    a. Dry ambient hydrogen with high strength steels
    b. $CO/CO_2/H_2O$ vapors with carbon steels
    c. Methanolic vapors with titanium alloys
    d. Iodine vapor with zirconium alloys
2. Non-Aqueous Fluids
    a. Methanol with titanium
    b. N_2O_4 with titanium
    c. NH_3 with carbon steel

These are simply examples. This list is no doubt as infinite as the possible material-environment combinations.

Where certain ions promote SCC it is interesting to note the wide range of their effect. While stainless steel is subject to SCC in 45% $MgCl_2$ at 154°C, it also cracks in the same kinds of times in 2 ppm solutions at 200°C.

5. Patterns in Stress Corrosion Cracking

5.1 Introduction

There are several general patterns emerging which permit correlating the SCC of certain groups of alloys. The boundary conditions and many details have yet to be defined, but these patterns are steadily emerging as useful concepts. These are correlations and are not necessarily mechanistic.

5.2 Stress Intensity at Crack Tip

The development of the stress intensity concept and its application to crack propagation has permitted the variable of stress to be correlated on a consistent basis.

The stress intensity provides the amplitude for the stress components at the crack tip. For example, in Figure 1, the value of σ xx is proportional to stress intensity.

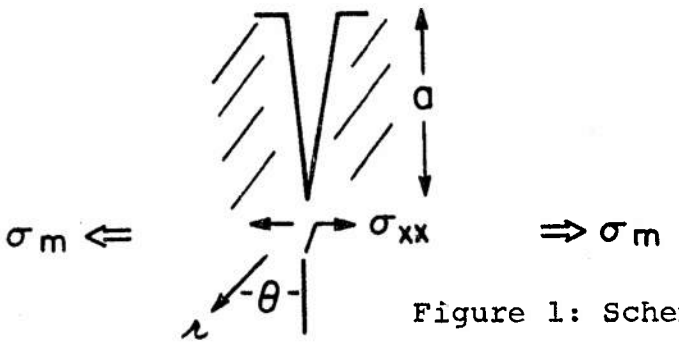

Figure 1: Schematic Diagram of Crack

In Figure 1, the value of σ_{xx} is given:

$$\sigma_{xx} \alpha K \times f\ (r,o) \qquad (1)$$

and K is the stress intensity which, depending on the overall geometry, has the general form:

$$K = \sigma\ m\ \sqrt{a} \qquad (2)$$

where σ m is the mean stress in the region of the defect having depth, a.

Since the key feature in the crack propagation is more obviously σ xx than σ m, the stress intensity approach would be expected to provide more valid correlations--and it does.

The stress intensity concept does not give either microstructural nor environmental definition. It is a continuum concept. But its introduction has provided an enormously useful tool.

This concept is limited to the condition of propagation since it is reasonable that no stress intensity can be defined for the case of initiation. This limitation is important since many SCC systems are limited by initiation conditions.

5.3 The V-K Curve

The workers at Boeing (Speidel, Blackburn, Beck, Feeny) have found that a large amount of data can be correlated according to a plot of crack velocity (V) versus stress intensity (K).

A typical V-K curve is illustrated in Figure 2. The key observation here is the existence of three stages. Stage

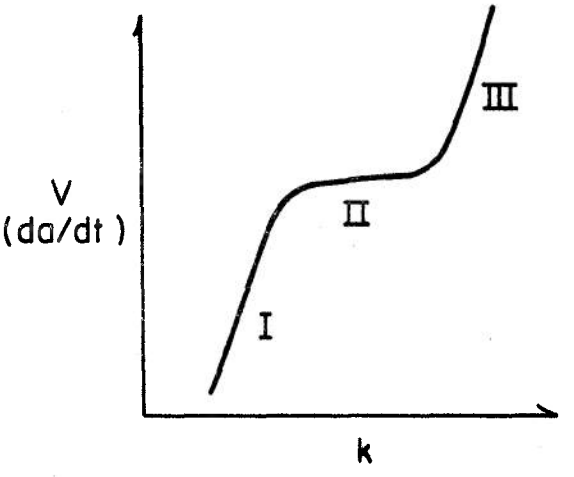

Figure 2: Typical V-K Curve Showing the Three Important Kinetic Regions

I and III have very steep dependencies of V on K whereas Stage II is independent of K. The remarkable feature of these curves is that they apply to a variety of alloys including titanium, aluminum, high strength steel, and magnesium. Also, at least for the tests conducted, they apply to a variety of environments including water, gaseous chlorine, and liquid metals.

The activation energies for Stages I and II differ. In Stage I, the activation energy is in the range of 25-30 Kcal whereas in Stage II, it is 5-10. Further, the concentration dependence of the critical species (Cl^-, H_2O, I^-, etc.) is quite different for Stages I and II.

The applicability of the V-K correlation to the more ductile alloys (copper, stainless steel, carbon steel, etc.) has not been pursued extensively because of the great tendency for

crack branching which renders the calculation of stress intensity more tedious. Some preliminary work is now being conducted by Scully.

The V-K concept grew out of a desire to put the K-t concept originally developed by Brown on a more quantitative basis. This concept which correlated initial stress intensity (K) versus failure time (t) produced the K_{Iscc} value which defined the stress intensity below which cracks would not propagate. This correlation is illustrated in Figure 3.

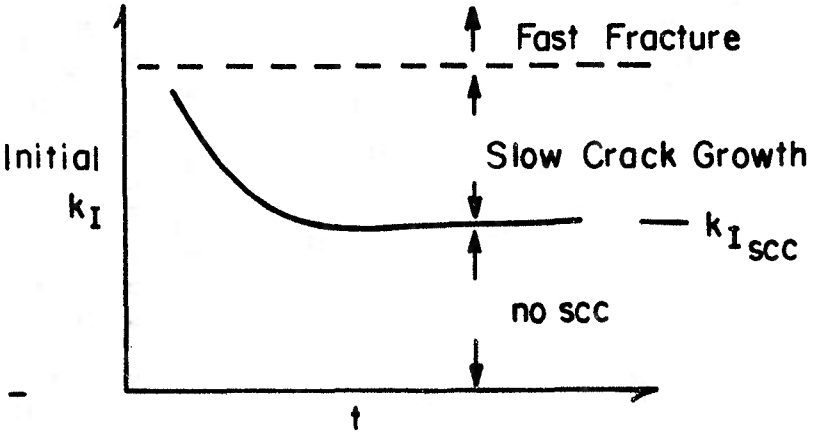

Figure 3: Schematic Illustration Showing Stress Intensity Versus Failure Time Plot

The V-K curve essentially provides K_{Iscc} as well as K_{Ic} although the matter of minimum or zero V at some low K is not yet well established.

5.4 The E-log i Correlation and the "Cracking Volume" Concept

The electrochemical polarization curve for alloys in electrolytes is a well known method for characterizing corro-

sion behavior. It has become clear in the last two years that this curve also identifies zones where SCC is more likely. These correlations work excellently for carbon steels and stainless steels. The basis for the correlation is involved with the unit process of slip-dissolution which is discussed later.

The correlation shows that SCC occurs at transitions between regions where stable protective films exist and where relatively rapid dissolution occurs as shown in Figure 4.

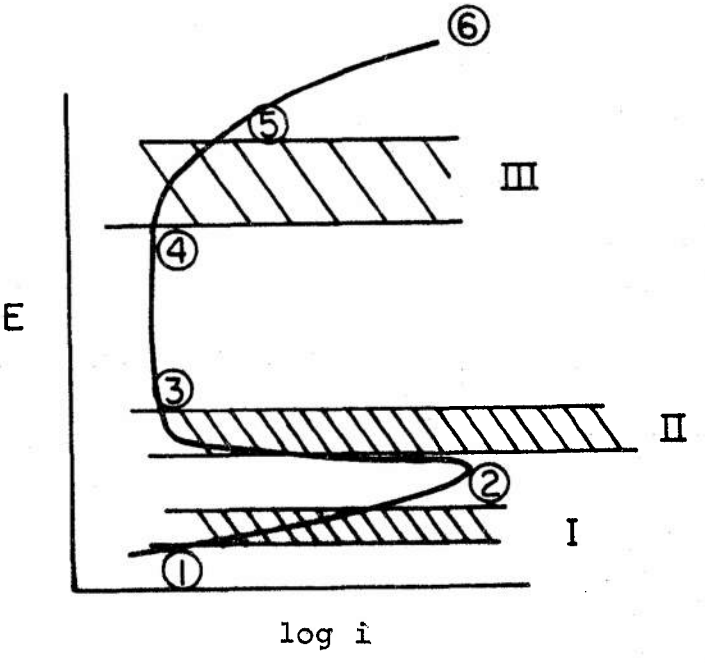

Figure 4: SCC Zones Related to the Polarization Curve

The Zones, I, II and III, do not all exist for every alloy-environment system. Their chief characteristic is their position relative to instabilities. Zone III lies in the passive region but is adjacent to a region where, at steady state, the protective film breaks down. Similarly, Zone II lies near the active

peak. The existence of Zone I depends on whether some kind of protective film exists between 1 and 2.

The SCC of stainless steel in boiling $MgCl_2$ occurs only at Zone III. The SCC of stainless steel in caustic solutions occurs in Zones I, II and III although the cracking modes are TG, TG, and IG respectively. The cracking of carbon steels in carbonates follows this pattern but cracking occurs in Zone II.

While not yet proven, this concept appears extendable to a "crack volume" with variables of potential, temperature, pH, environmental species (Cl^-, I^-, etc.). This concept begs the question of initiation versus propagation and also does not define the V-K but does provide a framework in which the cracking of a given alloy-environment system can fit.

The great value of the cracking volume approach is the possibility of defining it relative to other electrochemically significant processes such as pitting, intergranular attack, passivity, and general attack. A definition of the cracking volume permits designers to arrange alloy selection and environmental control in such a way as to assure the absence of SCC.

5.5 The Interface Between SCC and Corrosion Fatigue

The usual stress corrosion experiment involves a single application of load which remains constant until the specimen breaks prematurely. This, in fatigue terms, is simply a very low cycle fatigue test as illustrated in Figure 5.

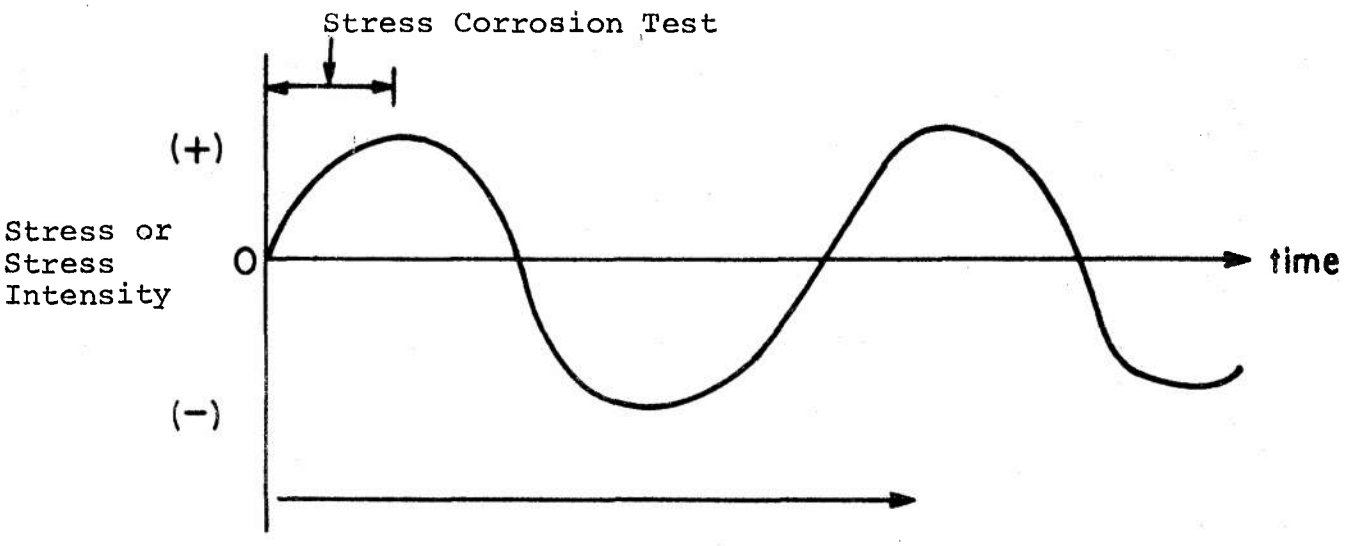

Figure 5: Schematic Illustration of Stress or Stress Intensity versus Time in Fatigue

The correlation between SCC and corrosion fatigue is best understood in terms of da/dN, the crack advance per cycle. Similar to the V-K curve of Figure 2, da/dN can be understood in terms of Figure 6 for da/dN versus Δ K.

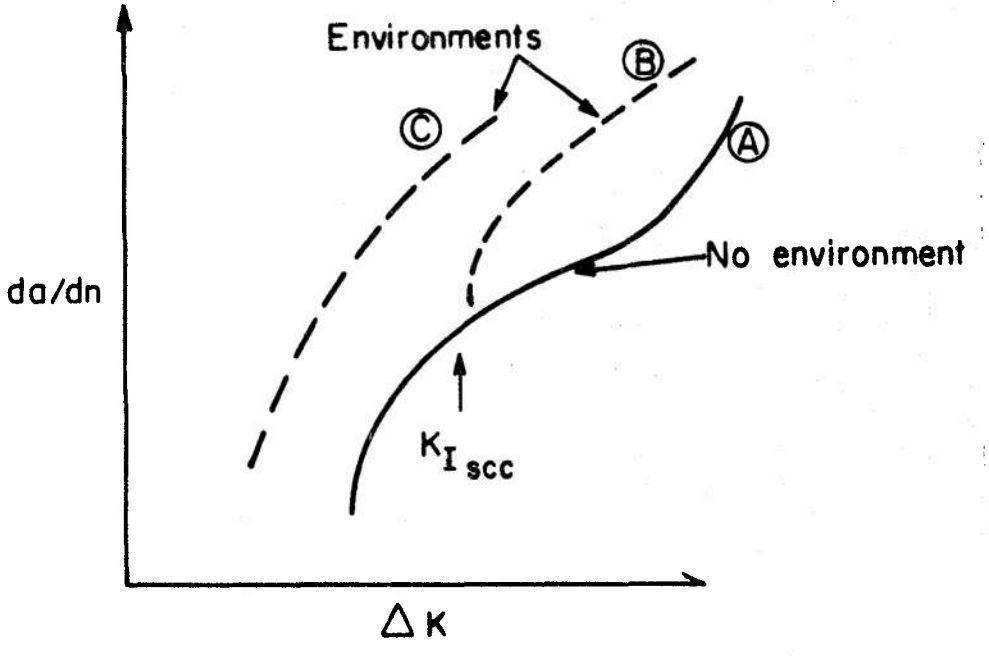

Figure 6: Schematic Illustration of Crack Advance Rate Versus Stress Intensity. Effects of environment are illustrated.

For K min = 0 the environmental contribution illustrated in Figure 6 as Curve B can, for some alloys, find its minimum at K_{Iscc}. However, for other alloys the minimum is lower than K_{Iscc} as illustrated in Curve C of Figure 6.

Cyclic frequency plays a major role in environmental effects with increasing frequency diminishing the environmental contribution.

5.6 The Strength Level Correlation

For environments where the crack process is clearly one involving the entry of hydrogen entry, there is a general correlation for increased susceptibility with increasing alloy strength. It is interesting that the reverse follows where anodic (oxidative) processes seem to dominate.

5.7 The Pure Metal Correlation

There is a general correlation existing that metals become more resistant to SCC as they become more pure. While the detailed reasons for this are not at all clear, the correlation has been found many times to be valid. The trend operates for the situation where all elements are removed and the direction of purity is toward the absolutely solute-free metal. There is a similar trend for high purity alloys where the interstitial impurities are removed.

There may be exceptions to the high purity idea in liquid metal SCC and in the SCC of zirconium by gaseous iodine. There may be still further cases of SCC of pure metals if we

can get people to stop testing only in environments like $MgCl_2$ and change the pH or temperature. However, the pattern of pure metal resistance is still one of general interest.

Mechanistically, the high purity correlation may relate to grain boundary composition, slip processes, or film formation behavior.

6. The Elements of Environmentally Influenced Cracking of Solids

The ultimate aim of any consideration here is to produce a basis for the quantitative prediction of environmentally influenced cracking (EIC) of solids.

This desirable objective is made very difficult because EIC involves the simultaneous interaction of a variety of individual processes which, by themselves, are not well understood. For this reason one may certainly ask "why try?".

The essential theme of this outline is that the situation is not hopeless and it may be constructively approached by (a) identifying the unit processes involved in EIC and (b) quantifying these processes. From these the overall nature of a given EIC system may be synthesized. Fortunately, certain unit processes may be neglected depending on the metal-environment system being considered.

We must emphasize also, relative to this section, that we are concerned about general environmentally-influenced cracking. This subject includes:

1. Stress causing cracking (static stress)

2. Creep rupture (when accelerated by an environment)

3. Corrosion fatigue including thermal fatigue (oscillating temperatures)

4. Oxidation induced cracking (cracks in uranium are induced because of coherency stresses at the oxide-metal interface)

There are also interesting peripheral areas. For example, the same factor which produces temper embrittlement--grain boundary segregation--renders the boundaries susceptible to SCC at certain potentials and solution chemistries. The case of sensitized stainless steel is similar; at very oxidizing conditions the grain boundaries corrode whereas at less oxidizing conditions, and under stress, the material is subject to SCC.

An objective of this outline is to make available to those in the component disciplines a perspective and a qualitative description of these elements.

6.1 Purely Mechanical Considerations

Since stress is an important aspect of EIC, this section outlines important ideas which are independent of environmental considerations. This section includes micro-structural as well as continuum ideas.

6.2 Slip Coplanarity

Coplanarity of slip, since 1960, has played an important role in understanding EIC. There are excellent positive correlations between EIC and coplanarity although it must be pointed out that other explanations can be found for these correlations. A good example of a correlation is the case of Ti-Al alloys.

Slip coplanarity is favored by low stacking fault energy, ordered structures (long and short range) and coherent precipitation.

Coplanarity is important at surfaces and within the metal. At the surface, a high degree of coplanarity gives more discrete steps as shown in Figure 7.

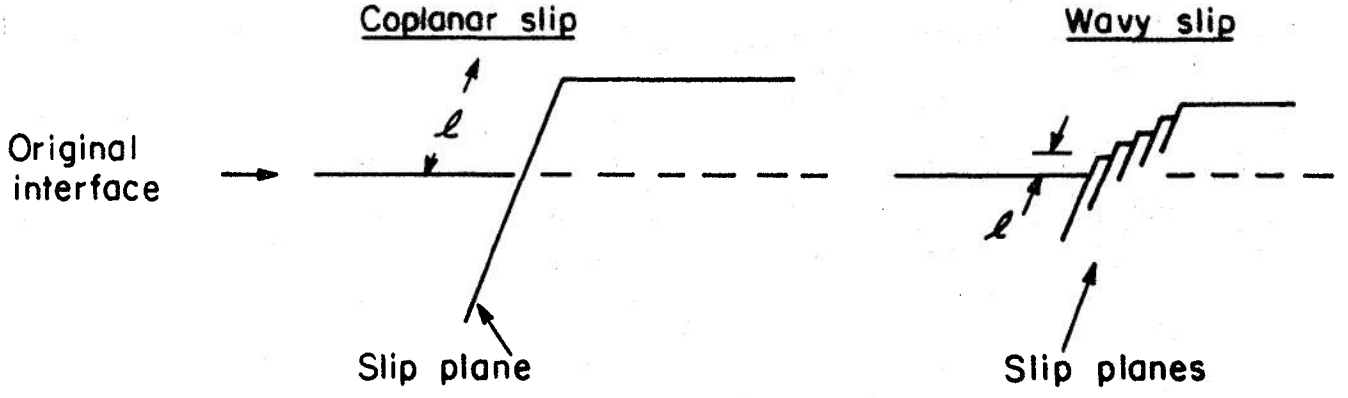

Figure 7: Schematic Illustration of Coplanar and Wavy Slip

If the step height, ℓ, for coplanar slip is large relative to the passive film thickness, then a substantial amount of unprotected underlying metal is exposed. In the case of wavy

slip, the average step height ℓ will be smaller and more on the order of the passive film thickness.

Slip coplanarity may also be important internally in the metal in connection with crack nucleation owing to pile-up stresses as shown in Figure 8.

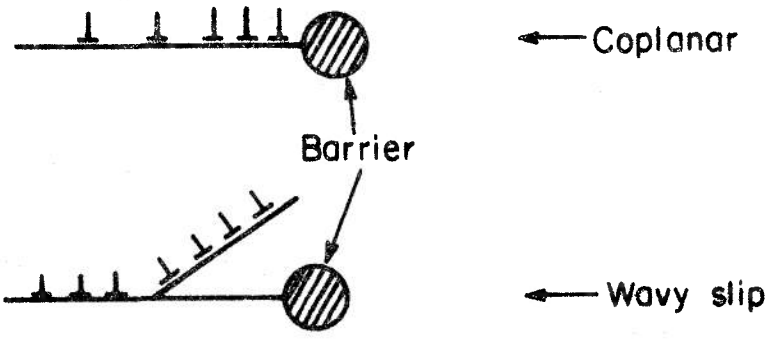

Figure 8: Schematic Illustration of Action of Dislocations at Internal Barriers Relative to Coplanarity

The degree of slip coplanarity may also affect the detailed geometry of the crack tip region.

6.3 Void Nucleation

Nucleation of voids ahead of advancing cracks in non-environmentally affected failure is a well documented observation. This void nucleation may be relevant environmentally in two ways. First, environmental species; i.e., hydrogen, could interact to stabilize voids. Second, the high strain rate in the ligaments may interact with the environment resulting in an accelerated reduction in area. The geometrical aspect

is illustrated in Figure 9 below.

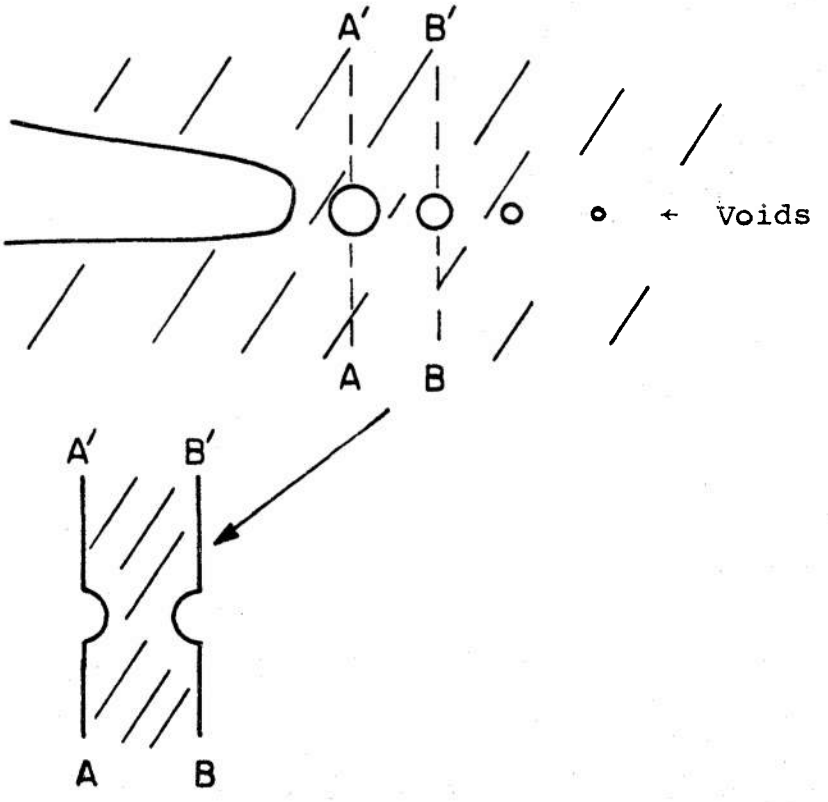

Figure 9: Schematic Illustration of Void Nucleation at a Crack Tip and Relation to a Tensile Test

6.4 Elastic-Plastic Continuum

This subject has been summarized by McClintock in this conference where he arranged approaches to considering cracks from a macro aspect to the micro-atomic scale. These are an appropriate part of this overall review, but the reader is referred to McClintock's contribution.

6.5 Dislocation-Solute Interaction

While the strain energy alone of a dislocation appears to contribute little to dissolution, there is a demonstrated effect on dissolution due to the attraction of solute atoms. While the dissolution aspect is the subject of a later section, the strain-solute interaction is important. Solutes may be either attracted or rejected and either of the following cases may accelerate localized dissolution:

1. Rejecting a passivating element (e.g., Cr, Si) from an iron dislocation.
2. Attracting an element that destroys passivity (P,S).

6.6 Mechanically Stable Tunnels

According to McClintock,* the crack tip can stabilize a mechanically induced tunnel geometry depending on the crack velocity, (å), stress intensity (K), and material properties. Detailed criteria (dimensions and precise ranges if å and K) are not available. A schematic geometry is shown in Figure 10.

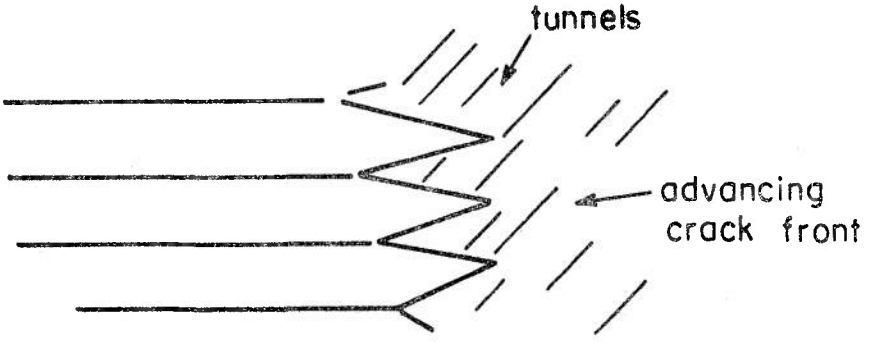

Figure 10: Schematic Illustration of Tunnel Arrangement at Advancing Crack Front

*Private communication at conference.

6.7 Adsorption of Gases

Gas adsorption may interact mechanically in several ways. This section considers only adsorption aspects of gas-metal interaction as opposed to oxide growth or significant inward diffusion. These important considerations are summarized below.

6.8 Fatigue Effects

In the opening and closing of a crack in fatigue, a certain amount of re-welding takes place in high vacuum in the absence of an adsorbing gas.

The significant consideration here is the duration the crack tip is open relative to the time required for coverage of some fractional amount.

6.9 Embrittling Effects

In this conference, Gilman described a model of crack advance involving simultaneously the stifling of slip at sides of the crack tip and promoting of decohesion by the environment.

6.10 Formation of Volatile Species

The formation of the volatile ZrI_4 appears to be the critical species in the SCC of Zr. By analogy there are other volatile species MoO_3, $TiCl_4$, TiI_4 and SiH_4. These species, like the ions in electrolytes, are "soluble" in the vapor.

The basis for mentioning this item here has to do with the competitive adsorption of reacting gases, some of which may form volatile species and others may block this process.

6.11 Reaction Processes

This section summarizes those reaction processes which are significant to understanding EIC. The variety of such processes is such that it is easier to discuss them directly than to introduce them.

6.12 The Double Layer

In electrolytes, the metal-solution interface is charged. The sign of the charge depends on the electrochemical potential. Schematically, the interface is depicted in Figure 11.

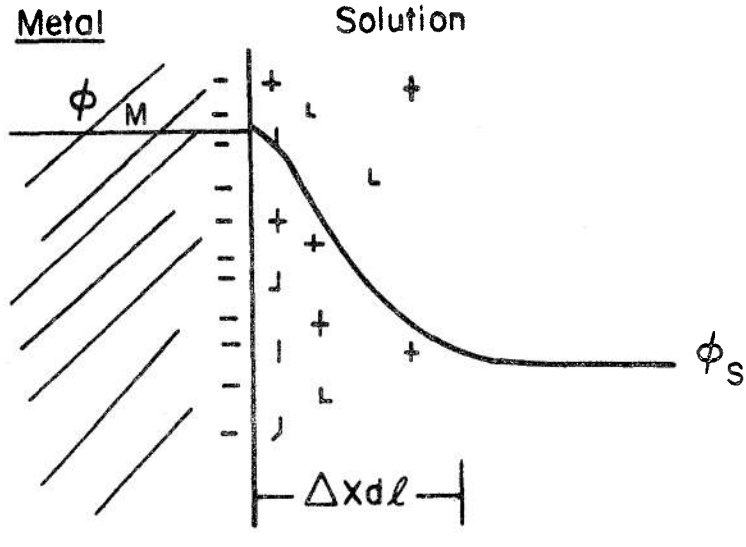

Figure 11: Schematic Potential Distribution at the Surface of a Metal in an Electrolyte

Here ϕ_M and ϕ_s are the inner potentials of the metal at solution and $\phi_M - \phi_s = E + K$, where E is the measured electrochemical potential and K is determined by the reference electrode.

The thickness of the double layer $\Delta X_{d\ell}$ depends on the solution concentration. The value of $\Delta X_{d\ell}$ is about 10Å for concentrated solutions ($\omega > 1$ M) at about 100Å for dilute solutions ($\omega > 0.001$ M).

This construction is shown only for the film free case. The detailed structure of this layer is less clear for the filmed case.

6.13 Dissolution Kinetics

The rate of dissolution of metals into electrolytes appears to be an important quantity both in cases where dissolution and hydrogen entry is important. In the absence of protective films, the general expression for dissolution ($M \rightarrow M^{n+} + ne$) is:

$$i_a = K[C_s]\, e^{\frac{-\Delta G^*_a}{RT}}\, e^{\frac{+ZF\alpha E}{RT}}$$

where C_s = concentration of surface sites

ΔG^*_a = anodic activation energy

Z = charge in activated species

F = Faraday constant

α = transmission coefficient

E = electrochemical potential

i_e = oxidation or anodic current density

Important quantitative considerations are the following:

1. Ranking by Standard Potential

In general, the $e^{\frac{-\Delta G_a^*}{RT}}$ term follows the pattern of the standard potential where:

for
$$M \rightleftarrows M^{n+} + Ne \qquad (2)$$

$$E_o = E_o^\circ + \frac{2.3\,RT}{nF} \log M^{n+} \qquad (3)$$

So, schematically in Figure 12, some important elements are arranged.

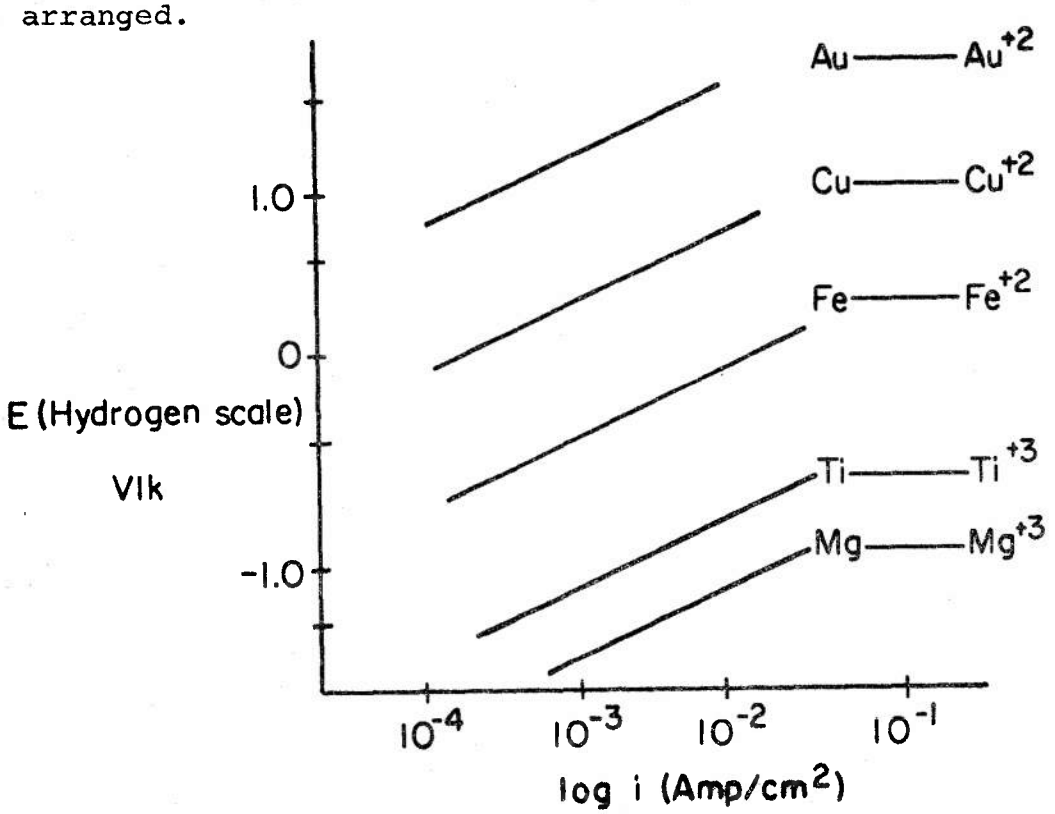

Figure 12: Schematic Relative Arrangement of i_a for Selected Metals

With respect to the SCC question, Figure 12 suggests that more active metals like Ti and Mg ought to propagate cracks faster than iron base alloys--they do!

The recession rate of the surface is given by the relationship:

$$\dot{X} = \frac{A}{Fn\rho} i \qquad (4)$$

where A = atomic weight (gms)

n = charge per ion

ρ = density (gm/cm^3)

i = current density (A/cm^2)

$\dot{X}$ = rate of surface recession (cm/sec)

For iron:

$$\dot{X} = (3.7 \times 10^{-5})i \quad (cm/sec)$$

where i is in units of A/cm^2

It is interesting to compare this rate with the plateau velocities of Ti and Al SCC which are in the same range as that given in Eq. (4). Currents of 1-10 A/cm^2 would give plateau velocities of 3-30 x 10^{-5} cm/sec.

2. Limitation Due to Mass Transfer

At current densities in the range of 10^{-1} to 10 amp/cm^2 the oxidation rate becomes mass transfer limited in static solutions.

3. Limitation Due to Film Formation

The easy dissolution into solution is limited by the formation of product layers. The maximum current reached when a protective film is present varies from 10^{-8} to 1 amp depending on the pH, the metal, and species in solution.

4. Enrichment of the Surface

In the absence of a protective film, the dissolution of alloys may be greatly reduced by enriching one of the alloy species. In the case of alloy AB, there are three important cases with respect to the electrochemical potential as depicted in Figure 13.

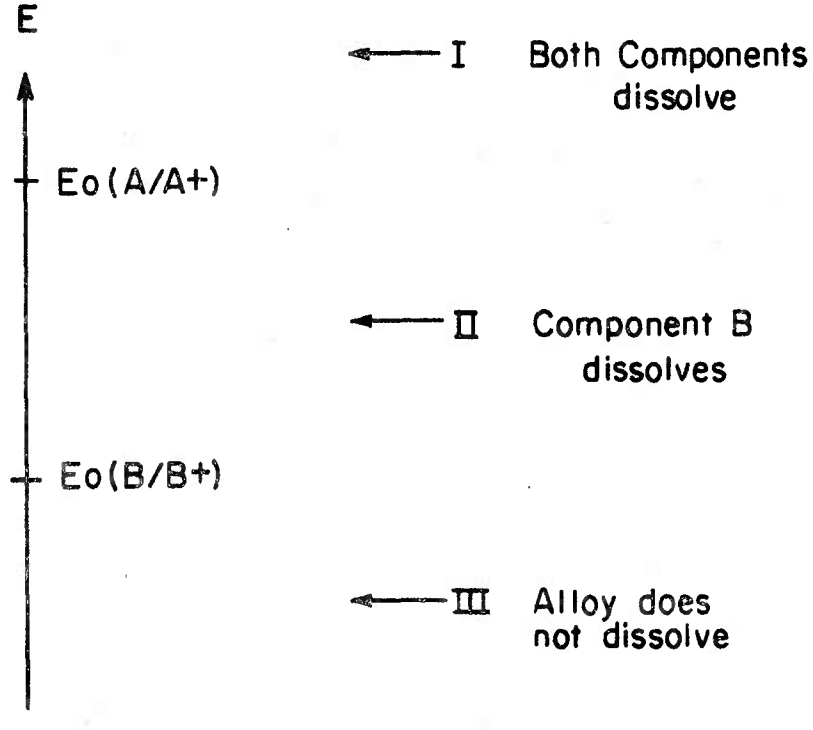

Figure 13: Three Cases of Possible Dissolution with Respect to the Standard Potentials of the Alloy Components A, B

If the potential is in Region III, no reaction occurs and the alloy is stable. This case is epitomized by Cu-Au alloys in deaerated aqueous solutions. If the potential is in Region II, Component B dissolves, but Component A remains inert. This case applies to Cu-Zn alloys in deaerated solutions or Cu-Au in solutions containing O_2 or Fe^{+3}. If the potential is in the range of III, both components may dissolve or one may have a much larger rate constant and enrichment will occur in one of the species.

For Region II, the i-t behavior of Component B follows the pattern of Figure 14.

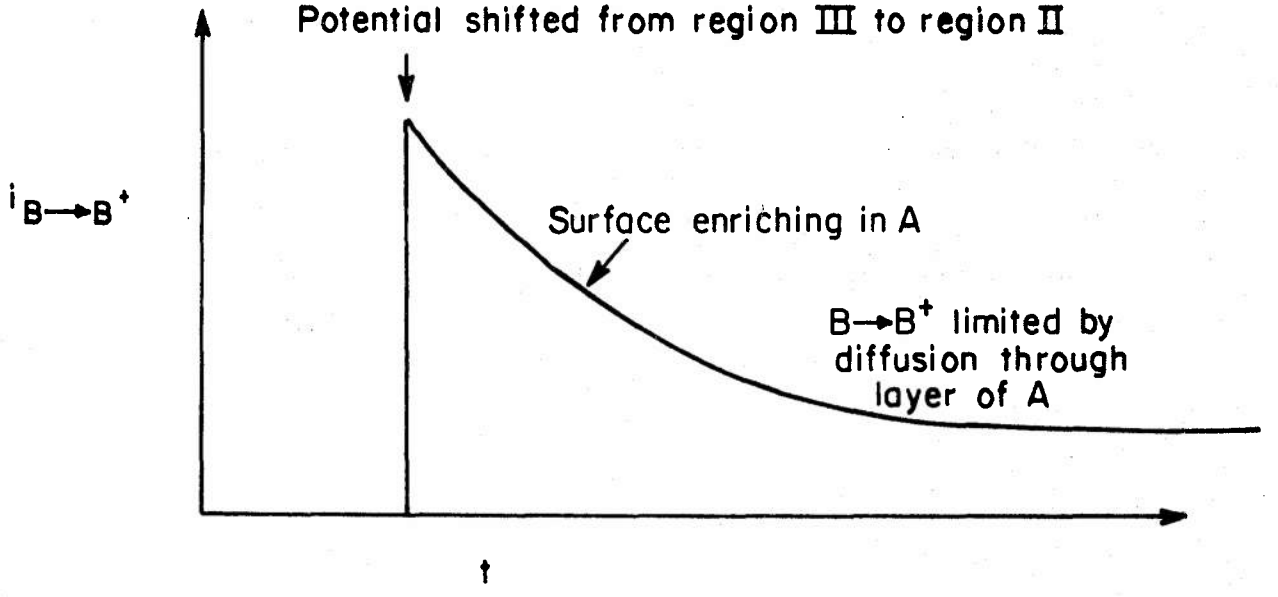

Figure 14: Schematic i-t Behavior for the Dissolution of B in Region II of Figure 13.

In Region I, the dissolution of either component may follow the pattern of Figure 14 or both components may dissolve with the same specific rate constant. There is an influence effect here wherein the rate constant of Species A may be affected by that of B according to:

$$\Delta G^* \text{ (of A in AB)} = N_A \Delta G^*_a + N_B \Delta G^*_B \qquad (5)$$

which gives a dissolution current at constant potential shown in Figure 15. Refer here to the equation (1) for anodic kinetics.

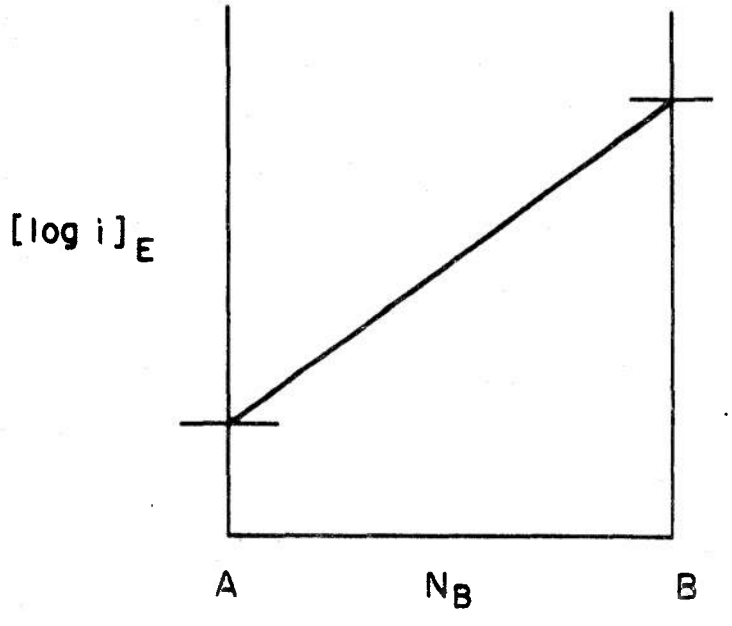

Figure 15: Dissolution Current of Species A in Alloy AB at Constant Potential

In Fe-Ni alloys in acid solution, the difference in the end points is approximately 10^3 with the iron being more reactive. The general pattern of SCC of Fe-Ni alloys follows this trend!

6.14 Product Layer Formation (Steady State)

Product layers form on metals either by direct oxidation or by precipitation. In the former case:

$$M + H_2O \rightarrow MO + 2H^+ + 2e \qquad (6)$$

or

$$M^{++} + H\,O \rightarrow MO + 2H^+ \qquad (7)$$

The criteria for existence of such reactions are summarized in the well known Pourbaix diagrams illustrated (approximately for iron) in Figure 16.

These diagrams define the existence of phases much the same as binary equilibria diagrams do in metallurgy.

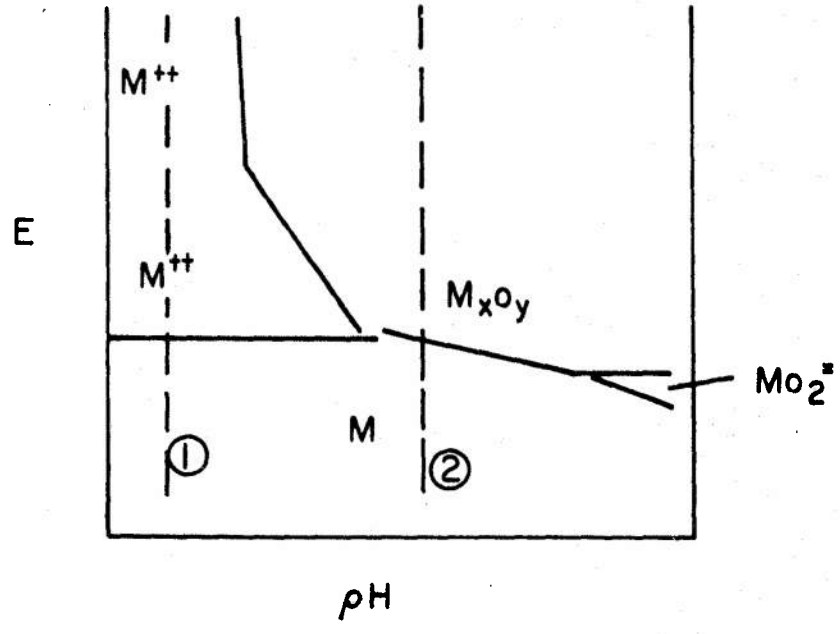

Figure 16: Schematic Pourbaix Diagram Showing Regions of Stability of Possible Species

While these diagrams furnish general guides, they do not predict films which are observed experimentally to form in the region of M^{X+} nor do they predict rates of reactions. These films provide barriers which reduce the reaction rate to 10^{-5} to 10^{-7} A.cm^2. Taking lines (1) and (2) of Figure 16, the i-E behavior would appear as shown in Figure 17.

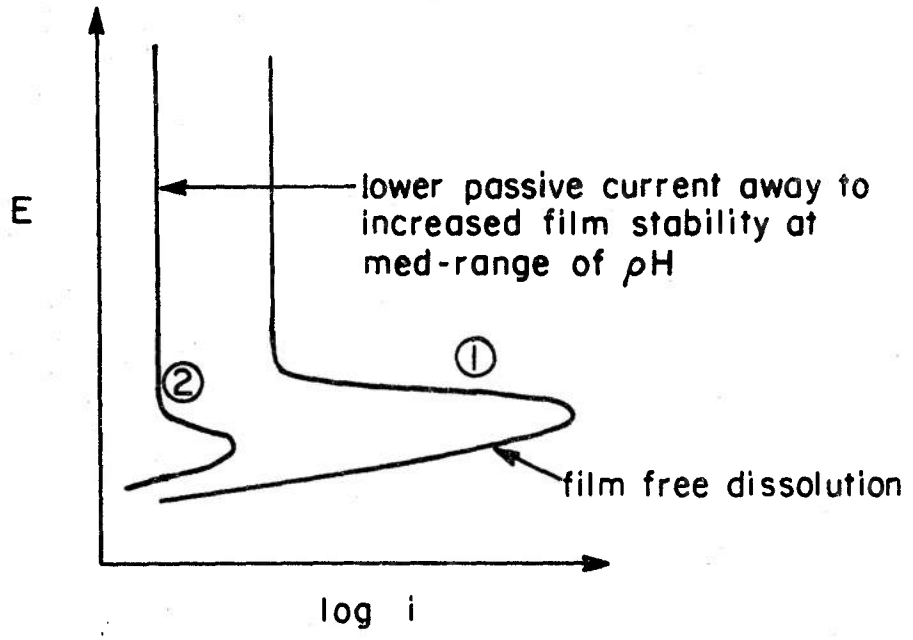

Figure 17: Schematic Illustration of Polarization Curves as a Function of pH

It is not necessary that the protective film be an oxide. It may also be a fluoride or sulfide. For example, the formation of MgF_2 gives a greatly increased range of stability of Mg. From:

$$Mg^{++} + 2HF \rightleftarrows MgF_2 + 2H^+ \qquad (8)$$

There is a greatly increased range of metal stability relative to the oxide.

$$Mg^{++} + H_2O \rightleftarrows MgO + 2H^+ \qquad (9)$$

Similar situations exist for sulfides, carbonates, etc. The relative effects of (8) and (9) are shown in Figure 18.

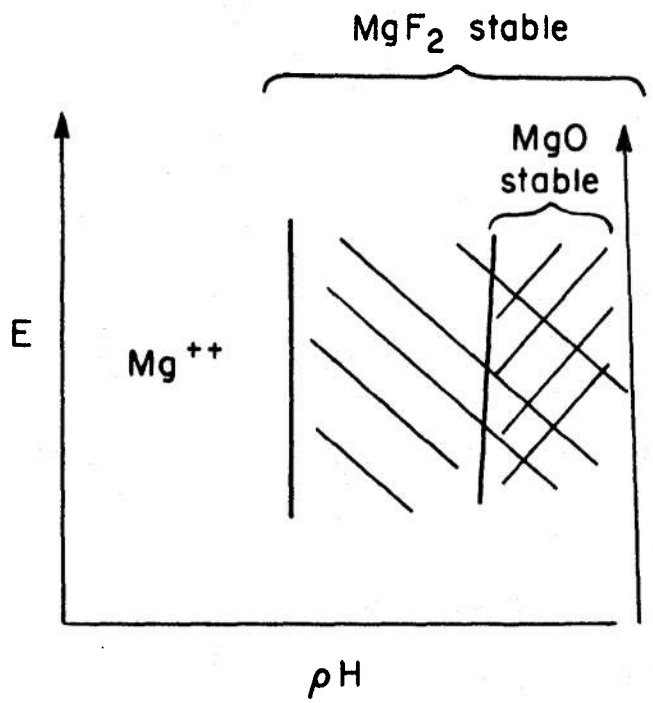

Figure 18: Schematic Effect of MgO Versus MgF on the Product Layer in Mg

In a wide range of metals including Ti, Fe, Ni, Cr, the growth law for the protective films follows an empirical law of the form:

$$\Delta X = (A + B \log t)\ (E-E_A) \qquad (10)$$

where ΔX = thickness of film

t = time

A,B = constants

E_A = potential at about $\Delta X = 0$

This shows that the films grow slowly and that the thickness is linearly proportional to potential. The constant A is of the order 10-50Å. The value of E_A corresponds about to the peak of Figure 17. Examples of data are shown in Figure 19.

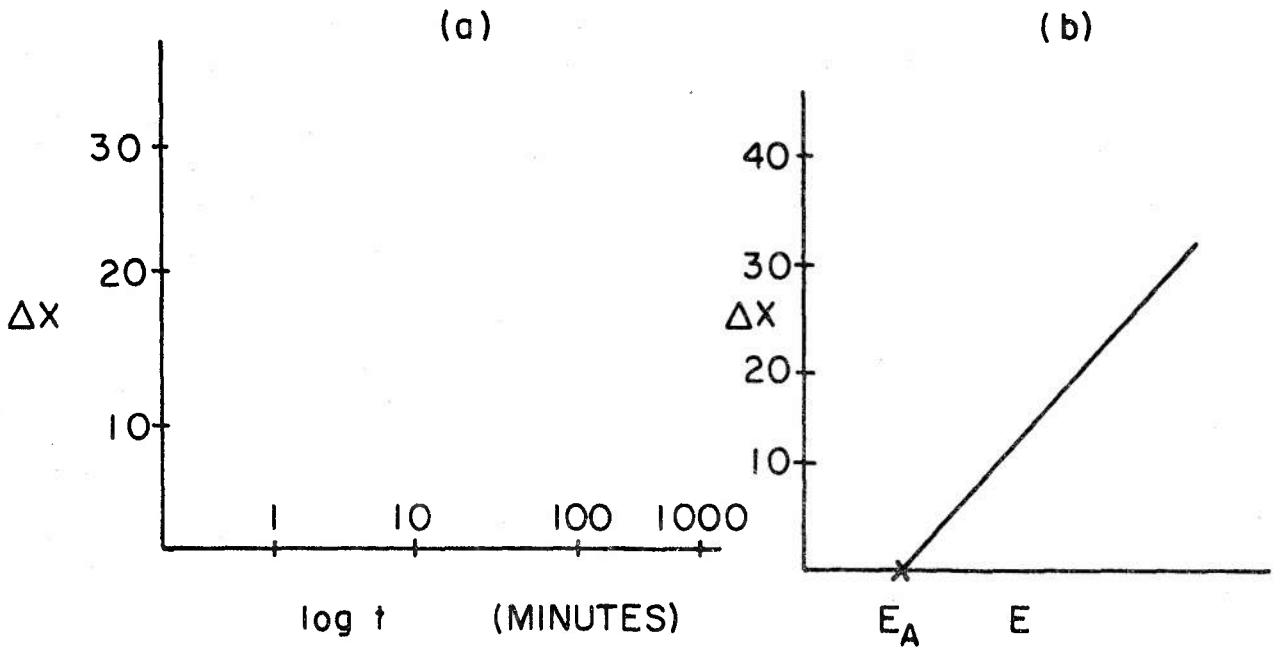

Figure 19: Approximate values for ΔX versus log t and ΔX versus E for iron at pH8 and room temperature. Figure (a) is typical of the behavior in the mid-range of passivity (~ + 0.400 volts) and (b) is for 100 minutes.

The film growth rates at low temperatures (i.e,, room temperature) are dominated by the field, $(\frac{V}{\Delta X}) = \varepsilon$, across the film. After a certain thickness, the film thickness tends to a limiting value. Times for such a limiting thickness depend but may be ascertained from the logarithmic behavior of Figure 19 (a).

The steady state film thickness depends also on the pH. The oxides may dissolve according to:

$$MO + H^{+} \rightarrow M^{++} + \Delta H^{-} \qquad \text{(acid)} \qquad (11)$$

or

$$MO + H_2O \rightarrow MO_2^{=} + 2H^{+} \qquad \text{(caustic)} \qquad (12)$$

Thus, the actual thickness depends on Eqs. 10, 11, 12 according to:

$$X(t) = \text{rate of formation - rate of dissolution} \qquad (13)$$

While the rate of film growth is well defined, the dissolution kinetics are not, so that a detailed expression for (13) is not available.

6.14 Transient Film Formation

When a protective film is instantaneously broken, clean surface is exposed. The competing processes are illustrated in Figure 20. Here at time t = 0+, there is a clean surface

where originally it was protected by a film.

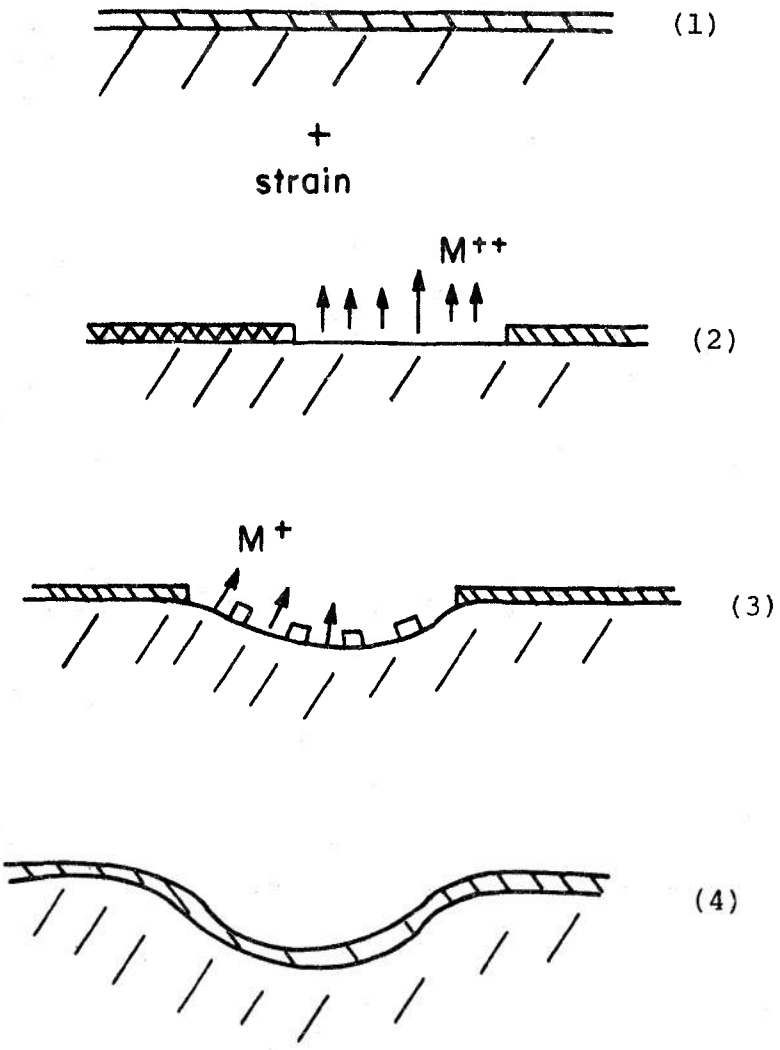

Figure 20: Schematic illustration of film breaking and reformation.

The time scale over which the processes of Figure 20

operates is given by Figure 21.

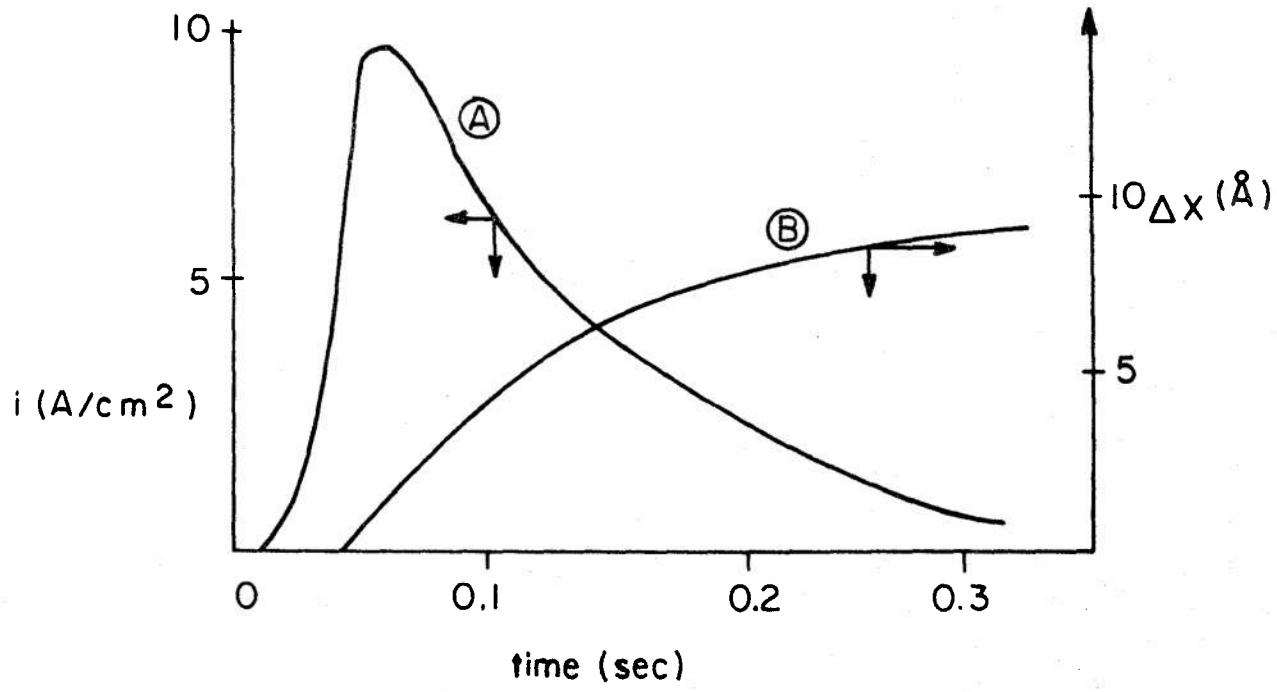

Figure 21: Approximate time dependence of the dissolution current (A) and the film thickness (B) for iron in neutral solution at room temperature.

The detailed nature of curves (A) and (B) depends greatly on the alloy, environment (E, anions, pH and temperature.) The number of coulombs, Q, under (A) or (B) may vary from $Q_A = Q_B$ to $Q_A >> Q_B$.

Of particular importance is the speed with which the film begins to reform. These same processes certainly operate at a crack tip.

6.15 Kinetics of the Reduction Processes

The kinetic processes in the reduction of oxidized species in the environment are crucial considerations in corrosion and EIC processes.

The key species which are reduced in electrochemical-industrial environments are water and oxygen according to:

$$O_2 + 4H^+ + 4e = 2H_2O \qquad (13)$$

$$E_o = 1.228 - 0.059\ pH + 0.014 \log P_{O_2}$$

and

$$H_2O + e = \frac{1}{2} H_2 + OH^- \qquad (14)$$

$$E_o = 0.0 - 0.059\ pH - 0.030 \log PH_2$$

There are other important reduction processes such as:

$$I_2 + 2e \rightarrow I^-$$

$$C\ell_2 + 2e \rightarrow C\ell^-$$

$$Fe^{+3} + e \rightarrow Fe^{+2}$$

$$MO = e + H^+ \rightarrow M + OH^-$$

etc.

For species in aqueous solution, the rate of reduction,

without mass transport limitation, follows an equation similar to (1):

$$i_c = K[C]\, e^{\frac{-\Delta G_c^*}{RT}}\, e^{\frac{-ZF\,(1-\alpha)\,E}{RT}} \qquad (15a)$$

$$i_c = i_{o,c}\, e^{\frac{-ZF\,(1-\alpha)\,E}{RT}} \qquad (15b)$$

For an iron substrate $i_{o,c}$ for water reduction is in the range of 10^{-5} A/cm^2 for pH = 0; and for oxygen reduction $i_{o,c}$ is in the range of 10^{-10} A/cm^2. i_c depends then on E, [C] and ΔG^*.

With respect to EIC, the reduction kinetics control two important aspects.

1. Open Circuit Potential

The open circuit potential is controlled by the rate of the reduction kinetics according to the concept of mixed electrode theory. For example, the open circuit potential on a stainless steel at reactor operating temperature is 400 mV higher for a BWR with ~1.0 ppm O_2 than for a PWR with ~0.001 ppm. This difference of potential is sufficient to move one in and out of the critical SCC region, as illustrated in Figure 22.

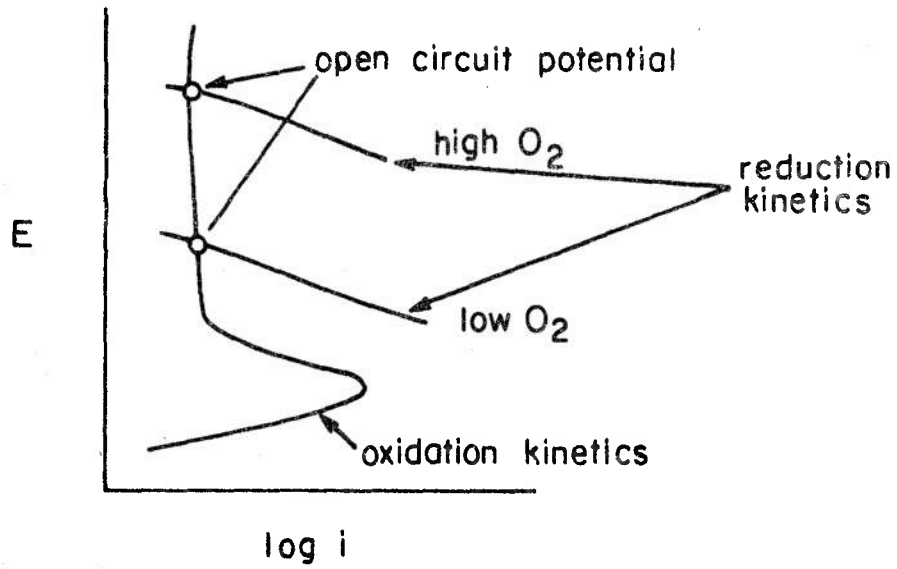

Figure 22: Schematic illustration of effect of oxygen on open circuit potential.

2. Availability of Hydrogen for Entry

Since an important aspect of EIC involves hydrogen entry, the kinetics of water reduction are relevant. The hydrogen available for entry into the metal is related to the step-wise process.

$$H_2O \rightarrow 2H_{ads} \rightarrow H_i \uparrow \qquad (16)$$

$$H_2O \rightarrow 2H_{ads} \rightarrow H_2 \uparrow$$

The amount of hydrogen which actually enters the metal depends on the rate of the reduction process. This amount is typically in the range of 1-10%. In many cases for iron, the

absorption rate follows a pattern:

$$i_{abs} = K(i_{total})^{\frac{1}{n}} \qquad (17)$$

where i_{total} is the total amount of hydrogen produced and $n \sim 2$.

6.16 Kinetics of the Hydrogen Entry Process

While (17) describes a general behavior, the actual amount absorbed is frequently influenced by "poisons" which can greatly influence the rate of entry. For example, arsenic greatly accelerates the entry process. The value of K in Eq. (17) may be increased by factors of 2-20, depending on the poison or the potential.

While it is commonly the approach to use arsenic in solution as the arsenite, $A_sO_2^-$, the presence of pure arsenic on the surface exerts the same effect. Thus, the possibility of arsenic alloyed in the metal or at grain boundaries would accelerate the entry at those sites where the arsenic concentration is significant. Sulfur similarly accelerates hydrogen entry.

6.17 Tunneling Processes

It is possible to produce in alloys penetrations of a high ℓ/d geometry. These processes produce a condition of one dimensional growth where the sides do not extend laterally to to any significant extent. Such a geometry is illustrated in

Figure 23 below:

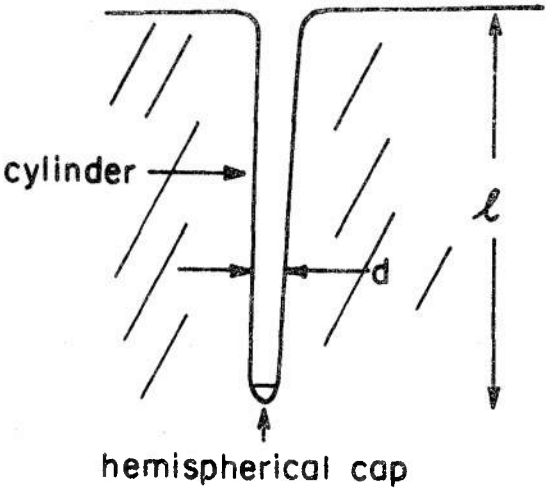

Figure 23: Schematic illustration of tunnel penetration into a solid.

The process of pitting involves the lateral progress of the side and there is the tendency to produce a hemispherical penetration. Below are described two processes which give these geometries. These two processes are not too different but do show differences in detail.

1. The Swann Model

This development is mainly due to Swann (Imperial College). Assume that a metal stops dissolving after a certain amount of reaction. Specifically, take the case of a Cu-Au alloy, described

in Figure 15; here, the dissolution essentially stops after several layers of gold have accumulated on the surface. If we now examine the behavior of a cylinder versus a hemispherical cap but at constant radius we find:

$$\left[\left(\frac{V}{S}\right)_{cyl} < \left(\frac{V}{S}\right)_{hemisphere}\right]_{r = k} \qquad (18)$$

This means that the hemispheral cap is always unstable with respect to a cylinder at the same radius and so the tunnel of Figure 23 will continue to propagate. The maximum velocity of this will again be governed by Eq. (4). This velocity will be diminished by concentration polarization.

The values of d observed are in the range of 50-500 Å with ℓ/d being 10-100.

These tunnels could not form as the noble component increases in the concentration since the critical amount of dissolution before cessation of significant propagate approaches one monolayer in the range of 50% Au.

A similar process appears to operate for the case of metals which form product layer films. Such tunnels have been observed in stainless steels. The d dimension of these tunnels appears to be about an order of magnitude greater than for the noble metal type.

2. The Westwood Model

Imagine the case where lateral ledge motion is stopped by adsorption of ledge poisons. In the absence of these poisons, the lateral ledge velocity is uninhibited and the material simply dissolves. If there is a superabundance of poison, the ledge motion is stopped almost instantaneously and no dissolution occurs. In an intermediate case, the ledges move some distance until sufficient poison accumulates to stop lateral motion. Simultaneously, a new ledge is nucleated and progresses laterally until stopping. This process produces a tunnel geometry depicted in Figure 24.

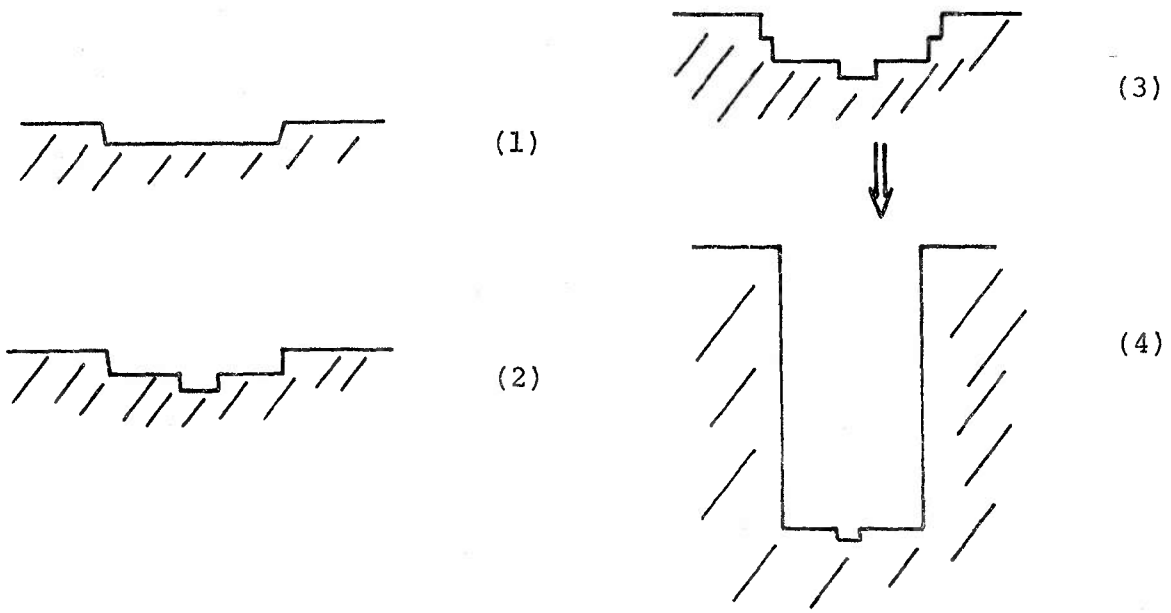

Figure 24: Schematic illustration of tunnel growth controlled by effect of poison on lateral ledge motion.

The rate of the tunnel growth is controlled by the nucleation of dissolution events in terrace. Diameters appear to be on the order of 1μ.

6.18 Effects of Straining on Dissolution

The rate of reaction as influenced by straining may be divided into the following categories.

1. Film Free Metals

The two components of straining involve surface slip and increasing the internal energy. The former dominates the observed effects; there is very little evidence that the internal energy contribution is significant.

If the dissolution current of a straining current is measured, the reaction is dominated by the increase in area and the increase in rate per unit area at any instant is increased by an amount on the order of a factor of two to four. This increase can be shown simply to result from less stable ledge configurations because, upon cessation of straining, the current decreases to a value linearly related to the increased area. Thus, the $\dot{X}_o$ of equation (4) is not significantly affected by straining the film free material. Schematically, this situation is illustrated in Figure 25.

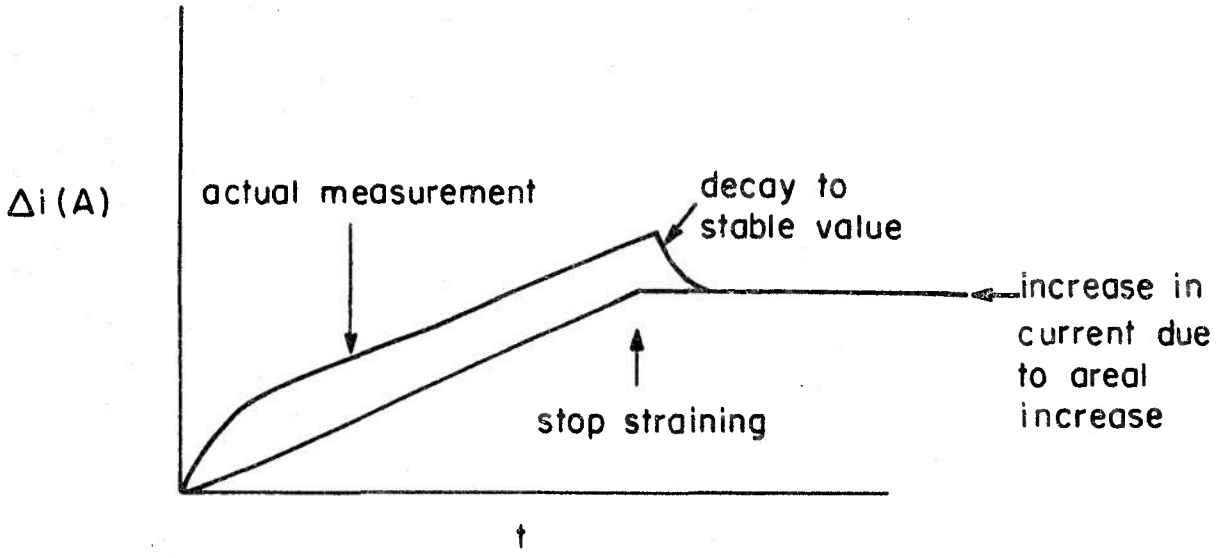

Figure 25: Schematic i-t behavior for straining a film free electrode at constant potential and constant strain rate.

2. Film Covered Metals

This subject was covered in the previous section on transient re-formation of protective films.

The upper limits of current density in the film free areas (made film free by straining) appear to be controlled by an extrapolation (log i versus E) of the film free kinetics to higher potentials operating in the region of film coverage. Thus, peak currents on transiently film free surfaces might approach 10-100 A/cm^2 at higher potentials although they would decay rapidly.

Typical steady state current densities for filmed surfaces are 10^{-9} to 10^{-5} A/cm^2.

6.19 Hydrogen Within the Lattice

Of the available environmental species, only hydrogen enters significantly into the metal in the lower temperature regime.

A most important characteristic of the hydrogen is its high mobility. In iron at room temperature the diffusivity is on the order of 10^{-5} cm^2/sec whereas in nickel it is about 10^{-11} cm^2/sec.

Hydrogen does not form a hydride in iron but does in a variety of metals like the Ti group, Ni and others. An important feature of the hydrides in the Ti-Zr-Hf group in their acicularity thereby enhancing the embrittling effects. Further, these hydrides are stable generally in the same electrochemical regimes as the hydrogen from water reduction; i.e.,

$$7\ Zr + 6H_2O = 2\ Zr_2H_3 + 3ZrO_2 \qquad (19)$$

There is a variety of deleterious processes which result from hydrogen in the lattice. These include:

1. Slow crack growth $K_I < K_{Ic}$ in high strength materials YS > 175,000 psi.

2. Hydrogen blistering which usually occurs in the ductile alloys.

3. Surface fissures in bcc Fe, fcc stainless steel, and fcc Ni.

4. Slow strain rate embrittlement.

5. Hydride embrittlement.

These failure processes appear to be related to a variety of possible hydrogen-metal interactions:

1. Hydrogen-solute (significant for cases where M-X bonds are strong).

2. Hydrogen-dislocation (not strong).

3. Hydrogen-grain boundary (may be related also to solute segregation at grain boundaries).

4. Hydrogen interaction with crack tip stress fields.

6.20 Metallurgical Aspects

SCC processes are significantly affected by the following:

1. Grain boundary composition.

2. Phase distribution and composition.

3. Grain size.

4. Preferred orientation.

5. Cold work.

6. Intermediate metastable phases.

6.21 Grain Boundary Composition - Precipitates

The grain boundary region can have three regions of significantly different chemical composition--each with its specific chemical and mechanical behavior. The grain boundary region is shown in Figure 26.

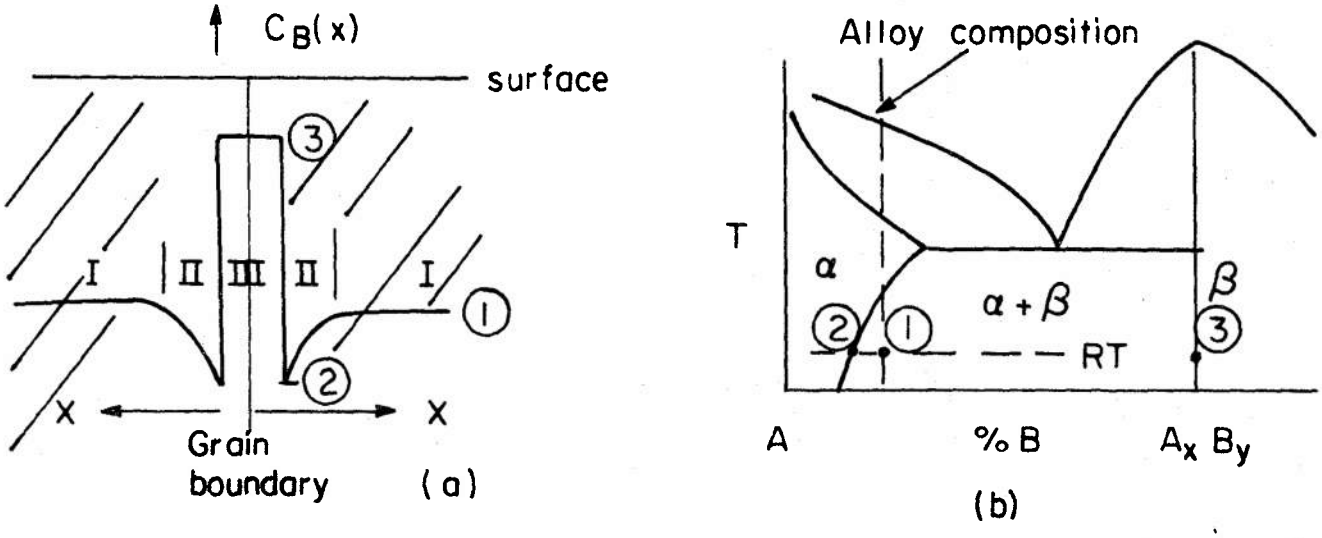

Figure 26: Schematic relationship between the phase diagram and the grain boundary composition profile for a metastable alloy.

The circumstance depicted in Figure 26 is relevant to aluminum alloys in particular; the sensitization of stainless steel involves a similar arrangement except that the chemical distribution, while similar to 26 (a) results from kinetic circumstances not too easily related to a phase diagram.

Depicted in Figure 26(a) are three zones: the precipitate of composite $A_x B_y$ (Zone III), the solute-depleted zone (Zone II), and the metastable region of intermediate composition (Zone I). These zones differ both in chemical composition and mechanical properties.

The polarization response of a Al-Mg-Zn type precipitate in a Al-Base alloy is different from that of either region I or II. Further, this precipitate is different from the Al-Cu precipitates. In the stainless steels, where TiC are present, an approximate polarization response of TiC relative to stainless steel in H_2SO_4 solution is shown in Figure 27.

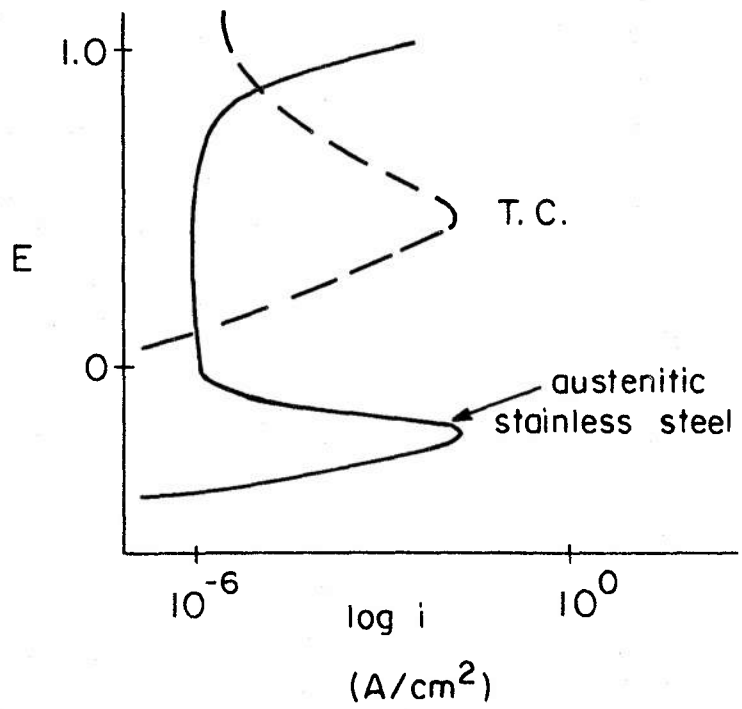

Figure 27: Schematic relationship of polarization response of an austenitic stainless steel and TiC (present in the Ti-stabilized Type 321).

Clearly, from Figure 27 the TiC is very unstable where the stainless steel exhibits its greatest stability. Thus, a crucial consideration here is related to the precipitate morphology and spacing.

If the Region II of Figure 26(a) is softer, the dislocation mobility will be high and will relate to repassivation considerations discussed in 6.14. The width of Zone II receives frequent consideration in the SCC of Al-Base alloys.

It is of parenthetical interest here that carbides in grain boundaries may be quite reactive both in oxidizing at reducing environments forming CO_2 in the former and CH_4 in the latter. Thus, cathodic protection may not be a panacea. Similarly, silicon-containing compounds may suffer similarly owing to the volatility of SiH_4 formed at lower potentials.

6.22 Grain Boundary Composition - Non-Precipitating

In a broad class of alloys solutes segregate to grain boundaries but do not precipitate. These segregations sometimes are mechanically deleterious as in temper embrittlement or lead to ordinary intergranular corrosion as in stainless steels (non-sensitized) at very oxidizing potentials (e.g., the Cr^{+6} +HNO_3 type environment).

These segregants may lead to premature breakdown of passivity as for phosphorous and sulfur or may have inherently different polarization responses. Figure 28 compares the polarization response of Fe and Cr in acid solutions relative

to the grain boundary composition profile.

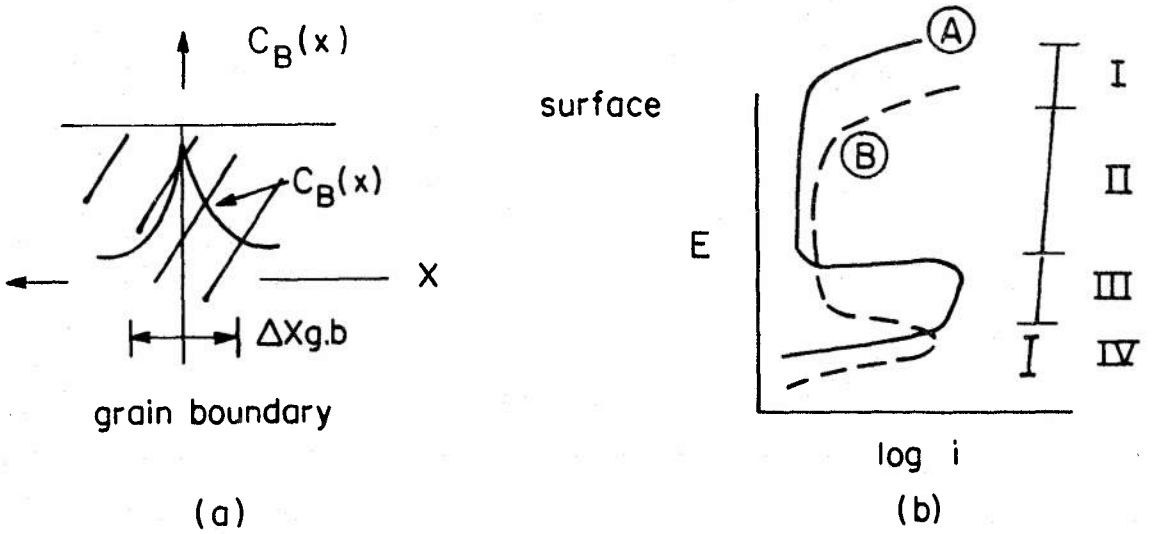

Figure 28: (a) Schematic composition profile resulting from segregation; (b) Polarization response of elements A and B.

If the potential lies at Zone II, both the g.b. and matrix are stable. In Zones I and IV, the g.b. will dissolve preferentially and in Zone III the matrix will dissolve preferentially. The schematic of Figure 28(b) is quite close to the situation actually existing for Fe-Cr alloys where A = Fe and B = Cr.

Parenthetically, the Figure 28 applies also to solute enriched dislocations and a similar discussion applies.

These solute segregations may also affect local hydrogen entry rate as for the previous discussion in 6.16.

Finally the solute segregation influences the mechanical

properties of the grain boundary either by softening or hardening.

The width of the zone, $\Delta X_{g.b}$, varies from a few atom layers as observed for segregation in temper embrittlement to 20μ as observed by microhardness profiles.

6.23 Phase Distribution

The relative reactivities of different phases as affected by their composition follows patterns already described by Figure 27.

It is interesting to note that various sulfides, phosphides, nitrides, etc., have reactivities possible quite different from the matrix material. The vagarious nature of the influence of phase distribution is readily seen from the SCC susceptibility of duplex stainless steels--some of which are very resistant and others very susceptible.

6.24 Grain Size

Increasing the grain size generally accelerates the EIC phenomenon patterns similarly to the Petch relationship. These grain size effects relate to distribution of impurities at interfaces, slip step height in surfaces, and pile-up internally.

Grain size does not generally affect the "yes or no" aspects but the degree.

6.25 Preferred Orientation

Preferred orientation affects EIC phenomena in two ways. First, pancake type grains prevent IGSCC in directions perpendicular to the pancake. This is the longitudinal case for aluminum alloys. Thus, where SCC is dominated by grain boundary reaction, a very substantial improvement can be made by arranging the plane of the pancake grains parallel to the plane of stressing.

Secondly, some IGSCC follows particular planes. In hexagonal metals like Ti or Zr, it is easy to orient the basal planes. Fortunately, the preferred SCC plane is approximately parallel (off $\sim$ 17°) to the basal plane. Thus, the advance of SCC can be shifted relatively easily in sheet materials.

While SCC susceptibility can be somewhat manipulated as above, fatigue effects are not so easily manipulated. Fatigue cracks in aluminum, for example, are transgranular; the environmental component is superimposed and is significant.

6.26 Cold Work

Cold working relative to SCC operates in a variety of ways. One is to break up grain boundaries. This approach has been very effective in ameliorating the IGSCC of carbon steels. The SCC susceptibility can be virtually eliminated in some cases.

In other cases of IGSCC cold working also diminishes

the SCC probably for reasons relating to surface slip geometry.

6.27 Intermediate Metastable Phases

The metastable phases of greatest interest are martinsite of the steels and the omega type phases in titanium.

The degree of metastability appears not to affect film-free dissolution kinetics; the stability of protective films seems to be somewhat affected but not to order of magnitude.

These metastable phases seem to have their greatest influence on mechanical properties, hydrogen interactions, and local details of deformation.

6.28 Mechanical Surface Interaction

1. Image Forces

The simplest consideration of a dislocation-surface interaction is the image force effect in which the attractive force (for an edge) is:

$$\frac{F_x}{L} = \frac{\mu b^2}{4n\ (1-\nu)\ \ell} \qquad (20)$$

where μ is the shear modulus, b the Burgers vector, ν Poisson's ratio, and ℓ the distance from the surface.

2. Effect of Surface Layers (Elastic Effects)

For a metal of elastic modulus E_m covered with a surface layer of modulus E_s, a dislocation is attracted when $E_s < E_m$ and

repelled when $E_s > E_m$.

3. Interfacial Dislocations at the Metal-Surface

Product layers such as oxides have structures which are certainly (although not identified in most cases) different from the substrate. At such interfaces, interfacial dislocations might be moderately effective in inhibiting slip.

4. Surface Energies in the Absence of Protective Films

When slip exposes new surface an additional increment of surface energy is required, $\gamma_s \Delta S$. With respect to systems which experience SCC, the pattern of liquid metals and aqueous solutions are of interest. Liquid metal embrittlement has been positively correlated with surface energy lowering.

The understanding of surface energy of metals in electrolytes is greatly obscured by the presence of protective films. The large bulk of work done on mercury is only of qualitative applicability but serves to demonstrate a minimum in surface energy with potential.

5. Surface Energies in the Presence of Films

One of the resistive aspects of deforming the surface is the creation of new oxide-environment surface.

6. Near Surface Charge Redistribution in Ionic Solids

In the presence of an adsorbed surface species which is

charged, a redistribution of charge occurs in the substrate of ionic solids. This charge redistribution interacts with the motion of dislocations which are also charged acting, in some cases, to embrittle the surface. While the available work has been conducted on bulk ionic solids, a similar effect might be relevant in oxide covered metals.

7. Surface Morphology

The surface heterogeneities mentioned earlier--pits and tunnels--may interact mechanically to accomplish part of the penetration of Stage I in fatigue.

These gross heterogeneities change local chemical processes to produce hydrogen and altered pH.

On a finer scale, dissolving surfaces of metals in electrolytes achieve step heights at a size of 0.01 - 0.1μ. Of course, they may be much smaller. Such steps may participate in the nucleation of surface slip.

8. Dislocation Layer at the Metal Surface

While this appears to be a complicated and controversial layer, it appears that some kind of dislocation debris layer does accumulate at the surface under appropriate circumstances. Such a layer hardens the surface.

6.29 Additional Forces Within Cracks

In addition to the obvious applied forces and the less obvious residual ones two other sources are available.

1. Reaction Products

The formation of reaction products in restricted geometries produces forces of substantial magnitude. A well known case has always been that of alumina in concrete where the formation of aluminum oxides cause the surrounding concrete to crack.

The effective hydrostatic stresses in a thin wall cylinder of Ti with a corroding insert (Fe) have been measured to be in the 7,000 psi range.

SCC in high temperature caustic solutions has been shown to be related to this effect. SCC of stainless steels has been propagated by this effect.

2. Double Layer Repulsion

Referring to Figure 11, one can imagine two surfaces--such as at the crack tip--approaching to within a distance of less than 100 $\mathring{A}$ and finding a repulsion due to the interaction of the double layer fields.

6.30 Crack Chemistry

1. The Hydrolysis Equilibrium

The general aspects of a crack chemistry are dominated by the equilibrium:

$$M^{++} + H_2O = MO + 2H^+$$

where (21)

$$\text{Log}[M^{++}] = K - 2pH$$

Here, a change in $[M^{++}]$ by two orders of magnitude causes a change of 1 pH unit.

The approximate location of the stable range of pH can be obtained for pure metals from Pourbaix's book. Taking M^{++} as unity, approximate pH's are:

Metal	pH
Fe^{++}	8
Fe^{+3}	3
Mg^{++}	10
Ti^{+4}	1
Cr^{+3}	2

If oxidizing species are added to solution, lower valence ions are oxidized thereby decreasing the solubility product.

2. The Crevice Effect

Since the crack in a region where environmental species do not easily gain access, especially since oxidized species are reduced as they diffuse, we can imagine a cell of high and low oxygen.

It is most appropriate to envision this not as an equilibrium cell, nor as a battery, but as sites for different kinetic processes as shown in Figure 29.

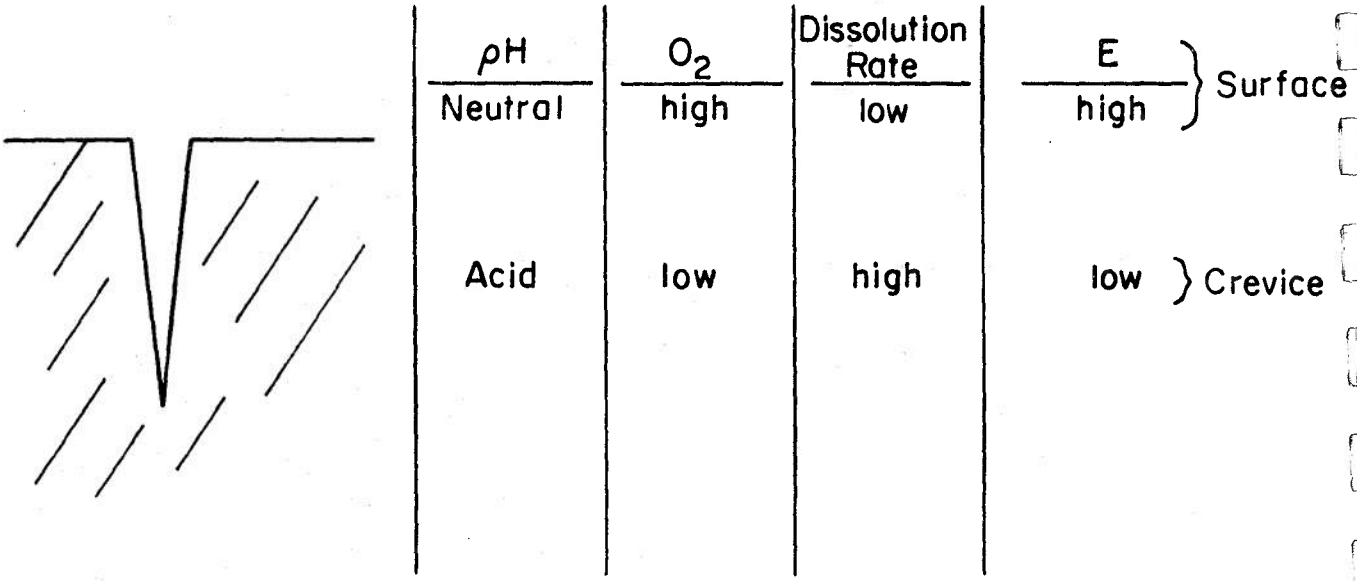

Figure 29: Schematic of crevice and general description of relative value of key variables.

Within the crevice, the oxygen is low so that dissolution tends to be accelerated to balance the relatively higher O_2 availability in the surface. The dissolution rate on the external surface tends to be low owing to the stability of the films

so that, on balance, there is a tendency to dissolve within the crevice. Whether accelerated dissolution actually occurs in the crevice, excepting SCC, depends on the range of potential over which the film is stable. A broad range of stability and a low anodic peak favor stability of the crevice walls.

It is not necessary that oxygen be the oxidized species. Depending on the system, Te^{+3}, Cl_2, NO_3^-, $CrO_4^=$, etc. will do as well.

3. Dynamic Stressing

The opening and closing of cracks as in the case of fatigue tends to produce a more uniform chemical situation within the crack. There is nothing quantitative here, but we might expect chemical conditions more nearly like those of the external environment.

4. Minimum Potential at the Crack Tip

The minimum potential at the crack tip under open circuit conditions is fixed by the $M = M^{n+} + ne$ equilibrium. This, then, fixes the maximum over-voltage (and rate) for the hydrogen reduction reaction.

5. Liquid Phase in Cracks

In a nominally gaseous environment, it is possible to stabilize a liquid at a narrow geometry according to a relationship where the radius of curvature is proportional to the partial

pressure of gas. We may thus have a liquid phase at a crack tip regardless of a normal gaseous environment. This may be the case in the water vapor SCC of high strength steels and aluminum alloys. Also, the vapor phase methanol-induced SCC of titanium may also be relevant.

6.31 External Observations

There are certain general observations which relate to EIC which need to be summarized.

1. Fractography

The fractographic appearance of EIC has not been systematically correlated. However, a variety of microstructures has been observed on SCC surface as follows:

a. Intergranular - Seen frequently in HSS as probably defined by prior austenite. Also, seen in stainless from ordinary intergranular SCC.

b. Cleavage - Frequently seen in the SCC of Ti.

c. Striated - Seen in the SCC of Cu base and Mg base.

d. Dimpled - Seen in high strength steels.

Thus, a variety of structures have been observed. A major controversy is involved in interpreting these structures relative to environmental action--i.e., if a dissolution process is involved, where is the dissolution?

2. Acoustical Emission

Acoustical emissions are produced in some but not all SCC systems. High strength steels have produced the most unambiguous emissions. Acoustical emissions have also been observed in titanium. No emission can be detected from cracks advancing in stainless steel.

So far the acoustical measurements have not measured emissions from stainless steels. This may be due to the background interference. However, for SCC of stainless steels, it is possible to hear hydrogen bubbles collapsing.

There is presently no correlation between the details of microstructure and acoustical emission.

3. Crack Branching

There appears to be a wide range of crack branching considerations as follows:

a. In aluminum alloys cracks tend to stay single if propagating in the short transverse node.

b. Crack branching is epidemic in stainless steels but no good fracture mechanics experiments have been seen.

c. Intergranular SCC of isotropic stainless steels has been observed to be extensively branched, but also to be single.

d. There is some suggestion that branching occurs in Regime II of the V-K curve if the plateau is wide enough. Thus, regardless of the reduction in K a wide range of K on the plateau would permit two cracks to propagate.

There appears to be no good fundamentally reliable base for the prediction of crack branching.

4. Cracking Plane

In the TG SCC of stainless steels and copper alloys, it is quite clear that SCC is initiated according to slip-defined sites. However, the nature of the propagation appears different. Cracking planes of {211} and {100} have been reported. This leads to the suggestion of a Stage I-Stage II type of process similar to fatigue where the Stage I is also slip related.

In the Ti base alloys, the SCC plane is 17° off the basal.

7.0 The Slip Dissolution Model of SCC

A large number of SCC systems involve breaking a surface film as a critical part of the process. These films and their associated breaking appear to fall into the following categories:

1. A very thin product layer film exists on iron base alloys, titanium base alloys, copper alloys in the

non-tarnishing environments. This film is usually less than 100 Å thick. It is doubtful whether such a film is of the brittle type. The breaking of this film appears to follow the pattern shown in Figure 30. It is this process that will be discussed further in this section. A detailed discussion of this model is presented in my NATO paper handed out at the same time as this paper. Only the essentials are sketched herein.

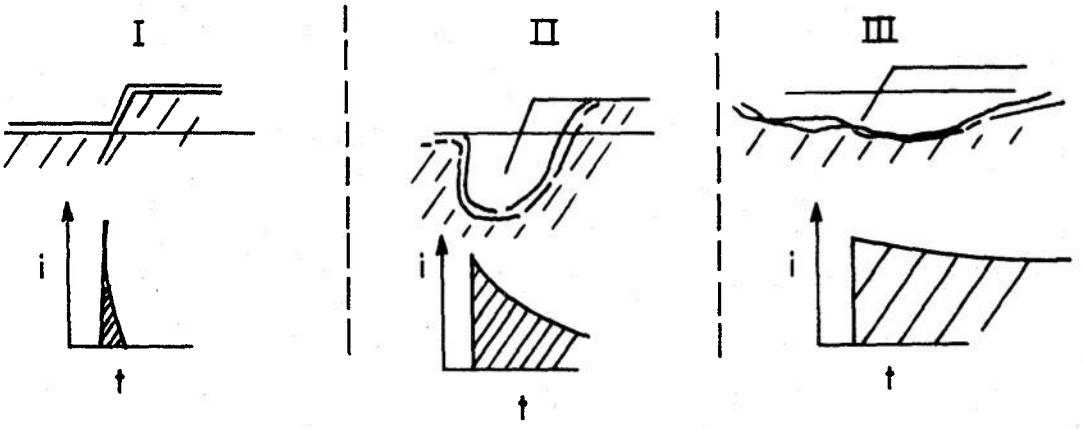

Figure 30: Three cases for slip-dissolution sequence. Upper figures show dissolution geometry resulting from broken film. Lower figures show corresponding current-time transients.

2. The brittle film concept was suggested in 1959. Here the brittle film could be a relatively thicker oxide or a surface region on the metal which had been previously embrittled by a variety of processes including preferential dissolution of the more active

species in an active noble alloy or by the inward diffusion by a species such as hydrogen.

The main objective of this section is to describe briefly the essence of the slip dissolution concept and its application to interpreting the SCC of a variety of materials. Here we are mainly concerned with the breaking of the thin films of Item No. 1 above.

7.1 Application of the Slip Dissolution Model to Transgranular SCC (TGSCC)

Following Case II of Figure 30, the propagation of transgranular SCC appears to be a succession of similar events or simply a continuous rupturing of the film at the crack tip. The dissolution in the lateral direction is restricted since the film is no longer breaking along the crack walls. Hence, a crack-like geometry results.

In summary, the essential sequence is depicted in Figure 31.

There are several objections to the essential model above. Chiefly, these are:

1. The fractography suggests very much a cleavage type process.

2. The fracture surfaces have been observed variously to be {211} {100} and {111} and therefore a simple

slip controlled process as illustrated in Figure 30 may not be involved.

3. Hydrogen evolution from the advancing cracks suggests that a hydrogen embrittlement process may, in some way, be involved. Of course, the evolution of hydrogen from advancing cracks does not define the site of hydrogen in reduction.

The detailed counter arguments to these objections to the hydrogen model as well as a detailed description of the application of this model to interpreting the SCC of stainless steels is given in a recent paper by me at the NATO meeting in Portugal, April 1971. (This has been published by NATO and was edited by J.C. Scully.)

For the present, it is sufficent to say that the slip dissolution concept probably provides the most effective interpretation of available data. It rationalizes a wide range of alloy dependence and electrochemical potential dependencies.

7.2 Application of the Slip Dissolution Model to Intergranular SCC (IGSCC)

One of the most difficult aspects of SCC models is explaining the transition between transgranular (TG) and intergranular (IG) SCC in a given alloy system. It serves no purpose to ennumerate all the circumstances in which such transitions occur so a single illustration of current industrial significance will be given.

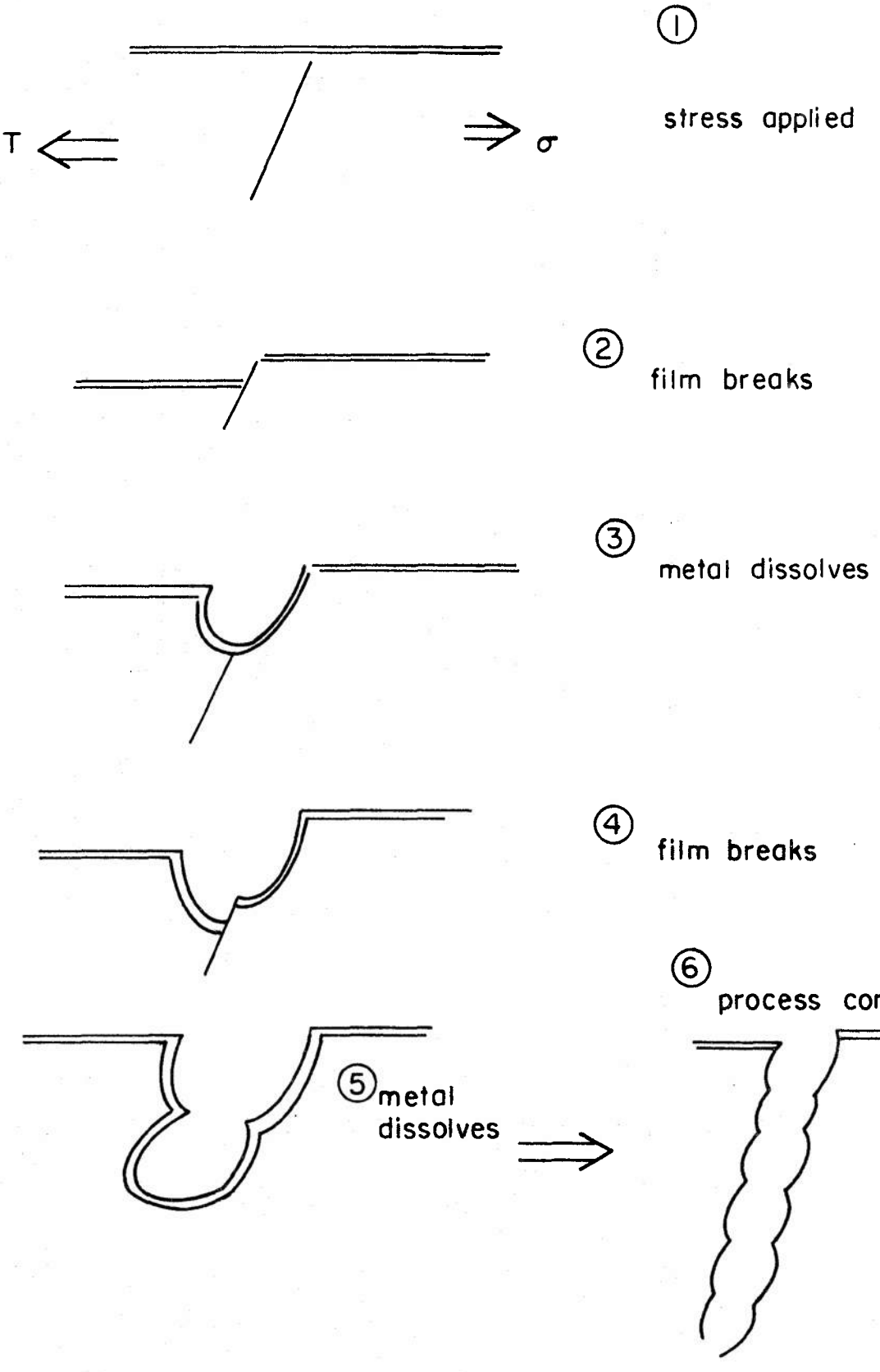
①
T
σ
stress applied
②
film breaks
③
metal dissolves
④
film breaks
⑤ metal dissolves
⑥
process contours

The austenitic stainless steels have been well known to experience TGSCC in chloride solutions since mid-1930. It was not until 1962 that SCC of non-sensitized material was observed. Unfortunately, it was observed that these alloys would crack by IG in Boiling Water (nuclear) Reactors (BWR) but not in Pressurized Water Reactors (PWR). There is a factor of 10-100 difference in the oxygen content with the BWR being higher and in the range 0.1-1.0 ppm.

The question now remains as to exactly why the BWR environment experiences IGSCC and the PWR does not.

Suppose that we have, at the grain boundary, solute segregation of the type that gives Case II (Figure 29) type transient attack; whereas the grain matrix has Case I at the same potential. Thus, the crack advance epitomized in Figure 30 is confined to the grain boundary. Such a situation is depicted in Figure 31.

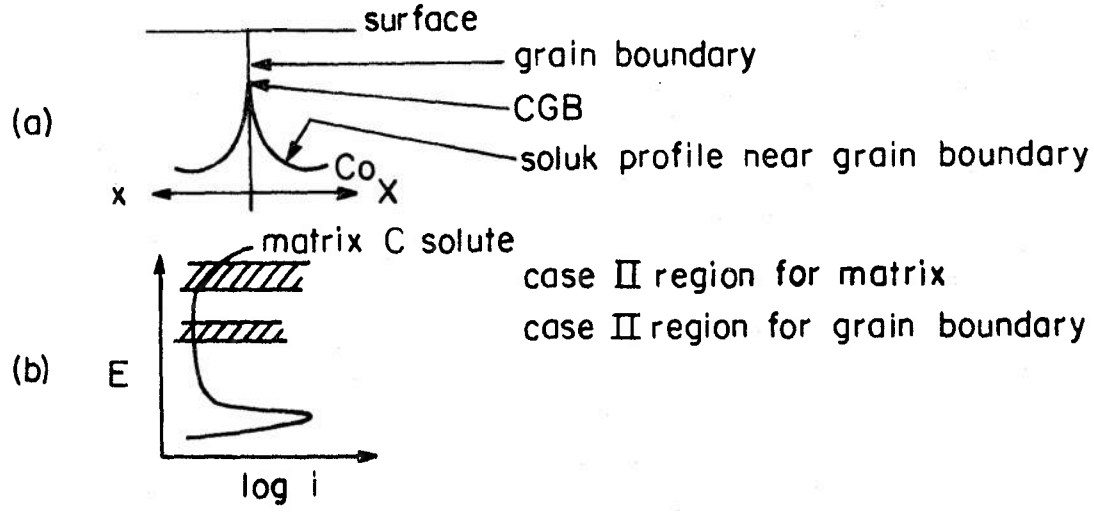

Figure 31: (a) Schematic of solute distribution with respect to grain boundary; (b) Polarization curves corresponding to grain boundary and matrix compositions.

It is of very substantial interest that still further increases in potential give simple intergranular attack for these non-sensitized alloys in the absence of stress.

The environmental case for PWR environments obviously lies below the IGSCC region of Figure 31 due to the lower oxygen--and no SCC occurs!

It is quite likely that the IGSCC of temper embrittled steels recently observed occurs because the phosphorous and antimony at the grain boundary slow the transient repassivation relative to that of the grain matrix.

7.3 Application of the Slip Dissolution Model to Slow Crack Growth in High Strength Steels

The essence of this idea has already been explained in Section 6.19. While the hydrogen entry seems primarily the causative agent, the availability of hydrogen is primarily related to the dissolution event--at least at open circuit.

An understanding of the transient dissolution process may, through its limitation of hydrogen produced, limit the rate of crack advance.

7.4 The Transition From Passivity to SCC to Pitting

The intimation of Figure 4 is that Zone III of SCC is between passivity (3) - (4) and pitting (5) - (6). Thus, as the potential first starts in the region (3) - (4) the alloy would be corrosion resistant whether stressed or not; as the potential moves into Zone III in the region (4) - (5) the tran-

sient dissolution changes from very rapid repassivation (Case I of Figure 29) to somewhat slowed repassivation (Case II of Figure 29).

As the potential is raised still higher, the repassivation rate is further decreased and becomes that of Case III of Figure 29. That this transition actually occurs is well documented.

IV. DEFECT PHYSICS IN STRESS-CORROSION CRACKING

by

R. Thomson and J. P. Hirth

In the belief that the field of defect physics has not been brought to bear fully in the solution of problems of fracture and stress corrosion cracking, the authors will attempt to assay the types of questions which are amenable from this viewpoint. In contrast to fracture mechanics, where one begins with visibly macroscopic concepts and works toward the invisible, in defect physics, one must begin with atomic lattice structures and force laws, and work back toward the large scale. Typically, one also has his eyes on behavior which is peculiarly structure sensitive. Thus, certain aspects of material failure will be only grossly dependent on atomic structure, for example, the elastic constants ultimately are atomic properties, but this fact is not essential in the use of the elastic constant in fracture mechanics. On the other hand, the very existence of an ultimate atomic structure is crucial to certain aspects of fracture and failure. We will discuss some of these in the following, and attempt some prediction of where help may be forthcoming from this general approach. For this reason, we must apologize at the onset for a somewhat mixed bag of topics.

1. Lattice Trapping[1,2,3]

One of the most dramatic effects in dislocation physics which depends entirely on the underlying atomic structure is the Peierls energy of a dislocation. A dislocation possessing a high Peierls energy will not move in a crystal except under very high stress. Similarly, a fracture crack is predicted to be trapped by the underlying regularity of a crystal lattice.

The simplest model which demonstrates the effect of a crack which is lattice trapped is depicted in Figure 1. In this model, we assume a wedge is forced between the atoms of an infinite crystal, and forces the atoms apart.

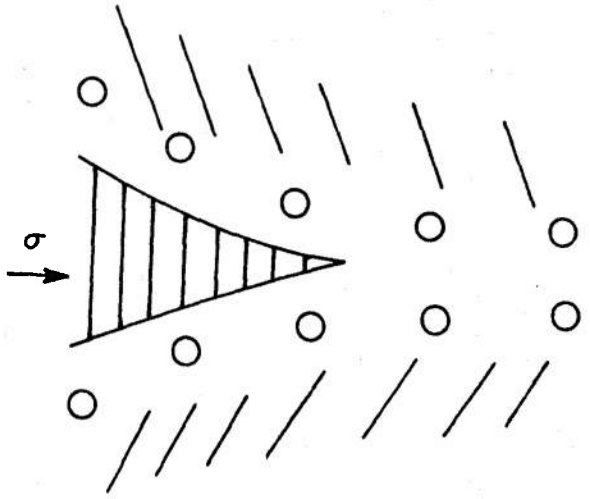

Figure 1 - Crack formed in a lattice by running a wedge in from the left.

We now assume that the elastic energy in the medium is a smooth function, which we deal with separately, and we calculate precisely the change in surface energy as a function of the wedge position. If we label an atom pair facing each other across the crack plane by n, assume that the energy of the bond between them is some function of the stretching of the bond, E'(y), and that the shape of the wedge pushing the

atoms apart is a function, y(n), then the total surface energy is:

$$S = \sum_{n=\infty}^{\infty} E'(y(n)) = \sum_{n=-\infty}^{\infty} E(n) \qquad (1)$$

This is a divergent sum if there are an ∞ number of broken bonds, and what we really require is the change in the surface energy as the wedge moves back and forth from a reference position. If we label the position of the wedge by x, then a rigid displacement of the wedge changes the surface energy by a finite amount given by:

$$S(x) = \sum_{n=-\alpha}^{\alpha} [E(n-x) - E(n)] \qquad (2)$$

For an arbitrary bond energy and crack shape, this sum is of course not informative, but if we give the function E(n) a functional form, we can perform the sum. A physically reasonable function is:

$$E(n) = \frac{E_o}{2}\left(1 - \frac{2}{\pi}\tan^{-1}\frac{n}{\alpha}\right) \qquad (3)$$

E_o is the total bond energy, and α is the "width" of the cohesive region of the crack.

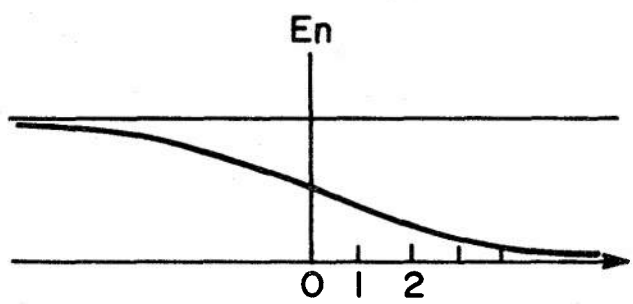

Figure 2 - Bond energy as a function of n for a crack.

To make a longer story shorter, the sum is analytic and depicted in Figure 3. The slope of the curve is the force on the ledge (neglecting the change in elastic energy), and displays a maximum and minimum value between $0 \leq x \leq 1$.

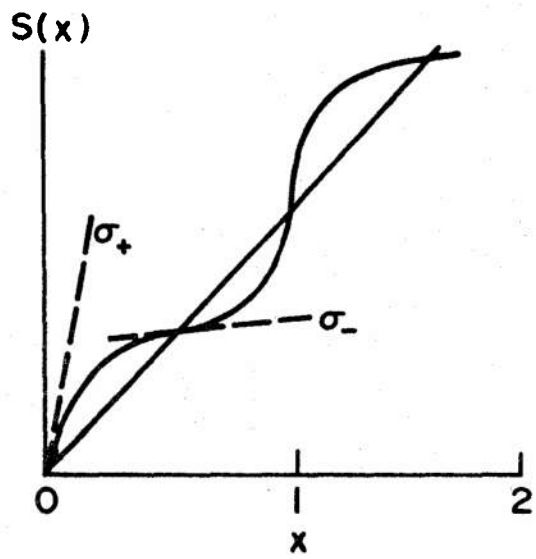

Figure 3 - S(x) as a function of x shows an oscillating form about its average continuum value. The slope shows a maximum and minimum value, σ_+ and σ_-.

Thus, for all values of the wedge force, σ, between these two values, the crack is stable at one atomic position. We define the maximum value of σ by σ_+ and the minimum by σ_- and the result is:

$$\frac{\sigma_+ - \sigma}{\sigma_-} \overset{\sim}{=} 4\, e^{-2\pi\alpha} \qquad \alpha > \frac{1}{2\pi} \tag{4}$$

$$\sim 1.14 \text{ for } \alpha = \frac{1}{0.607}$$

A more sophisticated model can be worked out for a two dimensional lattice in the so-called lattice statics approximation.

The mathematics of this model becomes quite involved and will not be repeated here. Briefly, one starts with a linear lattice in equilibrium with the applied forces:

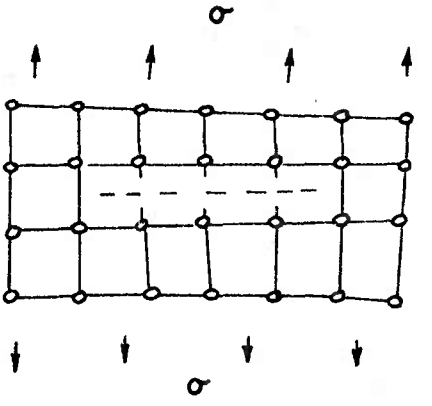

Figure 4 - A two-dimensional lattice under tension containing a number of broken bonds on an assumed crack plane.

$$\sum_{\underline{\ell}'kj} f'_{ij}\ (\underline{\ell},\underline{\ell}')\quad U_j\ (\underline{\ell}') \quad = \quad F_i\ (\underline{\ell}) \qquad (5)$$

$f'_{ij}\ (\ell,\ell')$ is the force constant between the atom at ℓ and the atom at ℓ', and is a tensor in the atom displacements, $U_j\ (\ell')$. As it stands, this equation applies to both good crystal, and to broken bonds, and cannot be manipulated further. If we write it for a perfect crystal, and add forces which separately annihilate the bonds to be broken, the symmetry of the crystal allows one to proceed further. Then:

$$\sum_{j\ell'} f'_{ij}(\underline{\ell}-\underline{\ell}')\ U_j(\underline{\ell}') \quad = \quad F_i(\ell) + \sum_{j\ell'}{}^{\Lambda}{}_{ij}\quad (\underline{\ell},\underline{\ell}')\ U(\underline{\ell}') \qquad (6)$$

The left hand side of (6) now depends only upon the distance between the atoms $\underline{\ell},\underline{\ell}'$, and is easily summed. The standard procedure is now to Fourier analyze the equation and

we find that when that is done and assumptions made about the crystal type, the equations can be solved, though for a long crack, machine numerical work is necessary.

The results are depicted in Figure 5. There the stress force to break N bonds is plotted as a function of F. The $1/\sqrt{N}$ Griffith result is shown for comparison. We see that the force for zipping the crack back together is also plotted, and is a curve displaced measurably from the bond breaking curve. The difference between these two curves shows the lattice trapping phenomenon already explained.

What has been said applies to rigorously two dimensional crystals, but it suggests that classes of crystals exist for which lattice trapping should be important if the crack is atomically sharp, and that for crystals which have high anisotropy on the crack plane so that the cohesive region of the crack is broad, the lattice trapping is negligible.

Computer calculations of the crack tip geometry in bcc Fe by Gehlen and Kaninen[3] have been reported, which confirm the general results of this qualitative discussion. They find that the crack tip region is narrow, and that it is stable under stresses larger than the Griffith stress.

If a crack is trapped in equilibrium at a line of atoms by some external stress, a small increase of the stress will not be sufficient to overcome the trapping stress. However, local thermal fluctuations occur, which permit the crack to move under stress at a speed set by the rate of thermal fluctu-

ations. Computer calculations have been reported[4] which show that in iron, the kink energy is of the order of 0.3 ev.

2. Brittle vs. Ductile Behavior

Kelly[5] and others have compared the theoretical shear stress with the theoretical tension stress in an attempt to predict the brittle vs. ductile behavior of a single sharp crack. The question is whether when a sharp crack is somehow placed in the crystal it automatically blunts itself due to the spontaneous shearing at the crack tip which will form a dislocation in the crystal. Of course, the question still remains whether any stress concentration can occur in a region sufficiently removed from sources of plasticity which will form the crack in the first place. (We discuss only the sufficient condition for a sharp crack, not its necessary condition.)

The formation of a dislocation out of the crack tip blunts the tip, as shown in Figure 6.

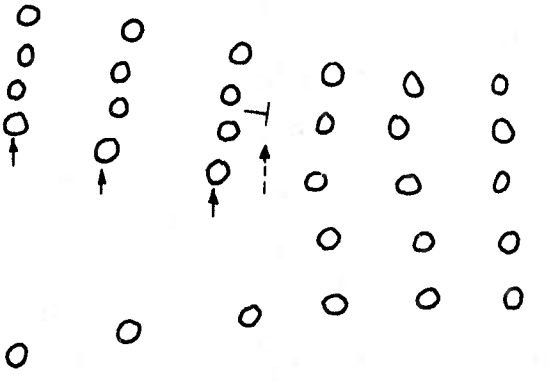

Figure 6 - As the dislocation is formed out of the sharp crack, a ledge is left behind which is equivalent to a blunted crack.

In the three dimensional process, a small dislocation loop is formed at a local position on the crack tip, as shown in Figure 7.

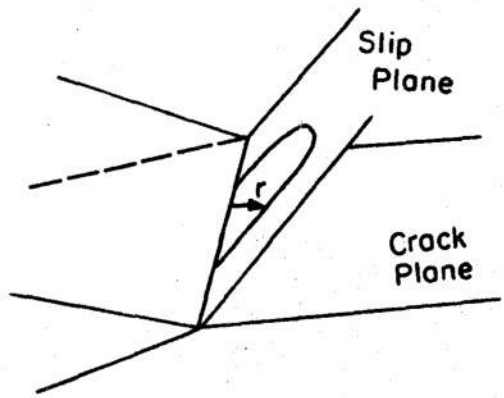

Figure 7 - Dislocation loop forming on a slip plane intersecting the crack tip.

There are three factors in the formation energy of the dislocation loop. These are (a) self energy of the dislocation, including the image force term from the crack geometry (positive), (b) stress on the dislocation due to the crack field (negative), and (c) the surface energy of the newly exposed ledge (positive).

Rice and Thomson have shown[6] that the image stress on a straight edge dislocation in the presence of the crack is exactly the same as for an infinite plane mirrored in the crack tip. We have consequently used half the self energy of a dislocation loop in our calculation.

The total energy, E, of the crack as a function of a radius r is:

$$\frac{E}{r} = E_o \ell n\, r/ro + E_\ell \left(1-\frac{ro}{r}\right) - E_\sigma \left(r^{\frac{1}{2}}-\frac{ro^{\frac{1}{2}}}{r}\right) \qquad (7)$$

E_o, E_ℓ, E_σ are material constants, and r_o is the cut-off.

The various terms as a function of the radius of the loop have the variation shown in Figure 8, and the total energy may or may not have a maximum. When a maximum occurs, the loop will expand for radii larger than the critical loop, due to the long range stress field of the crack.

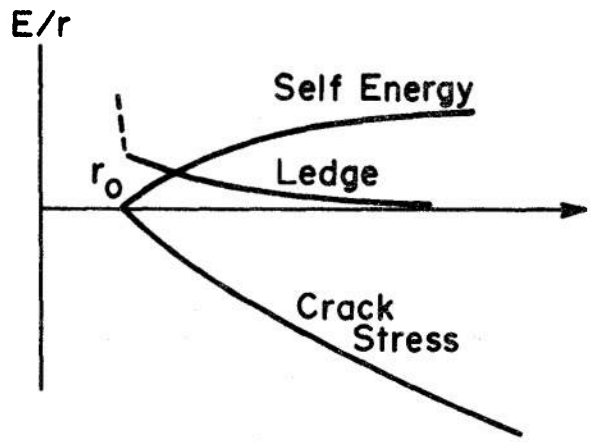

Figure 8 - Three contributions to the dislocation loop energy as a function of loop radius.

Our results are shown in the accompanying table. Briefly, it seems that for a combination of reasons, the face centered cubic materials will not sustain a sharp crack in the lattice. Neither will sodium. Iron has a small activation energy for dislocation formation and it appears to be a borderline case. The other materials shown have such large activation energies that once a sharp crack is formed, it would appear to be completely stable against spontaneous blunting.

Table 1

Activation Energy for Homogeneous

Dislocation Nucleation at a Crack Tip

Crystal	Act. Energy (eV)	Critical Loop Radius (r/b)
Copper	-----	
Silver	-----	
Gold	-----	
Lead	-----	
Aluminum	-----	
Nickel	-----	
Iron	2.2	5.1
Tungsten	33	12.7
Sodium	0.02	1.5
NaCl	241	95.3
LiF	59	32.4
MgO	205	36.8
Diamond	351	27.0
Ge	260	42.5
Si	111	20.5
Be	181	22.5
Zn	3445	282

3. Stress Activated Reactions

Tiller and Schrieffer[7] have recently called attention to the effect of stress on the electron-chemistry of a crack tip. We believe their suggestion is typical of a class of phenomena which can take place at the crack tip because of changes in the chemical potential in the solid.

Tiller and Schrieffer noted that the band width of the electrons in a metal depends upon the local pressure, and the fluctuating band width near a crack tip causes electrochemical potentials to be set up in the vicinity of the crack tip. These electrochemical potentials are shown to be cathodic in agreement with experimental findings. Gomer in unpublished work has refined their picture in a way which changes the quantitative results of their findings, but he still predicts a cathodic reaction at the tip.

The purpose of these comments is to note that other classes of crystals show analogous behavior. For example, in a semiconductor, the surface states will be modified by the local stress at the crack tip through the deformation potential. Depending on the position of the Fermi level, the local charge on the surface of the semiconductor will thus be modified at the crack tip, setting up conditions for similar electrochemical reactions there.

In a somewhat different vein, Charles and Hillig[8] have derived a stress activated theory of dissolution at a crack tip, in which both the surface energy and the volume of acti-

vation play a role. It is conceivable to us that a combination of lattice trapping modified by chemical dissolution may be playing a role in this regime.

4. The Role of Dislocation Structure and Scale

As shown by McClintock and Rice[9], there are various scales within which different viewpoints prevail in describing the situation about a crack tip. Here, we wish to focus on the penultimate fine scale: that of the dislocation structure. To place this in a concrete context, let us consider a planar crack. At the grossest scale the solution is the elastic K_I solution, next the small scale yielding solution of Rice[10], or various elastic-plastic solutions reviewed elsewhere[9], next a region of size nominally related to discrete dislocation spacings, and finally the atomic configuration at the crack tip.

There is substantial evidence that coplanarity of slip enhances SCC sensitivity. Brown[11] finds greater SCC sensitivity with planar arrays of dislocations in titanium alloy systems than with tangled arrays. Hyatt and Speidel[12] find SCC enhancement when aluminum precipitation systems involve G-P zones which are sheared, leading to coplanar pileup arrays. There is evidence for SCC enhancement by lowering of stacking fault energy[13,14] which would give greater coplanarity of slip.

On the other hand, the mechanism of enhancement remains obscure. One possibility was that of the requirement for a large slip step to initiate the slip dissolution model[14,15], or

the variant[16] of requiring a large slip event to rupture a film followed by dissolution as in the slip-dissolution case. However, Latanision and Staehle found that the presence of a protective film on model led to finer slip in cases where SCC was enhanced. The other notion is related to the increased likelihood of large stress concentrations with coplanar arrays[17], but a detailed mechanism has not been put forward. Here we shall attempt to indicate qualitatively that coplanar slip together with a fixed microstructure scale can influence cracking susceptibility. Since no detailed observations are available at such a scale, however, we first briefly consider the case of slip around a nondeforming particle for which observations are available and then extend the arguments to the case of the crack.

Consider a spherical, nondeforming particle in a single crystal deformed by simple shear on a single slip system and suppose that dislocations not captured by the particle pass through the region in question. The elastic field of the captured dislocations can be determined by a method due to Eshelby[18], in which the particle is removed, the medium sheared uniformly, and the particle then reinserted, deforming the medium[18,19], as shown in Figure 9.

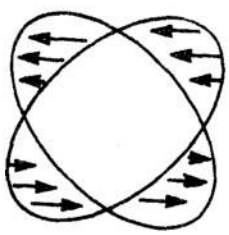

Figure 9

The resultant field is equivalent to a set of closely spaced Orowan dislocation loops in the interface of the particle[20] and corresponds reasonably with expectation from a continuum mechanics calculation[21] for a strain-hardening elastic-plastic case, which is the two dimensional analog of Figure 9. On observing such particle microstructures, however, relaxation is observed over a scale corresponding to the inter-particle spacing λ, occurring by the formation of punched out loops and helices, as illustrated in Figure 10. Thus, only on a scale of size > λ will the discrete relaxed dislocation result and the continuum result coincide.

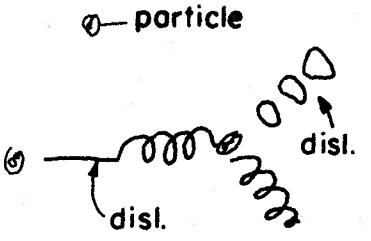

Figure 10

Now consider a mode I crack tip, Figure 11, on the scale of the dislocation microstructure denoted by S, the source spacing, which could be particle spacing, dislocation cell wall spacing, grown in dislocation spacing, as microstructural scale parameters.

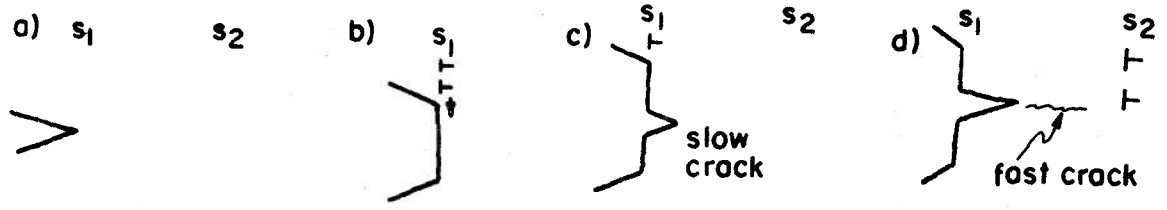

Figure 11

To make the point, suppose that the sources are such as to produce glide on a plane and in a direction both normal to the crack plane. In configuration (a) the stress field of the crack will be such as to operate S_1 to produce blunting of the crack as in (b). Let a new crack now start to grow on an atomically sharp basis as in (c), say by a mechanism such as discussed in the previous section, with some relaxation continuing at source S_1. With the crack in configuration (d), the stress field will be such as to operate source S_2. In this case, however, the dislocation motion, while relaxing the total strain energy of the crystal, will increase the local normal stress at the crack tip.[23] One possible result would be that the local critical stress intensity is exceeded so that the crack will grow rapidly until it reproduces configuration (a), whereupon the cycle repeats.

The picture is obviously speculative, but it does show a possible role of structure on the discrete dislocation scale. An alternative would be for the crack to emit dislocations rather than activating sources. Also, sources could operate as a variety of systems inclined to the crack plane, to cite two different possibilities.

Consider now the role of coplanarity in the model of Figure 11. In materials where slip is coplanar (fcc, low stacking fault energy; hcp, basal slip), the situation of Figure 11 would be favored. The intrinsic slip pattern would be one of multipolar arrays of dislocations of one slip system which could act as the sources in Figure 11. Moreover, the low

stacking fault energy (fcc or hcp) or low Peierls stress (hcp) would tend to restrict slip to a single plane, as shown in the figure. With non-coplanar slip, Figure 12, the dislocation

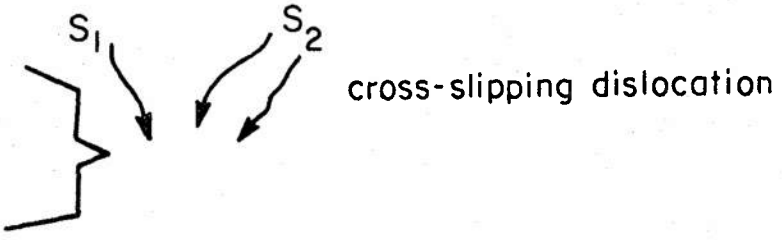

Figure 12

arrangement will tend to be one of cell walls containing dislocations of several glide systems. Further, systems of this type coincide with those in which cross-slip is a relatively easy process. Thus, both from the viewpoint of more slip systems and cross-slip, the situation of Figure 11(c) is less likely to occur. Instead, as indicated in Figure 12, continual blunting of the crack would occur.

The above discussion is entirely qualitative and conjectural, since no observations on such a scale are available for a crack tip: however, it is plausible on the basis of the dispersion particle case discussed beforehand. The thrust of both discussions is that detailed dislocation models are necessary for description of a crack on a sub-microstructural scale level[9], usually of the order of hundreds of Angstroms, and that the mechanism on this scale can differ from that extrapolated

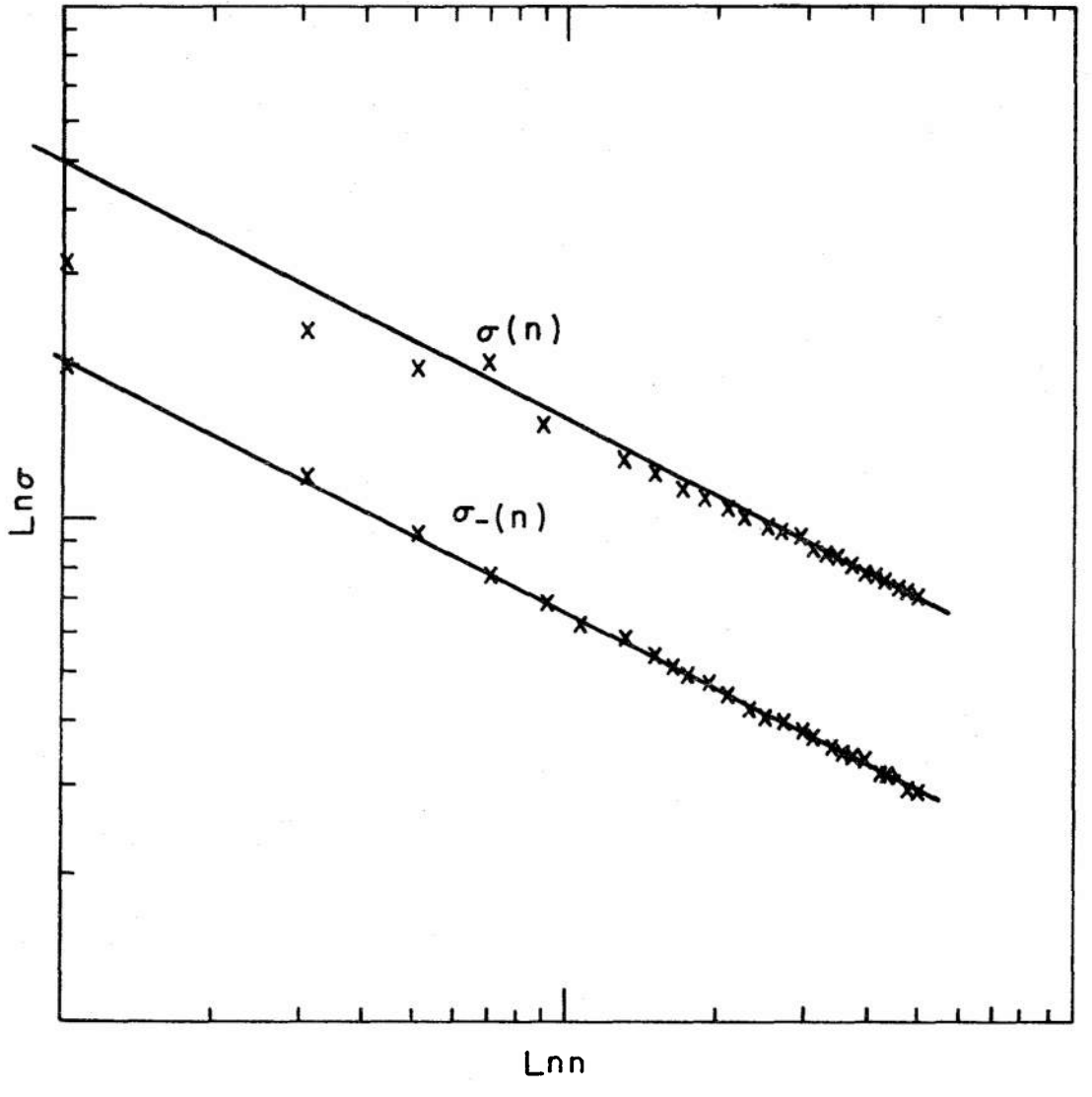

Figure 13: Crack length versus stress. The $1/\sqrt{n}$ Griffith law is superposed for comparison. Two curves result for forward and reverse crack motion.

from a more macroscopic scale. On a larger scale, the alternating flow, slow crack, fast crack cycle of Figure 11 would be describable by an elastic-plastic solution.

5. Conclusion

We have listed a number of instances where detailed atomic pictures based on fundamental properties of lattices should play a major role in the description of the mechanics and chemistry of fracture. We believe stress corrosion cracking to be a ripe area for development of the traditional interplay of theory and experiment.

REFERENCES

1. R. Thomson, C.Hsieh, and V. Rana, "Lattice Trapping of Fracture Cracks," to be published, J. Appl. Phys.

2. C. Hsieh, W. Cochran, and R. Thomson, "Theory of a Static Crack in a Two Dimensional Square Lattice," APS "March Meeting," 1971.

3. P. Gehlen and M. Kanninen, "Inelastic Behavior in Solids," ed. by Kanninen et. al., McGraw-Hill, 1970, p. 587.

4. P. Gehlen and M. Kanninen, Battelle-Northwest Conference on Atomic Force Laws, 1971.

5. A. Kelly, "Strong Solids," Cambridge Univ. Press, 1968.

6. J. Rice and R. Thomson, Summary Report ARPA Materials Council Summer Conference, 1970, in press.

7. R. Tiller, and J. Schrieffer, Summary Report, ARPA Materials Council Summer Conference, 1969.

8. R. Charles and W. Hillig, Symposium on Mechanical Strength of Glass and Ways of Improving It. Florence, Italy, 1961, pp. 511-527.

9. F.A. McClintock and J.R. Rice, this symposium.

10. J.R. Rice, Int. J. Fracture Mech. 2, 426 (1966).

11. B.F. Brown, in ARPA Coupling Program on Stress Corrosion Cracking, Final Technical Report, 21 Sept. 1970, Naval Research Laboratory, Washington, D.C.

12. M.V. Hyatt and M.O. Speidel, Rept. D6-24840, Boeing, June 1970.

13. H.W. Pickering and P.R. Swann, Corrosion, 19, 373 (1963).

14. R.M. Latanision and R.W. Staehle, in Fundamental Aspects of Stress Corrosion Cracking, Nat. Assn, of Corrosion Eng., Houston, 1969, p. 214.

15. R.W. Staehle, Proc. NATO Conf. on Stress Corrosion Cracking, Portugal, 29 March 1971.

16. S.F. Bubar and D.A. Vermilyea, J. Electrochem. Soc. 114, 882 (1967).

17. A.H. Cottrell, Dislocations and Plastic Flow in Crystals, Oxford Univ. Press, 1953.

18. J.D. Eshelby, Proc. Roy. Soc. (London) A241, 376 (1957).

19. M.F. Ashby, Phil, Mag. 14, 1157 (1966).

20. L.M. Brown and W.M. Stobbs, Phil. Mag. 23, 1185 (1971).

21. W.C. Huang, Rept. SM-45, Harvard Univ., October 1970.

22. P.B. Hirsch and F.J. Humphreys, in Physics and Strength of Plasticity (The Orowan Volume), Mass. Inst. Tech. Press, Cambridge, 1969; Proc. Roy. Soc. (London) A318, 45 (1970).

23. J.R. Rice, ARPA Materials Research Council, Summer Session, 1970: Summary Report in press.

V. FRACTURE MECHANICS FOR STRESS-CORROSION CRACKING

by

Frank A. McClintock and J.R. Rice

1. Introduction

The mechanics of fracture can be viewed at scales of observation differing from each other by as many as eight orders of magnitude. Different scales reveal different features: the size of the plastic zone, the roughness of the crack front, and the microstructure of the material. The microstructure can in turn be viewed at the scales of grains, inclusions, precipitate particles, subgrains, dislocation networks, dislocations, and finally atoms and electrons. In this paper, we first consider in detail the mechanics of two limiting regimes or scales of observation, one in which the material under consideration is primarily elastic, and a finer scale view or a situation at higher stress level, where the material under consideration is primarily plastic. We later consider in a much more tentative way some of the other scales of observation mentioned above.

A number of features characterize the mechanics of stress corrosion cracking:

a) The opening mode of loading a crack is much more important than either shear mode in causing crack growth.

b) The important stress and strain fields are those arising during crack growth, rather than during crack initiation from a sharp notch, because as indicated in Figure 1, cracks grow at stress levels that are only a fraction of those required for fast, dynamic fracture.

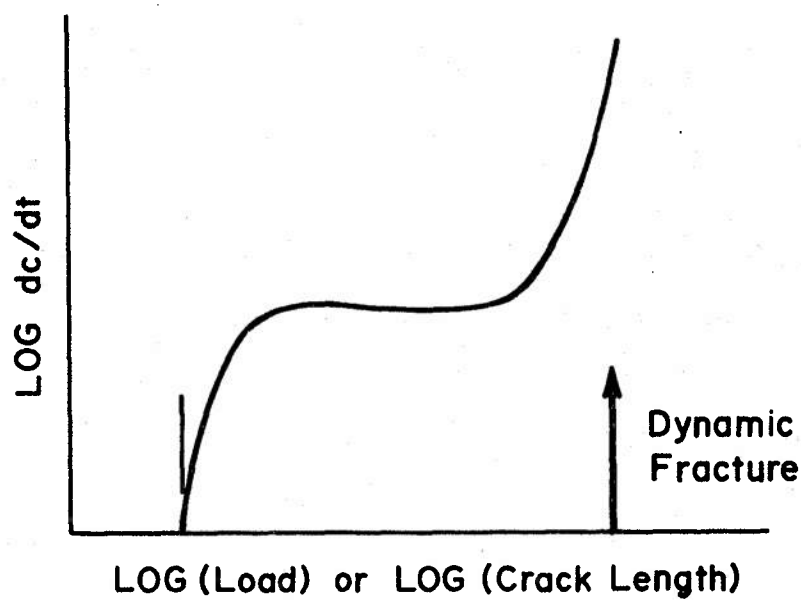

Figure 1. Schematic diagram of stress corrosion crack velocity.

c) Landmark features of Figure 1 to be explained are the existence of a plateau of constant rate of

crack growth and the possible limiting combination of stress level and crack length below which there will be no crack propagation.

d) The formation of cracks in unnotched parts must be considered because at typical working stresses, cracks can propagate when they are so short as to be lost in the microstructure. Initiation sites are corrosion pits, crevices, and phase or grain boundaries. Cracks can form without visible corrosion, as in stainless steel. There may be a critical stress level below which such crack formation will not occur. For instance, in ordinary low-carbon steel, there can be both corrosion and stress without stress corrosion cracking. In summary, where production is reliable and the consequences of failure are not too critical, design can be based on unnotched data; where parts are critical, the design must be based on crack growth from the largest undetected crack.

e) The plastic zone at a crack tip may be either larger or smaller than the structural features of the material. Therefore, either the elastic or the plastic idealization may be best for studying the effects on crack growth of such features as crack branching or grain size.

2. The Macroscopic Mechanics of Crack Tip Deformation

2.1 Elastic Stress Fields

a) Mode I - Plane Strain Tensile Opening Mode

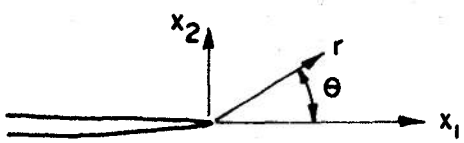

$$\sigma_{ij} = \frac{K_I}{\sqrt{r}} fij(\theta) + \cdots$$

bounded terms

Figure 2

i.e., $$\frac{\sigma_{11} + \sigma_{12}}{2} = \frac{K_I}{\sqrt{2\pi r}} \cos(\theta/2)$$

$$\frac{\sigma_{22} - \sigma_{11} + i\sigma_{12}}{2} = \frac{i K_I e^{-3ie/2}}{2\sqrt{2\pi r}} \sin\theta \qquad (i=\sqrt{-1})$$

$$U_2 \Big|_{\theta = \pm\pi} = \frac{4(1-2r^2)K_I}{E}\sqrt{\frac{r}{2\pi}}$$

b) Example

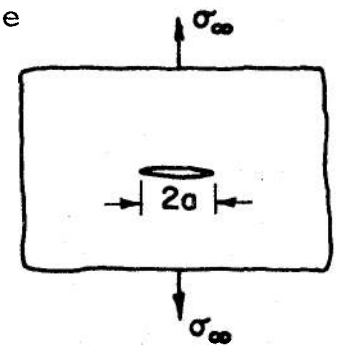

Figure 3

$$K_I = \sigma\infty\sqrt{\pi a} = \kappa_1\sqrt{\pi}\,; \quad K_1 = \sigma\infty\sqrt{\alpha}$$

c) Energy Release Rate

$$-\frac{d\,(\text{total potential energy})}{d\,(\text{crack length})} = G = \frac{1-\nu^2}{E} K_I^2$$

d) Small Scale Yielding - Elastic Fracture Mechanics

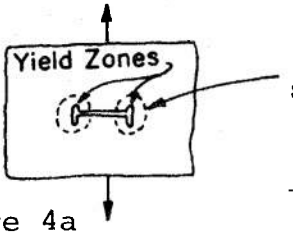

Figure 4a

same elastic K_I

→ same crack extension behavior

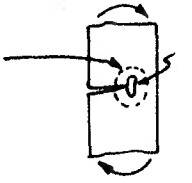

Figure 4b

yield zone

e) Three Modes

I

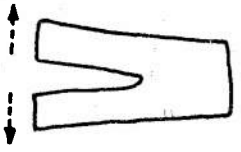

Figure 5a

II

Figure 5b

III

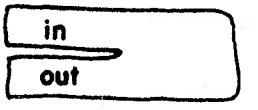

Figure 5c

2.2 Fully Plastic Flow Fields

a) Rigid-Plastic Material Model (Non-Hardening)

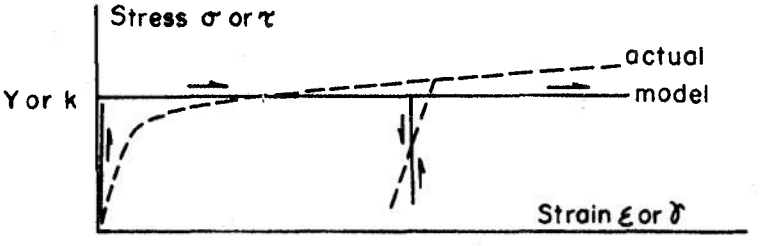

b) Some Limit Flow Fields

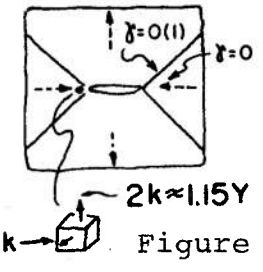

Figure 7a

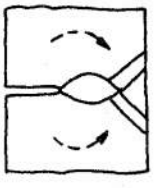

Figure 7b

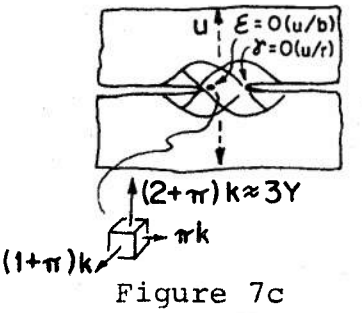

Figure 7c

c) Solutions Which Include Crack Advance

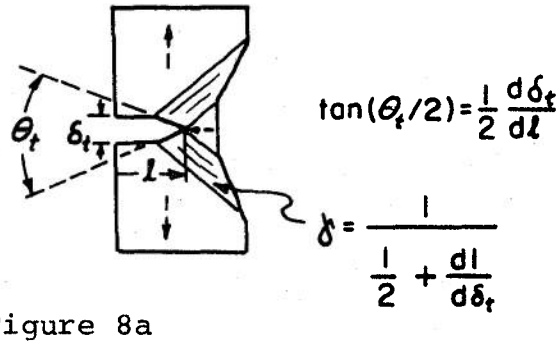

Figure 8a

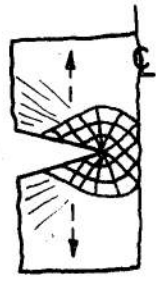

Figure 8b

Note: In these solutions, the ratio of boundary displacement increments to increments of crack length is prescribed apriori.

A special class of solutions involves no crack growth by "cutting" ahead, but the crack grows by alternate sliding off at the tip.

Figure 8c Meandering

2.3 Contained Plastic Deformation: Elastic-Plastic

a) Non-Hardening Material: Stress State as r → o

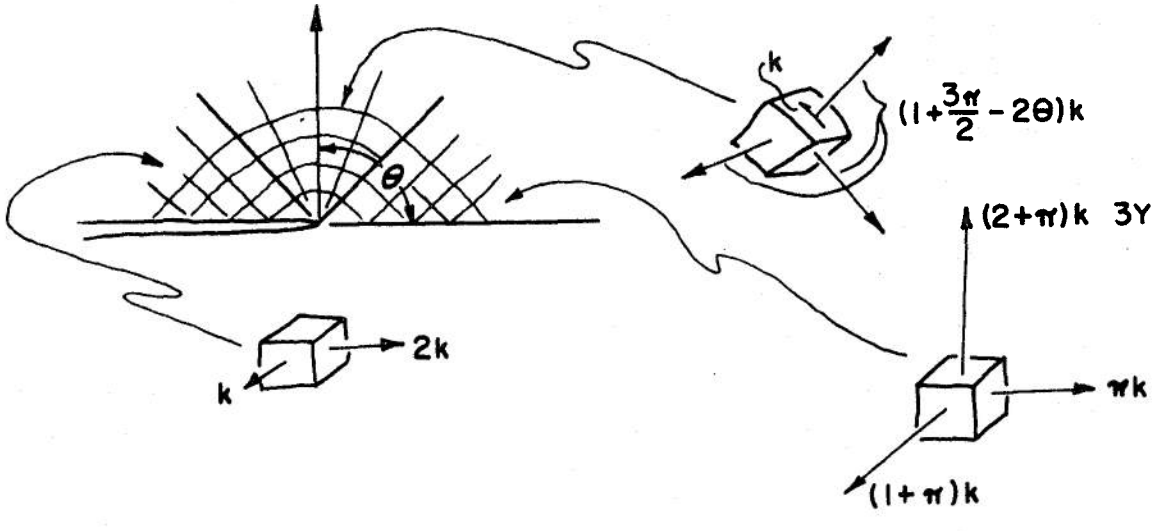

b) Stationary Crack: Small Scale Yielding

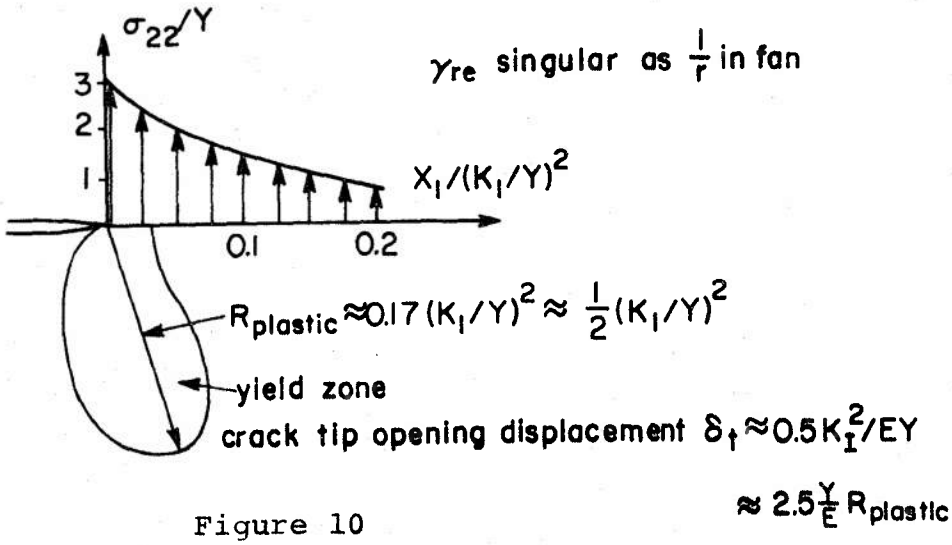

Figure 10

c) Power Law Strain Hardening

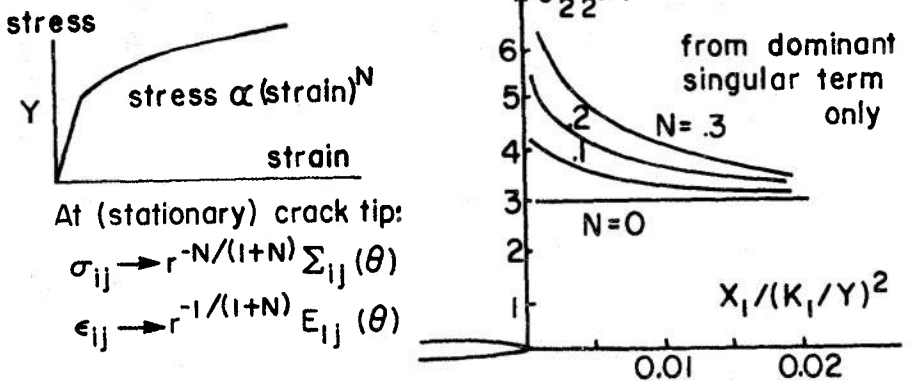

d) Crack Tip Blunting by Deformation

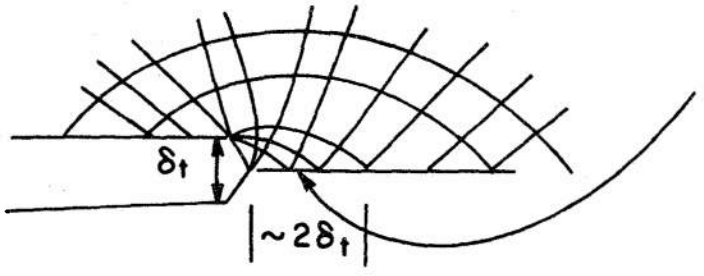

Figure 11

large strain region (strains on order unity) created ahead of tip by blunting

(for macroscopically stationary crack)

Blunted shape may depend on growth from initial defects.

e) Advancing Cracks

Very little is known about elastic-plastic fields accompanying crack advance. For steady-state crack advance, assuming continuously sharp tip:

$$E_{ij} \text{ singular as } \log\left(\frac{1}{r}\right), \text{ versus } \frac{1}{r} \text{ (stationary)}$$

$$U_2 \Big|_{\theta = \pi} \to r \log\left(\frac{\text{const}}{r}\right), \text{ versus crack tip opening } \delta_t$$

but this gives blunt tip, so consider finite rotations.

f) Simple Model for Crack Advance - Steady State

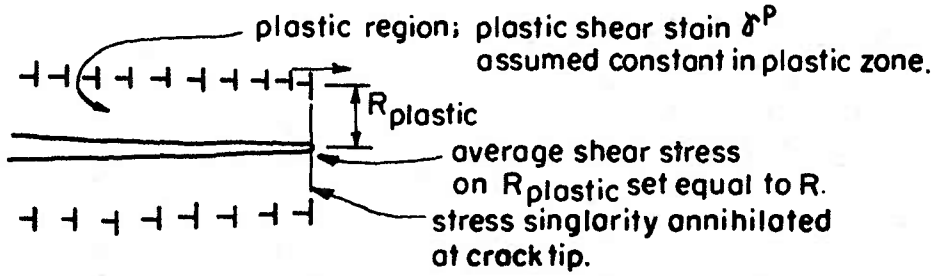

Figure 12

$$R_{plastic} = \frac{1}{16\pi}\left(\frac{K_I}{k}\right)^2 \simeq 0.06\left(\frac{K_I}{\gamma}\right)^2$$

$$\gamma^P = \frac{8\pi(1-\nu^2)\,k}{E} = 4\pi(1-\nu)\,\frac{R}{G} \simeq 8\,\frac{R}{G}$$

3. Microstructural Mechanics

3.1 De-Cohering Layer with Elastic Surroundings

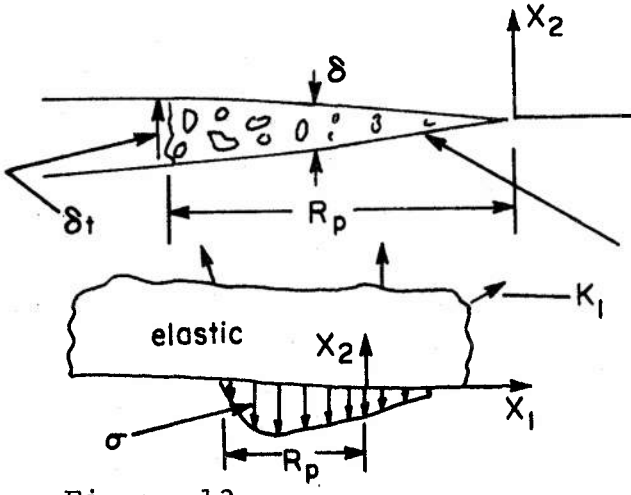

flow localization by local weakness may destroy plastic zone above and below the crack

Figure 13

boundedness condition: $\sqrt{\frac{2}{\pi}} \int_{-R_p}^{0} \frac{\sigma(\chi_1)}{\sqrt{-\chi_1}} \, d\chi_1 = K_I$

a) $\sigma = \sigma$ (porosity)

b) d (porosity) = $\underbrace{A \, d\,\delta}_{\text{hole growth by plastic deformation}} + \underbrace{B \, dt}$ - dissolution, etc.?

c) Diffusion equation, including channel porosity and thickness. How thick should the channel be initially? What processes go on within?

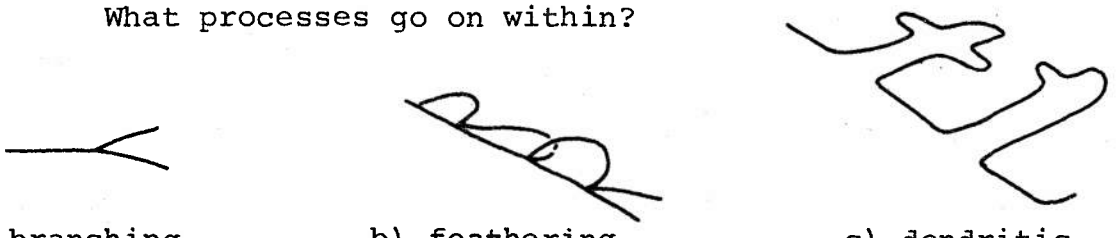

a) branching b) feathering c) dendritic tunneling

Figure 14: Forms of irregular crack fronts approximated by a de-cohering layer.

3.2 Anisotropic Plasticity (1 μ)

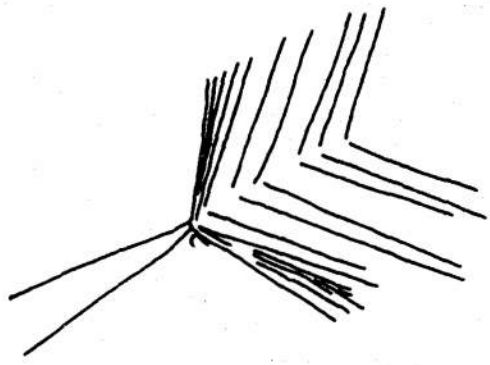

Crack advancing along a grain boundary with numerous sources. Stress limited to order of $\frac{Y}{\rightarrow}$ by flow in adjacent fans.

3.3 Dislocation Mechanics Region (.01 μ)

a) If sources are spaced a distance ℓ, continuum plasticity does not apply within ℓ. For highly hardened alloys, with high dislocation densities,

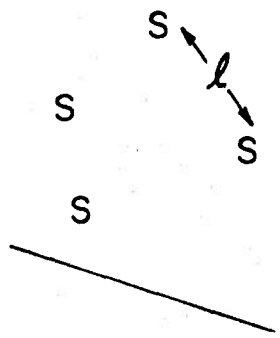

$$\ell \simeq E\, b/Y$$

Spacings ℓ are history-dependent; low near a free surface and high near a rigid film.

b) Dislocation fields near cracks

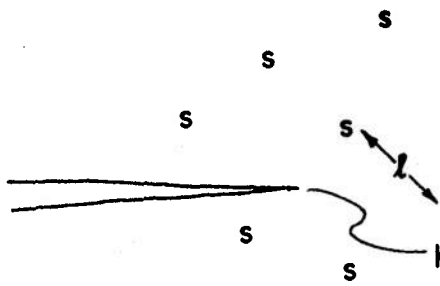

$K_I \approx Y\sqrt{\ell}$; for $Y \approx Eb/\ell$

$K_{Ic} \approx \frac{E}{15}\sqrt{b}$; when $K_{Ic} = \frac{Eb}{\ell}\sqrt{\ell}$

or $\frac{\ell}{b} = \frac{E}{Y} = 200$, can get cleavage

Figure 15: Limitation of stress between dislocation source.

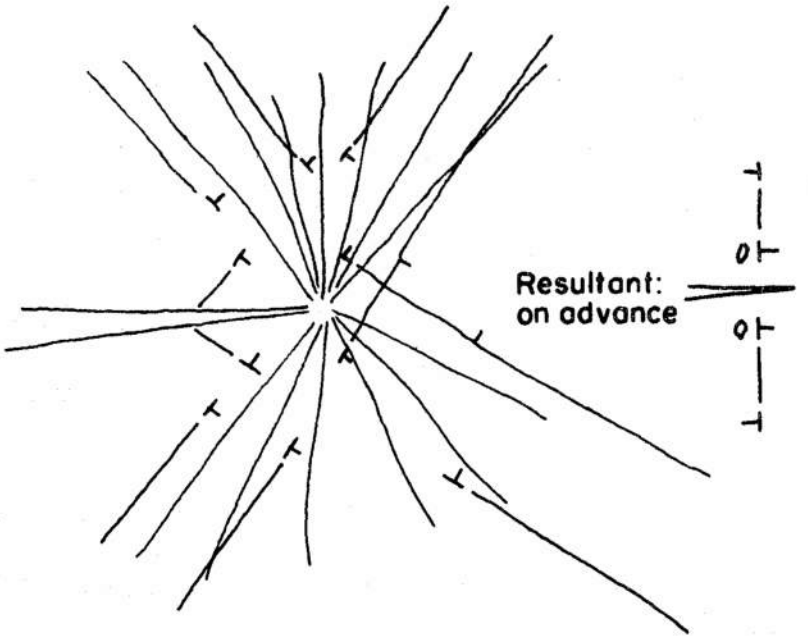

Figure 16 - Dislocation motion around a crack.

4. Atomistic Mechanics (10 Å)

4.1 Cohesive Strength - E/15

Note: A 700,000 psi steel would achieve this in front of a crack with plastic constraint.

Grain Boundary Strength

(of the order of 1/2 cohesive strength)

Grain Boundary Energy

(of the order of 1/4 surface energy)

Cohesive Strength of a Dislocation

(of the order of 1/2 cohesive strength)

4.2 Stress and Curvature Affected Dissolution

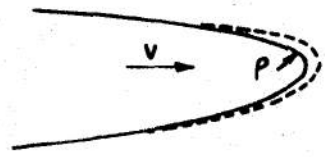

$$\nu = \nu_o \, e^{-(E - b\sigma + \gamma^1/\rho)/kT}$$

4.3 Dislocation Blunting for γ/Gb High Enough (Or High σ_{coh}/τ - Kelly)

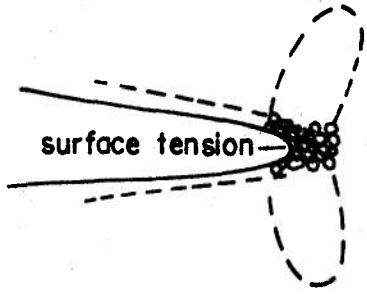

non-linear elastic region

"fluidized region" of high tension and low shear strength.

Non-linear regions at the tip of a crack arising from force laws of the type.

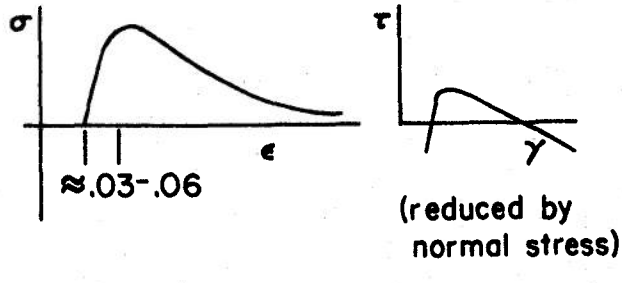

VI. BOUNDARY SEGREGATION EFFECTS IN ENVIRONMENTAL DEGRADATION

by

J. H. Westbrook

Segregation, the development of positive or negative compositional gradients of solutes or impurity atoms, may take place at various types of interfacial boundaries. The present discussion will mostly treat grain boundaries and the oxide-metal interface although stacking faults, anti-phase domain walls, and other types of interfaces within solids may be expected to give analogous environmental degradation behavior whenever there is some path of communication with the environment.

The types of environment considered include oxidizing atmospheres, aqueous corrosion media and liquid metals. Given that segregation is present, the ways in which it may act to bring about the degradation of a solid materials in an aggressive environment are many. These may be divided into four main classes:

(a) A chemical effect of the segregate in which it alters the electrochemical difference between bulk and boundary.

(b) A chemical effect of the segregate in which the segregate accelerates the degradation process by enhancing the diffusion penetration of the

active species from the environment.

(c) A mechanical effect of the segregate in which it embrittles the material locally at the boundary or surface. Stressing of the material then initiates cracks whose propagation is accelerated by the environment.

(d) Effects of the segregate (either chemical or mechanical as above) exerted not in the substrate but in the normally protective oxide film whose invulnerability is thereby compromised.

With regard to the mechanism of segregation itself it is argued that although surface energy driven segregation may occur, a more prevalent and potent segregation mechanism is the non-equilibrium redistribution of solutes induced by vacancy flows to or from interfaces which may act as sources or sinks in any process in which the total concentration of vacancies is caused to seek a new equilibrium value.

Although all the degradation mechanisms above are plausible, and in certain particular cases can be strongly inferred to be operative from the experimental results, it is usually very difficult to prove unambiguously that solute segregation is the causative agent. The reasons for this situation are several: even ppm quantities of solute are effective as segregants, the width of the

concentration gradient is very small (tens of Å to a few microns), interferences exist from two or more solutes present simultaneously and other extraneous phenomena can mask the true effect. Some suggestions are made for an experimental program which will elucidate the situation.

REFERENCES

1. V. I. Arkharov "Intercrystalline Internal Adsorption of Dissolved Additional Elements and Its Significance in Intercrystalline Corrosion" from Intercrystalline Corrosion and Corrosion of Metals under Stress I. A. Levin, ed., transl. from the Russian. Consultants Bureau 1962.

2. J. H. Westbrook "Segregation at Grain Boundaries" Metallurgical Reviews 9 (1964) 415.

3. J. H. Westbrook "Solute Segregation at Interfaces" Interfaces R. C. Gifkins, ed. Butterworths (1970) 283.

VII. FRACTOGRAPHY OF STRESS-CORROSION FAILURES--MECHANISTIC ASPECTS

by

E.N. Pugh

SUMMARY

The purpose of this talk was to illustrate the nature of fracture surfaces in stress-corrosion systems and to discuss existing fractographic evidence in terms of the major proposed models of SCC. The models considered are listed in the following table:

Proposed Mechanism	Predicted Characteristics of Crack Propagation		
	Mode	Continuous or Discontinuous	Crack Path
Film Rupture	Dissolution	Continuous	Transgranular
Adsorption	Mechanical (Brittle)	Continuous	Transgranular or Intergranular
Brittle Film	Mechanical (Brittle)	Discontinuous	Transgranular or Intergranular
Tunnel Model	Mechanical (Ductile)	Discontinuous	Transgranular or Intergranular
Hydrogen Embrittlement	Mechanical (Brittle)	Discontinuous	Transgranular

It was pointed out that significant differences exist in the characteristics of crack propagation predicted by the various models (see table). According to the film-rupture model, cracking proceeds by preferential anodic dissolution at the crack tip, so that the fracture surfaces should exhibit a corroded appearance. The other models consider that the crack propagates by mechanical fracture, either brittle or ductile, and hence the resulting fractures should be characterized by cleavage markings (e.g., river patterns) and a dimpled structure, respectively. Several of the models predict discontinuous propagation and in these cases, the fracture surfaces would be expected to show evidence of discontinuities.

It is apparent from a consideration of the fracture surfaces actually observed in stress-corrosion systems that the various failures cannot be characterized by a single type of fracture surface, and thus selected systems were discussed. It was shown that the intergranular fracture surfaces of Al-Zn-Mg alloys[1,2] exhibit a corroded appearance which is consistent with the film-rupture model. Other workers[3] have reported the presence of striations on the fracture surfaces in this system, but it was argued that these were in fact slip steps. The characteristics of striations were then discussed and it was emphasized that such markings must be matching on both halves of the fracture surfaces, this distinguishing them from slip steps.

Evidence was presented for the existence of striations in the case of the complex-ion embrittlement of AgCl[4] and the

cracking of an 8-1-1 Ti alloy in gaseous hydrogen.[5] It was pointed out that similar markings have been observed on the intergranular fracture surfaces of alpha-brass in tarnishing NH_3[6,7] and alpha-titanium in liquid N_2O_4[8], but that it has not yet been established that they are matching on both halves of the fractures. Brittle oxide films are produced in both these systems, so that if the presence of striations is confirmed then these failures would appear to occur by the brittle-film model.

The transgranular failures of alpha-titanium alloys in aq NaCl and other media[9,10], and 304 type austenitic stainless steels in boiling $MgCl_2$[11-13] were shown to be characterized by fractures similar in appearances to cleavage. It was argued that such surfaces cannot be rationalized in terms of a dislocation mechanism and that they supported either the adsorption or hydrogen-embrittlement models. Based on the existing fractographic evidence, it is not possible to establish whether cracking is continuous or discontinuous in these alloys so that it is not yet possible to distinguish between these models.

REFERENCES

1. A.J. Sedriks, P.W. Slattery, and E.N. Pugh, Trans. ASM, 62, 238, 1969.

2. A.L. Jacobs, Proc. of Conf. of Fundamental Aspects of Stress-Corrosion Cracking, Ohio State University, 1967, p. 530, published by NACE, Houston, Texas, 1969.

3. A.J. McEvily, J.B. Clark, and A.P. Bond, Trans. ASM, 60, 661, 1967.

4. A.R.C. Westwood, D.L. Goldheim, and E.N. Pugh, Ref. 2, p. 84.

5. D. Meyn, unpublished work at Naval Research Labs.

6. A.J. McEvily and A.P. Bond, J. Electrochem. Soc., 112, 131, 1965.

7. E.N. Pugh, J.V. Craig, and A.J. Sedriks, Ref. 2, p. 118.

8. W.K. Boyd, unpublished work at Battelle Memorial Institute.

9. B.F. Brown, NRL Report 7168, Final Technical Report of the ARPA Coupling Program on Stress-Corrosion Cracking, September 1970, Naval Research Laboratory, Washington, D.C.

10. G. Sandoz, Ref. 2, p. 684.

11. N.A. Nielsen, Ref. 2, p. 308.

12. N.A. Nielsen, 1970 Gillett Memorial Lecture, Journal of Materials, JMLSA, 5, 794, 1970.

13. J.D. Harston and J.C. Scully, Corrosion, 26, 387, 1970.

VIII. PRACTICAL PROBLEMS OF STRESS-CORROSION CRACKING IN HIGH-STRENGTH METALLIC MATERIALS

by

Markus O. Speidel

1. Introduction

In these notes we try to point out where, why, and how much stress-corrosion cracking of high-strength metallic materials is a practical problem. We attempt to put into proper perspective the influential parameters which cause the practical stress-corrosion cracking problems; i.e., the alloys, the environments, and the stresses involved. Finally, suggestions are presented and questions raised about what could be done to alleviate the problem.

No attempt is made to discuss the fundamental aspects or the mechanisms of stress-corrosion cracking.

2. Where is Stress-Corrosion Cracking a Practical Problem?

It is now an accepted fact that SCC can be a problem in almost all branches of industry, notably:

* the chemical and petroleum industry
* the power-generating industry
* the construction of marine structures, bridges, etc., and
* the aerospace industry.

Above all, it is the aerospace industry which depends most on high strength materials, especially:

* high-strength aluminum alloys
* high-strength steels
* high-strength titanium alloys
* high-strength magnesium alloys.

The experience gained by the aerospace industry with these materials may therefore serve well as an indication of the overall performance of the alloys.

In advanced structures, such alloys are often exposed to extreme conditions of stress and environment and thus, the possibility of stress corrosion cracking is obvious and must always be checked. However, some of the most widely used high-strength alloys can develop stress corrosion cracks under surprisingly mild conditions--humid air and residual stresses only.

Just how much of a problem stress corrosion cracking of high strength alloys is in the aerospace industry has been a matter of dispute. We have therefore tried to find out in a quantitative way to what extent SCC occurs in various alloy systems. The result is shown in Figure 1. It is based on over three thousand individual failure reports from six aerospace companies and a number of government agencies and research laboratories in the U.S. and four countries in Western Europe. It concerns such items as small aircraft (the majority of failures), helicopters, jet aircraft, and rockets.

We have plotted the estimated number of stress corrosion service failures which occurred within aerospace products in Western Europe and North America versus the year in which these failures* were reported. A certain amount of extrapolation was necessary since it is impossible to get reports from all failures. Moreover, all classified information is excluded. Apart from that, the order of magnitude, the trend and the relative number of failures for the various alloy systems is considered to be correct, and the following conclusions can be drawn from Figure 1:

* Stress corrosion cracking of high strength aluminum alloys is by far the most often occurring problem, followed by stress corrosion cracking of high strength steels. On an average, high strength magnesium alloys account for less than ten percent of all failures encountered, and the number of service failures of titanium components is completely insignificant.

* The number of stress corrosion service problems has been on the rise from 1960 until 1968 and it may be

---

*Alloys 7079-T6, 7075-T6, and 2024-T3 contributed to more than 90% of the service failures of all high-strength aluminum alloys.

Steels 4340, 4330, and 17-7 PH contributed to more than 80% of the service failures of all high-strength steels.

Magnesium alloys AZ 91C-T6 and AZ 80A-F contributed to more than 70% of the service failures of all high-strength magnesium alloys.

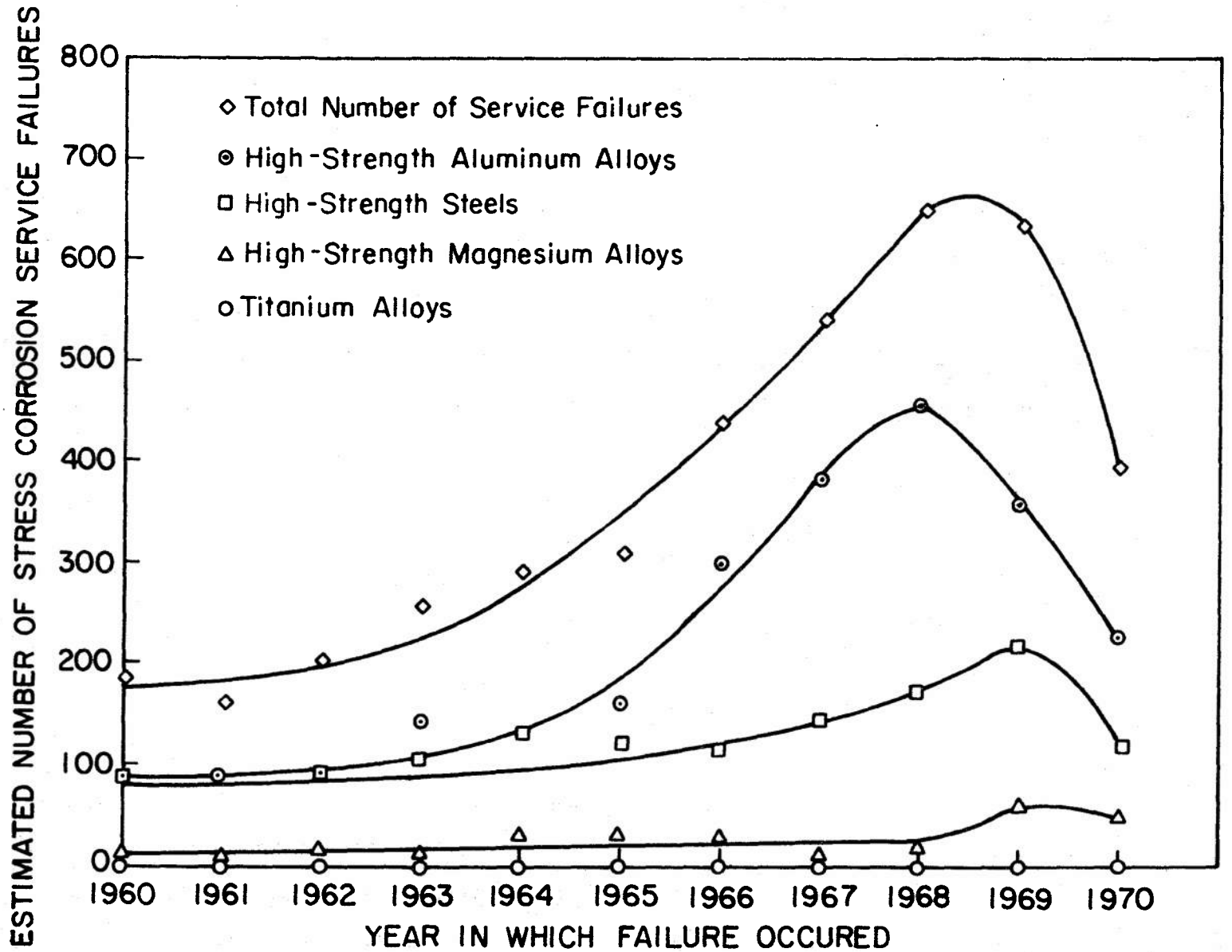
ESTIMATED NUMBER OF STRESS CORROSION SERVICE FAILURES
800
700
600
500
400
300
200
100
0
◇ Total Number of Service Failures
⊙ High-Strength Aluminum Alloys
□ High-Strength Steels
△ High-Strength Magnesium Alloys
○ Titanium Alloys
1960
1961
1962
1963
1964
1965
1966
1967
1968
1969
1970
YEAR IN WHICH FAILURE OCCURED

FIGURE 1.

interesting to speculate on the reasons that brought a reversal of this trend in 1969 and 1970. Among the possibilities:

1) designers have learned from their failures and introduced less susceptible alloys, better surface protection, inhibited environments, and reduced sustained stresses;
2) government-funded research has paid off and provided better alloys as well as a greater awareness of the problem;
3) the declining market situation in the aerospace industry has resulted in less aerospace products and thus less failures.

However, it should not be overlooked that even in 1970 the number of stress corrosion service failures with high strength alloys was greater than in 1965.

One of the lessons that we can learn from Figure 1 is that we should pay more attention to stress corrosion cracking of high strength aluminum alloys and high-strength steels than to stress corrosion cracking of titanium alloys. However, SCC of titanium alloys, although insignificant at present, should not be neglected, partly because titanium is used under more severe conditions and thus, possible failures might be more spectacular. Finally, we would like to point out that the service failures listed in Figure 1 almost never resulted in

catastrophic failures. The vast majority of the failures was with structural parts which were routinely replaced during inspection and maintenance. However, the failures resulted in significant economic losses, due to the cost of replacement and (often more significant) due to the cost of down time.

3. What Are The Specific Causes For The Practical SCC Problems?

With most service failures, specific causes for initiation or propagation of stress corrosion cracks have been observed. The various causes usually belong to one of the following three classes:

* metallurgical
* environmental
* mechanical

This follows quite naturally from the old observation that for stress corrosion cracking to occur, three conditions have to be fulfilled:

* the alloy must be "susceptible" to SCC;
* the environment must be "damaging"; and,
* the stress (intensity) must be "sufficient."

In the following tables (Table 1 through 4), we have listed some of the specific causes for stress corrosion crack initiation and propagation in the two groups of high-strength alloys which cause the most numerous stress corrosion problems.

Table 1

Initiation Sites of Stress-Corrosion Cracks in High-Strength Aluminum Alloys

* stress raisers due to design (bore hole, sharp radius, etc.)	25%
* holes for interference fit bushings	15%
* corrosion pits	12%
* Fatigue cracks	5%
* galling, fretting, wear	5%
* intergranular corrosion, exfoliation	4%
* not known	34%

Table 2

Initiation Sites of Stress-Corrosion Cracks in High-Strength Steels

*	corrosion pits	30%
*	stress raisers due to design (holes, slots, small radii, fillets)	20%
*	fatigue cracks	10%
*	untempered martensite	8%
*	machine marks, scratches	8%
*	cracks in plating	7%
*	not known	17%

Table 3

Sources of Stresses Causing Propagation of Stress Corrosion Cracks in High-Strength Aluminum Alloys

* residual stresses (from heat treatment and fabrication)	40%
* installation stresses (fit-up stresses, improper shimming, torque)	25%
* service stresses (amplified due to stress raisers)	25%
* not known	10%

Table 4

Sources of Stresses Causing Propagation of Stress Corrosion Cracks in High-Strength Steels

* service stresses (amplified by stress raisers)	60%
* residual stresses (e.g., from bending)	10%
* installation stresses (high torque, etc.)	10%
* not known	20%

Again, these tables are based on an evaluation of the enormous number of failure reports from a wide variety of sources mentioned above in Section 2. These tables may well provide starting points to discuss potential technical solutions to the stress corrosion problem in high strength alloys, since we could alleviate the problem by either making crack initiation or crack propagation more difficult.

Titanium alloys. The number of known service failures due to SCC of titanium alloys is too small to be treated in a "statistical" manner. The following list contains the majority of the known service failures due to stress corrosion cracking of titanium alloys.

1) Failure of a jet engine turbine compressor disk made of Ti-4 Al-4Mn. The cracking was associated with areas of the disk in intimate contact with cadmium plated bolts. Stress corrosion cracking occurred due to the presence of cadmium. The problem was solved by eliminating the cadmium from the engine.

2) Failure of a jet engine compressor rotor assembly made of Ti-7Al-4Mo and Ti-5Al-2.5Sn. The cracking originated at the bolt holes where silver plated bolts were in intimate contact with the disk. Cracking was shown to result from the presence of silver chloride. The problem was solved by eliminating the silver from the engine.

3) Stress corrosion cracking of titanium fasteners by solid cadmium. One of the possible solutions is the elimination of the cadmium plating of the bolts.

4) Stress corrosion cracking (or corrosion fatigue) of cast high-speed propellers made of Ti-6Al-4V. Cracking occurred at the site of weld repairs.

5) Stress corrosion cracking of pressurized Ti-6Al-4V tanks filled with Liquid N_2O_4 . The problem is eliminated by adding about 1% H_2O which acts as an inhibitor.

6) Stress corrosion failure of a pressure vessel by anhydrous methanol. The problem is solved by adding a small quantity of water to the methanol. Just as in Case 5) above, the water acts as an inhibitor.

7) Stress corrosion cracking in trichlorethylene of a welded component made of Ti-5Al-2.5Sn. The problem is solved by adding an inhibitor ("stabilizer") to the chlorinated hydrocarbons which are used as degreasers. A better solution appears to be the avoiding of this environment altogether.

In summary, stress corrosion cracking of titanium alloys is relatively easily controlled, because with those alloys nor-

mally used, SCC occurs almost exclusively in "exotic" environments (another example is red fuming nitric acid). Either inhibiting or avoiding the environment appears to be sufficient.

This is very much in contrast to high strength aluminum alloys and high strength steels which can fail by stress corrosion cracking in such ubiquitous environments as moist air--a service environment which is difficult to inhibit or to avoid. However, if marginally susceptible titanium alloys (e.g., Ti-6Al-4V) are used in their highest strength condition, they will become susceptible to environments as little exotic as sea water--and this is a problem to watch in the future.

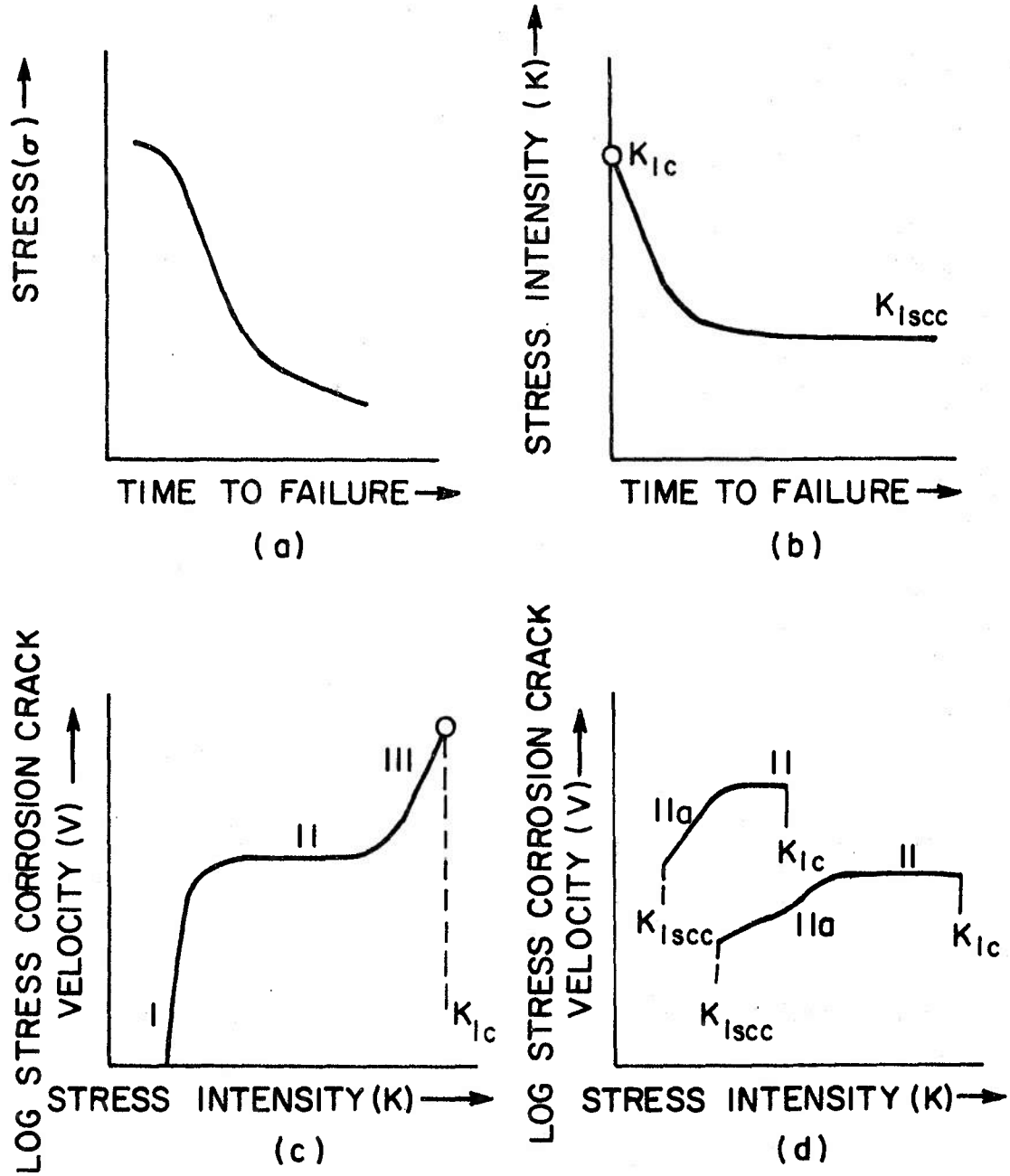

FIGURE 2. Methods of presenting SCC data for (a) Smooth specimens and (b) and (c) Notched (and precracked) specimens and (d) Typical curves for α or (α+β) titanium alloys tested in aqueous solutions.

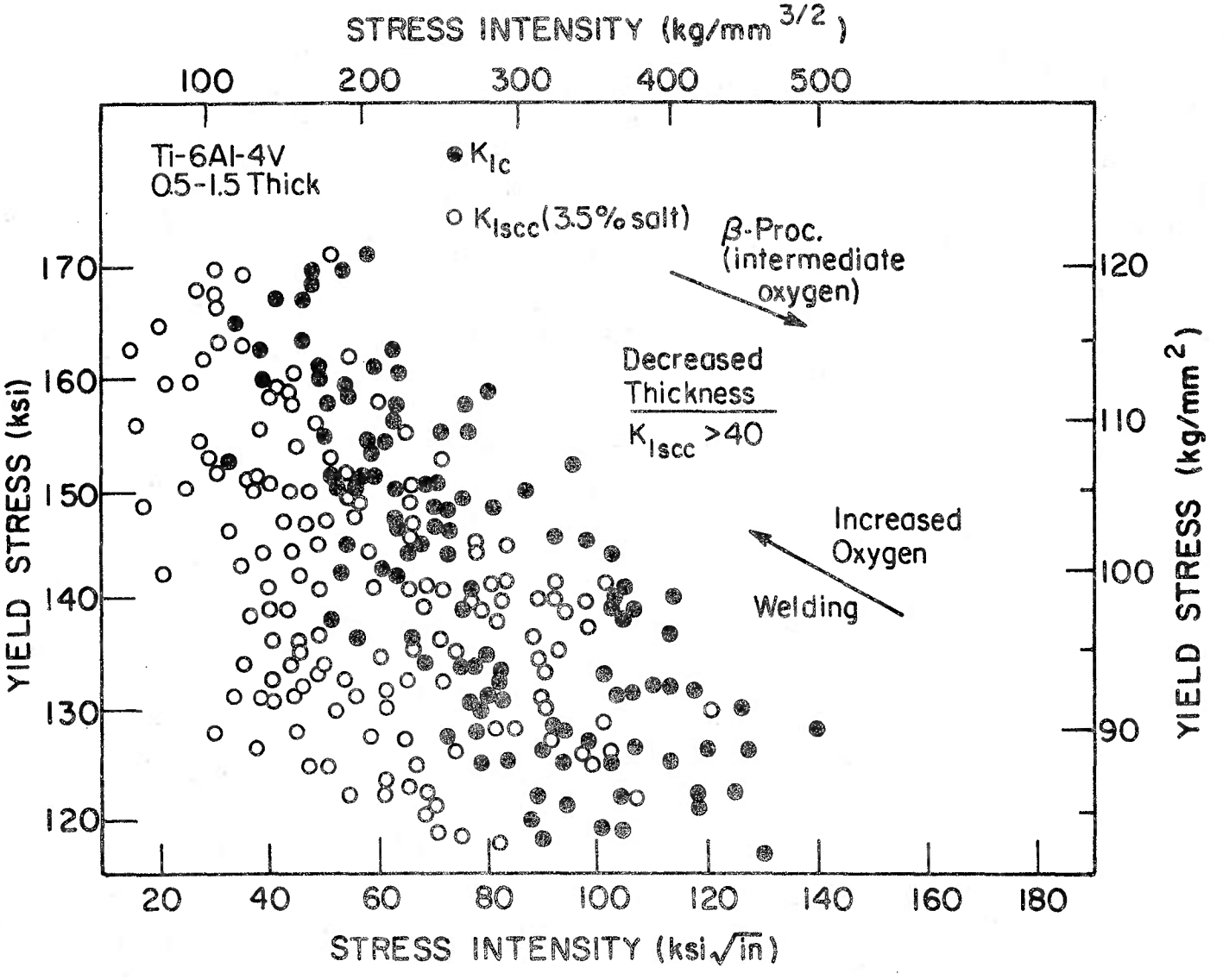

FIGURE 3. The variation of K_{Ic} and K_{Iscc} with yield strength for the alloy Ti-6Al-4V.

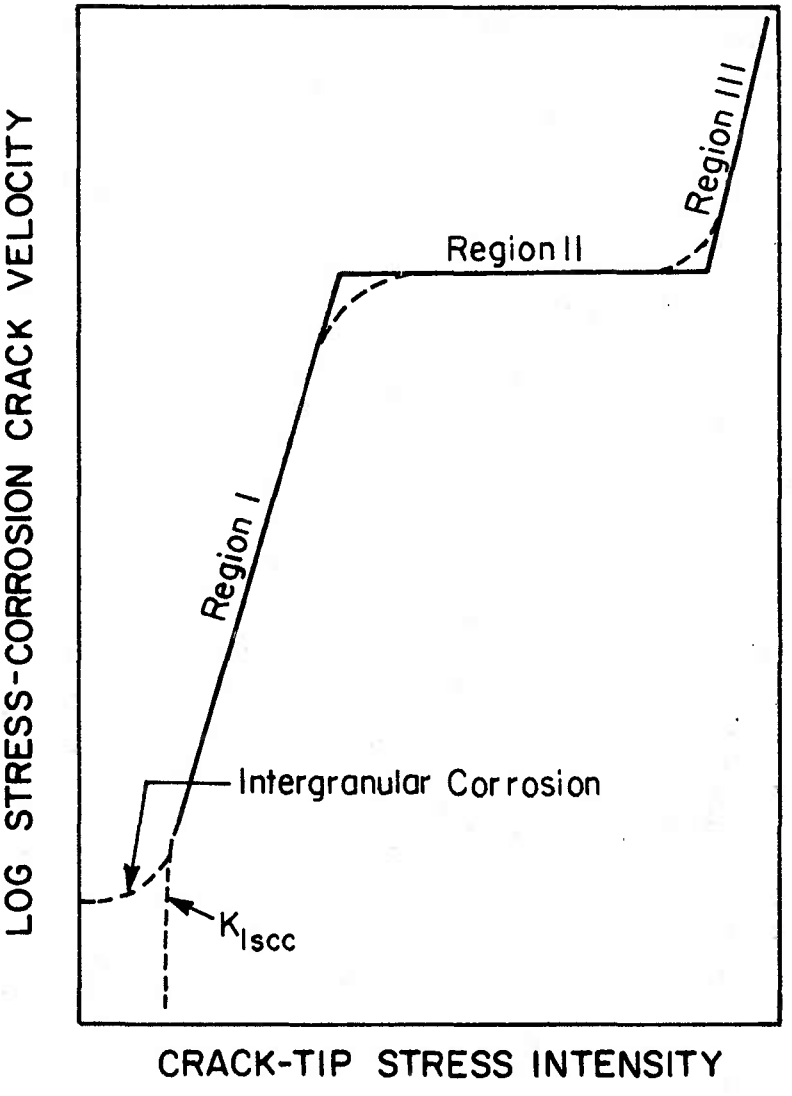
LOG STRESS-CORROSION CRACK VELOCITY
Region III
Region II
Region I
Intergranular Corrosion
K_{Iscc}
CRACK-TIP STRESS INTENSITY

FIGURE 4.

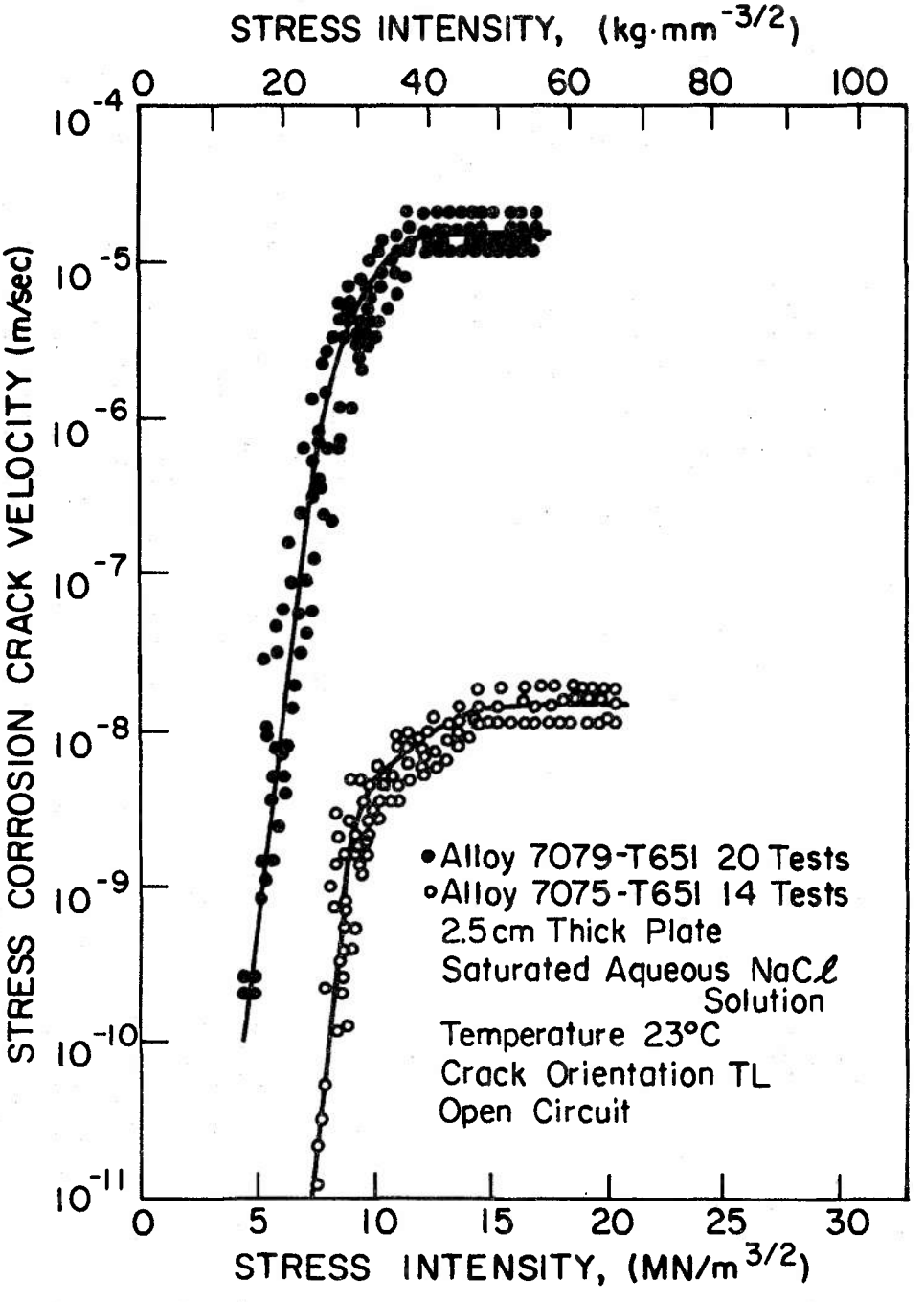
STRESS INTENSITY, (kg·mm$^{-3/2}$)
0
20
40
60
80
100
10^{-4}
10^{-5}
10^{-6}
10^{-7}
10^{-8}
10^{-9}
10^{-10}
10^{-11}
STRESS CORROSION CRACK VELOCITY (m/sec)
•Alloy 7079-T651 20 Tests
∘Alloy 7075-T651 14 Tests
2.5cm Thick Plate
Saturated Aqueous NaCℓ Solution
Temperature 23°C
Crack Orientation TL
Open Circuit
0
5
10
15
20
25
30
STRESS INTENSITY, (MN/m$^{3/2}$)

FIGURE 5.

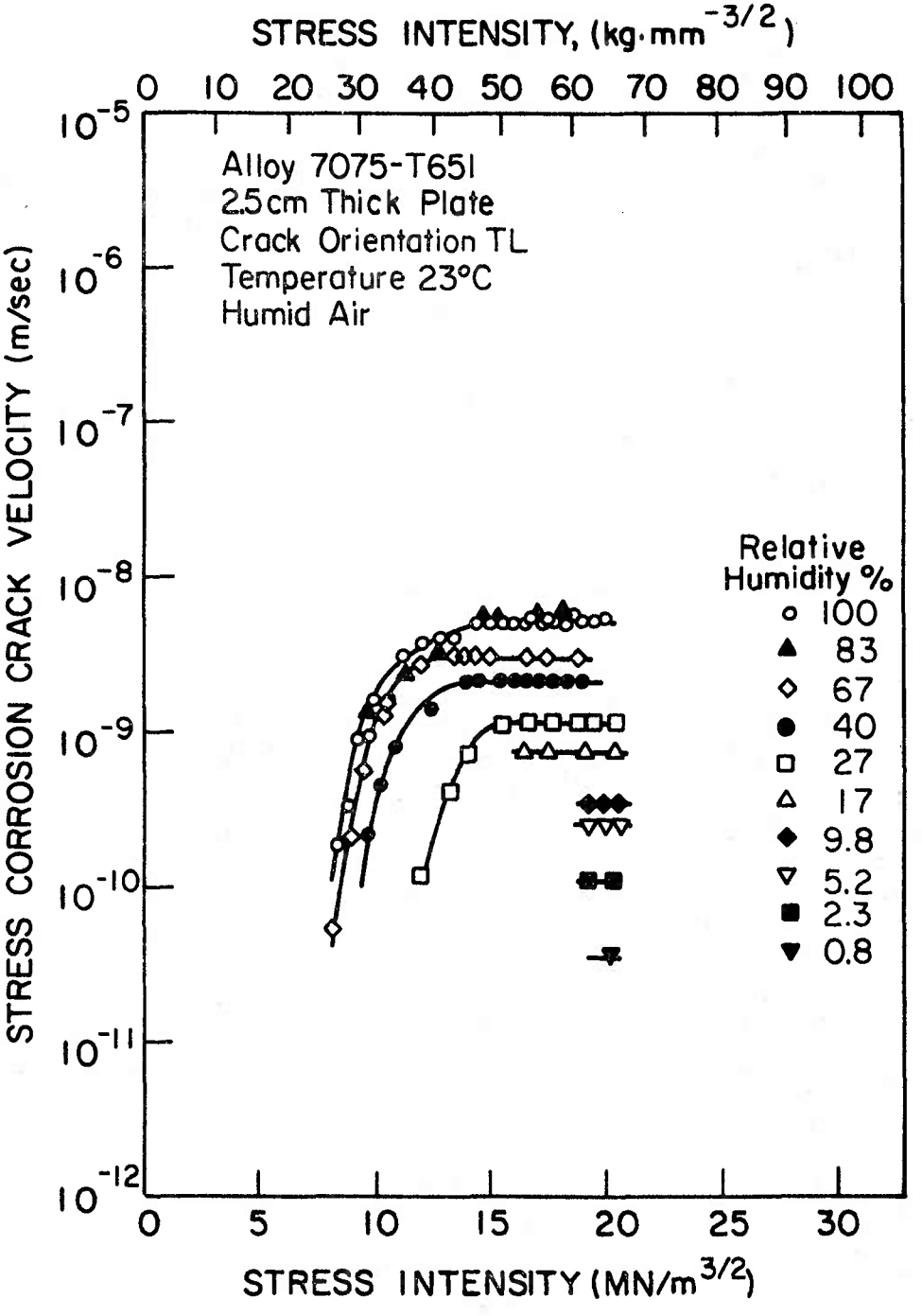

FIGURE 6. Effect of humidity and stress intensity on stress corrosion crack velocity of a high strength aluminum alloy in air.

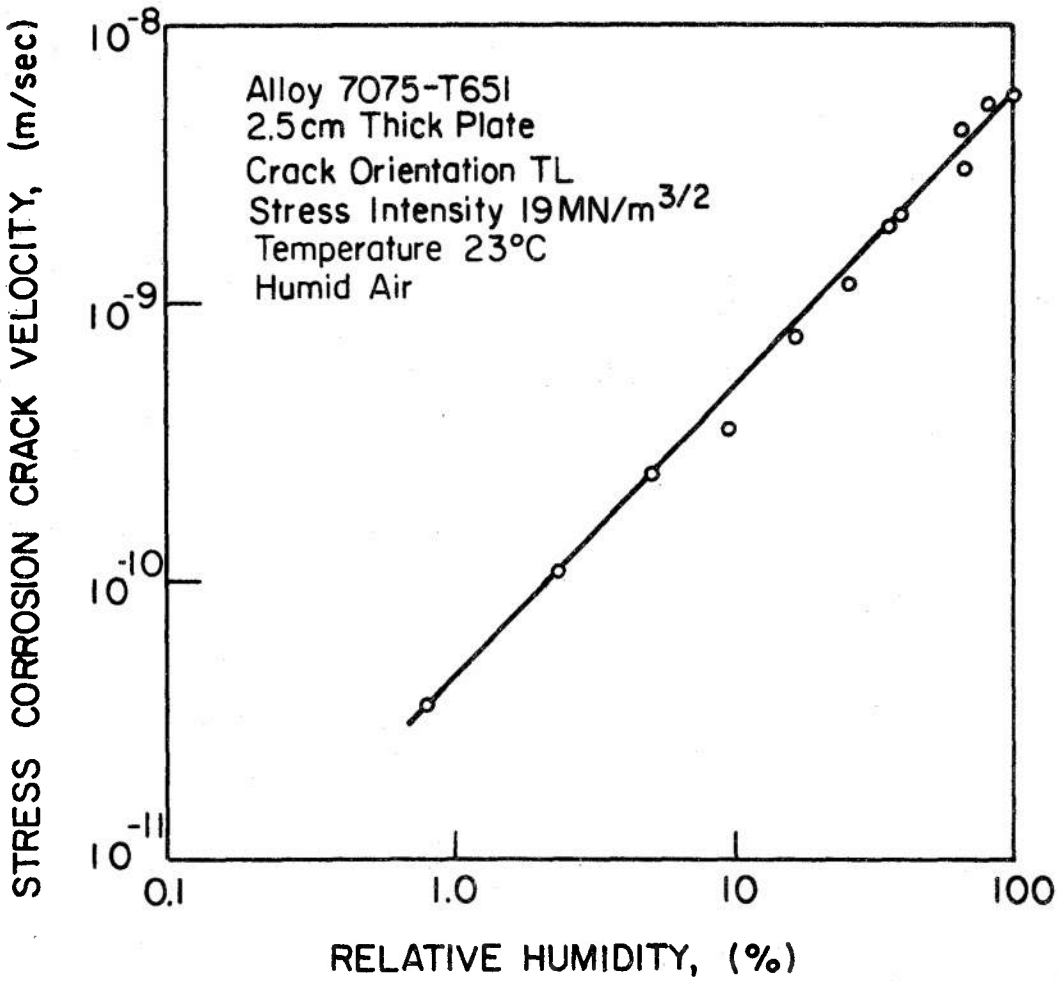

FIGURE 7. Effect of humidity of air on stress-independent stress-corrosion crack velocity of a high strength aluminum alloy.

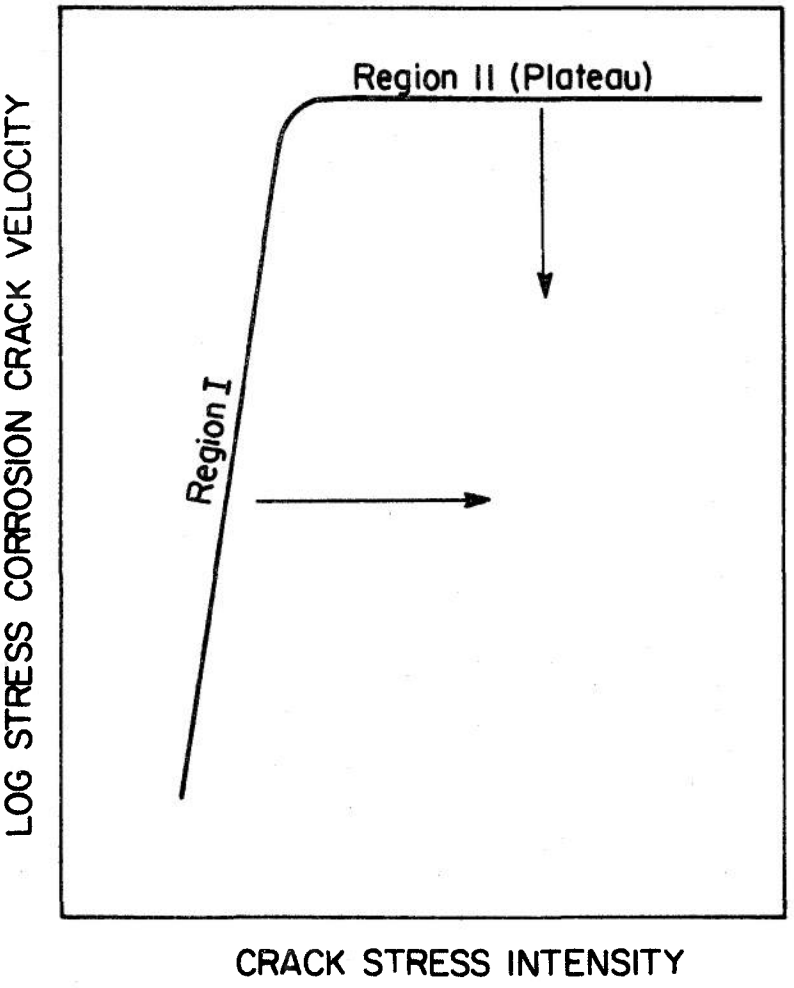

FIGURE 8. Schematic representation of the possible effects of overaging on stress corrosion crack velocity in precipitation hardened aluminum alloys.

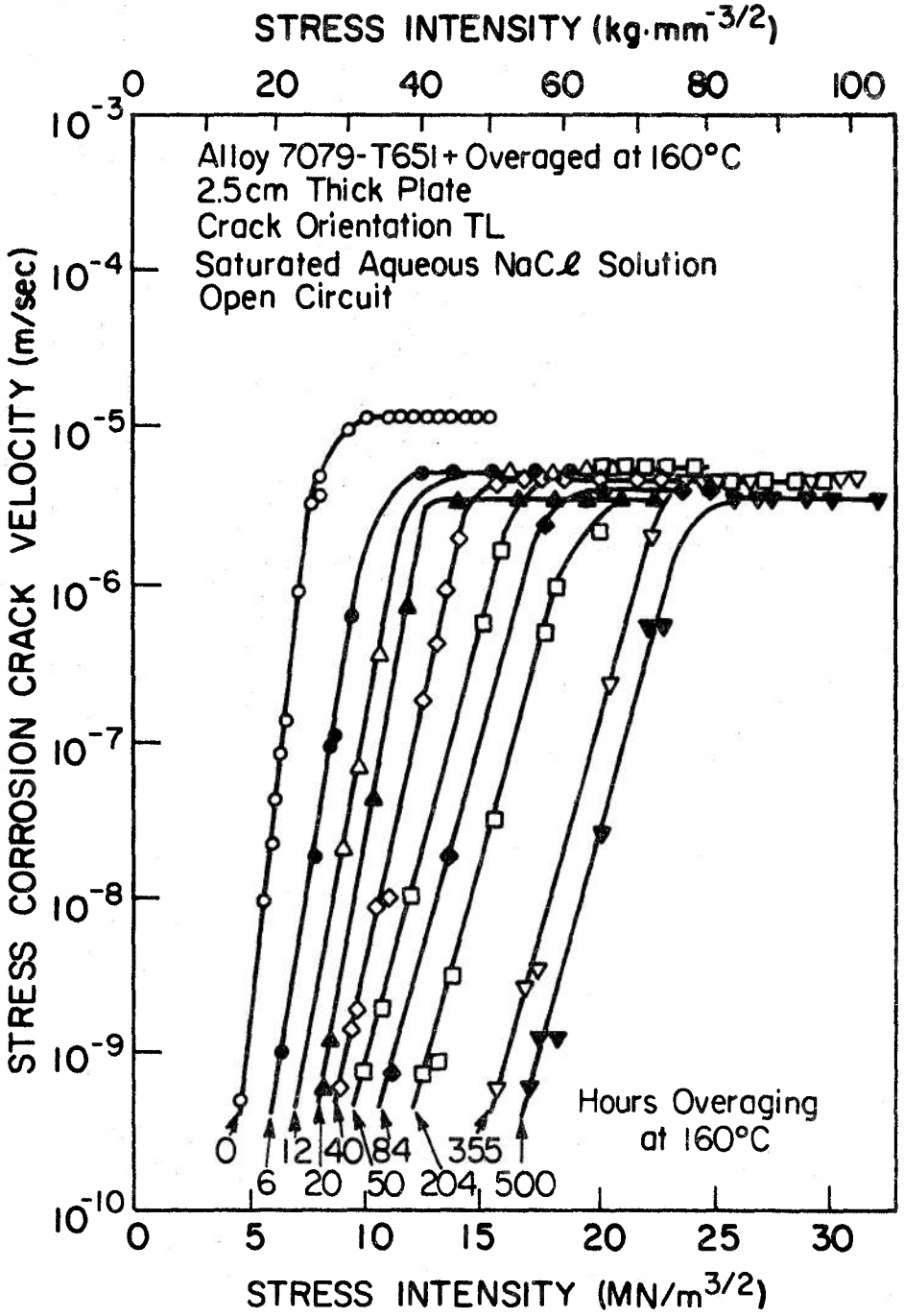

FIGURE 9. Effect of overaging on stress corrosion crack velocity of high strength aluminum alloy 7079.

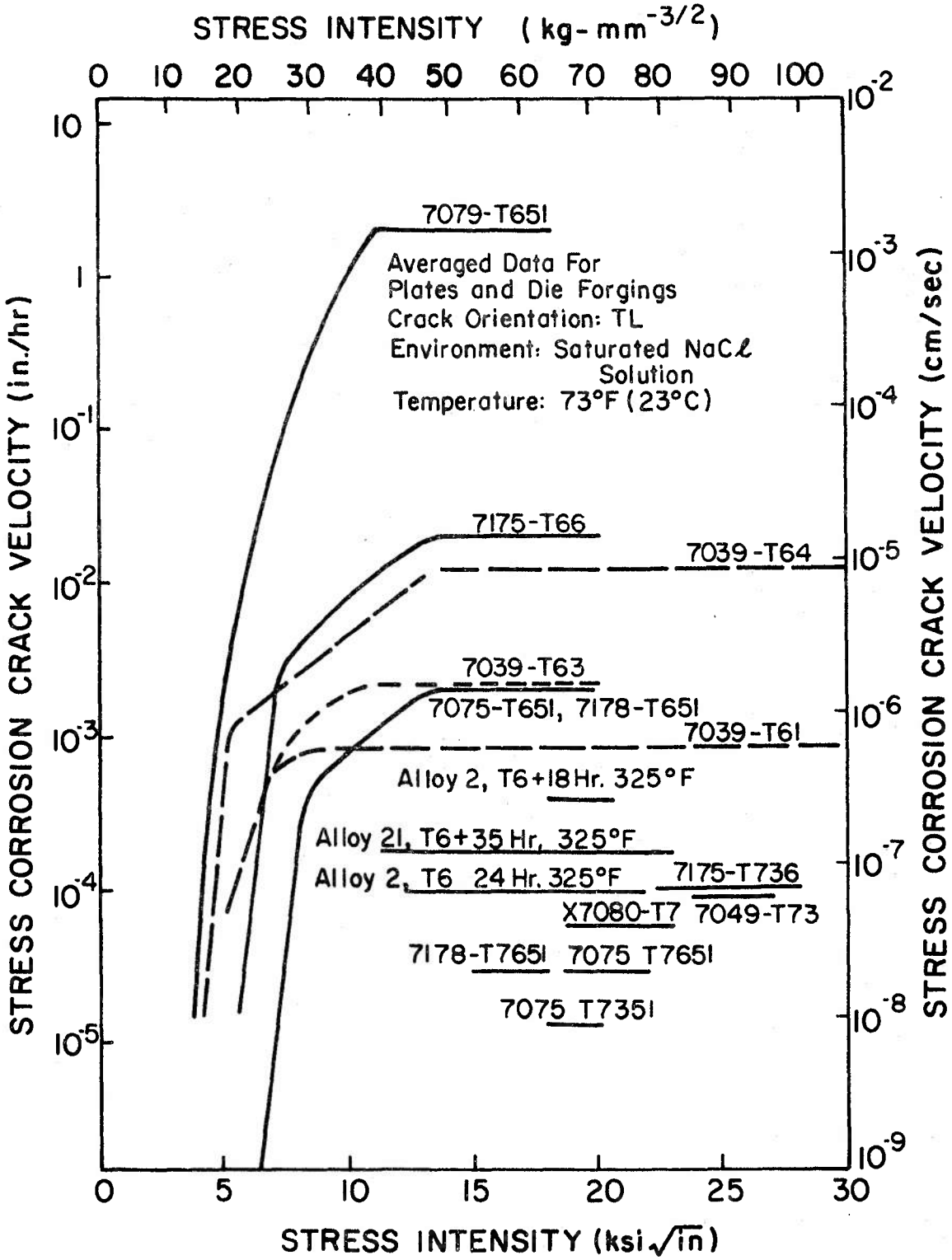

FIGURE 10. Effect of stress intensity on stress-corrosion crack velocity for several commercial and experimental aluminum alloy.s

IX. STRESS CORROSION IN NUCLEAR SYSTEMS

by

S. H. Bush

1. Introduction

The following discussion is limited to an engineering assessment of the variables playing a significant role in stress corrosion. Most of the examples cited are culled from direct or indirect experience with nuclear reactors. A substantial percentage of the downtime of nuclear power plants has been due to stress corrosion induced failures of various components in the reactor primary or secondary systems. Some idea of the components affected is given in Table I compiled from a decade of power reactor experience.

While particular attention will be paid to the austenitic stainless steels, three other materials are of interest due either to a history of stress corrosion in nuclear reactor systems or their use as a part of the primary system. These materials are 17-4 PH, Incoloy-800, and Inconel Alloy-600.

The critical parameters affecting stress corrosion can be grouped under the four factors--material, fabrication, design, and operational. An attempt is made in Table II to assess the significance of the listed parameters on stress corrosion as

applied to nuclear power systems. No claim is made that the table includes all critical parameters; however, I believe that most of the significant parameters are included, together with the role a given parameter plays--significant, minor, or controversial. Table II represents a culling from the various case histories cited later. Hopefully, there will be no contradictions insofar as the effect of single parameters is concerned. The interaction of parameters is difficult to assess in such a table. This will be done through reviewing case histories.

2. Materials

Four classes of materials will be discussed. These are: 17-4 PH (martensitic precipitation hardening) Fe-17 Cr - 4 Ni - 0.05 C; 304, 316, 347 SS (austenitic) essentially Fe-18 Cr - 8 Ni + Mo, Nb, etc.; Incoloy-800 (high nickel SS) Fe-21 Cr - 34 Ni - 0.05 C, and Inconel Alloy-600 (Ni-Cr-Fe alloy) Ni - 16 Cr - 7 Fe - 0.05 C.

2.1 17-4 PH

The critical factor increasing the susceptibility of 17-4 PH to stress corrosion cracking (SCC) is the high hardness and strength resulting from a low temperature precipitation hardening treatment. While this steel is susceptible to stress corrosion after an H-900 (900°F) heat treatment, it is essentially immune after H-1100. Some idea of the differ-

TABLE I
TYPICAL REACTOR PROBLEMS IN PAST DECADE

REF. - D.S. BRIGGS "OPERATING EXPERIENCE WITH NUCLEAR POWER PLANTS IN MEMBER STATES" - ATOMIC ENERGY REVIEW 7 NO. 4, 1969, pp. 167-214.

CAPACITY FACTOR (GCR, BWR, PWR,LMFBR) > 50%

$$\frac{\text{TOTAL TIME - DOWN TIME}}{\text{TOTAL TIME}} \times 100 = \text{CAPACITY}$$

FUEL AND CLADDING

METALLIC FUEL BOWING - IRRADIATION CREEP (GCR'S)
MAGNOX CLADDING CAVITATION - (GCR'S)
VIBRATION FAILURES
STRESS CORROSION CRACKING - STAINLESS STEEL - BWR'S
CRUD FAILURES
FUEL MEETING (THERMAL AND FAST)

HEAT EXCHANGERS, STEAM GENERATORS, CONDENSERS

MAJOR FACTOR IN SHUTDOWNS
- VIBRATION
- CORROSION (STRESS CORROSION, ETC.)
- EROSION

TURBINES, GENERATORS, ALTERNATORS

BLADE DAMAGE AND FAILURE
LOSS OF OIL
STEAM LEAKAGE THROUGH CASING
- SHAFT FAILURE
- LOSS OF LUBRICATION

CONTROL ROD DRIVES

BLADE FAILURES - STRESS CORROSION
STUCK RODS
ELECTRICAL FAILURES

ON-LINE REFUELING EQUIPMENT

NUMEROUS FAILURES DUE TO DESIGN ERRORS

GAS CIRCULATORS AND PUMPS

FATIGUE FAILURES OF BLADES
OIL LEAKAGE AT SEALS

ROTOR DAMAGE
LOSS OF REACTOR COOLANT AND MOTOR BURNUP
BEARING FAILURE

VALVES

LEAKAGE
TURBINE VALVE MALFUNCTION

MISCELLANY

PCRV CABLE CORROSION (G-2)
EXCESSIVE TEMPERATURE IN CONCRETE PCRV (CHINON)
THERMAL INSULATION DETACHED (PEACHBOTTOM)
THERMAL SHIELD FAILURE (YANKEE, SELNI, SENA, BIG ROCK)
PIPE FAILURES AND LEAKAGE (CONN, YANKEE, DRESDEN, CHINON AGESTA, GUNDREMMINGEN, DOUNREAY FAST REACTOR)
VESSEL CLADDING CRACKS (JPDR)
STRESS CORROSION CRACKING OF STAINLESS STEEL NEAR VESSEL (ELK RIVER, LACBWR, OYSTER CREEK, NINE MILE POINT, TARAPUR)

TABLE II

STRESS CORROSION
REVIEW OF SOME CRITICAL PARAMETERS

Role played by specific factor with given material in promoting stress corrosion.

S = Significant; M = Minor; C = Controversial

Material	Martensitic	18/8 Austenitic		High Nickel	
	17-4 PH	304 316	347	Incoloy 800	Inconel Alloy-600
Ferrite Percent		S			
Carbon Effect					C
Fabrication					
Cold Work		M			C
Cleanliness		S			
Heat Treatment					
Solution					
Sensitizing		S	M	S	
Precipitation Hardening	S				
Welding Heat Input		S			
High Strength & Hardness	S				
Low Strength & Hardness					
Pickling		S			S
Design					
Stress		S	S	S	S
Weld-Residual					
Thermally Induced					
Loads					
Crevices (Concentrator)		S	S		S
Galvanic Coupling	S				
Cyclic Loading		S			

Operational	Martensitic 17-4 PH	18/8 Austenitic 304 316	18/8 Austenitic 347	High Nickel Incoloy 800	High Nickel Inconel Alloy-600
Temperature		M		S	S
Local Heat Flux		S			
Neutron Irradiation	C	M			
pH		M→S			
Additives					
Alkaline-LiOH,NaH,NaOH		S	S		M
Borax		M			
Acid					
Residuals					
Oxygen	S	S		S	S
Chlorides		S			M
Fluorides		C			
Lead					S

ences in mechanical properties for the different heat treatments is given in the table.

Heat Treatment	PSI UTS	PSI Y.S.	% R.A.	% Elongation
H-900	200,000	------	45.5	11.5
H-1100	149,000	139,000	63	15

Another important factor appears to be oxygen content. Cracking occurred rapidly in 17-4 PH (H-900) control rod index tubes in Dresden-1, a boiling water reactor (BWR) while lead screws (H-875) used in Shippingport, a pressurized water reactor (PWR), did not crack. PWR's such as Shippingport inject hydrogen in the coolant to scavenge the oxygen. While cracking of 17-4 PH has been observed in PWR's and attributed to SCC, hydrogen embrittlement also can cause cracking. Since it is difficult to examine highly radioactive components, it cannot be said unequivocally that SCC occurred.

Galvanic coupling may aggravate SCC due to hydrogen embrittlement. This has occurred when an aluminum alloy was adjacent to a 17-4 PH part.

A specific instance of SCC of 17-4 PH is seen in Figure 1. A four inch valve stem broke soon after initiation of operation. While an H-1100 treatment had been specified, both hardness and microstructure indicated a heat treatment nearer 950-1050°F. The water contained a scavenger for oxygen, but it was not effective.

The critical factors promoting SCC in 17-4 PH are hardness and oxygen in the coolant. Lowering the hardness and the oxygen content are beneficial.

2.2 Nickel-Chromium-Iron Alloy 600 (Inconel 600)

The Ni-Cr-Fe alloys had been considered to be immune to SCC; however, late work by Coriou, Copson, et al., and Staehle determined that SCC can occur under certain circumstances. There is general agreement that stresses near or exceeding the yield strength are virtually essential to initiate SCC. Crevices appear to be important, possibly as a concentrator of trace ions. Oxygen is believed to be necessary, but the lower limit has not been determined. Cracking has been observed with lithium hydroxide additions to the normal compound used for pH control in many PWR's. Trace quantities of lead are known to promote cracking while chlorides and fluorides do not appear to be important.

There is some evidence that the alloy after a sensitizing heat treatment is more susceptible to SCC than the alloy with a solution heat treatment. Pickling a sensitized alloy seems to render it more susceptible to intergranular (IG) SCC, the only cracking mode observed with Inconel-600. The roles of carbon and of cold work are more controversial. There seems to be no definitive experiments confirming or denying their effect.

Inspection tubes fabricated of Inconel-600 have failed in the Swedish Ågesta reactor. Operating conditions were 217°C in water containing 1-4 ppm of LiOH. The alloy contained 0.08% carbon, definitely higher than usual. In addition, there were

substantial crevices present together with high, thermally-induced, stress levels. In addition, the picture is clouded by use of a high sulfur fuel gas for heat treatment which may have caused some sulfidation. Also, it is quite possible that oxygen was present. Several of the conditions cited as being required for IG SCC of Inconel-600 did exist. Their interaction is less certain.

2.3 Incoloy-800

There are relatively limited data on the sensitivity of Incoloy-800 to SCC. Apparently, it will be attacked under conditions similar to those cited for Inconel Alloy 600. Incoloy-800 in the 1100°F sensitization condition has cracked after exposure to 550°F water containing 100 ppm of oxygen with stress levels of 14000-17000 psi. SCC can occur in the absence of crevices when the Incoloy-800 is in the sensitized condition. Times to initiate SCC were substantially more than for 304 SS under similar conditions. Also, the magnitude of cracking was less in Incoloy-800. Incoloy-800 appears to be somewhat more resistant to SCC than Inconel-600; however, direct comparisons are difficult.

3. The 18/8 Austenitic Stainless Steels (304, 316, 347)

Stress corrosion cracking of austenitic stainless steels was relatively straightforward in the texts used ten to twenty years ago. Two types were discussed; the first covered chloride SCC in the presence of oxygen and stress; the second dealt with

caustic SCC occurring in the absence of oxygen. No particular differentiation was made between sensitized and unsensitized stainless steels. In the past decade this clearcut picture has become badly blurred. We no longer can state unequivocally that chlorides are critical and SCC response of sensitized stainless steels has modified our concepts to a major degree.

In the nuclear industry, we have been plagued with many SCC failures as can be seen from Table I. I have decided that the memory span of people must be about seven years. We have a rash of failures due to some specific design, fabrication or operational error. Corrective measures are determined and applied. Then, the same failure mechanism recurs again six or seven years later. Of particular concern is the failure to eliminate sensitized stainless steels from reactor systems when only nominal design and fabrication changes are required to accomplish this goal.

3.1 Unsensitized Stainless Steel

A reasonable assumption is that any combination of variables that cause SCC in an unsensitized austenitic stainless steel will cause SCC in the same steel in the sensitized state. The converse is not true. A sensitized steel may undergo SCC under certain circumstances while the same steel solution heat treated so that it is unsensitized and subjected to the same test conditions will be resistant to SCC.

The following discussion will deal with parameters affecting initiation of SCC in the unsensitized state.

3.2 Chlorides and Fluorides

There appears to be a threshold of chloride ion concentration to initiate SCC. However, this is influenced by stress levels and oxygen concentrations. Usually several ppm of oxygen are required. Care must be taken that chlorides are not generated from unexpected sources. SCC has occurred due to chlorides resulting from the radiolytic decomposition of freon used as a leak detector in a nuclear system. In this case, both chlorides and fluoride ions were formed. Similar cases have been recorded where elastomeric materials were decomposed thermally or radiolytically. The chloride ions formed soon caused SCC.

Most evidence confirms that fluorides will cause cracking of sensitized but not unsensitized stainless steels. However, there are at least two instances where SCC was reported in unsensitized steel. The SlC reactor pressure vessel cladding exhibited cracks after two weeks at 480°F in pH 10 water (NH_4OH). In this instance, a temporary gasket of Viton-A was used during the hydrostatic test, then not removed during start-up. The gasket underwent thermal decomposition releasing fluoride ions that were said to cause transgranular SCC up to three-eighths inch in depth in the cladding. Similar results had been reported by Bettis Laboratories. Not enough is known of these case histories to eliminate the possibility of chlorides being present, at least in my opinion.

3.3 Bases (Hydroxyl Ions)

The phenomenon of caustic SCC of stainless steels is well documented. Oxygen need not be present in caustic SCC. There is evidence that there is a decreasing tendency to cause SCC from sodium hydroxide (the worst) to potassium hydroxide, lithium hydroxide and ammonium hydroxide. The latter two, LiOH and NH_4OH, are used for pH control in PWR's. Concentrations at pH 10 to 11 are insufficient to cause SCC even when NaOH is used. However, any mechanism to concentrate the hydroxyl ions such as crevices or steam blanketing can result in SCC. Additives such as orthophosphates minimize, but do not eliminate, caustic SCC. Heat exchangers with high steaming rates such as at Shippingport are susceptible to steam blanketing and caustic concentration.

3.4 Concentration Effects

The preceding cases describe caustic concentration in crevices or through steam blanketing. Similar cases have been reported for chlorides where initial levels were very low. Carry-over in wet steam is a typical mechanism. Moisture shields in turbines have failed by chloride buildup. A more interesting case occurred with the first superheat fuel elements where very careful attention was given to keeping chloride levels to a few parts-per-billion. Due to carry-over of moisture in steam that flashed on the hot fuel element surfaces, chlorides built up from a few ppb to greater than 10,000 ppm in a few weeks.

The thermally induced stresses, plus chlorides, plus a few ppm of oxygen soon cracked the 304 SS cladding. Incoloy-800 was an adequate substitute immune to chloride ions. Another example of concentration of chloride from wet steam occurred in a safety valve. The design permitted collection of chlorides in the hollow interior of the plug seal and the plug finally broke away from the stem.

At Savannah River some of the heat exchangers contained double tube sheets of 304-L, to minimize contamination of the D_2O primary coolant with the H_2O secondary coolant, or loss of D_2O to the H_2O. The D_2O contained <6 ppb chlorides, the H_2O 1-6 ppm chlorides. Some water (H_2O) leaked into the gap between the tube sheets and vaporized, depositing chlorides. Another source of chlorides in the water was decomposition of elastomeric gaskets containing 8% chloride in the heat exchanger. Concentrations as high as 300 ppm chloride were measured in the deposited layers, sufficient to cause gross transgranular SCC after five years, leading to rupture of one and leakage in other tubes.

3.4 Stress

Stress is an essential factor in SCC. There can be direct loads, thermally induced stresses or residual stresses from welding or other fabrication operations. The lower stress threshold depends on time, temperature, impurities present and their levels, and concentrating mechanisms. High stresses may lead to rapid cracking while low stresses may delay SCC for

years. Residual stresses are difficult to predict so high levels may exist, causing rapid failure. An example of rapid SCC induced by high residual stresses occurred in the Oyster Creek and Tarapur BWR pressure vessel stub tubes. These stub tubes consisted of relatively short sections of thick-walled 304 SS tubing welded into the bottom head of the vessel. The stub tubes are transition pieces to which the control rod drive (CRD) thimbles are welded. The procedure consisted of counter-boring holes partially through the head; setting in the stub tubes, and making a partial penetration weld. Since the head was A-533, a low alloy steel, and the stub tubes were 304 SS, it was necessary to make the weld with INCO-82, a high nickel alloy matching the coefficient of expansion of the alloy steel. The weld between the stub tube and the CRD thimble introduced a bending moment so that the shorter stub tubes had very high stresses near the toe of the INCO weld. Chloride contamination was sufficient to cause severe cracking around the circumference near the weld region. An additional factor was the residual stress introduced due to mechanically straightening the stub tubes after welding. The stub tubes underwent the same 1100°F stress relief as the vessel, an ASME code requirement, so they were severely sensitized. This probably accelerated SCC, but I am convinced that the tubes would have cracked even if unsensitized. Fundamentally, the design was poor and contaminants accentuated the problem.

Another example of high loading, leading to accelerated SCC, occurred at the Nine Mile Point BWR. The pipe supports

were installed on the basis of the cold system at room temperature. On heatup, the reactor vessel expanded axially so that bending moments were introduced near the nozzle region. These high stresses on the sensitized safe end transition pieces resulted in very rapid circumferential SCC.

3.5 Neutron Irradiation

Exposure to a neutron flux appears to be relatively unimportant insofar as SCC is concerned. There are limited data that fast neutrons will damage oxide films and increase the susceptibility to SCC in 316 SS. If so, the effect appears to be minor.

3.6 Ferrite Level

Austenitic castings or welds usually contain greater than 5% ferrite. This is sufficient to minimize SCC except in the more aggressive environments. SCC can occur if the ferrite is too low. Cases of SCC have been observed where retained ferrite was less than 1%. In these instances, the system was sensitized and cracking occurred in the presence of very low concentrations of chloride and oxygen.

3.7 Welding Heat Input

Welding procedures vary a great deal with austenitic piping. Earlier procedures used heat inputs as high as 100,000 Joules/inch. Current practice is nearer 30,000 Joules/inch. With high heat inputs the heat-affected-zones (HAZ's) become

sensitized and SCC has occurred in BWR systems 5 to 10 years after initiation of operation. Lowering the heat input eliminates this problem.

3.8 High Heat Fluxes

One class of fuel cladding investigated for BWR's was non-freestanding 304 SS. This thin-walled tubing was used with uranium dioxide fuel. When operated at high heat fluxes approaching 500,000 BTU/ft^2/hr, the cladding soon failed intergranularly by a mechanism akin to SCC. The 304 SS was not sensitized, but almost all failures were intergranular. The coolant contained $\sim$ 1 ppm oxygen and $<$ 1 ppm chlorides. There seemed to be no concentrating mechanism so the high heat flux seems to be a significant factor, Figure 2.

3.9 Cyclic Loading

The addition of a cyclic load to a static load may lead to very rapid failure. I define this as corrosion-fatigue which is incorrect albeit quite descriptive. Apparently, there is continuous notch sharpening by the corrodent so that the number of cycles to failure are a small fraction of those predicted by ASME design procedures for cyclic fatigue. An example of failure by cyclic loading is given in Figure 3. In this case, the component is a sensitized 304 SS tube in a steam generator. Several tubes failed in a few weeks due to the cyclic loading. Both oxygen and chlorides were below 1 ppm.

Thermal fatigue may result in rapid failure of austenitic stainless steel. The structure often resembles transgranular SCC so closely that it is often mistakenly diagnosed as SCC. The usual mechanism of thermal fatigue is injection of colder water into a hot stream at a tee. Systems are often designed with thermal shields, but they are not considered necessary when the Δt is small. Due to their high coefficient of thermal expansion, austenitic stainless steels are particularly susceptible to such thermal fatigue. An example is given in Figure 4.

3.10 Sensitized Stainless Steel

Sensitization of the austenitic stainless steels makes them much more susceptible to SCC. The following examples are cases where failures occurred in sensitized steel, but almost certainly would not have occurred in an unsensitized steel. The temperature and times of sensitization may affect susceptibility to SCC. There is some evidence that the plate-like morphology of carbides produced below 1100°F is more susceptible to SCC than the isolated particles typical of 1200°F sensitization.

SCC can be expected to occur at lower levels of stress, chlorides, and oxygen. A limiting case is SCC in the presence of oxygen and stress with no measurable chlorides. There have been several instances of intergranular SCC in pH 7 high purity water such as used in BWR's. Usually oxygen levels are high enough to promote cracking, Figure 5.

3.11 pH

The principal effect of pH is to change the cracking mode of sensitized stainless steels. For example, at pH 5 cracking is transgranular, at 4.5 it is mixed; at 3.0-3.5 it may be intergranular. Stress level sometimes shifts the values.

3.12 Fluorides

There is definite evidence of cracking of sensitized steel in the presence of fluoride ions as low as 1 ppm in alkaline or neutral solutions. This could be significant in some nuclear operations.

3.13 Pickling

Care should be taken in the pickling of sensitized stainless steels with HNO_3-HF solutions. Grain boundary attack to depths of greater than 0.015 inches is known to occur. This deep attack results in crevices for concentration of impurities.

An example of failure believed to be induced by pickling occurred at Savannah River. Nozzles used as a part of the reactor system were sensitized, then pickled, prior to welding into the system. The design was such as to lead to residual stresses. The coolant was D_2O kept to 3 micro mhos/cm. Impurity levels were 0.5 ppm NO_3^-, 0.5 ppm $SO_4^=$, 0.02 ppm Cl^-, 2 ppm O_2, pH 5 by HNO_3 plus oxygen. These nozzles cracked near

the weld at the point of suspected maximum stress, due to concentration of chlorides in the crevices.

Another type of attack may result from incomplete cleaning after pickling. If tubes are sensitized with pickle solution remaining, severe intergranular attack may occur from the very low pH acids. Examples have been seen of hemispherical regions of gross intergranular attack believed to result from residual droplets of acid, Figure 6.

3.14 Potential Problems

One concern with nuclear systems is that they may fail by SCC before operation because of contaminants introduced during construction. This is of continuing concern in liquid-metal-fast-breeder (LMFBR) reactor pressure vessels such as shown in Figure 7. Due to the vessel geometry, it may not be possible to solution heat treat the vessel so there will be sensitized regions that could be attacked. After operation, the entire system becomes sensitized due to the operating temperature of 950-1050°F and the problem of protection against contaminants remains.

4. Closing

This has been a brief survey of some of the more significant factors influencing SCC in alloys of interest to the nuclear industry. No attempt has been made to discuss fundamental mechanisms.

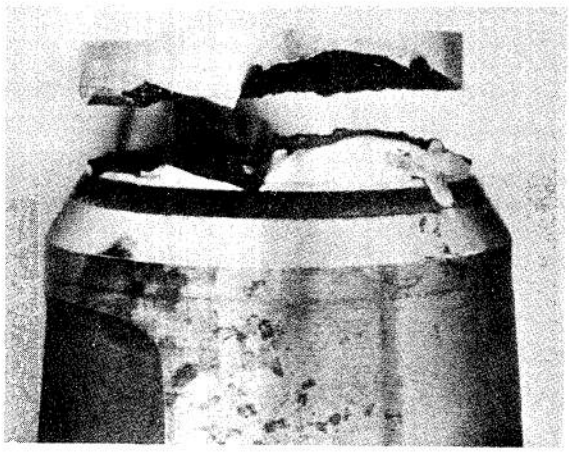

a) Side View of Break

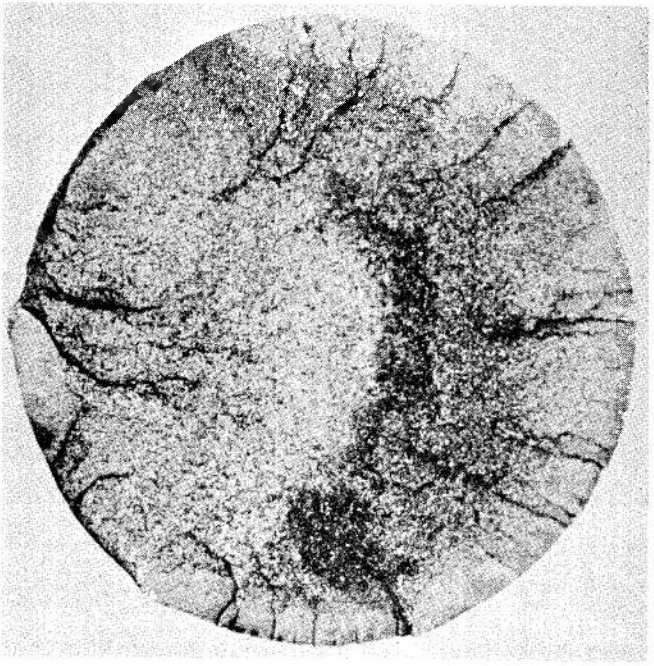

d) Broken Surface. Staining Indicates Propagation

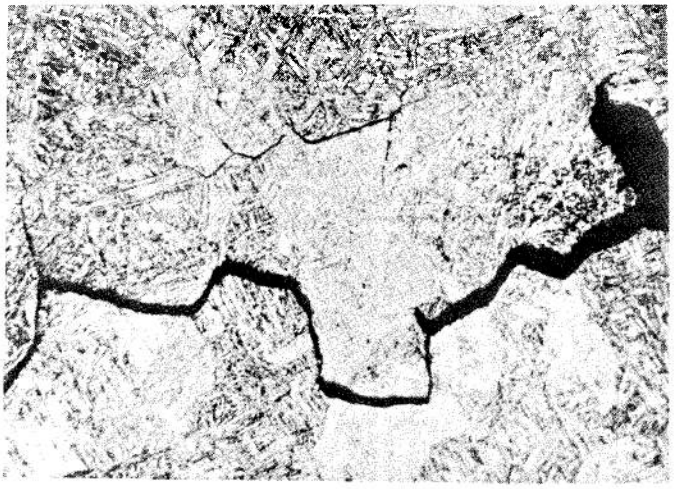

c) Cracks off Main Break. The Intergranular Nature is Typical of Stress Corroded Martensitic Alloys

FIGURE 1: Stress corrosion cracking in a 17-4 PH valve stem supposedly given a 1025° to 110°F heat treatment. Results were more consistent with 900°F treatment.

FIGURE 2: An example of complete intergranular failure in 304 stainless steel fuel element cladding. This failure occurred during irradiation in water by a mechanism akin to stress corrosion. Electrolytic oxalic acid etch.

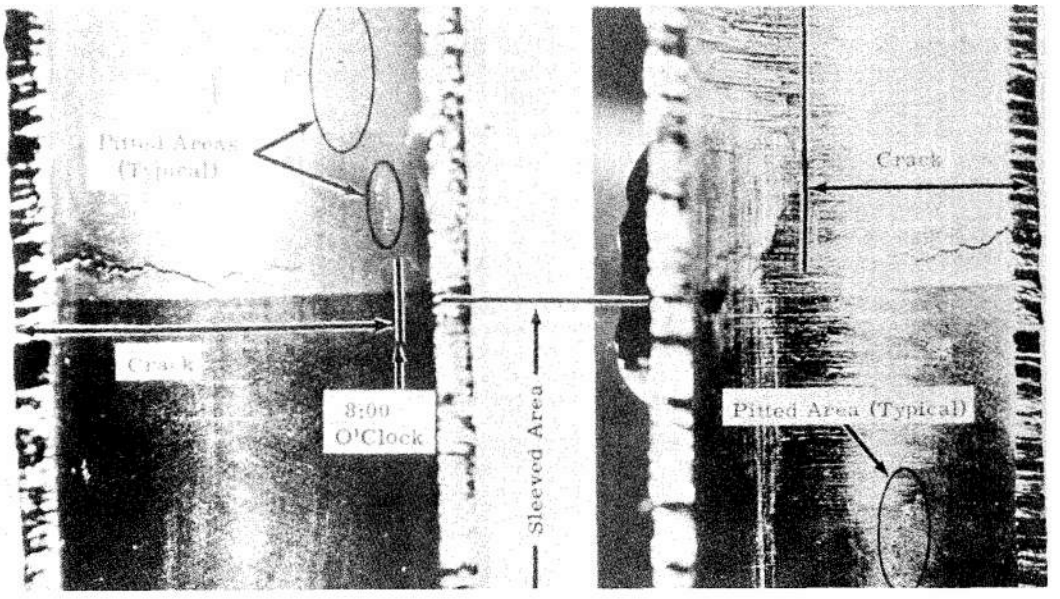

a) Inner Surface of Tube Showing Circumferential Crack

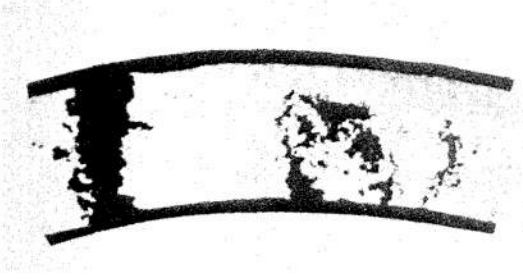

b) Micrograph Displaying Severe Corrosion-Fatigue Attack

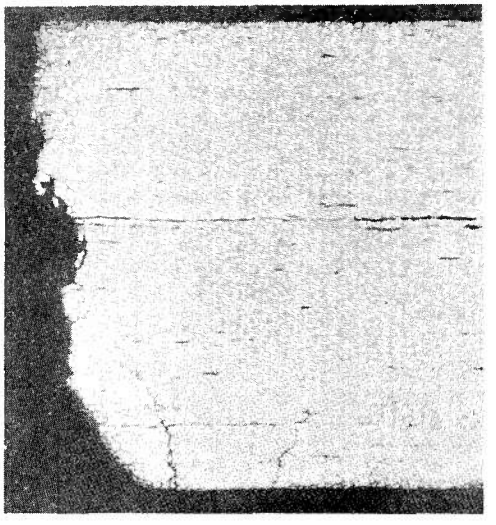

c) Micrograph of Fracture Surface

FIGURE 3: An example of corrosion-fatigue failure in a steam condenser tube.

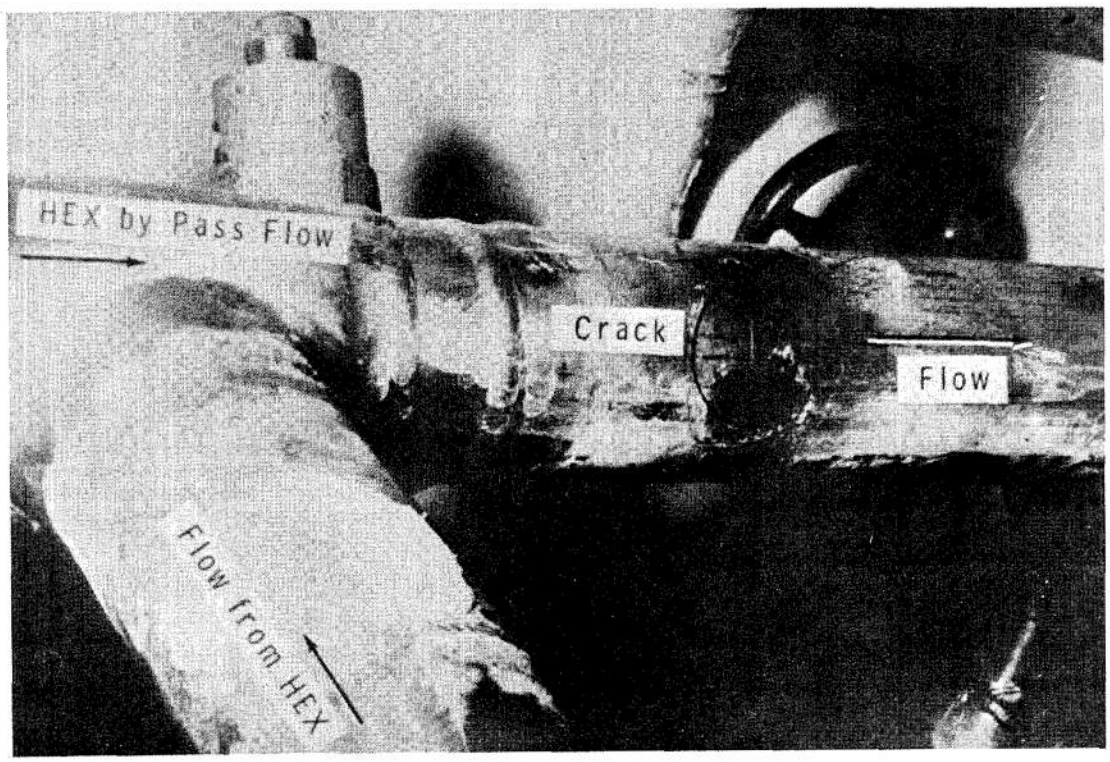

a) Cracking Due to Injection of Cold Water from Heat Exchanger into Bypass Line

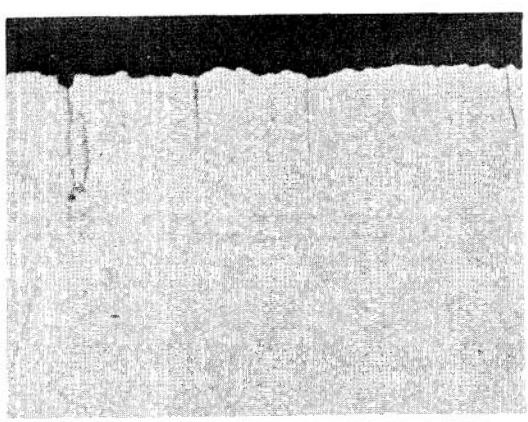

b) Surface Cracking

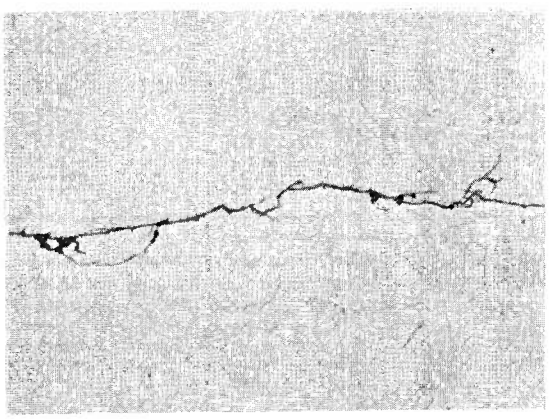

c) Through Cracking

FIGURE 4: An example of failure due to thermal fatigue resulting from injection of colder water into a hot stream.

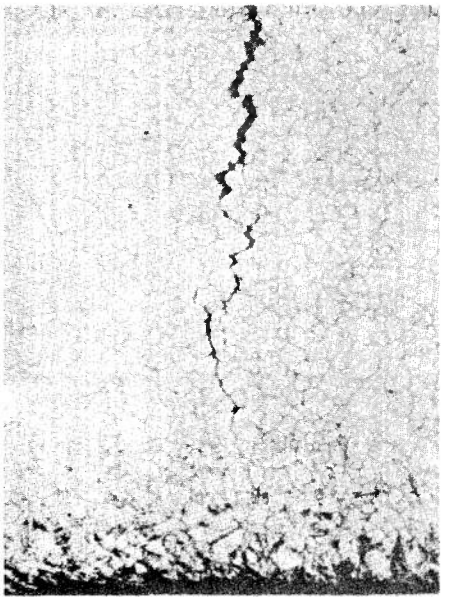

a) Intergranular Cracking of Sensitized 304 SS

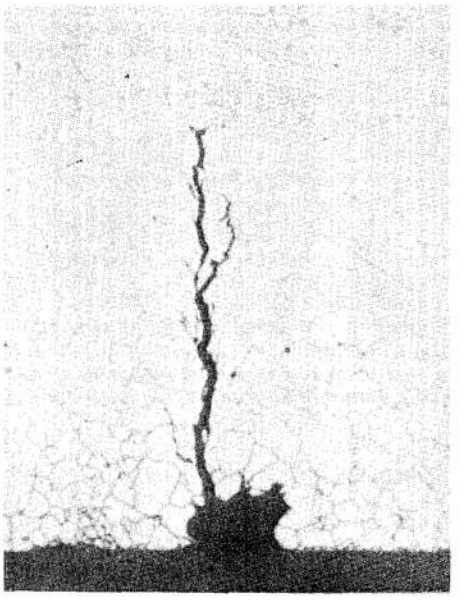

b) Transgranular Cracking Initiating at Pit in Sensitized 304 SS

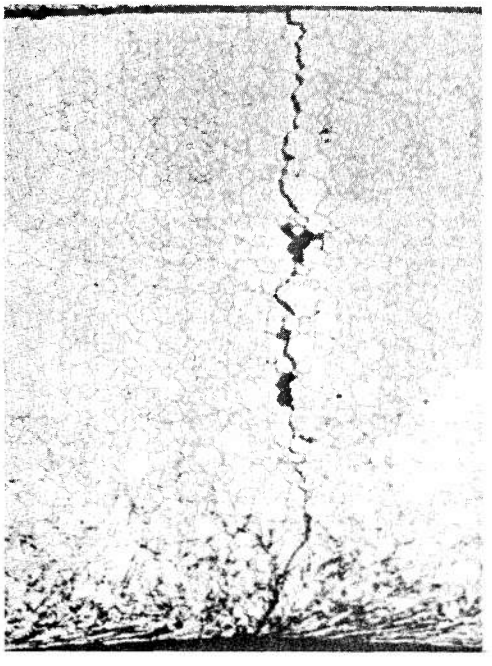

c) A Mixture of Intergranular and Transgranular Cracking in Sensitized 304 SS

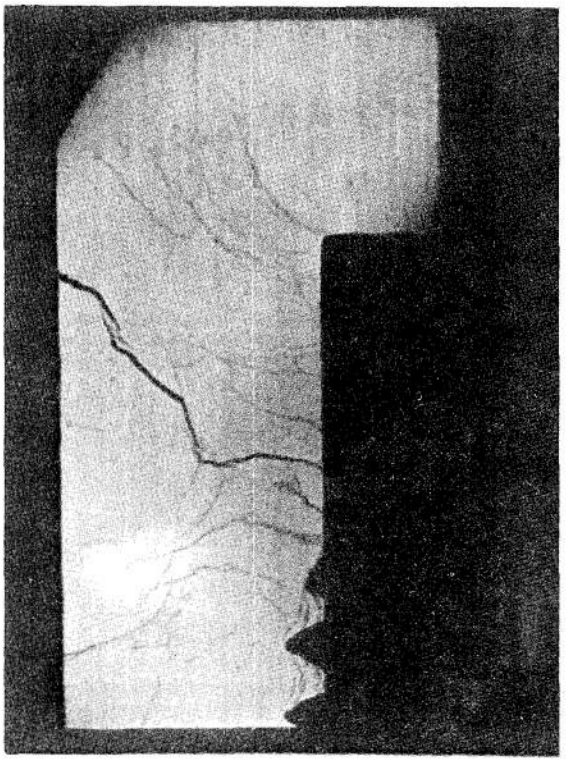

d) Macrograph of cracking in pH-10 (NaOH) After Concentration of Caustic Occurred. A Stainless

FIGURE 5: Typical examples of stress corrosion cracking in a 304 stainless steel. This attack was probably due to chlorides and oxygenin a, b, c caustic in d.

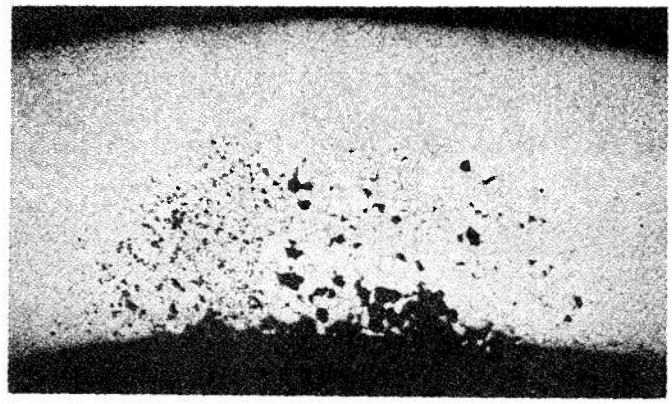

a) Selective Intergranular Attack of Sensitized Austenitic Stainless Steel

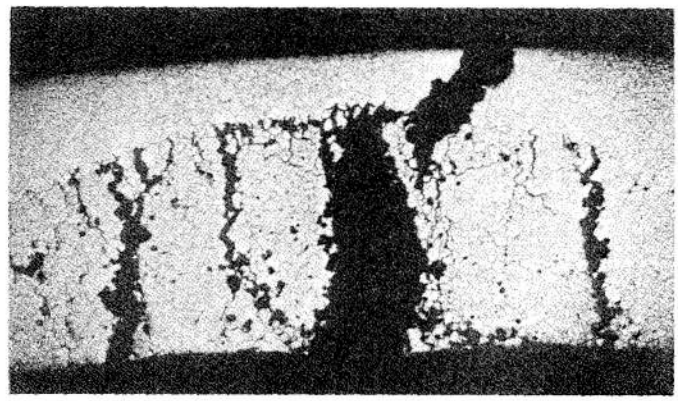

b) Failure Under Hydrostatic Loading of a Section Similar to 1C

FIGURE 6: Examples of General Corrosion

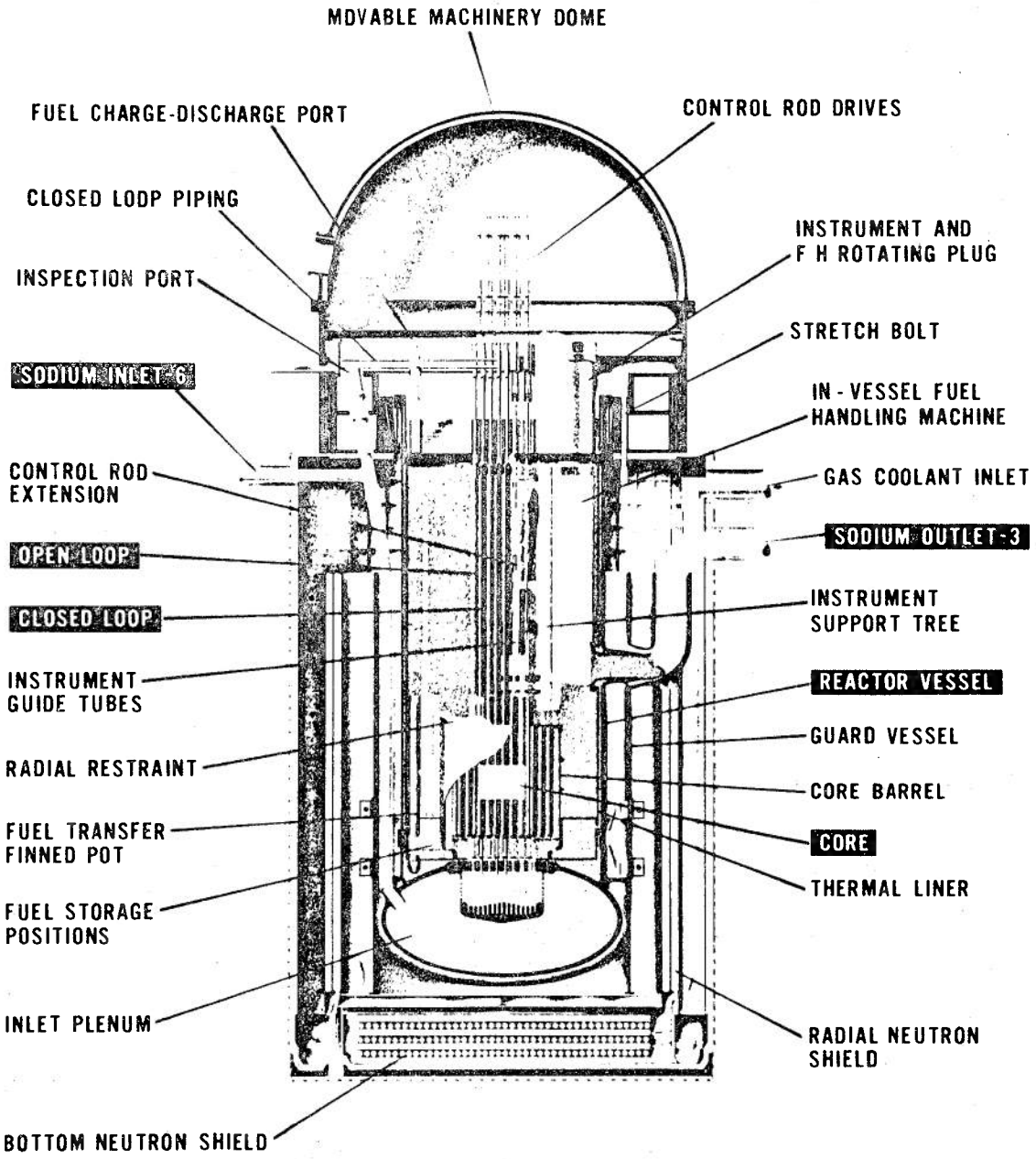

FIGURE 7: General arrangement of a liquid metal fast breeder reactor - the fast flux test reactor.

Component(s) - Control-Rod Drives

Type(s) of Failure - Axial and circumferential cracking of 17-4 PH index tubes and guide roller mounts of control rod drives due to stress corrosion.

Mechanism(s) of Failure - Complete separation of a control rod poison blade from the drive occurred in Dresden-I. Subsequent examination revealed axial and circumferential cracking in index tubes and guide roller mounts. The material used in these drives was 17-4 PH aged at 900°F to maximum strength. This alloy is very sensitive to stress corrosion even in high purity hot water.

Summary of Failure Mechanism(s) - Stress corrosion cracking of of 17-4 PH in a condition of maximum hardness.

Corrective Action(s) - A change in aging temperature from 900°F to approximately 100°F essentially eliminates sensitivity to stress corrosion cracking without undue loss of strength. This action was taken.

Lesson(s) Learned - The 17-4 PH alloy was used for a critical application without adequate information on its properties in the operating environment.

Pertinent Reference(s) - ASME-61-WA-268.

Component(s) - Inconel-600 inspection tubes in the Swedish Agesta reactor.

Type(s) of Failure - Intergranular stress corrosion cracking.

Mechanism(s) of Failure - Inconel-600 inspection tubes in the Agesta reactor were observed to suffer from intergranular stress corrosion cracking after exposure to 217°C water containing small (1-4 ppm) quantities of LiOH or KOH. The alloy was atypical in having a high (0.08%) carbon content with heavy precipitation of carbides, and the pieces probably contained substantial levels of residual stress. These are known to be deleterious, but no definite assessment of their role in the failure can be made.

Summary of Failure Mechanism(s) - Intergranular stress corrosion of Inconel-600 containing high carbon or high residual stresses after exposure to relatively pure water.

Corrective Action(s) - Apparently both high carbon and cold work may initiate stress corrosion in Inconel-600. These should be replaced with stress relieved tube with lower carbon.

Lesson(s) Learned - Minimize residual stress levels and carbon content of Inconel-600 when used in high temperature water.

Pertinent Reference(s) - Swedish Report AE-245, 1966.

Component(s) - Austenitic stainless steel primary reactor system.

Type(s) of Failure - Generalized cracking.

Mechanism(s) of Failure - Various portions of a reactor primary were leak-checked using a freon detector. Not all the freon was removed and a combination of radiolysis and hydrolysis partially decomposed the freon, forming chloride and fluoride ions. These ions caused stress corrosion in the austenitic stainless steel, developing cracks in the system.

Summary of Failure Mechanism(s) - Stress corrosion cracking due to chloride and possibly fluoride ions formed by the decomposition of freon.

Corrective Action(s) - Thoroughly flush the system and replace cracked sections.

Lesson(s) Learned - Any material potentially capable of decomposition to products known to attack reactor components should be avoided. This encompasses most organic compounds.

Pertinent Reference(s) - None

HEAT EXCHANGERS

Component(s) - Shippingport Steam Generator

Type(s) of Failure - Caustic stress corrosion cracking of 304 stainless steel steam generator tubes.

Mechanism(s) of Failure - The relatively small size and high steaming rates of the Shippingport steam generators posed difficulties in control of the secondary coolant. The pH, free caustic, and chloride contents all varied, and considerable difficulty was experienced in retaining the correct ratio of phosphate to caustic. One unit suffered severe transgranular stress corrosion cracking initiating on the outer surface of the tubes and propagating inward. The attack was typical for either caustic or chloride stress corrosion cracking in an uastenitic stainless steel; however, most of the evidence favored caustic as the culprit.

Summary of Failure Mechanism(s) - Stress corrosion of 304 stainless steel due to sodium hydroxide.

Corrective Action(s) - Minimize steam blanketing and concentration of solids by relocation of steam risers. Use a base other than sodium hydroxide to control pH (LiOH); use orthophosphate for phosphate control; remain at least 0.2 pH units below the Whirl-Purcell curve of stoichiometric neutrality for trisodium phosphate.

Lesson(s) Learned - Excess caustic is as severe an agent promoting stress corrosion as is chloride in the presence of oxygen.

Pertinent Reference(s) - Proc. of the American Power Conference V2, 1959, pp. 748-68; BMI-1764, February, 1966.

Component(s) - Stainless steel safety valve.

Type(s) of Failure - Plug in safety valve broke off.

Mechanism(s) of Failure - A type 304 stainless steel safety valve used in 300 pound steam service failed by severe stress corrosion cracking after some years of operation. Chlorides from the wet steam collected in the hollow interior of the plug seal in the valve. The stress corrosion cracking became so severe that eventually the plug broke away from the stem.

Summary of Failure Mechanism(s) - Stress corrosion cracking of valve plug due to collection in stagnant region.

Corrective Action(s) - Redesign the valve to eliminate hollows or crevices where salts could collect.

Lesson(s) Learned - Any region where chlorides can collect may result in chloride concentration and stress corrosion.

Pertinent Reference(s) - Materials Protection June 1965, pp. 28-35.

Component(s) - 304 stainless steel heat exchanger tubes.

Type(s) of Failure - Transgranular stress corrosion cracking of 304-L stainless steel heat exchanger tubes in region between double tube sheets.

Mechanism(s) of Failure - These Savannah River heat exchangers were equipped with double tube sheets to minimize loss of D_2O by leakage into the H_2O secondary coolant. The D_2O contained < 6 ppb of chloride, the H_2O 1-6 ppm of chlorides. In addition, the heat exchanger contained elastomer gaskets containing 8% chlorides. There was some leakage of H_2O into the gap between the tube sheets. This water vaporized, depositing chlorides (from water or decomposed gaskets) and iron oxides on the outside of the heat exchanger tubes. Chloride concentration as high as 300 ppm were measured in these films. This concentration was sufficient to cause gross transgranular corrosion in the tubes after five years, leading to the rupture of one and leakage in other tubes.

Summary of Corrosion Mechanism(s) - Concentration of chlorides by evaporation leading to stress corrosion cracking of 304-L stainless steel.

Corrective Action(s) - Eliminate double tube sheet to minimize concentration mechanism.

Lesson(s) Learned - The use of 304-L stainless steel will not

insure against stress corrosion cracking if a concentrating mechanism exists to increase the chlorides in contact with the 304-L.

Pertinent Reference(s) - DP-539, November 1960.

Corrective Action(s) - Install a flow diverter in the pipe to prevent direct impingement of the colder water on the wall.

Lesson(s) Learned - Design plays an important role in the minimization of thermal fatigue. Anytime two coolant streams mix with a substantial temperature differential, thermal fatigue is possible. Another lesson is the similarity of cracking caused by thermal fatigue and stress corrosion. A cursory evaluation of the factors would have suggested stress corrosion.

Pertinent Reference(s) - HW-68125.

X. SOME THOUGHTS ON SCC PROBLEMS

by

B.F. Brown

The status of SCC of high strength alloys in DoD hardware has changed markedly in recent years. During the early 1960's it was pandemic, but by 1970 it is no longer credible to me that a major DoD hardware program could experience a SCC surprise. The reason for this development is that macroscopic test methods are now available and widely known which will anticipate SCC failures in service hardware providing the environment is adequately characterized. What is more, we now have laboratory tests which generate homogeneous data which have the added advantages of being "worst case" with respect to mechanics and of having predictive capability with respect to other geometries. We do not have predictive capabilities with respect to fundamentally new chemical environments. It is easy to rationalize experience, but not to predict. I do not think this situation will change very rapidly because not only is the chemical predictability problem difficult, but students of chemistry these days are so busy trying to make like solid state physicists that they do not have time to learn the descriptive chemistry needed for predictability.

We have not seen much development in SCC theory to parallel the development of useful test concepts and methods. That state of affairs is neither surprising nor, to me, dismaying. In retrospect, it is astonishing that, until the work at NRL, only Edegleanu and Marshakov seem to have considered local deviations from bulk chemistry in connection with SCC, and neither of them had any data at all on the local chemistry within stress corrosion cracks. (Marshakov's "narrow crevices" are sometimes mistranslated "cracks.") It is clear that an "uphill diffusion" process is operative, the significance of which wants wider consideration.

There has been an excessive numbers-collecting campaign--making bricks--in this field, as I suppose is true of most other fields as well. If the current budgetary squeeze would only squeeze out this brick-making, it would be a good thing. Alas, I am afraid that a kind of Gresham's law will prevail, particularly if those who control such things do not wake up to the inadequacy of the "any complete theory of SCC must explain" argument.

Despite corrosion being a kinetic phenomenon, the thermodynamic arguments of the grand architects of corrosion science--Evans, Hoar, and Pourbaix--have proven their usefulness in building up this science. Just as I have little respect for the abstract artist who has not proved that he is able to first paint a hand which looks like a hand, so I am very suspicious of those avant garde corrosion scientists who do not understand the work of the grand architects.

XI. NOTES ON ELECTROCHEMISTRY

by

R.A. Oriani

Electrochemical reactions have as their chief distinctive characteristic that the oxidative (electron-yielding) portion of the reaction is spatially separated from the reductive (electron-absorbing) portion, with the electron traveling through the substrate from one spatial region to the other. As a consequence, kinetic control of the overall reaction may be in the oxidation or in the reductive portions. Another consequence is that charged species are necessarily involved in each portion, so that electric fields are generated and in turn applied electric fields can be used to control the reactions.

The effects of varying the electrical potential drop across the inner portion of the electrical double layer at a metal-water interface has both thermodynamic and kinetic effects. For example, a well known effect of varying that potential drop is that the interfacial free energy (surface tension) of the liquid mercury-water interface is a strong function of potential. Though such "electrocapillary curves" have never been measured for solid metals in contact with water, the effect is undoubtedly real for solid metals. A clear inference from this is that the adatom and surface vacancy populations, as

The problem of the diffusion and translation of existing corrosion science and lore into practice remains a major obstacle. Frank LaQue's magnificent "Sea Horse Institute" serves well in this respect for seawater corrosion. I doubt that carbon copies would work for other areas, but somewhat similar approaches might be worth trying in certain special areas. The building industry, with corrosion problems in heating, plumbing, and external metal trim and structural components would be an example of the latter. But that is not a Navy problem.

well as the density of kinks on atomic surface steps, should also be functions of potential, leading to the conclusion that surface mobilities and also growth and "ungrowth" kinetics should be functions of potential. Also, along with the change of interfacial free energy with potential there should also be a change of surface step free energy; this in turn would lead to large changes in nucleation frequency of surface deposits, and hence to changes in deposition and in dissolution kinetics. In addition, the chemical and crystallographic nature of corrosion products may change as the electrical potential drop is changed, not only for thermodynamic reasons (e.g., Pourbaix diagrams), but for kinetic factors. Furthermore, the nature and amount of adsorbed species upon the surfaces of the corrosion product will change with potential, and since the chemical and electrical structure of the adsorbed layers probably affects strongly how the crystallites of the corrosion products bond together, the protective character of the corrosion products should be expected to be a function of the electrical potential.

In considering problems such as the embrittlement of metals by hydrogen, or the extent and kinetics of the absorption of hydrogen by steels, it is important to know the thermodynamic fugacity of hydrogen corresponding to the dissolved hydrogen concentration in the metal just below the surface because this is the quantity that sets the driving force for diffusion of hydrogen, or that controls the equilibrium amount of hydrogen that can be absorbed. In particular, charging in of hydrogen by cathodic deposition, a common way of presenting hydrogen to

metals, leads to a sub-surface hydrogen concentration which is, in general, kinetically determined and that cannot be calculated from thermodynamics (Nernst equation). Cathodic charging involves the following three steps:

1. H^+ (aq.) + e → H (adsd.)

2. H (adsd.) + H (adsd.) → H_2(g)

or

H (adsd.) + H^+ + e → H_2(g)

3. H (adsd.) → $\underline{H}$

Only if the discharge reaction (1.) is by far the fastest step can the activity of sub-surface dissolved hydrogen, $\underline{H}$, be given by the Nernst equation. If that is not the case, then the kinetics of the recombination reaction (2.) and/or the kinetics of the dissolution step (3.) will set the sub-surface activity of the hydrogen. The kinetics of these steps is very sensitive to the content of impurities, both ionized and unionized, at the interface, and it is well known that small amounts of sulfide ion, for example, will greatly increase the amount of hydrogen taken up by steels from water solutions.

It is therefore necessary to measure the sub-surface hydrogen concentration for any given set of cathodic charging parameters. This may be done by measuring the steady-state permeation of hydrogen through a thin sheet of the desired metal. The input surface is maintained in contact with the

desired charging medium and at a given cathodic potential. The output surface is maintained at very nearly zero hydrogen activity, and transmits the permeated hydrogen to some detector, electrochemical, mass spectrometer, etc. Since the permeability-concentration gradient relationship is already known from measurements in gaseous hydrogen temperatures above 100°C where surface impedances become negligible, one may extrapolate this relationship to the temperature in question, obtaining thereby the sub-surface input concentration of dissolved hydrogen multiplied by the normal lattice diffusivity of hydrogen. Since the latter value is known, one may obtain the sub-surface concentration from the product, and from the known relationship between concentration, temperature, and fugacity of hydrogen, the latter may be calculated.

This admittedly circuitous method may be replaced, for a limited range of fugacities, by the method of Podgurski. A large, totally enclosed artificial void is produced within the metal desired to study. This may be done by hot-pressing the ends of a tube held within very clean hydrogen at low pressure. The outer surface of what is now an ampoule is contacted to the cathodic charging medium and charging under constant conditions is continued until constant weight is attained, as observed by sensitive gravimetric techniques. Knowing that the weight gain is due to gaseous hydrogen in the void in equilibrium with the sub-surface concentration of dissolved hydrogen, knowing the final volume of the void from measurement of the apparent density, and knowing the equation of state of hydrogen

at the temperature of charging one can calculate the fugacity of the hydrogen gas in the void, and hence the fugacity generated by the charging medium and conditions. This method is restricted to fugacities that correspond to pressures not so large so that the metal ampoule is ruptured. Only by such laborious techniques would it be possible to investigate, for instance, how embrittlement phenomena for any one steel under cathodic charging vary with hydrogen fugacity, or at a given, known fugacity, how they vary with chemical composition or with heat treatment of a steel.

Once the hydrogen has entered the metal, its diffusivity (though not in a steady-state permeation) will be decreased by attractive interactions with dislocations and interfaces, and at room temperature for iron-based b.c.c. alloys the effective diffusivity can thereby be diminished by as much as four orders of magnitude. Indeed, such attractive interactions are responsible for the uptake, from an environment of a given hydrogen fugacity, of an amount of hydrogen far in excess of the normal lattice solubility. Elastic stress fields also increase the lattice solubility, for a given thermodynamic fugacity, and stress field gradients must be considered explicitly in the diffusion equation.

Tiller and Schrieffer have deduced that a localized tensile elastic stress will produce an enhanced concentration of Fermi electrons in a metal in that stressed region. From this, they have concluded that the driving force for hydrogen input from an aqueous solution will thereby be increased. This argu-

ment, however, cannot be right on thermodynamic grounds, even if we accept their quantum-mechanical argument about the electron concentration due to tensile stress. Careful examination of this problem shows that the stress-induced polarization can affect only the kinetics of hydrogen entry, and this only if the discharge step (1.) above is rate-controlling.

XII. A MECHANISM OF STRESS-CORROSION CRACKING IN PLASTIC SOLIDS

by

J.J. Gilman

ABSTRACT*

Small changes in surface environments can change the energy needed to create a surface shear step. Increases in this energy tend to shift a delicate balance between glide and cleavage initiation at a crack tip. By inhibiting plastic deformation, this causes an increased tendency for cleavage. Thus, a material that is ductile in a vacuum can become quite brittle in the presence of certain surface active environments; particularly atomic hydrogen.

The quantitative criterion for deciding whether flow or cleavage will prevail is the ratio of the appropriate glide plane's surface energy to the cleavage plane's surface energy.

A survey of the strengths of the interactions between hydrogen and metals has been made. Throughout the periodic

*The complete manuscript of this paper is published in another volume of the Report of ARPA Materials Research Council, 1971.

table strong diatomic interactions occur. At surfaces, the interactions remain strong although they are somewhat weaker. In solid hydrides, they tend to be much weaker or non-existent. Thus, the strength of the interaction depends on the metal-metal distance. It is shown that for a typical transition metal, the interaction with hydrogen is strong enough to readily cause embrittlement.

XIII. ENVIRONMENTALLY INDUCED BRITTLE DELAYED FAILURE: THE STRESS-CORROSION PROBLEM

by

A.R. Troiano

The delayed failure of steel and many other alloys, even in relatively mild environments, has been a problem for a long time. However, it has become increasingly acute as environments become more aggressive, temperatures and pressures rise, strength levels and applied stresses increase, alloys become more complex, etc. Interpretation and analysis of the problem has been mired partially in semantics and partially in controversy relative to the mechanisms, particularly in terms of anodic dissolution* vs. hydrogen embrittlement. Considering the semantics of the situation, stress corrosion cracking is an observable phenomenon and not an explanation, hence the term should not be employed interchangeably with the concept of anodic dissolution under stress as opposed to a hydrogen embrittlement phenomenon. Stress corrosion cracking should refer to a brittle type failure in a cor-

*Including all the suggested non-hydrogen mechanisms in anodic dissolution may be somewhat of an oversimplification, but it does generally cover most of the situation. A stress-sorption concept, largely a take-off of the Petch and Stables surface-energy reduction model has received some consideration, but can be dismissed as applying to anything but completely brittle solids.

rosive environment under stress and not be viewed as simply corrosion failure accelerated by stress.

It is the position of the writer that virtually all SCC is related to hydrogen embrittlement and more specifically to the factors which will allow the production and entry of hydrogen into the metal. Research in the Case Institute Laboratories has developed a theory of hydrogen embrittlement and brittle delayed failure which appears to be quite compatible with a generalized theory of SCC.

Briefly, the theory (see Campbell Memorial Lecture, Trans. ASM, 1960) involves the stress-induced diffusion of the solute to a region of high triaxial stress beneath a notch or other stress raiser (i.e., metallurgical). Highly localized plastic flow occurs at the root of the notch. This is followed by crack initiation beneath the notch, and discontinuous propagation after a measurable crack incubation period, all of which leads to ultimate failure. There is a critical threshold stress for failure, rationalized on the basis of the interaction energy between the solute and a dislocation array (crack embryo) to achieve the critical solute concentration for crack initiation. The yield strength provides a "cut-off" value for the interaction energy which must be elastic. The higher the yield strength, the greater will be the interaction energy, and hence the greater will be the driving force for the concentration of hydrogen. This, of course, explains the greater sensitivity of the high strength steels to hydrogen.

Even the above very brief outline indicates many points of common behavior with accepted SCC phenomena. For example, crack incubation time, discontinuous crack propagation, threshold stress for failure, crack nucleation below pits (notches), greater susceptibility of higher-strength materials, brittle fracture surface appearance (admitted even by those who espouse any of the anodic dissolution theories of SCC), etc. These and other more recent studies involving hydrogen permeability, pitting and delayed failure in various environments, have led us to the conclusion that the same fundamental mechanism, with perhaps only slight, if any, modification operates in the general case of stress-corrosion cracking. Here, the embrittling agent (hydrogen) is in the outside environment of the metal rather than distributed within the metal in any or all of a number of different forms. Thus, the hydrogen must enter the steel (chemical or physical action), and diffuse through the lattice to the region of triaxial stress (the crack embryo).

Regions of high triaxiality are produced in many different ways. Corrosion pits are, of course, ideal loci. However, there are other more subtle, but equally effective, regions. These include segregates (both nonmetallic and metallic), and the elastic-plastic interface resulting from plastic deformation even on a microscale well below the engineering yield stress.

Research by the writer and a number of his students as well as by others has established the discontinuous nature of environmentally induced crack propagation. This is, of course,

similar to that observed for hydrogenated alloys and presages a strong similarity in the mechanism. Stress-corrosion cracking has been reported to have an incubation period and, significantly time to failure is "essentially the same" whether the stress is applied from the outset or only during the latter stages.

Of the greatest engineering importance as well as fundamental interest is the threshold or the lower critical stress below which failure will not occur. The measured dependent variable is usually "time to fail" where the really significant variable is the stress below which failure will not occur; more recently these values have been examined in terms of K_{Iscc}. The stress-corrosion literature makes repeated reference to a threshold stress for failure. This, in our opinion, is the same phenomenon as observed in hydrogen-charged specimens, another example of great similarity between hydrogen delayed failure and stress-corrosion cracking. Thus, it becomes evident that the focus of all variable parameters should be primarily on their influence on the threshold value of stress for crack initiation and propagation.

Stress-corrosion cracking studies conducted in potentiostatically controlled environments provide an opportunity to delineate the conditions for SCC failures. Some of the more recent studies involving these techniques have attempted to differentiate between anodic dissolution and hydrogen embrittlement as the controlling mechanism in stress-corrosion failures.

The usual procedure is to examine the time to fail under stress over a range of both cathodic and anodic controlled potentials relative to the natural potential. The time to failure exhibits a maximum as a function of applied potential and it is claimed that this abrupt change in slope indicates a change of electrochemical mechanism. This peak is considered to represent the most positive potential at which the hydrogen embrittlement mechanism functions. At higher potentials, the failure mechanism is considered to be stress-corrosion cracking, with the inference that this occurs by simple anodic dissolution, film breakdown or related phenomena.

There are a number of observations that indicate that this approach may not be discriminatory. For example, as we have shown, corrosion pits give rise to hydrogen entry even under anodic polarization. Presumably, this results largely from the very low pH developed within the pits. For structural steels, it has been demonstrated that hydrogen permeation accompanied by SCC develops under anodic polarization in those steels that exhibit pitting. On the other hand, steels that suffer general dissolution without pitting do not exhibit either hydrogen permeation or SCC. Thus, cracking under anodic polarization relative to the natural potential does not exclude a hydrogen-embrittlement mechanism for the cracking phenomenon, nevertheless, this has been offered as refutation of the hydrogen concept.

It is generally agreed that the maximum in failure time as a function of potential is the result of cathodic protection. This

is also used as an argument against hydrogen. Briefly, it goes as follows: it is experimentally observed and theoretically consistent that increased hydrogen is evolved at the anode under cathodic protection; yet, it is under these very conditions that optimum resistance to SCC is observed. Hence, hydrogen cannot be involved. This line of reasoning makes the necessary and unjustified assumption that the absorption of hydrogen is directly proportional to its adsorption or, in other words, that the relative rates do not change. Recent research at the Case Laboratories have demonstrated that the oxygen-reduction reaction plays a major role in decreasing the entry of hydrogen and protecting against delayed failure. In the absence of oxygen, there is no cathodic-potential failure maximum and there is substantial hydrogen permeation not observed in the aerated solutions.

One of the last remaining arguments against a generalized hydrogen mechanism for SCC, cites the evidence that ferritic stainless steels do not have SCC in boiling $MgCl_2$ yet they are sensitive to hydrogen embrittlement; while just the opposite is true for austenitic steels. Of course, austenitic steels (and other fcc alloys) will lose substantial ductility from hydrogen. Preliminary studies at the Case Laboratories appear to indicate that the above behavior can be rationalized in terms of the hydrogen model.

One of the most intriguing aspects of the SCC phenomenon is its marked specificity which has been cited in support of a stress-sorption mechanism. We cannot subscribe to this, but

rather adopt the principle that this phenomenon is simply related to "the factors which will allow the production and entry of hydrogen into the metal." Specificity is a most important aspect of the SCC problem with broad practical ramifications and should receive intense systematic study with all the tools available, such as low-energy electron diffraction, permeability, etc.

For passive metals, pitting occurs only when the electrode potential exceeds a critical value that depends on many environmental factors including pH, temperature and the concentration of specific ions such as sulfates and nitrates in the electrolyte. Sulfides (H_2S) are known to catalyze the entry of hydrogen into metals and, in view of their prevalence in sea water as well as in brackish waters, etc., their influence on pitting and SCC in terms of hydrogen may directly contribute to failure. It is evident that pitting or some form of selective non-uniform film breakdown, hydrogen entry, and SCC are intimately related. Indeed, for the face-centered cubic alloys (i.e., austenitic steels) it is not certain that SCC can occur in the absence of pitting at anodic potentials, natural or applied.

Another aspect of the relation of pitting, hydrogen and SCC involves the action of stress in nucleating pitting. It is intriguing to speculate that, depending upon environmental circumstances, if there is a significant influence of stress on pit nucleation and pitting will allow hydrogen entry, then there may be a close relation between the pitting stress and the threshold stress for SCC.

Pitting corrosion does not invariably lead to cracking and this is particularly true for stainless steels, Monel, and similar alloys. For example, these alloys often exhibit pitting in salt solutions at ambient temperatures as well as at elevated temperatures; however, cracking occurs only in the elevated temperature tests, as in boiling $MgCl_2$. The relatively low mobility of hydrogen in stainless steels appear to be the principal factor responsible for this temperature sensitivity of the cracking phenomenon. That is, the temperature must be high enough to provide the hydrogen mobility required for crack propagation. This is perhaps best illustrated in studies of the hydrogen embrittlement of Monel. For cathodically charged samples, maximum embrittlement occurs at temperatures in the range from 300° to 400°F with virtually no embrittlement exhibited within reasonable lengths of time in static fatigue tests conducted at room temperature. This, again, indicates the close relation between hydrogen embrittlement and SCC.

For the most part, this report has been slanted towards liquid environments, but there is little doubt in our mind that the same principles and model applies to gaseous environments. Johnson, Chandler, and others in the United States, Hofmann in Germany, and Fidelle in France have contributed substantially to the knowledge of gaseous environmentally induced failure. These investigators have generally indicated the close relation with hydrogen embrittlement. That is a vital aspect of the gas problem and its study involves, in a sense, a type of "gaseous

electrochemistry." Here, again, the practical implications are broad and even embrace considerations of fuel-cell technology, catalysis, etc.

XIV. REMARKS ON STRESS-CORROSION CRACKING

by

H.H. Uhlig

In discussing mechanisms of stress-corrosion cracking (SCC), it is important to differentiate between intergranular corrosion which proceeds without stress, and SCC which requires some definite tensile stress in order for failure to occur. I mention this because in some of the discussions at this meeting, I noted that sensitization leading to carbide precipitation in stainless steels has been included in the category of factors contributing to stress-corrosion cracking. I would be inclined to exclude this factor because the causes and remedies that apply are quite different from those applying to the transgranular cracking observed in stressed austenitic stainless steels exposed to damaging environments.

The present discussions of stress-corrosion cracking so far have emphasized fracture mechanics and metallurgical factors. However, there is a whole area of environmental factors that are equally important and which deserve serious consideration at any conference of this kind. For example, one can entirely avoid SCC of metals in aqueous media by the process of cathodic protection, accomplished through either an impressed

electric current or by use of electrochemically more active metals and alloys. Furthermore, one can avoid SCC by use of inhibiting salt additions. Boiler waters of steam power plants are regularly treated with salts like phosphates, Quebracho extract, or nitrates which, as small additions, prevent incidence of SCC caused by alkalis that are common constituents of such waters. In the chemical industry, industrial waters or chemical solutions containing chlorides are treated with small additions of nitrates in order to avoid SCC of austenitic stainless steels.

Focusing on cathodic protection, one finds that SCC of carbon steels (in nitrates), stainless steels, brasses and perhaps of most other metals as well, occurs only when a well-defined critical potential is exceeded. For type 304 stainless steel in magnesium chloride solution boiling at 130°C, the measured value is -0.145 V (S.H.E.). At a controlled potential 5 to 10 mV above this value, rapid transgranular failure occurs within 1 to 2 hours; but for a controlled potential at a few mV below the critical value, resistance to cracking exists for the entire test period of 50-100 hours. It is important to note, particularly in view of several discussions at this meeting, that crack growth already initiated can also be stopped at this same approximate potential. In other words, if a specimen of type 304 stainless steel [0.040 in.(1 mm) thick] is precracked by applying a potential slightly above the critical value, the ensuing crack stops growing if the potential is then shifted to a value that is slightly below the critical value. The crack

starts growing again if the potential is shifted to the former more noble value. Obviously, the environment in this case is all-important, not only in determining crack initiation, but also crack growth.

The information supplied by critical and corrosion potentials has permitted us to inhibit SCC by simple galvanic coupling. For example, a stainless steel which, uncoupled, normally undergoes SCC in $MgCl_2$ solution does not fail up to the maximum test period of 200 or more hours when coupled to a stainless steel of somewhat different composition having the proper more-active corrosion potential. Similarly, other galvanic couples can act to accelerate SCC depending on prevailing corrosion and critical potentials. Basic information of this kind has obvious practical relevance.

Many salts that are inhibiting act, by and large, to shift the critical potential to a more noble value. When the shift brings the critical potential above the corrosion potential, SCC is no longer observed. Present considerations indicate that inhibitors can act not only to prevent cracks from initiating, but they also can prevent their continuing growth in a precracked specimen.

It is likely that if a specimen is deeply precracked, that is, the crack extends more than perhaps a fraction of a millimeter, cathodic protection and the use of inhibitors become less effective. Throwing power of the current is then not adequate, or the chemistry of the solution at the base of the

crack undergoes marked changes. The critical crack depth under a variety of environmental conditions deserves detailed study.